АПРЕЛЬ-ИЮНЬ 2016 ТОМ 8 № 2 (29)

ISSN 2075-8243

# ActaNaturae

## Биоинженерия искусственных лимфоидных органов

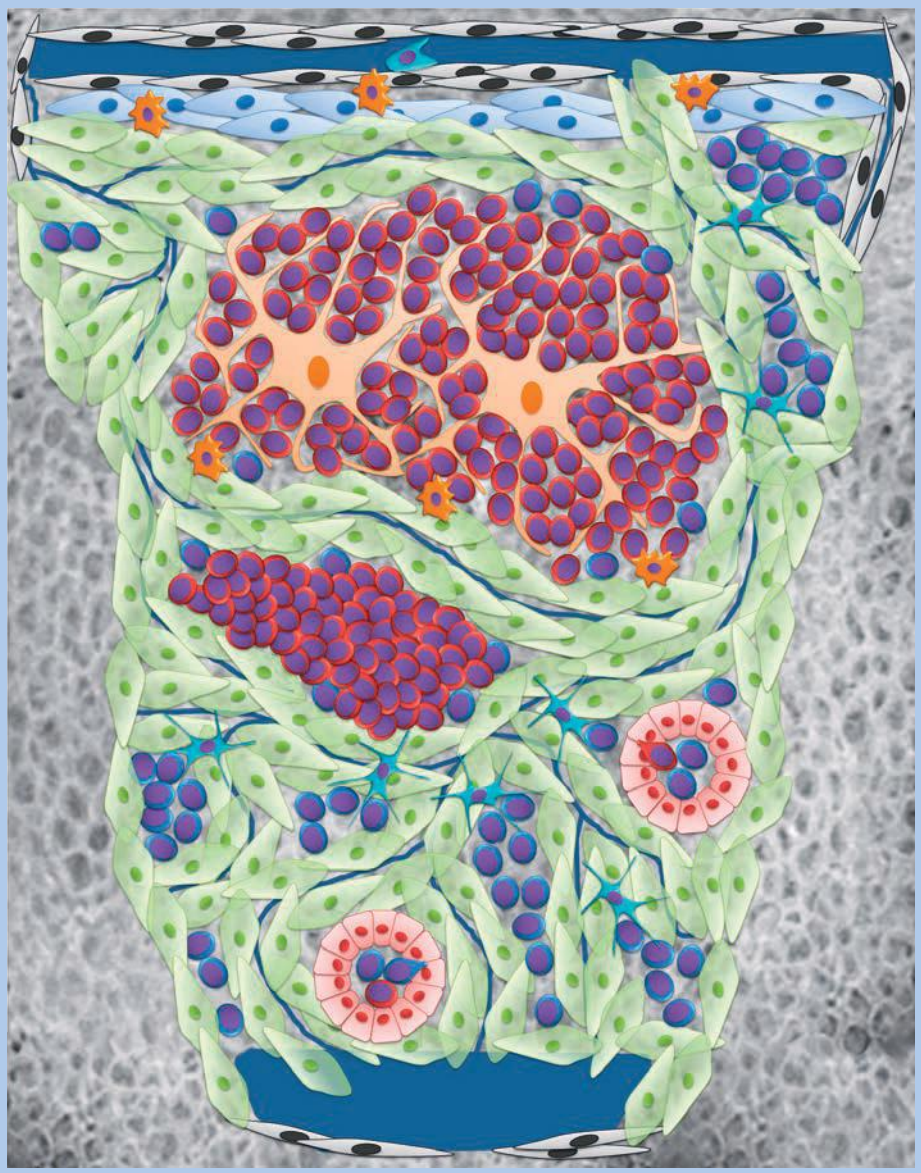

ПОДПИСКА НА ЖУРНАЛ

# ActaNaturae

Журнал *Acta Naturae* уделяет особое внимание междисциплинарному характеру исследований и разработок, которые находятся на стыке различных сфер биологических специальностей - молекулярной биологии, биохимии, молекулярной генетики и биологической медицины.

*Acta Naturae* издается компанией «Парк-медиа» на русском и английском языках и входит в Перечень ведущих периодических изданий Высшей аттестационной комиссии Министерства образования и науки РФ и реферативную базу данных PubMed.

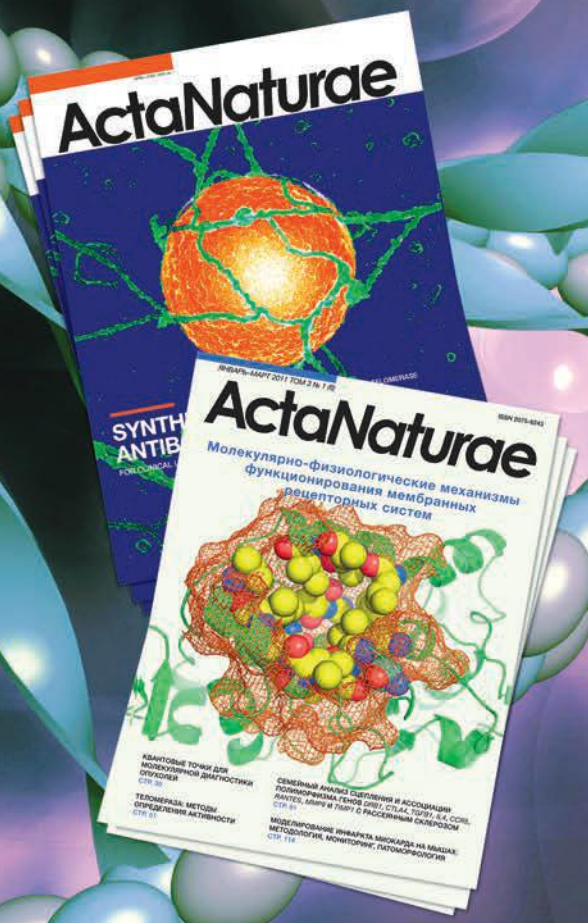


## ПОДПИСКА В РЕДАКЦИИ:

119234, Москва, Ленинские горы, 1, владение 75Г
Телефон: +7 (495) 930-87-07, 930-88-51
Bio-Mail: podpiska@biorf.ru
Web site: www.actanaturae.ru

## ПОДПИСКА ПО КАТАЛОГАМ НА ПОЧТЕ И ЧЕРЕЗ ИНТЕРНЕТ:

| РОСПЕЧАТЬ | ИНФОРМНАУКА | ИНТЕР-ПОЧТА |
|---|---|---|
| Индексы: 37283, 59881 | Индекс: 59881 | Индекс: 17510 |
| www.pressa.rosp.ru | www.informnauka.com | www.interpochta.ru |

**ИНФОРМАЦИЯ ДЛЯ АВТОРОВ:**
Если Вы хотите опубликовать свою работу в журнале *Acta Naturae*, пишите на journal@biorf.ru и звоните по телефону: 8 (495) 930-87-07

# Letter from the Editors

Dear readers of ActaNaturae,

We bring you in this issue reviews and research articles focused on areas of life sciences that we consider of current interest. You will find the very interesting review in the field of regenerative medicine (Nosenko *et al.*) discussing the modern studies devoted to the bioengineering of lymphoid organs. Most articles in this issue are in some way related to biomedicine: from in silico modeling of the structure of complexes of voltage-gated potassium channels with peptide blockers (review by Novoseletskii *et al.*) to clinical and molecular genetic aspects of monogenic arrhythmia syndromes (review by Golukhova *et al.*). These reviews echo the study by Nikitskaya *et al.*, who investigated the effect of cytomegalovirus infection on the development of the acute coronary syndrome. The problems associated with the development of cardiac insufficiency are also discussed in the study by Tapilina *et al.* devoted to the functioning of the system of muscarinic receptors. The immunological topic of this issue is continued by the research article by Stepanova *et al.*, who are designing novel recombinant vaccines, including anti-influenza A virus ones, based on fragments of the hemagglutinin subunit.

We also discuss the problems associated with innate immunity. In their review, Finkina *et al.* analyze the functioning of one of the key components in the plant innate immunity system: lipid-transfer proteins. The plant-related theme of our issue is continued by Lebedev *et al.*, who design herbicide-tolerant transgenic tree varieties. The study by Nilov *et al.* demonstrating that 7-methylguanine, metabolite of nucleic acids, can inhibit poly(ADP-riboso)polymerase and interfere in the DNA repair system also contributes to the topic of *in silico* design of inhibitors of a critical enzyme pathway. The authors discuss the prospects of using the revealed activity in combination chemotherapy for cancer patients. DNA integrity under thermal stress is discussed in a mini review by Kantidze *et al.* This problem is also extremely important for the biomedical prospects of studying the thermal shock system. Despite using the "conventional molecular biological" approach, the research article by Elizar'ev *et al.* devoted to the regulation of gene expression using the Drosophila melanogaster model is also promising for modern medical biotechnology.

Summing up, we would like to urge our readers and potential authors once again to collaborate with us in a broad range of intriguing areas of modern biomedicine. ●

*The Editorial Board*

# INNOVATION RUSSIA

## Discussion club

We create a dialogue between all socially active groups of people: students, scientists, lecturers, businessmen, managers, innovators, investors, designers, art critics, architects, photographs.

## Learn more at WWW.STRF.RU

Everyone with something to say and ideas to share is welcome to visit our events

Tel.: +7 (495) 930-87-07, 930-88-50
E-mail: seminar@strf.ru

# Inhibition of Poly(ADP-Ribose)Polymerase by Nucleic Acid Metabolite 7-Methylguanine

D. K. Nilov, V. I. Tararov, A. V. Kulikov, A. L. Zakharenko, I. V. Gushchina, S. N. Mikhailov, O. I. Lavrik, V. K. Švedas

The ability of 7-methylguanine, a nucleic acid metabolite, to inhibit poly(ADP-ribose)polymerase-1 (PARP-1) and poly(ADP-ribose)polymerase-2 (PARP-2) has been identified in silico and studied experimentally. The amino group at position 2 and the methyl group at position 7 were shown to be important substituents for the efficient binding of purine derivatives to PARPs. The activity of both tested enzymes, PARP-1 and PARP-2, was suppressed by 7-methylguanine with IC50 values of 150 and 50 μM, respectively. At the PARP inhibitory concentration, 7-methylguanine itself was not cytotoxic, but it was able to accelerate apoptotic death of BRCA1-deficient breast cancer cells induced by cisplatin and doxorubicin, the widely used DNA-damaging chemotherapeutic agents.

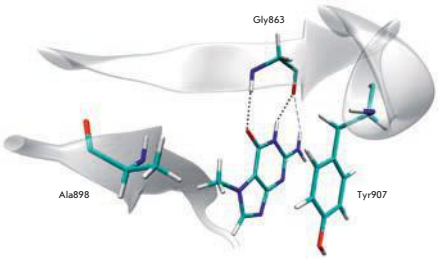


The position and interactions of the 7-methylguanine molecule in the PARP-1 active site revealed by molecular modeling: two hydrogen bonds of the lactam group with Gly863 shown as dotted lines, an electrostatic interaction of the amino group as dashed line, pi stacking of purine rings with Tyr907, and hydrophobic interaction of the methyl group with Ala898.

One-year control and transgenic aspen plants (genotype Pt) 7 days after treatment with water or Basta herbicide at a dose of 2.5, 5, 10 l/ha in 2014. Left – untransformed control plant, right – transgenic line PtXIBar14a

# Testing Transgenic Aspen Plants with Bar Gene for Herbicide Resistance under Semi-natural Conditions

V. G. Lebedev, V. N. Faskhiev, N. P. Kovalenko, K. A. Shestibratov, A. I. Miroshnikov

A number of transgenic lines of European aspen plants expressing the *bar* gene for resistance to phosphinothricin-containing herbicides were produced. Resistance of the resulting lines to a twofold normal field dosage of herbicide Basta was demonstrated under semi-natural conditions. Four lines with high resistance both to herbicides and extremely low temperatures were selected. These plants are promising for further research, in particular, for field studies.

# A New Approach To the Diagnosis of Point Mutations in Native DNA Using Graphene Oxide

A.A. Kuznetsov, N.R. Maksimova, V.S. Kaimonov, G.N. Alexandrov, S.A. Smagulova

A new approach to designing graphene oxide-based test systems for the diagnosis of point mutations in native DNA was developed. This new approach is based on using graphene oxide for absorption and quenching of fluorescently labeled primers in a post-amplification PCR mixture followed by detection of fluorescently labeled PCR products.

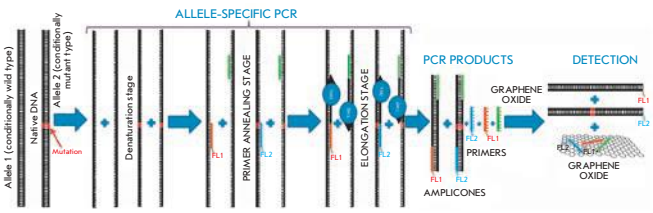


Schematic representation of point mutation diagnosis in native DNA using the developed approach

ActaNaturae
APRIL-JUNE 2016 VOL. 8 № 2 (29)

**Founders**
Ministry of Education and
Science of the Russian Federation,
Lomonosov Moscow State University,
Park Media Ltd



Address: 119234 Moscow, Russia, Leninskiye Gory, Nauchny
Park MGU, vlad.1, stroeniye 75G.
Phone/Fax: +7 (495) 727 38 60
E-mail: vera.knorre@gmail.com, actanaturae@gmail.com



Номер подписан в печать 26 мая 2016 г.
Тираж 200 экз. Цена свободная.
Отпечатано в типографии «МИГ ПРИНТ»

**Indexed in Pubmed, Web of Science, Scopus, and RISC**

# CONTENTS

## RESEARCH ARTICLES



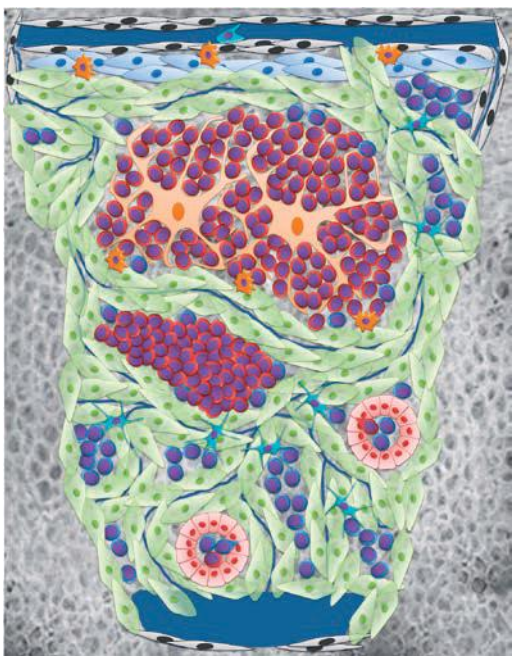

**IMAGE ON THE COVER PAGE**
(see the article by Nosenko *et al.*)

# Biological Collections: Chasing the Ideal

P. A. Kamenski*, A. E. Sazonov, A. A. Fedyanin, V. A. Sadovnichy
M.V. Lomonosov Moscow State University, Leninskie Gory 1, 119991, Moscow, Russia
*E-mail: kamenski_pa@mail.bio.msu.ru

This article is based on the results of an analysis of existing biological collections in Russia and abroad set up in the framework of the project "Scientific Basis of the National Biobank – Depository of Living Systems" by M.V. Lomonosov Moscow State University [1].

**What is a "biological collection"?** Today, the terms "biological collection" and "biobank" are not interchangeable. A biological collection is typically defined as a systematized repository of a combination of any biological material type specimens. The term "biobank" is usually used only for collections of human biospecimens [2]. Hence, the term "biological collection" is broader than the term "biobank": so, the former term will be used hereinafter in this study.

Based on the definition given above, several types of biological collections can be distinguished, depending on the types of biological material stored and the storage methods.

**Cryogenic collections** with material stored in frozen state are most often meant when talking about biological collections. These collections are created for long-term storage of biospecimens that are always supposed to retain their viability and normal functioning after being thawed. Cryogenic collections are typically used to store cells rather than entire organisms (of course, unicellular organisms are an exception). This storage method is applicable to cells of organisms of all life kingdoms on Earth. The cryostorage protocols are elaborated to the least extent for higher plant cells, which lose their viability relatively quickly during the freeze/thaw cycle because of their cytological features [3]. Nevertheless, these cells can also be successfully stored in cryogenic collections. Furthermore, nucleic acids extracted from living organisms can also be stored in frozen form; hence, the corresponding collections are also supposed to be classified as cryogenic collections.

**"Classical" collections** are another type of biological collections. First of all, they include collections of zoological museums and herbaria. Classical collections were the first collections of biological material in the world; some of them go back over two centuries. Recently, it has become clear that these collections of biological material, in addition to being used to study biodiversity, are a valuable source of DNA that can be extracted from the specimens stored and analyzed using the methods of molecular genetics [4]. This enables large-scale molecular phylogenetic studies for big samples amounts, which yield more statistically significant results.

When talking about biological collections, **collections of biological information** are often not included. This category is extremely important for the development of science and technology and mainly includes computer databases containing information about the primary, secondary, and tertiary structures of biological molecules. Such databases as GenBank (nucleotide sequences of the genomes of various organisms, http://www.ncbi.nlm.nih.gov/genbank/) and the Protein Data Bank (tertiary structures of proteins, http://www.rcsb.org/pdb/home/home.do) can be mentioned as examples. The main distinctive feature of collections of biological information is their global character, which means that they can be freely accessed from any location via the Internet.

**Why do we need biological collections?**

In addition to the types of specimens stored, the purpose of biocollections can be viewed as a criterion for their classification.

Most collections that currently exist in the world are **research collections**. This term is used for sets of biological specimens that are stored in research laboratories and are needed in daily routines. Types of specimens in these collections may vary largely, from individual biological molecules to entire organisms. Research collections typically are small; however, they are today the main contributors to the development of fundamental life sciences and allow scientists to carry out comparative research. It should be mentioned that such collections can also be extensive. For example, collections of natural history museums and herbaria often comprise several million specimens and are actively used in research. The previously mentioned global collections of biological information are also used as research collections.

**Commercial collections** (i.e., collections of biological material that is intended for sale to external consumers) have recently acquired wide usage. In fact, these

collections began emerging several decades ago, but the specimens stored were intended exclusively for research. Several collections of baker's yeast strains can be given as an example [5]. The later created commercial collections most typically store donated human biological material (sex cells, blood cells, etc.) and belong to private institutions. Consumers of specimens from commercial collections may be both individuals (e.g., those using *in vitro* fertilization) and pharmaceutical companies that use human cell material for preliminary clinical trials of drugs.

Finally, **"state" collections** (i.e., the ones that are created and maintained for the sake of the state) need to be mentioned. First of all, this category includes collections intended for the preservation of biodiversity. Zoological and botanical gardens (although they are used both for research and common cultural purposes), as well as nature reserves and wildlife refuges, are examples of such collections. Collections for the preservation of biodiversity are not necessarily state-sponsored; they can be created by the initiative of an academic community, such as the Frozen Ark International Consortium that has been organized on the basis of several dozen research laboratories storing frozen cell material collected from rare and endangered species [6]. Along with preservation of biodiversity, state collections can be created to optimize the efficient use of biological resources. For example, the Natural Product Repository at the National Institute of Health (USA) [7] has over 100,000 extracts from various animals and plants that are used to search for novel biologically active agents. The All-Russian Collection of Industrial Microorganisms is an example of this type of collections in Russia; it is the only organization thus far that has been given the status of a national bioresource center by the state [8]. This collection includes microorganisms that are critically important for biotechnology. We would also like to mention such All-Russian collections as the All-Russian Collection of Microorganisms and the Russian Cell Culture Collection.

One should remember that preservation of biodiversity is also related to national security. First and foremost, such collections are meant for the preservation of producer cells for industrial and medical biotechnology, as well as bio-objects for cattle breeding and crop production. Under crisis conditions, Russian industry and agriculture will be thrown back decades if there are no Russian collection repositories.

**Russian and foreign biocollections.** *Table* summarizes the data on the largest Russian collections of biological materials.

As it has been mentioned previously, the main objectives of creating and maintaining biocollections include preservation, research, and the beneficial use of biodiversity. Speaking about Russian biological collections, the research function is the best-developed. The *Table* demonstrates that the vast majority of large Russian collections perform research activities and annually publish hundreds of studies focused on a thorough investigation of the specimens stored.

The situation with biodiversity preservation is more complex. Under the current state of technology development, the problem of biodiversity preservation needs to be solved at two levels; namely, the organism and cell levels. At the former level, work is being carried out in zoological and botanical gardens and nature reserves; Russia is in a rather strong position here. As of 2014, there were 104 nature reserves in Russia [9]; this number is significantly larger than that in any other country. On the other hand, it cannot be denied that nowadays the traditional measures of preservation of rare and endangered living species need to be supplemented with high-tech measures; that is, the storage of cell material harvested from these organisms in cryogenic collections. This aspect contributes most significantly to Russia's lag behind other industrialized countries. Whereas the international consortia preserving cell material harvested from rare species have been operating abroad for an appreciably long time (e.g., the aforementioned Frozen Ark), such work in Russia has just started.

The beneficial use of Russian biological resources is also far from perfect. Living systems are practically used mainly in biotechnology and medicine. When it comes to biotechnology, it is noteworthy that the performance of Russian biocollections is rather active. This mostly relates to the collections of microorganisms (Russian National Collection of Industrial Microorganisms, All-Russian Collection of Microorganisms, several small collections of microalgae) that have been successfully implementing the results of their activity for a long time by creating and optimizing strains producing various compounds. On the other hand, the use of biocollections in medicine in Russia is currently at its lowest level. In Europe and the U.S., 5 years ago there were already several dozen both global and specialized large collections of human cell material [10] and their number has increased since then. The specimens in these collections are actively used in biomedical research and pilot projects. Today, when medical cellular technologies develop in explosive fashion, these collections become particularly important. Finally, it cannot go unmentioned that there are no large collections related to cattle breeding in Russia. Undoubtedly, this fact significantly

Table. The largest Russian biological collections (in descending order of the amount of repository items) according to the official websites of the corresponding organizations

| Collection | Organization | Type of specimens stored | Amount of specimens stored | Purposes of specimens stored | Pipelines |
|---|---|---|---|---|---|
| Collection of Zoological Institute | Zoological Institute, RAS | Animal biomaterial (non-living) | 60,000,000 | Research, museum affairs | https://www.zin.ru/Collections/ |
| Zoological Museum, MSU | Moscow State University | Animal biomaterial (non-living) | 10,000,000 | Research, museum affairs | http://zmmu.msu.ru/ |
| Collection of Botanical Institute | Botanical Institute, RAS | Dried plant and small amounts of plant cell cultures | 7,000,000 | Research | http://www.binran.ru/collections/ |
| Herbarium, MSU | Moscow State University | Dried plants | 1,000,000 | Research | http://herba.msu.ru/russian/departments/herbarium/General_Information/Collection/ |
| N.I. Vavilov collection of cultivated plant seeds | N.I. Vavilov Institute of Plant Genetic Resources, RAS | Cultivated plant seeds | 300,000 | Preservation of the beneficial biodiversity, agriculture | http://vir.nw.ru/otd_r.htm#dept |
| All-Russian collection of microorganisms | Institute of Biochemistry and Physiology of Plants and Microorganisms, RAS | Frozen microorganisms | 20,000 | Delivery of specimens to the external consumers, research | http://ibpm.ru/index.php?option=com_content&view=article&id=249:vkm&catid=4&Itemid=15 |
| Biological Resource Center "Russian National Collection of Industrial Microorganisms" | All-Russian Institute of Genetics and Selection of Industrial Microorganisms | Frozen microorganisms | 20,000 | Biotechnology, research | http://vkpm.org/o-bioresursnom-tsentre/ |
| Russian cell culture collection | The collection is stored in 9 different organizations. Principal organization: Institute of Cytology, RAS | Frozen human, animal and plant cells | 3,000 | Delivery of specimens to the external consumers, research | http://www.cytspb.rssi.ru/rkkk/rkkk_ru.htm |

slows the development of agriculture as a key sector of the Russian economy.

Having analyzed the current state of biological collections, we are certain that these collections represent a tremendous research and technological capability which is currently not being exploited for several reasons. So, **what are the challenges that Russian specialists who organize and maintain biological collections face today**? First of all, it is worth mentioning once again that the cryogenic collections of state status aimed at the preservation and beneficial use of the biodiversity of Russia are poorly developed (see text above).

A serious problem affecting modern biocollections (not only in Russia but worldwide) is that they are disaggregated. This is especially true for the small research collections that most research laboratories have, as was mentioned previously. It is quite typical that scientists maintaining and working with their local collections do not notify the research community at large of the specimens stored in their collections. This happens either because the scientists lack the resources to do so, or sometimes because they are oblivious to the fact that their material can be extremely useful to their colleagues from other organizations. Meanwhile, virtual integration of research (and not only research) collections into a consolidated information system would be extremely efficient today, as large-scale studies using big amounts of samples of different biological objects become increasingly important. Understanding of this problem also exists at the state level. In 2014, a working group was established by the Ministry of Education and Science of the Russian Federation to elaborate approaches to creating national biological resource centers on the basis of the existing biological collections. One of the main tasks of the working group was to perform a global auditing of existing biological collec-

tions in Russia, creating an integrated database that would include these collections, and elaborating a mechanism for reorganizing them into national bioresource centers. In 2015, a similar initiative was proposed by the Russian Academy of Sciences and the Federal Agency for Scientific Organizations by establishing a working group to maintain and develop bioresource collections. Its objectives include auditing research collections and elaborating recommendations for their centralization, standardization, and accessibility. Beyond any reasonable doubt, the activity of these working groups will increase the output of Russian scientists.

It should be mentioned that it is almost impossible to obtain funding for work related to direct maintenance of biocollections. Scientific foundations and the research programs of the ministries do not classify this field as research and usually do not consider the applications submitted. Neither does this activity fall within state assignments for higher educational institutions and research institutes. As a result, biocollections either get whatever funds remain or are maintained out of sheer enthusiasm (those are the two most common terms to describe the situation around the maintenance of biocollections).

Finally, it should not go unmentioned that there is virtually no legal framework for Russian biological collections. Meanwhile, establishment of a legal framework for working with biocollections is absolutely critical, mainly due to the close connection between biological collections and the concept of "national biological resources." This concept is similar to the term "biological diversity" but is broader, since it includes genetic resources of the country's population, biotechnological resources, and natural resources. Bioresources fall under strict legal regulations all over the world; however, regulation in Russia is weaker than in other industrialized countries. Moreover, the import and export of biological material for scientific purposes is unregulated. Because of the lack of accurate procedures, exchange of biomaterial – one of the key aspects of international scientific collaboration – either is impossible (which closes the door on Russian researchers' participation in many important and prestigious scientific consortia) or forces scientists to act as smugglers, which is unacceptable.

Furthermore, no laws that regulate work with human biomaterial exist yet (in 2015, the Law On Biomedical Cell Technologies was adopted only in the first reading in the Russian State Duma); the situation around the regulation of genetic modification of living organisms is not fully clear (the corresponding draft bill is been consideration by the Russian State Duma since 2015). On the other hand, Russian government agencies now understand the importance of elaborating such documentation; work towards it is under way, and members of the scientific community are involved. However, the entire state apparatus, including its executive and legislative branches, needs to consolidate in order to overcome the existing administrative barriers.

Based on the aforementioned, we would like to suggest measures to be taken in order to use biological collections in the Russian Federation with maximum efficiency:

Auditing the existing collections;

2. Sharing best practices in the field of biocollections; elaborating uniform protocols to work with biospecimens of the same type;

3. Creating a single database that would contain information about the maximum possible number of collections; in the long run, establishing a national information and analysis system;

4. Establishing a research center based on large collections under state assignment; establishing a national network of biocollections;

5. Collaboration between members of the scientific community involved in dealing with biocollections and state agencies to develop adequate measures for regulating the activities of biocollections and the related fields of science and technology; and

6. Creating a global "biocollection information space."

*The authors are grateful to the staff of the Ministry of Education and Science of the Russian Federation, I.V. Kazeev and O.A. Egorova, for their kind assistance in preparing the manuscript.*

*This study was supported by the Russian Science Foundation (grant no. 14-50-00029).*

REFERENCES

1. Sadovnichy V.A. // Science and Life. 2015. № 12. P. 2-13.
2. De Souza Y.G., Greenspan J.S. // AIDS. 2013. V. 27. № 3. P. 303–312.
3. Volkova L.A., Urmantseva V.V., Popova E.V., Nosov A.M. // Cryo Lett. 2015. V. 36. № 4. P. 252–263.
4. Krinitsina A.A., Sizova T.V., Zaika M.A., Speranskaya A.S., Sukhorukov A.P. // Biochemistry (Moscow). 2015. V. 80. № 11. P. 1478–1484.
5. Scherens B., Goffeau A. // Genome Biol. 2004. V. 5. № 7. P. 229.
6. MacKenzie-Dodds J., Clarke A., Lermen D., Rey I., Astrin J.J., Seberg O., Oste C.C. // Biopreserv Biobank. 2013. V. 11. № 3. P. 182–188.
7. Brown E.C., Newman D.J. // J. Environ. Monit. 2006. V. 8. № 8. P. 800–805.
8. Order of Russian Ministry of Education and Science № 982, August 11, 2014.
9. The Russian Federation National Environmental report, 2014. Russian Ministry of Natural Resources and Environmental Protection, 2015.
10. Vaught J., Kelly A., Hewitt R. // Biopreserv Biobank. 2009. V. 7. № 3. P. 143–150.

# Bioengineering of Artificial Lymphoid Organs

M. A. Nosenko[1,2,3*], M. S. Drutskaya[1], M. M. Moisenovich[2], S. A. Nedospasov[1,2,3]
[1]Engelhardt Institute of Molecular Biology, Russian Academy of Sciences, Vavilova str. 32, 119991, Moscow, Russia
[2]Lomonosov Moscow State University, Faculty of Biology, Leninskie Gory 1, bldg. 12, 119991, Moscow, Russia
[3]Deutsches Rheuma-Forschungszentrum (DRFZ), Charitéplatz 1, 10117, Berlin, Germany
*E-mail: maxim-nosenko@yandex.ru
Received: 02.09.2015


**ABSTRACT** **This review addresses the issue of bioengineering of artificial lymphoid organs.Progress in this field may help to better understand the nature of the structure-function relations that exist in immune organs. Artifical lymphoid organs may also be advantageous in the therapy or correction of immunodefficiencies, autoimmune diseases, and cancer. The structural organization, development, and function of lymphoid tissue are analyzed with a focus on the role of intercellular contacts and on the cytokine signaling pathways regulating these processes. We describe various polymeric materials, as scaffolds, for artificial tissue engineering. Finally, published studies in which artificial lymphoid organs were generated are reviewed and possible future directions in the field are discussed.**
**KEYWORDS** **artificial lymphoid organ, bioengineering, polymeric scaffold, stromal cells.**
**ABBREVIATIONS** **Ag – antigen, BEC – blood endothelial cells, DC – dendritic cells, FDC – follicular dendritic cells, FRC – fibroblastic reticular cells, HEVC – high endothelial venule cells, HSC – hematopoetic stem cells, iPSC – induced pluripotent stem cells, LEC – lymphatic endothelial cells, LTiC – lymphoid tissue inducer cells, LToC – lymphoid tissue orginizer cells, M - macrophages, MEF – mouse embryonic fibroblasts, MRC – marginal zone reticular cells, RA – retinoic acid, S1P – sphingosine-1-phosphate, TEC – thymus epithelial cells, $T_{FH}$ – T-follicular helper cells.**

## INTRODUCTION

In recent years, bioengineering technologies have attracted a lot of attention, because they provide new approaches to resolving current theoretical and practical issues in biology and medicine. The development of artificial biocompatible materials opens up broad prospects for regenerative medicine, transplantation, treatment of infectious diseases and cancer, as well as for fundamental studies of a number of important aspects of tissue organization in living organisms, which require preservation of the spatial structure of the object under study. A fairly wide range of biocompatible and non-toxic biotechnological materials have been developed that can maintain the functions of different cells in three dimensional space. Furthermore, these biomaterials, particularly scaffolds or matrices, which will be discussed later, can be "functionalized" for a particular task. This has served as a stepping stone for the development of artificial organs and tissues based on polymer scaffolds, including artificial bones [1–4], skin [5, 6], cardiac tissue [7], and other tissues and organs. The potential development of functional artificial lymphoid organs, mainly secondary or tertiary ones, e.g. lymph nodes and lymphoid follicles, attracts particular attention [8–10], because such structures can in theory be used for the correction of immunodeficient states and for the treatment of autoimmune and infectious diseases and malignant neoplasms. It is assumed that bioengineered immune organs will be partially or completely responsible for the protective function in a human body with underlying pathological conditions [10]. Functional artificial secondary lymphoid organs (e.g. artificial lymph nodes) will make it possible to study and model some as-of-now poorly understood aspects of the immune response, and in the future they may find application in the immunotherapy of a whole range of diseases. An important difference between new immunomodulation approaches and the current systemic techniques (e.g., systemic cytokine or anti-cytokine

therapy, depletion of lymphocyte populations, etc.) is the fact that the former act on the level of recognition of specific antigens by the immune system and will, therefore, minimize the negative impact of systemic immunotherapy and focus primarily on the cause of the disease. Their advantage over classical vaccination lies in the creation and long-term maintenance of the most favorable microenvironment, which enables all the key cellular interactions involved in the immune response to take place. In many cases, this can be the decisive factor for the success of a therapy [11, 12].

## STRUCTURE OF LYMPHOID ORGANS AND THEIR ROLE IN THE IMMUNE RESPONSE

Lymphoid organs are integral structural parts of the immune system, and disorders that affect them can result in immunodeficiency in humans and animals [13, 14]. There are three groups of organs: primary, secondary, and tertiary. In a normal adult organism, primary and secondary lymphoid organs are present at all times, whereas tertiary organs are generated locally at the site of a strong and sustained immune response: for example, at the site of a tumor or chronic inflammation [15]. Primary lymphoid organs – thymus and bone marrow – generate immune cells and define the repertoire of T- and B-lymphocytes receptors, whereas secondary and tertiary organs ensure their survival, interaction with other cells, interplay between innate and adaptive immune responses, as well as activation and maintenance of the immune response. Therefore, modeling of various lymphoid organs will help to resolve a variety of issues both in fundamental science and in medicine.

The functionality of immune organs relies on their unique microarchitecture and the wide range of cells and factors involved. Therefore, the challenge of bioengineering is to reproduce them in model systems, since functional activity can only be achieved through proper organization of all components. It is essential to understand the mechanisms of cell organization in the natural organs of a body in order to be able to construct their artificial analogues.

All immune organs are characterized by the presence of the stroma, which often consists of several types of cells of endothelial, mesenchymal, and, in some cases, epidermal origin [16, 17]. The main functions of the stroma include the recruiting and spatial organization of immune cells in the organ, maintenance of their viability, proliferation, and the enabling of effective interaction with other cells and antigens. Each organ has a type of stroma that is necessary for its functioning. The bone marrow of an adult organism produces all hematopoietic cells, including all types of leukocytes, from hematopoietic stem cells (HSC) and hematopoietic progenitor cells. The bone marrow maintains the HSC population via special niches that ensure long-term HSC repopulation, their differentiation into hematopoietic progenitor cells, and the generation of all necessary germs of differentiation [18, 19]. In addition, bone marrow, via certain bone marrow stromal cells, plays an important role in the differentiation and functionalization of B-lymphocytes, memory cells, plasma, and other immune cells [20].

Many types of hematopoietic cells completely, or almost completely, mature within the bone marrow. However, progenitors of T-lymphocytes must undergo several further stages of maturation in the thymus. The stroma of the thymus, i.e. thymic epithelial cells (TEC), enables the survival and selection of thymocytes, and different TEC subpopulations implement both positive and negative selection [21]. The key role in negative selection belongs to stroma-associated dendritic cells that actively present autoantigens [22]. Another important component of the thymus is the mesenchymal compartment responsible for the functioning of both epithelial and hematopoietic cells. Numerous interactions between hematopoietic, mesenchymal, and epithelial cells play an important role in all these processes [23]. The stroma facilitates the release of "trained" mature T-lymphocytes from the thymus, which, in the context of MHC molecules, can recognize the widest repertoire of foreign antigens while simultaneously being the least aggressive against autoantigens [16, 24].

In lymph nodes, the white pulp of the spleen and other secondary and tertiary lymphoid organs, the stromal cells recruit mature immune cells and enable antigen presentation and activation of T- and B-lymphocytes, which leads to their further differentiation, proliferation, and implementation of their effector functions, as well as the formation of memory cells [25–27]. Lymphoid organs associated with the intestines (mesenteric lymph nodes, Peyer's patches, isolated lymphoid follicles, and cryptopatches) play a special role [28]. They are involved in the regulation of the relationship between host and symbiotic microflora, the development of tolerance to non-pathogenic bacteria and food-borne antigens, and the response to pathogenic microorganisms [29–31].

Secondary and tertiary immune organs are of particular importance in the bioengineering of artificial lymphoid organs, since they play the central role in the initiation of the adaptive immune response [26], and, therefore, the processes occurring in them are of great interest for fundamental research and as the basis for potential clinical interventions in different pathological conditions. Therefore, the development and the structure of these organs will be discussed in more detail using lymph nodes as an example. The structure of a

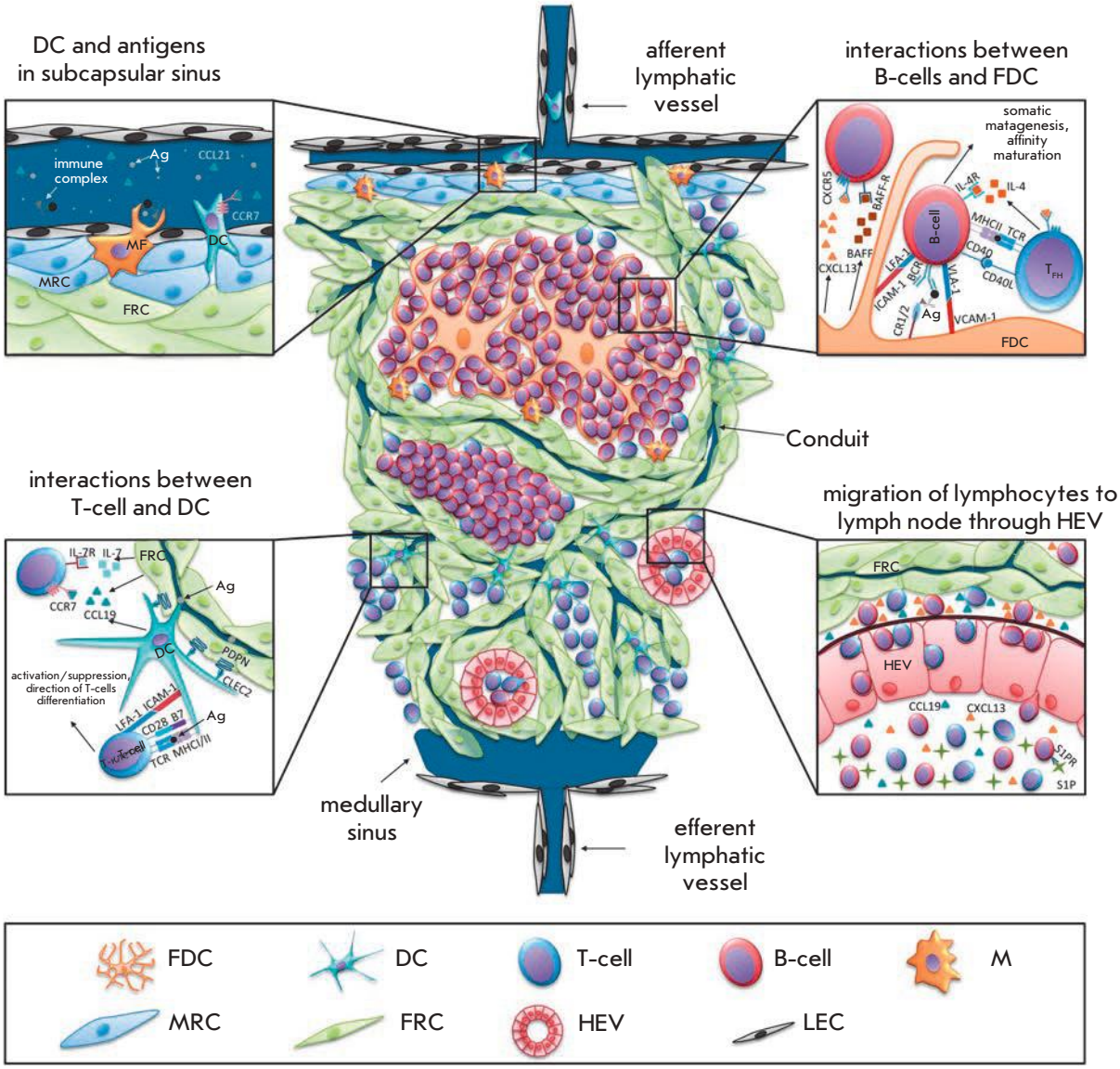


Fig. 1. Schematic representation of a lymph node structure. The key events are shown in detail. Lymph from afferent lymphatic vessels enters the organ through the conduit system. It is then collected in the medullary sinus from which efferent lymphatic vessels originate. Soluble antigens, immune complexes, and antigen-presenting DCs enter LN with the afferent lymph. Other hematopoetic cells enter LN with blood vessels through HEV in response to attracting chemokines (CCL19, CXCL13 and others). All these cells then become distributed between the T- and B-zones of the organ. Egress of lymphocytes from LN is controlled by S1P that is produced by endothelial cells outside the organ. Stromal cells play an important role in regulating all these processes. They produce all necessary factors, cytokines, chemokines, adhesion molecules, and form the appropriate organ structure to support the functions of immune cells

typical lymph node and the major steps of the adaptive immune response within it are presented in *Fig. 1*.

Anatomically, lymph nodes are bean-shaped encapsulated organs connected to the circulatory and lymphatic systems by a network of vessels. Two major groups of lymph nodes are identified based on their location in the body: mesenteric ones that are involved in the immune response and development of antigen tolerance in the intestines, and peripheral ones that collect the lymph from various regions of the body, primarily from barrier tissues. This distinction is based not only on their anatomical localization, but also on their functional differences, as these two groups of organs have different origins and functions [32–35]. Cervical lymph

nodes hold a special place among peripheral lymph nodes due to the nature of their development during embryogenesis and their involvement in mucosal immunity [36, 37]. Despite the differences in their origin and functions, the anatomic structure of all lymph nodes is rather similar. They have two main sections: the cortex, forming the main parenchyma of the organ, and the medulla, which communicates with the efferent lymphatic vessels carrying the lymph from the organ [38]. The area of the cortex bordering the medulla is called paracortex. On the outside, a lymph node is enclosed in a capsule through which the organ communicates with the afferent lymphatic vessels. Connective septa (trabecula) originates from the capsule and goes inside the organ, up to the medullary sinus that forms the lymph node gate [39]. The area between the capsule and the cortex is called the subcapsular space.

The blood vessels are connected to the organ through the gate; then they go into the paracortex, which is also called the T-zone, where a network of capillaries is formed. Lymphoid follicles, also called B-zones, are located in the cortex of the lymph node [38]. The name of the zones corresponds to the location and function of these two major groups of lymphocytes in a lymph node, although it does not reflect many details of cell migration and interactions, which have only been discovered in recent years (thanks to the development of techniques that allow for the intravital imaging of individual cells in tissues and organs [40]). B-lymphocytes primarily function in the B-zone; whereas T-cells are generally located in the paracortex, except for follicular helper lymphocytes, which play an important role in the functioning of B-lymphocytes [41]. The presence of separate B- and T-zones in lymph nodes is possible due to the development of special microenvironments within them, which produce both lymphocyte survival factors and "homeostatic" chemokines (for example, BAFF and CXCL13 cytokines are the key factors for B-zones; and IL-7, CCL21, CCL19 are the key factors for T-zones) [25, 42–44]. These molecules are synthesized mostly by lymph nodes stromal cells, as well as by other cell types, including endothelial and dendritic cells [42]. B-zones contain follicular dendritic cells that are involved in the maturation of B-lymphocytes, which are of mesenchymal origin [45], whereas T-zones have dendritic cells of hematopoietic origin, which are involved in antigen presentation to T-lymphocytes [46]. Dendritic cells of hematopoietic origin mostly arrive with the afferent lymph from different areas of the body, mainly from the barrier tissues where they have encountered antigens, have been activated, and have begun to express the CCR7 chemokine receptor that is responsible for their migration into lymph nodes T-zones. There are also resident lymph node dendritic cells, which are always present in an organ [47]. Their role is to present antigens absorbed directly from the lymph flowing into the lymph node through a special system of channels, called conduits. These channels are formed by an extensive network of polymers, including collagen I, II, IV, laminin, fibronectin, ER-TR7 *et al.* [48].

lymphocytes are constantly re-circulated in the body, periodically being recruited into different lymph nodes under the influence of chemokines. The appearance of these cells in the lymph node is very important for homeostasis of the immune system, as lymph nodes stromal cells are the main source of survival factors for mature lymphocytes [42]. The time which a lymphocyte spends in a lymphoid organ is defined by the balance of chemotactic signals. Once a lymphocyte enters the lymph node paracortex via special high endothelial venule cells under the influence of the "homeostatic" chemokine concentration gradient, the expression of the sphingosine-1-phosphate (S1P) receptor in the lymphocyte gradually increases. The concentration of this factor in the blood and lymph is very high, but its production in lymph nodes is almost absent [49]. Under the influence of the gradient of S1P concentration, lymphocytes arrive in the medulla and subsequently egress through the efferent lymphatic vessels into lymph circulation. The interaction of the receptor with its ligand S1P results in the internalization of the complex and disruption of the chemotactic signal, allowing the cells to regain their ability to penetrate lymph nodes under the influence of the gradient of chemokine concentration in the blood [50]. This system enables efficient re-circulation of lymphocytes in the body, which is necessary for the selection of lymphocytes with the optimal specificity of T- and B-cell receptors (TCR and BCR) for the antigens at the time present in the body [51].

In addition to recruiting and maintaining the homeostasis of immune cells, lymph nodes also enable all the interactions necessary for an effective immune response, which is mediated not only by the properties of antigen-presenting and effector cells, but also by the spacial architecture of a lymph node [26]. For example, the cortex is permeated by a system of conduits, which has optimally arranged antigen-presenting cells and through which the lymphocytes move. This spatial arrangement provides the best chance for these two types of cells to meet, which facilitates the search for receptors specific for a particular antigen presented on dendritic or other antigen-presenting cells, among the vast repertoire of T-cell receptors [8, 48, 51].

## LYMPH NODES STROMAL CELLS

The contribution of individual types of stromal cells to the maintenance and functioning of the lymph nodes,

their interactions, and origins remain poorly understood. To date, the most studied mesenchymal stromal cells of the secondary lymphoid organs are fibroblast reticular cells (FRCs) and follicular dendritic cells (FDCs) [33, 40, 43, 50, *Fig. 1*]. The former are primarily involved in T-lymphocytes functioning, whereas FDCs are necessary for full functionality of B-zones [25, 42]. FRCs form and maintain a system of conduits required for the migration and interaction of immune cells and delivery of antigens from the lymph [48, 52]. Three main types of endothelial cells are essential for the functioning of a lymph node: lymphatic endothelial cells (LEC), blood endothelial cells (BEC), and their variant, high endothelial venules cells (HEVC) [33, 42]. The role of these cells is to maintain constant contact between the node and the lymphatic and circulatory systems, or, more precisely, to ensure the exchange of immune cells and antigens. LECs ensure the recruitment and penetration of migratory dendritic cells into a lymph node, as well as the transfer of antigens from the lymph to the system of conduits inside lymph nodes [53, 54]. Conventional BECs line the blood vessels inside the node, whereas HEVC facilitate lymphocyte migration from the blood into the lymph node paracortex whence they are distributed to the respective zones of the node [42]. Recently, another type of stromal cells has been discovered which is located in the subcapsular zone of the lymph nodes and are present in other secondary lymphoid organs, but they are absent from tertiary ones; they are called marginal zone reticular cells (MRCs) [55, 56]. It has been shown that MRCs are the immediate precursors of FDCs, including being involved in the formation of germinal centers in follicles [57]. It has also been suggested that they play a role in maintaining the FDCs pool, but this requires further evidence.

The main obstacle in this field of research is the lack of consensus in the proper definition of different stromal cell types; despite fairly comprehensive characterization of the stromal cells functions, their exact phenotype is still a matter of debate and different authors adhere to different points of view [33, 42, 45, 58]. This can partly be attributed to the fact that only some stromal cells have universal surface markers. Many surface molecules are non-specific markers present in many cell populations. For example, the adhesion molecules ICAM-1 and VCAM-1 are considered to be the major markers for most of the mature lymph nodes stromal cells and their progenitors; these molecules enable both intercellular contacts in the stroma and interaction with incoming immune cells that express appropriate integrins on their surface [32, 59]. A glycoprotein podoplanin (gp38) is an important marker for some types of lymph node stromal cells, primarily LECs and FRCs. This molecule plays an important role in maintaining a normal state of vascular endothelial cells and a lymph node capsule, regulates the supply of blood and lymph to the node, migration of dendritic cells, and adaptive FRC reaction in case of a strong inflammation [54, 60]. All endothelial cells express CD31 as the primary endothelial marker. Specific surface markers are unknown for most lymph nodes stromal cells, and they are classified either by a combination of several "pan-markers" or based on the expression of specific genes and production of respective factors; however, this classification has not been fully accepted yet. For example, until recently the expression of CXCL13 chemokine in a mature lymph node had been attributed solely to FDCs, putative key players in the B-cell response. However, there is now evidence that marginal zone reticular cells (MRCs) and even FRCs can also synthesize CXCL13, and disruption of its production by these cells has a significant impact on the function of B-lymphocytes and the immune response [42, 44]. Nevertheless, a portion of stromal cells can be identified by the expression of a combination of several surface markers. For example, FDCs express CD35, CD21 (complement receptors), FcγRIIB, which detect immune complexes for subsequent presentation to B-lymphocytes in the germinal centers, and do not express typical hematopoietic surface markers (e.g., CD45) [45]. MRCs and, possibly, FDCs express MAdCAM-1 adhesion molecules [55]. FRCs are often identified on the basis of production of extracellular matrix components, which are necessary for conduits assembly, e.g. ER-TR7 [58]; however, these markers can only be used in immunohistochemical staining of lymph nodes sections, but not in cytometry when the cells are not bound to the matrix components. LECs typically express the Lyve-1 marker, and in mature lymph node HEVCs, in contrast to BECs, specifically express PNAd adressin and MAdCAM-1 adhesion molecules [42].

To summarize, the stromal compartment of lymph nodes and other secondary lymphoid organs is under active investigation and many aspects still have to be elucidated to fully understand the functions of all participating cells. This insight is important for the bioengineering of artificial lymphoid organs, the purpose of which is to create a functional organ from a minimum number of well-characterized components. The data on the functioning of lymphoid organs suggest that in order to be effective an artificial lymph node must have the appropriate infrastructure, which is mainly represented by a properly organized stromal compartment. The presence of all the necessary components of the stroma will define the effectiveness of a particular immune response that occurs in the system, and it will allow one to track the development of an artificial

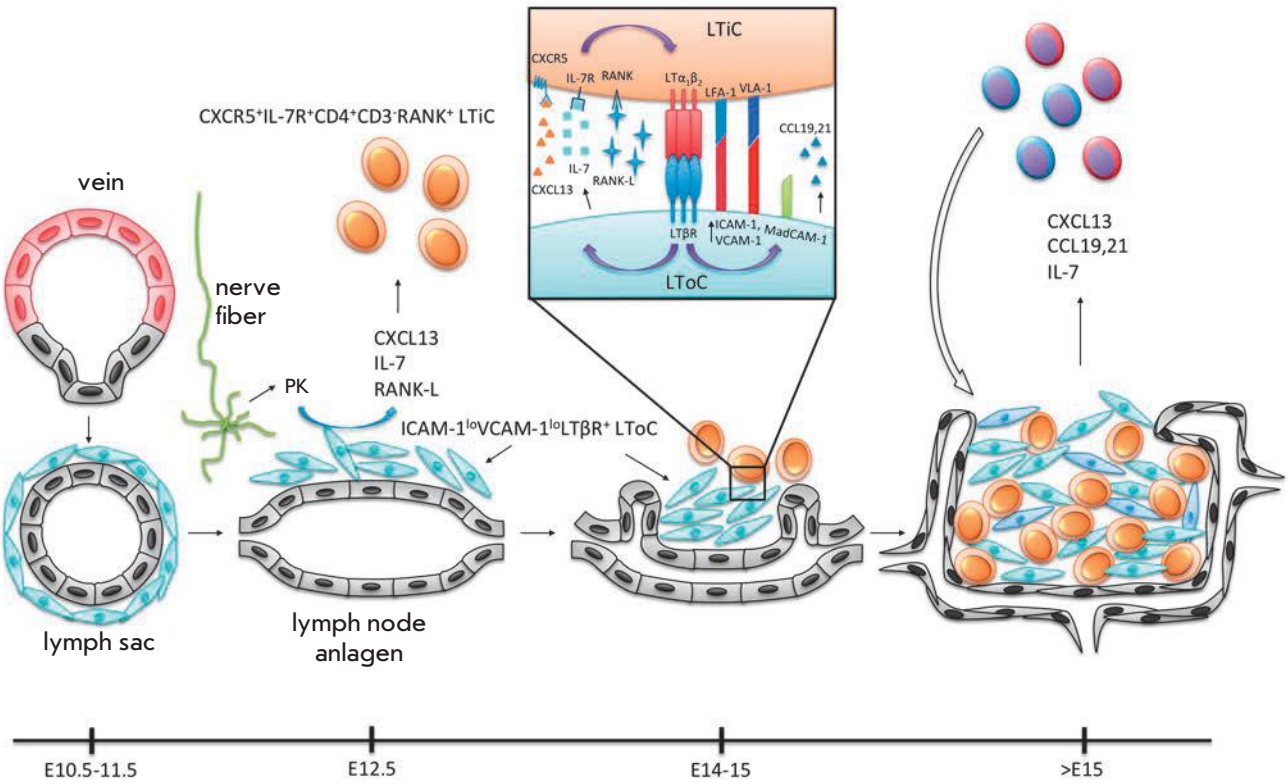


Fig. 2. Schematic representation of mouse lymph node development. It begins with lymph sacs formation from venule endotelial cells. These sacs then produce the entire lymphatic system and some of them produce lymph nodes. Initiation of lymph node development seems to be dependent on retinoic acid (RA) production by proximal nerve fibers. RA probably signals through its receptor on mesenchymal cells around lymph sacs and stimulates them to produce CXCL13 chemokine and other cytokines. CXCL13 promotes migration of LTiC to the lymph sac, leading to the formation of lymph node anlagen. LTiC express on their surface LTαβ that interacts with LTβR on mesenchymal cells, converting them to LToC. This process is key in the development of most of the secondary lymphoid organs, including the lymph nodes. Activation of LTβR leads to further differentiation of LToC from which all mature lymph node stromal cell subtypes seem to originate. LToC produce many LN-specific chemokines and cytokines. They also start to express adhesion molecules on their surface, such as MAdCAM-1 and PNAd, which are required for the migration of lymphocytes to the lymph nodes. Lymphocytes act on stromal cells in many ways, engaging different members of the TNF superfamily, like TNF itself , LT, LIGHT and others. This promotes further maturation of the lymph node stromal cells and the formation of T- and B-zones.

organ based on the analysis of the stromal cells' composition.

## EMBRYONIC DEVELOPMENT OF LYMPH NODES

Successful bioengineering of artificial lymph nodes requires good understanding of the processes that define the development of lymphoid organs during the embryogenesis. Such knowledge may allow one to differentiate all necessary types of cells from their progenitor cells extracted from fetal tissue or make it possible to develop the whole organ from the progenitor cells. Lymphoid organ development is shown in *Fig. 2*, using a lymph node as an example. It has been established that during the embryogenesis a lymph node anlagen is created in certain areas as a result of venules endothelial cells differentiation into lymphatic endothelium [61] and the formation of an endothelial lymph sac, which later participates in the development of the capsule and network of conduits in the lymph node and connects the organ to the lymphatic and circulatory systems [32]. Further development involves poorly differentiated mesenchymal cells around the vessels (pericytes), which are progenitors of FDCs, and, apparently, of all other stromal cells except for endothelial ones [45]. This has recently been demonstrated for the development of the spleen: FDCs, FRCs, and other stromal cells were derived from progenitor cells which expressed the transcription factors Nkx2-5 and Islet-1,

important for the embryogenesis of spleen and pancreas [62]; however, for lymph nodes the origin of all types of stromal cells from a single population of progenitor cells requires more rigorous evidence. Lymph sacs originate the lymphatic system of the body, as well as lymph nodes. Lymph node location is defined by local secretion of retinoic acid (RA) by nerve fibers endings [63]. Under the influence of RA, mesenchymal progenitors begin secreting CXCL13 chemokine, which attracts lymphoid-tissue-inducer cells (LTiC), with the adhesion molecules ICAM-1 and VCAM-1 on their surface. From that moment onward, the mesenchymal progenitor cells are called lymphoid-tissue-organizer cells (LToC). LTiCs migrate to the lymph node anlagen, primarily under the influence of the CXCL13 chemokine concentration gradient and interact with LToC [63]. It has been established that signal transmission through LTβR located on the LToC surface is crucial at this stage [64]. The LTα1β2 heterotrimer is the main LTβR ligand involved in the lymph node embryogenesis, and it appears on the LTiCs surface after their interaction with a soluble factor, TRANCE (RANK-L), the exact source of which is unknown, but it is assumed that LTiCs can themselves be the source [59, 65, 66]. Mice deficient in LTβR or LTα have no secondary lymphoid organs (except for the nasal-associated lymphoid tissue [67]), and mice with genetic LTβ inactivation develop only cervical and mesenteric lymph nodes, which suggests that this signaling pathway is critically important for embryonic development [34, 59]. This signal pathway triggers further LToCs differentiation, which leads to increased expression of adhesion molecules and appearance of MAdCAM-1 and PNAd on the cell surface, as well as to increased expression of chemokines that attract new hematopoietic cells to the location of the future lymph node [32, 59, 64]. Signaling through the TNFR1 receptor is another important molecular cascade for the development of lymphoid organs. It has been demonstrated that genetic inactivation of either TNF or TNFR1 in mice leads to disruption of FDCs development and, consequently, to the absence of germinal centers in lymphoid organs [68]. It should be noted that members of the TNF superfamily play an important role in the development and maintenance of not only lymph nodes, but also all other lymphoid organs [34, 59, 65, 68–71]. Therefore, there is a synergy of different signaling pathways, which eventually results in a fully developed and functional immune system.

The next step of development, apparently, involves the accumulation of hematopoietic cells in the forming lymph node, which results in its growth, further differentiation of stromal cells, development of high endothelial venules, primordial follicles, and other compartments characteristic of lymph nodes [32, 59, 72]. At the initial stages, the development of structural compartments in lymph nodes does not involve T- or B-lymphocytes; however, at the later stages they actively penetrate into the organs and participate in the final maturation of lymphoid follicles and further maintenance of the stroma infrastructure via LTβR and TNFR signaling [26, 36]. In addition to LTα1β2, another LTβR ligand, LIGHT, plays a crucial role in this process [65]. Thus, the development and functioning of a mature lymph node (as well as other secondary lymphoid organs) depends strongly on the interaction between mesenchymal and hematopoietic cells, which should be taken into account in the bioengineering of these organs. Both cell components (as mature cells or, possibly, progenitor cells) must be properly arranged in the lymph node development site for its effective maturation and subsequent functioning.

## BIOMATERIALS FOR ARTIFICIAL ORGANS ENGINEERING

In addition to the minimum set of cell types required for the functioning of an artificial lymph node, it is important to create a framework that will serve as a structural scaffold for a proper spatial arrangement of the cells, a prerequisite for their effective interaction. During ontogenesis, the stromal cells create the necessary structure themselves and it consists primarily of polymeric, preferably collagen, fibers [58, 59]. In the case of bioengineering of an artificial lymph node, it is necessary to initially create a three-dimensional scaffold on which the cells will create a three-dimensional cell culture, and, subsequently, a fully fledged node. This is extremely important at the early stages, when the cells have not yet created their own polymeric scaffold necessary for further differentiation, survival, and functionality.

Artificial scaffolds based on biomaterials appear to be the most promising ones for the bioengineering of lymphoid organs. Such materials consist primarily of modified polymers of natural origin, both polysaccharides and proteins: fibroin (main component of the silk cocoon of silkworm *Bombyx mori*) (*Fig. 3*) [35, 36], spidroin (primary component of a spider's web) [73–75], alginate (mixture of polysaccharides from algae cell wall) [76], collagen [77], etc. Synthetic polymers are also used, e.g., PLG (polylactate-co-glycolate), PLA (polylactate), PGA (polyglycolate), etc [78]. Various modifications of the substrate (e.g. by hydroxyapatite or collagen (gelatin)) are used to improve certain polymer properties such as elasticity, immunogenicity, adhesiveness, and resistance to outside factors [79].

The absence of antigenic, carcinogenic, toxic, and other properties limiting their use in medicine is a mandatory requirement for bioengineering materials. Such effects are typically associated with the presence

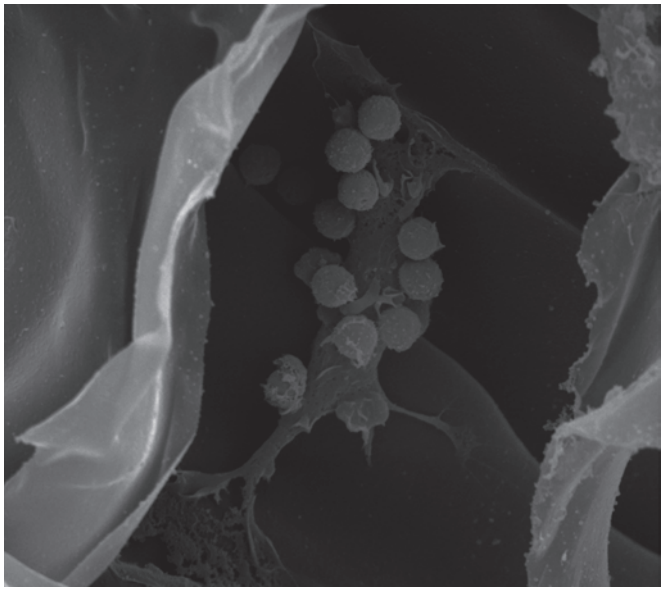

Fig. 3. Polymeric fibroin scaffolds for artificial lymphoid organ bioengineering. A SEM image of a mixed culture of bone marrow-derived dendritic cells and splenocytes is shown. A dendritic cell (in the middle) interacts with a group of lymphocytes (around the DC) on the surface of the scaffold seen on the periphery

of reactive groups formed by monomers or initiators of a polymerization reaction in the polymer substrate. Therefore, for future use it is necessary to carefully monitor the composition of the material and its purification and modifications [80]. Adverse effects *in vivo* are the main reason why many biomaterials have not yet found wide clinical application. There have been attempts to improve the properties of bioengineered materials; several types of structures which have been shown to be biocompatible in animal experiments have already been selected [11, 75]. However, it is impossible to avoid the immune response entirely, since most materials are allogenic. The main objective in the development of these materials is to avoid a systemic response and acute inflammation.

All these biomaterials usually come in the form of three-dimensional scaffolds with a cellular structure which is as close as possible to the fibrous structure of the extracellular matrix in animal tissues. By analogy, such bioengineered structures are also referred to as matrices, emphasizing their use as scaffolds; three-dimensional backbones for the cultivation of plated cell populations. This approach has been applied primarily in the preparation of 3D cell cultures, since it is known that many features of cell interaction in a functioning organ cannot be reproduced *in vitro* on plate surfaces [81]. The matrix may be a gel-like polymer network, for example, a collagen matrix, or it can have a more solid structure which retains its shape during mechanical manipulations, such as implantation into an animal model. The latter is the most important for the potential use of the material in medicine, direct studies of cell behavior in living models, and for the bioengineering of artificial organs. A variety of approaches are used to create the appropriate shape and texture of the matrix [78]. Polymerization of a monomer which will form the matrix has to create the appropriate three-dimensional porous structure; otherwise, the scaffold space will not be available for colonization by cells or saturation by any other substance.

In some studies, natural extracellular matrices from animal organisms, freed from inhabiting cells, are used to improve biocompatibility [82]. These materials do not induce an immune response upon implantation, since they are not allogenic, but they are usually more susceptible to enzyme degradation, which can be both advantageous and undesirable, depending on the task at hand.

However, scaffolding for an artificial organ is not the only implementation for such systems. Recently, the use of scaffolds for binding various kinds of soluble biological factors and their subsequent gradual diffusion from the matrix have been attracting increasing attention, since it ensures a gradual and extended release of biologically active substances over time. In the context of the bioengineering of artificial lymph nodes, this approach is promising, because it allows one to create an artificial gradient of chemokines and growth factors which may be necessary for the initiation of the maintenance program for organ development. As discussed above, during embryogenesis cells are recruited to the lymph node site and subsequently differentiated via the expression of, primarily, CXCL13 chemokine by stromal cell progenitors. In constructing artificial organs, special polymer particles can become sources of this chemokine, and they are being developed by several research groups at the moment. For example, a group of authors [83] has reported on the development of alginate microspheres which can be saturated by a chemokine and will be subsequently gradually released into the medium. Such microspheres have a size of 5–20 μm, which allows for various manipulations; e.g., they can be used as a source of substances that attract cells for organs and tissues modeling *in vitro*. Another approach to the development of materials that ensure a controlled release of factors is to use biodegradable polymers covalently crosslinked by an active substance. The action of the enzymes or spontaneous hydrolysis will also gradually release the factors linked to the matrix, allowing them to perform their biological function [84].

## ADVANCES IN BIOENGINEERING OF ARTIFICIAL LYMPHOID ORGANS

As we have noted, bioengineering of artificial organs is important, first and foremost, due to its potential clinical application. The possible use of these organs for reprogramming the immune response in a number of diseases is very appealing. For each specific task, the final system does not even have to have all the characteristics of normal organs, but rather only those that are relevant to the necessary function. If artificial lymph nodes are able to ensure recruitment, survival, interaction, activation and functioning of immune cells, it will be possible to direct the immune response towards the specific, most effective, direction. Artificial lymph nodes can be populated *in vitro* by activated DCs that are loaded with specific antigens. After implantation of such systems, dendritic cells will interact with incoming lymphocytes, regulating their differentiation and functional activity. The advantage of such systems over vaccination with antigens or administration of a suspension of activated DCs lies in the fact that they will represent the vast majority of antigen-presenting cells in an artificial lymph node, and therefore there is a high probability that every incoming lymphocyte, specific to the antigen, will be influenced by certain cytokines and costimulatory molecules at the DCs surface. The implantation of such systems directly into the center of tumor growth or autoimmune reactions is expected to allow one to reprogram the specific lymphocytes and, therefore, will afford therapeutic effect. Although the implementation of this idea still requires a lengthy process of development of a fully functional artificial lymph node, it is already possible to create truncated systems that may have some clinical significance. The major published advances in this field are summarized in the Table.

For example, the feasibility of using a matrix for vaccination against melanoma has been demonstrated in mice [11, 85]. For this purpose, a PLG-matrix was saturated with a granulocyte-macrophage colony-stimulating factor (GM-CSF), a synthetic oligonucleotide containing unmethylated CpG repeats, and with partially lysed melanoma cells. The study measured the therapeutic effect on the melanoma. Previously, it has been established that GM-CSF is essential in recruiting and activating murine dendritic cells. CpG was added to stimulate DCs differentiation towards a direction leading to the activation of type I T-helper cells, which are considered to be the most appropriate response to a tumor [86]. It has been shown that implantation of such "structural vaccines" as a three-dimensional matrix leads to the recruitment of murine skin DCs, their activation, and subsequent migration into the draining lymph node. In the node, they are involved in the maturation of specific T-helper type I cells, which ultimately leads to an increased anti-tumor response in a mouse, which manifests itself as reduced mortality in transplanted tumor models. In this paper, the matrix, which was saturated with factors of differentiation, recruitment of dendritic cells, and tumor antigens, partially functioned as a tertiary lymphoid organ. This is the simplest possible model that, nevertheless, allowed functional interaction between the implanted structure and the mouse lymphatic system that resulted in a specifically directed immune response. It has been shown that tumors are rejected due to the induction of a strong cytotoxic response of $CD8^+$ lymphocytes. Importantly, this treatment regimen has already been adapted to humans and is currently in the first stage of clinical trials (https://clinicaltrials.gov/show/NCT01753089).

In another model, which was closer to a real immune organ [10], the authors tried to create a prototype of a human lymph node *in vitro*. To that end, they developed a bioreactor that imitated the organ's position relative to the vascular system of the body. It consisted of a first chamber that contained the matrix with dendritic cells and represented a lymph node, and a second chamber that contained a suspension of lymphocytes to model blood flow. The chambers communicated with each other through a porous membrane that enabled free circulation of both the soluble factors and the cells. It has been shown that, subject to regular change of the medium, such a culture is quite stable and can survive for at least 2 weeks with preserved activity of the cells. After 2 weeks of cultivation, the matrix was found to contain T- and B-lymphocytes populations which came from the adjacent chamber of the bioreactor, in addition to the dendritic cells. Both the lymphocytes and dendritic cells formed clusters within the matrix, which could be an indication of their potential functional activity. This model was proposed as a possible test system for studying the effects of certain drugs, as well as for studying cellular interactions *in vitro*. The model is a rather faithful representation of some of the processes in a lymph node; namely, the migration of lymphocytes and their interaction with dendritic cells.

However, despite the advances in the bioengineering of truncated models of lymph nodes, it has become clear that a fully fledged organ cannot exist and function without its special constituent stroma. This resulted from both extensive studies of stromal cells biology and attempts to use them to model lymphoid tissue. These two lines of research were combined into one in [87]. A sufficiently strong local inflammation is known to results in increased size and cellularity of the draining lymph nodes. This adaptive reaction is supported by an elevated rate of FRCs divisions in the lymph node

Published models of artificial lymphoid organs

| Type of object | Polymeric scaffold | Cellular composition | Functional activity | Reference |
|---|---|---|---|---|
| Bioengineered vaccine against melanoma | PLG-matrix saturated with GM-CSF, CpG and tumor cells lysate | Myeloid dendritic cells | Recruiting of dendritic cells, resulting in their maturation, and subsequent migration into the draining lymph node, activation of anti-tumor immune response | [11, 49, 51] |
| *In vitro* model of a human lymph node, a bioreactor | Polysulfone bioreactor with polypropylene fibers as vessels and agarose matrix on which the cells were grown | Myeloid dendritic cells, T- and B-lymphocytes | After the system is initiated: secretion of cytokines and specific antibodies, formation of immune memory in response to an antigenic stimulus | [10, 52] |
| FRCs compartment of a murine lymph node | Polyurethane matrix modified with collagen | Fibroblast reticular cells (FRCs) | Adaptive FRCs response to changes in the fluid flow rate through the matrix, including increased production of the CCL21 and CCL19 chemokines and elevated rate of cell division | [50] |
| Artificial murine lymph node | Collagen matrix | Thymic epithelial cell line which produced LTα, and myeloid dendritic cells | After implantation of the matrix with the cells under the kidney capsule: migration of lymphocytes, formation of T and B-zones, production of antigen-specific antibodies. After the transfer of the artificial lymph node into immunodeficient mice production of antibodies was restored | [53, 54] |
| Artificial murine thymus | No polymeric scaffold | Aggregates of fetal thymocytes, mesenchymal cells and *Foxn1*$^+$ fibroblasts | After implantation into athymic mice: the aggregates ensured full thymic function, generated naive T-lymphocytes of all major subtypes | [55] |

proximal to the inflammation site and increase in the level of expression of the CCL21 and CCL19 chemokines, which attracts a lot of lymphocytes and dendritic cells to this lymph node. Since one of the first changes in local inflammation is a significant increase in the lymph flow rate through the draining lymph node [88], it has been suggested that FRCs may react to changes in the lymph flow rate in the system of conduits, which initiates a number of functional changes, such as an increase in chemokines production by these cells. To test this hypothesis, the authors constructed an *in vitro* lymph node model consisting of a matrix populated with a stable line of fibroblast reticular cells, with controlled flow of the lymphatic fluid through the model. It was shown that the secretion of CCL21 and CCL19 by the cells was higher under fluid flow conditions than in the static system. Moreover, the lymph flow affected not only the expression of the chemokines, but also the rate of cell division, as well as their spatial organization in the matrix.

Remarkably, in the case of fluid flow, some cells formed specific channel-like structures oriented along the direction of the flow. This organization was not observed under the static conditions. In addition, the lymph flow resulted in a reorganization of the matrix by the cells located within it and creation of spatially oriented structures. Presumably, in addition to being involved in the lymph node response to inflammation, the lymph flow may also play a role in the organization of the organ structure, adjusting the position and function of the stromal cells.

This is a very interesting observation, made for a simple lymph node prototype consisting of just one type of stromal cells, which nonetheless clearly demonstrated a complex systemic interaction between all components that can be explored entirely in a model of an artificial lymphoid organ.

The biggest success in the bioengineering of artificial lymph nodes has been achiev by Japanese scientists, who have developed a system based on a collagen matrix [89, 90]. They populated these matrices with a TEL-2 thymic epithelial cell line [91] previously transfected with a vector containing a lymphotoxin α (LTα) gene, as well as DCs derived from a bone marrow culture. They implanted these structures under the kidney capsule of a mouse and observed the migration of recipient lymphocytes into the matrix and a spatial cluster-like organization of T- and B-cells in the matrix, similar to their organization in the lymph node. They have also demonstrated that prior population of the matrix with dendritic cells is necessary for efficient migration of recipient cells into it. Furthermore, cells

expressing endothelial markers were detected in the matrix, which indicated blood vessels growth. After some time in a mouse model, the matrix was recovered and transferred into mice with severe, combined immunodeficiency (SCID). After transplantation, the immunodeficient mice displayed a migration of cells from the matrix into the spleen and secretion of IgG antibodies. If the populated matrices were initially implanted into mice previously immunized with a protein antigen (modified ovalbumin NP-OVA was used in the experiment), their subsequent transfer to immunodeficient mice resulted in the latter producing antibodies specific to that antigen. The wealth of data suggests that it is reasonable to call the system 'an artificial lymph node'. It should be noted that this work used collagen matrices which quickly degraded and shrunk in size, which could have affected their efficiency in the long-term experiments. Bioengineered scaffolds should use more inert materials to ensure the long-term presence and functioning of an artificial lymphoid organ in a recipient's body.

Development of artificial thymus is another equally important task. It may play an important role in medicine, since thymus evolution with age results in a decrease in the number of new T-lymphocytes in the human body and subsequent deterioration of the immune response to new infections. Development of artificial thymus could help solve this problem. Recently, a promising study [92] was published which describes a system for producing thymic epithelial cells (TECs), which are required for thymus functioning, using *in vitro* reprogramming of mouse embryonic fibroblasts (MEF) under the influence of Foxn1, a transcription factor important for TECs. It was shown that over the course of their differentiation the transformed cells acquired a normal TECs phenotype: they expressed surface markers (EpCAM) and genes for factors that are important for their functional activity (Dll4, CCL25, Kitl et al.). In addition, despite the involvement of the Foxn1 factor in the development of skin epithelial cells, the transformed MEFs do not express genes specific to them, which indicates their orientation towards thymic, rather than skin, epithelium. The resulting cells were then characterized by their ability to ensure *in vitro* maturation of T-cells progenitors, imitating the process that occurs in normal thymus. It has been shown that co-cultivation of a transformed MEF and T-cells progenitors leads to the formation of a transient population of thymocytes ($CD4^+CD8^+$), as well as terminally differentiated $CD4^+$ and $CD8^+$ naive T-cells in quantities comparable to those obtained when TECs isolated from embryonic mouse thymus are used as the stroma. Untransformed MEF did not enable thymocytes maturation. It is important that the resulting cells expressed MHC class II molecules at a level comparable with that of normal TECs. These MHC class II molecules were only expressed after T-lymphocytes progenitors were added to the culture, emphasizing the importance of interaction between stromal and hematopoietic cells for the functioning of the lymphoid tissues. It is well known that MHC class II molecules on the surface of TECs are important for the selection of thymocytes in the thymus by their ability to recognize major histocompatibility complex molecules and only insignificantly bound autoantigens in order to generate autotolerant functional cells. Notably, the latter function depends on the TECs *AIRE* gene that is expressed by *Foxn1*-transformed fibroblasts, as well. Finally, the resulting cells were used as a base for an artificial thymus model. For this purpose, tissue aggregates were produced from three cell types: T-lymphocyte progenitors, fetal thymus mesenchymal stroma as a source of survival factors, and transformed MEFs. Once these aggregates were produced, they were implanted under the mouse kidney capsule and thymic tissue formation was observed after 3–4 weeks. An examination of this tissue's composition revealed that aggregates obtained using the transformed fibroblasts reproduced normal thymus tissue in terms of its structure and function. These organelles were comparable to the artificial tissue obtained by implantation of embryonic TECs, whereas cell aggregates with non-transformed MEFs were unable to produce thymus tissue. The resulting system can be confidently called a prototype of artificial thymus. Just like the normal thymus, it had two subtypes of TECs necessary for proper thymocytes selection and their spatial zoning. The expression profiles of TEC-specific genes and surface markers were comparable to the profiles in the normal embryonic thymus. The artificial thymus was able to support T-lymphocytes differentiation towards both TCRαβ $CD4^+/CD8^+$ and TCRγδ T-lymphocytes. Finally, the implantation of the systems to athymic (nude) mice resulted in detection of mature naive T-lymphocytes in their peripheral blood and spleen, which confirms the full functionality of the organ. This work is an important step on the way towards bioengineering of artificial thymus, including for clinical purposes [92]. However, the issue of the mesenchymal compartment remained unaddressed, since in this work it was formed by the fetal thymus tissue, which would be impossible if the artificial organ is produced for an adult organism. Overcoming this obstacle will open the way to the development of fully functional bioengineered active organs that can promote better understanding of the nature of the thymocyte selection process occurring in the thymus and can become an important tool in the treatment of human immunodeficiency.

It should be stressed that while the approaches relying on transformed cell lines are useful for research, they have no potential clinical use. Moreover, even in the laboratory such models are limited to a single line of animals from which the culture is derived. Two possible approaches to resolving this issue have been proposed: the use of cell-free systems or primary cell cultures. The first idea is based on the introduction of a pre-defined mixture of factors into the matrix, which will be used as the basis for an artificial organ, in order to attract and ensure the survival and differentiation of lymphoid and stromal progenitor cells imitating normal lymph node development. Additional biomaterials ensuring a gradual release of substances, such as alginate microspheres, can be used to create a concentration gradient of these factors. Candidate factors include the CCL19, CXCL13 chemokines, the BAFF, IL-7, VEGF, PDGF cytokines, and others. Regulation of the dynamics of individual release for each factor can ensure recruitment of progenitor cells from the bloodstream and their subsequent differentiation, without prior colonization of the matrix by any cells. Recently, a model was described in which the matrix included two cytokines, VEGF and PDGF [93]. It has been shown that tailored release dynamics for each factor can effectively stimulate angiogenesis at the site of the matrix implantation, which is necessary for the migration of cells and nutrients into it. Construction of artificial organs using this approach will, of course, require a combination of a higher number of factors.

If a cell-free system proves not enough for the bioengineering of clinically efficient artificial lymphoid organs, it will become necessary to develop a protocol for the use of cells. In this case, the most promising approach appears to be associated with the use of induced pluripotent stem cells (iPSC), which are expected to be the "next big thing" in the field of personalized medicine [94]. To date, there are several published works in which iPSCs were successfully used to create models of human organs: e.g. small intestine [95, 96]. In the context of artificial lymphoid organs, iPSCs can serve as a source of stromal compartment which ensures functional activity of the organ. This possibility has recently been discussed in a review of artificial thymus bioengineering [97]. In the future, this promising approach can be applied to other lymphoid organs.

## CONCLUSION

Even though several models of artificial lymphoid organs have been developed to date, a critical analysis has identified several problems that still need addressing. The use of transformed cells places obvious limitations on clinical application. Organ bioengineering using primary cell cultures has also been of limited use, mostly due to the fact that there are no adequate experimental protocols for many types of cells, especially stromal cells, describing their isolation, cultivation, and maintenance of their differentiated state. The most promising approach for clinical use is to obtain all or most of the cell types either from their progenitors or by transdifferentiation of mature cells; e.g. via iPSCs. Some cell types are readily available in primary cultures, including those of human cells, and this has already become the basis of several therapy regimens, such as adoptive transfer of dendritic cells or lymphocytes. It is only natural to suggest a combination of the two approaches: introduce some cells directly into the artificial lymph node scaffold as primary cultures, and compensate for the lack of others by adding factors, anticipating that such a combination would be enough to initiate the process of organ formation, and that all other cells will develop there later from the recruited progenitor cells. Today, many studies are conducted in this field.

In summary, the development of artificial lymphoid organs is an important task in modern immunology and biomedicine both from the theoretical and practical points of view. Success in this area is associated not only with advances in bioengineering, but also with recent progress in understanding the processes of lymphoid organs formation and functioning. This subject is at the crossroads of several scientific fields: bioengineering, immunology, systems biology, and regenerative medicine and, therefore, requires a comprehensive approach to research which would combine different ideas and take into account all or most of the factors responsible for the functioning of such complex systems as lymphoid organs.

*The authors would like to thank AA Kruglov for valuable discussions and helpful comments. Electron microscopic images of the matrices were obtained by A.Yu. Arkhipova with the support of the SKC of the Moscow State University and with the financial support of the Ministry of Education and Science of the Russian Federation.*

*The studies of the interactions of immune cells and cytokines as regulators of this process were supported by the program of the Presidium of the Russian Academy of Sciences "Molecular and Cell Biology"; the studies of development and research of multidimensional cell systems were supported by the RFBR (grant № 14-04-01799).*

REFERENCES


1. Hussain A., Takahashi K., Sonobe J., Tabata Y., Bessho K. // J. Maxillofac. Oral Surg. 2014. V. 13. № 1. P. 29–35.
2. Rose F.R.A.J., Oreffo R.O.C. // Biochem. Biophys. Res. Commun. 2002. V. 292. № 1. P. 1–7.
3. Rezwan K., Chen Q.Z., Blaker J.J., Boccaccini A.R. // Biomaterials. 2006. V. 27. № 18. P. 3413–3431.
4. Lutolf M.P., Hubbell J.A. // Nat. Biotechnol. 2005. V. 23. № 1. P. 47–55.
5. Nayak S., Dey S., Kundu S.C. // PLoS One. 2013. V. 8. № 9. P. 1–17.
6. Sun B.K., Siprashvili Z., Khavari P.A. // Science. 2014. V. 346. № 6212. P. 941–945.
7. Scarrit M.E., Pashos N.C., Bunnell B.A. // Front. Bioeng. Biotechnol. 2015. V. 3. P. 43.
8. Tan J.K.H., Watanabe T. // Adv. Immunol. 2010. V. 105. P. 131–157.
9. Cupedo T., Stroock A.D., Coles M.C. // Front. Immunol. 2012. V. 3. P. 1–6.
10. Giese C., Demmler C.D., Ammer R., Hartmann S., Lubitz A., Miller L., Müller R., Marx U. // Artif. Organs. 2006. V. 30. № 10. P. 803–808.
11. Ali O.A., Huebsch N., Cao L., Dranoff G., Mooney D.J. // Nat. Mater. 2009. V. 8. № 2. P. 151–158.
12. Martino M.M., Brkic S., Bovo E., Burger M., Schaefer D.J., Wolff T., Gürke L., Briquez P.S., Larsson H.M., Gianni-Barrera R., et al. // Front. Bioeng. Biotechnol. 2015. V. 3. P. 45.
13. Facchetti F., Blanzuoli L., Ungari M., Alebardi O., Vermi W. // Springer Semin. Immunopathol. 1998. V. 19. № 4. P. 459–478.
14. Owen J.J., Jordan R.K., Raff M.C. // Eur. J. Immunol. 1975. V. 5. № 9. P. 653–655.
15. Dieu-Nosjean M.-C., Goc J., Giraldo N.A., Sautès-Fridman C., Fridman W.H. // Trends Immunol. 2014. V. 35. № 11. P. 571–580.
16. Rodewald H.-R. // Annu. Rev. Immunol. 2008. V. 26. P. 355–388.
17. van de Pavert S.A., Mebius R.E. // Nat. Rev. Immunol. 2010. V. 10. № 9. P. 664–674.
18. Clark B.R., Keating A. B: Annals of the New York Academy of Sciences. // 1995. V. 700. P. 70–78.
19. Anthony B.A., Link D.C. // Trends Immunol. 2014. V. 35. № 1. P. 32–37.
20. Tokoyoda K., Zehentmeier S., Chang H.D., Radbruch A. // Eur. J. Immunol. 2009. V. 39. № 8. P. 2095–2099.
21. Klein L., Kyewski B., Allen P.M., Hogquist K.A. // Nat. Rev. Immunol. 2014. V. 14. № 6. P. 377–391.
22. Koble C., Kyewski B. // J. Exp. Med. 2009. V. 206. № 7. P. 1505–1513.
23. Anderson G., Jenkinson E.J. // Nat. Rev. Immunol. 2001. V. 1. № 1. P. 31–40.
24. Manley N.R., Richie E.R., Blackburn C.C., Condie B.G., Sage J. // Front. Biosci. 2011. V. 17. P. 2461–2477.
25. Bajénoff M., Egen J.G., Koo L.Y., Laugier J.P., Brau F., Glaichenhaus N., Germain R.N. // Immunity. 2006. V. 25. № 6. P. 989–1001.
26. Malhotra D., Fletcher A.L., Turley S.J. // Immunol. Rev. 2013. V. 251. № 1. P. 160–176.
27. Junt T., Scandella E., Ludewig B. // Nat. Rev. Immunol. 2008. V. 8. № 10. P. 764–775.
28. Eberl G., Lochner M. // Mucosal Immunol. 2009. V. 2. № 6. P. 478–485.
29. Newberry R.D. // Curr. Opin. Gastroenterol. 2008. V. 24. № 2. P. 121–128.
30. Forchielli M.L., Walker A.W. // Br. J. Nutr. 2005. V. 93. Suppl 1. P. S41–S48.
31. Mowat A.M. // Nat. Rev. Immunol. 2003. V. 3. № 4. P. 331–341.
32. Randall T.D., Carragher D.M., Rangel-Moreno J. // Annu. Rev. Immunol. 2008. V. 26. P. 627–650.
33. Buettner M., Pabst R., Bode U. // Trends Immunol. 2010. V. 31. № 2. P. 80–86.
34. Alimzhanov M.B., Kuprash D.V, Kosco-Vilbois M.H., Luz A., Turetskaya R.L., Tarakhovsky A., Rajewsky K., Nedospasov S.A., Pfeffer K. // Proc. Natl. Acad. Sci. USA. 1997. V. 94. № 17. P. 9302–9307.
35. Cupedo T., Vondenhoff M.F.R., Heeregrave E.J., De Weerd A.E., Jansen W., Jackson D.G., Kraal G., Mebius R.E. // J. Immunol. 2004. V. 173. № 5. P. 2968–2975.
36. Rennert P.D., Browning J.L., Hochman P.S. // Int. Immunol. 1997. V. 9. № 11. P. 1627–1639.
37. Luther S.A., Ansel M.K., Cyster J.G. // J. Exp. Med. 2003. V. 197. № 9. P. 1191–1198.
38. Crivellato E., Vacca A., Ribatti D. // Trends Immunol. 2004. V. 25. № 4. P. 210–217.
39. Willard-Mack C.L. // Toxicol. Pathol. 2006. V. 34. № 5. P. 409–424.
40. von Andrian U.H., Mempel T.R. // Nat. Rev. Immunol. 2003. V. 3. № 11. P. 867–878.
41. Crotty S. // Immunity. 2014. V. 41. № 4. P. 529–542.
42. Chang J.E., Turley S.J. // Trends Immunol. 2014. V. 36. № 1. P. 30–39.
43. Allen C.D.C., Cyster J.G. // Semin. Immunol. 2008. V. 20. № 1. P. 14–25.
44. Cremasco V., Woodruff M.C., Onder L., Cupovic J., Nieves-Bonilla J.M., Schildberg F.A., Chang J.E., Cremasco F., Harvey C.J., Wucherpfennig K.W., et al. // Nat. Immunol. 2014. P. 1–11.
45. Aguzzi A., Kranich J., Krautler N.J. // Trends Immunol. 2014. V. 35. № 3. P. 105–113.
46. Banchereau J., Briere F., Christophe C., Davoust J., Lebecque S., Liu Y.-J., Pulendran B., Palucka K. // Annu. Rev. Immunol. 2000. № 18. P. 767–811.
47. Steinman R.M. // Annu. Rev. Immunol. 1991. V. 9. P. 271–296.
48. Sixt M., Kanazawa N., Selg M., Samson T., Roos G., Reinhardt D.P., Pabst R., Lutz M.B., Sorokin L. // Immunity. 2005. V. 22. № 1. P. 19–29.
49. Pappu R., Schwab S.R., Cornelissen I., Pereira J.P., Regard J.B., Xu Y., Camerer E., Zheng Y.-W., Huang Y., Cyster J.G., et al. // Science. 2007. V. 316. № 5822. P. 295–298.
50. Matloubian M., Lo C.G., Cinamon G., Lesneski M.J., Xu Y., Brinkmann V., Allende M.L., Proia R.L., Cyster J.G. // Nature. 2004. V. 427. № 6972. P. 355–360.
51. Bajénoff M., Egen J.G., Qi H., Huang A.Y.C., Castellino F., Germain R.N. // Trends Immunol. 2007. V. 28. № 8. P. 346–352.
52. Link A., Vogt T.K., Favre S., Britschgi M.R., Acha-Orbea H., Hinz B., Cyster J.G., Luther S.A. // Nat. Immunol. 2007. V. 8. № 11. P. 1255–1265.
53. Randolph G.J., Angeli V., Swartz M.A. // Nat. Rev. Immunol. 2005. V. 5. № 8. P. 617–628.
54. Acton S.E., Astarita J.L., Malhotra D., Lukacs-Kornek V., Franz B., Hess P.R., Jakus Z., Kuligowski M., Fletcher A.L., Elpek K.G., et al. // Immunity. 2012. V. 37. № 2. P. 276–289.
55. Katakai T. // Front. Immunol. 2012. V. 3. P. 200–205.
56. Katakai T., Suto H., Sugai M., Gonda H., Togawa A., Suematsu S., Ebisuno Y., Katagiri K., Kinashi T., Shimizu A. // J. Immunol. 2008. V. 181. № 9. P. 6189–6200.

57. Jarjour M., Jorquera A., Mondor I., Wienert S., Narang P., Coles M.C., Klauschen F., Bajénoff M. // J. Exp. Med. 2014. V. 211. № 6. P. 1109–1122.
58. Fletcher A.L., Acton S.E., Knoblich K. // Nat. Rev. Immunol. 2015. P. 1–12.
59. Mebius R.E. // Nat. Rev. Immunol. 2003. V. 3. № 4. P. 292–303.
60. Astarita J.L., Acton S.E., Turley S.J. // Front. Immunol. 2012. V. 3. P. 1–11.
61. Nicenboim J., Malkinson G., Lupo T., Asaf L., Sela Y., Mayseless O., Gibbs-Bar L., Senderovich N., Hashimshony T., Shin M., et al. // Nature. 2015. V. 522. P. 56–61.
62. Castagnaro L., Lenti E., Maruzzelli S., Spinardi L., Migliori E., Farinello D., Sitia G., Harrelson Z., Evans S.M., Guidotti L.G., et al. // Immunity. 2013. V. 38. № 4. P. 782–791.
63. van de Pavert S.A., Olivier B.J., Goverse G., Vondenhoff M.F.R., Greuter M., Beke P., Kusser K., Höpken U.E., Lipp M., Niederreither K., et al. // Nat. Immunol. 2009. V. 10. № 11. P. 1193–1099.
64. Bénézech C., White A., Mader E., Serre K., Parnell S., Pfeffer K., Ware C.F., Anderson G., Caamaño J.H. // J. Immunol. 2010. V. 184. № 8. P. 4521–4530.
65. Lu T.T., Browning J.L. // Front. Immunol. 2014. V. 5. P. 47.
66. Yoshida H., Naito A., Inoue J.-I., Satoh M., Santee-Cooper S.M., Ware C.F., Togawa A., Nishikawa S., Nishikawa S.-I. // Immunity. 2002. V. 17. № 6. P. 823–833.
67. Bienenstock J., McDermott M.R. // Immunol. Rev. 2005. V. 206. P. 22–31.
68. Ware C.F. // Annu. Rev. Immunol. 2005. V. 23. P. 787–819.
69. Fütterer A., Mink K., Luz A., Kosco-Vilbois M.H., Pfeffer K. // Immunity. 1998. V. 9. № 1. P. 59–70.
70. Kuprash D. V, Alimzhanov M.B., Tumanov A. V, Anderson A.O., Pfeffer K., Nedospasov S.A. // J. Immunol. 1999. V. 163. № 12. P. 6575–6580.
71. Kuprash D. V, Tumanov A. V, Liepinsh D.J., Koroleva E.P., Drutskaya M.S., Kruglov A.A., Shakhov A.N., Southon E., Murphy W.J., Tessarollo L., et al. // Eur. J. Immunol. 2005. V. 35. № 5. P. 1592–1600.
72. Blum K.S., Pabst R. // J. Anat. 2006. V. 209. № 5. P. 585–595.
73. Altman G.H., Diaz F., Jakuba C., Calabro T., Horan R.L., Chen J., Lu H., Richmond J., Kaplan D.L. // Biomaterials. 2003. V. 24. № 3. P. 401–416.
74. Agapov I.I., Moisenovich M.M., Vasiljeva T. V, Pustovalova O.L., Kon'kov A.S., Arkhipova A.Y., Sokolova O.S., Bogush V.G., Sevastianov V.I., Debabov V.G., et al. // Dokl. Biochem. Biophys. 2010. V. 433. № 5. P. 201–204.
75. Moisenovich M.M., Pustovalova O.L., Shackelford J., Vasiljeva T.V., Druzhinina T.V., Kamenchuk Y.A., Guzeev V.V., Sokolova O.S., Bogush V.G., Debabov V.G., et al. // Biomaterials. 2012. V. 33. № 15. P. 3887–3898.
76. Shapiro L., Cohen S. // Biomaterials. 1997. V. 18. № 8. P. 583–590.
77. Perez R.A., Kim M., Kim T.-H., Kim J.-H., Lee J.H., Park J.-H., Knowles J.C., Kim H.-W. // Tissue Eng. 2013. V. 20. P. 103–114.
78. Lu T., Li Y., Chen T. // Int. J. Nanomedicine. 2013. V. 8. P. 337–350.
79. Moisenovich M.M., Arkhipova A.Y., Orlova A.A., Drutskaya M.S., Volkova S.V., Zaharov S.E., Agapov I.I., Kirpichnikov M.P. // Acta Naturae. 2014. V. 1. № 20. P. 20–26.
80. Gombotz W.R., Pettit D.K. // Bioconjug. Chem. 1995. V. 6. № 4. P. 332–351.
81. Li Z., Cui Z. // Biotechnol. Adv. 2013. V. 32. № 2. P. 243–254.
82. Uriel S., Labay E., Francis-Sedlak M., Moya M.L., Weichselbaum R.R., Ervin N., Cankova Z., Brey E.M. // Tissue Eng. 2009. V. 15. № 3. P. 309–321.
83. Wang Y., Irvine D.J. // Biomaterials. 2011. V. 32. № 21. P. 4903–4913.
84. Tessmar J.K., Göpferich A.M. // Adv. Drug Deliv. Rev. 2007. V. 59. P. 274–291.
85. Ali O.A., Emerich D., Dranoff G., Mooney D.J. // Sci. Transl. Med. 2009. V. 1. № 8. P. 1–22.
86. Zavala V.A., Kalergis A.M. // Immunology. 2015. V. 145. P. 182–201.
87. Tomei A.A., Siegert S., Britschgi M.R., Luther S.A., Swartz M.A. // J. Immunol. 2009. V. 183. № 7. P. 4273–4283.
88. He C., Young A.J., West C.A., Su M., Konerding M.A., Mentzer S.J. // J. Appl. Physiol. 2002. V. 93. № 3. P. 966–973.
89. Okamoto N., Chihara R., Shimizu C., Nishimoto S., Watanabe T. // J. Clin. Invest. 2007. V. 117. № 4. P. 997–1007.
90. Suematsu S., Watanabe T. // Nat. Biotechnol. 2004. V. 22. № 12. P. 1539–1545.
91. Nakashima M., Mori K., Maeda K., Kishi H., Hirata K., Kawabuchi M., Watanabe T. // Eur. J. Immunol. 1990. V. 20. № 1. P. 47–53.
92. Bredenkamp N., Ulyanchenko S., O'Neill K.E., Manley N.R., Vaidya H.J., Blackburn C.C. // Nat. Cell Biol. 2014. V. 16. № 9. P. 902–908.
93. Richardson T.P., Peters M.C., Ennett A.B., Mooney D.J. // Nat. Biotechnol. 2001. V. 19. № 11. P. 1029–1034.
94. Sasai Y. // Stem Cell. 2013. V. 12. № 5. P. 520–530.
95. Forster R., Chiba K., Schaeffer L., Regalado S.G., Lai C.S., Gao Q., Kiani S., Farin H.F., Clevers H., Cost G.J., et al. // Stem Cell Reports. 2014. V. 2. № 6. P. 838–852.
96. Watson C.L., Mahe M.M., Múnera J., Howell J.C., Sundaram N., Poling H.M., Schweitzer J.I., Vallance J.E., Mayhew C.N., Sun Y., et al. // Nat. Med. 2014. V. 20. № 11. P. 1310-1314.
97. Bredenkamp N., Jin X., Liu D., O'Neill K.E., Manley N.R., Blackburn C.C. // Regen. Med. 2015. V. 10. № 3. P. 317–329.

# Mycoplasmas and Their Antibiotic Resistance: The Problems and Prospects in Controlling Infections

O.A. Chernova[1,2*], E.S. Medvedeva[1,2], A.A. Mouzykantov[1,2], N.B. Baranova[1,2], V.M. Chernov[1,2]
[1]Kazan Institute of Biochemistry and Biophysics, Kazan Scientific Center, Russian Academy of Sciences, Lobachevskogo Str., 2/31, 420111, Kazan, Russia
[2]Kazan (Volga Region) Federal University, Kremlevskaya Str., 18, 420008, Kazan, Russia
*E-mail: chernov@mail.knc.ru
Received 25.08.2015


**ABSTRACT** **The present review discusses the problem of controlling mycoplasmas (class Mollicutes), the smallest of self-replicating prokaryotes, parasites of higher eukaryotes, and main contaminants of cell cultures and vaccines. Possible mechanisms for the rapid development of resistance to antimicrobial drugs in mycoplasmas have been analyzed. Omics technologies provide new opportunities for investigating the molecular basis of bacterial adaptation to stress factors and identifying resistomes, the total of all genes and their products contributing to antibiotic resistance in microbes. The data obtained using an integrated approach with post-genomics methods show that antibiotic resistance may be caused by more complex processes than has been believed heretofore. The development of antibiotic resistance in mycoplasmas is associated with essential changes in the genome, proteome, and secretome profiles, which involve many genes and proteins related to fundamental cellular processes and virulence.**

**KEYWORDS** **mycoplasmas, antibiotic resistance mechanisms, omics technologies, bacterial resistome**

**ABBREVIATIONS** **MIC – Minimum Inhibitory Concentration, MLSK – macrolide-lincosamide-streptogramin-ketolide antibiotic group, ABC – ATP-binding cassette, COG – Clusters of Orthologous Groups of Proteins, MATE – Multidrug and Toxic Compound Extrusion family, MDR – Multidrug Resistance, MFS – Major Facilitator Superfamily, SMR – Small Multidrug Resistance family, QRDR – Quinolone Resistance-Determining Region, RND – Resistance-Nodulation-Cell Division superfamily, SNP – Single Nucleotide Polymorphism**

Mycoplasmas are of particular interest not only because of the unique organization of these tiny bacteria lacking cell walls, but also for practical considerations. Mycoplasmas are parasites of higher eukaryotes, the causative agents of socially significant infections, and the main contaminants of cell cultures and vaccines. Controlling mycoplasma infections is a serious problem [1–3].

Various mycoplasma inhibition methods have been under development for several decades, but no effective remedies have been discovered [4, 5]. The basic method for inhibiting mycoplasma infections and contamination is based on the administration of antibacterial drugs [2–4]. The rapid development of resistance to antimicrobial agents in mycoplasmas, whose mechanisms are not entirely clear, represents a significant problem. It is believed that the problem of controlling mycoplasma infection and contamination can be cracked by investigating the molecular and genetic adaptation mechanisms of mycoplasmas to stress conditions, which determine the survival of bacteria in various conditions [1–5]. Obviously, such research necessitates the use of an integrated approach involving both conventional and modern methods of analysis of biological material.

In this review, we summarize and analyze data on the mechanisms determining the antibiotic resistance of mycoplasmas. What we know about these mechanisms was largely developed in the period preceding the post-genomic era. Meanwhile, successful implementation of genomic projects and the discovery of omics technologies have led to the development of new approaches in the investigation of the molecular and genetic basis of bacterial adaptation to stress conditions and the discovery of resistomes, the ensemble of all genes and their products involved in the formation of antibiotic resistance in microorganisms [6–13]. This integrated approach produced results indicating that the

antibiotic resistance of bacteria may be caused by more complex processes than has previously been thought.

Since Mollicutes class representatives lack cell walls, the main classes of antimicrobial agents, such as beta-lactam antibiotics, glycopeptides, and fosfomycin, do not affected them. The biological characteristic features of mycoplasmas also result in the ineffectiveness of a number of other substances (sulfonamides, trimethoprim, rifampin, polymyxin, nalidixic acid, linezolid, and some others). Tetracyclines, fluoroquinolones, and macrolides are the most effective anti-mycoplasma agents. They are widely used to suppress mycoplasma infection and contamination of cell cultures. [4] However, recent reports have appeared on a new class of bacteriostatics, deformylase inhibitors, which are active against urogenital mycoplasmosis [5]. However, long-term clinical trials in various regions of the world are required to assess the prospects of these antibiotics.

Antimicrobial peptides (melittin, isolated from bee venom, globomycin, gramicidin C, surfactin, and valinomycin produced by bacteria, alamethicin detected in fungi, A and P1 cecropins, and magainin 2 derived from animal tissues) are not widely used to control mycoplasma at the moment [14–20]. It was found that mycoplasma successfully develops resistance to these drugs [19, 21]. Since data on the mechanisms of mycoplasma resistance to antimicrobial peptides are not yet available, a study of the adaptation of Mollicutes class representatives to antimicrobial agents should focus mainly on the formation of resistance to tetracyclines, fluoroquinolones, and macrolides.

The knowledge about the mechanisms responsible for the resistance of microorganisms to these groups of drugs is based mainly on the results of studies of classical bacteria. This is partly due to the peculiarities of Mollicutes biology, which determine the complexity of their isolation in artificial media and clonal analysis of axenic cultures. The results of a bioinformatics analysis [22–24] are not always consistent with experimental data. Thus, based on an *in silico* analysis of five efflux systems making a substantial contribution to the adaptation of classical bacteria to antibiotics, MATE (the multidrug and toxic compound extrusion family), MFS (the major facilitator superfamily), SMR (the small multidrug resistance family), RND (the resistance-nodulation-cell division superfamily), and ABC (the ATP-binding cassette superfamily) [25, 26], the MATE, MFS, and ABC genes are present in the genomes of some Mollicutes. However, experimental evidence of the contribution of efflux to mycoplasmas antimicrobial resistance has been established only for ABC transporter systems [24, 27, 28].

Either way, the development paths of resistance to tetracyclines, quinolones, and macrolides observed in classic bacteria are largely characteristic of Mollicutes, as well. However, the formation of antimicrobial resistance has different characteristic features in different mycoplasma species. Moreover, even in the case of similar mechanisms, the level of strain sensitivity to the drug can significantly vary *(Table 1)*. Furthermore, the mechanisms that determine antibiotic resistance cannot be identified in some mycoplasma species [5]. This may indicate the existence of as-of-yet undiscovered paths of resistance development in Mollicutes and/or more complex mechanisms of microbial adaptation to antibiotics than was previously thought.

Tetracyclines are the most widely used agents to control mycoplasma infection of urogenital and respiratory tracts in adults [30, 31]. Additionally, they are frequently used to treat mycoplasma infections in farm animals [5]. The bacteriostatic activity of tetracyclines is based on their capability of reversible binding to the 30S subunit of the bacterial ribosome, inhibition of the interaction between aminoacyl-tRNA and the acceptor site, and thus prevention of the protein synthesis characteristic of these antibiotics [32]. Active cellular efflux of the antibiotic, production of ribosome-protecting proteins (Tet (M), Tet (O), Tet (S), Tet (W), Tet (32), Tet (36), TetB (P), Otr(A), Tet, Tet(Q), and Tet (T)), inhibition of drug influx into the cell, target modification, and antibiotic degradation with enzymes [33, 34] are considered to be *the main mechanisms of tetracyclines resistance in classic bacteria*. Intensive growth of bacterial resistance to tetracyclines is believed to be associated with the active exchange of genes of the key factors involved in the respective processes in bacterial populations [35–38]: the plasmids and mobile genetic elements that are believed to be the main mediators of the horizontal transfer of genetic material.

*The development of tetracycline resistance in mycoplasmas* in some cases is associated with the acquisition of tet(M) determinants located at the Tn916 transposon [39]. The transposon encodes the TetM protein, protecting ribosomes from the effects of tetracyclines. This protein is homologous to the eF-Tu and eF-G elongation factors. It can cause conformational changes in the 30S ribosomal subunit, preventing it from binding to tetracyclines. A high level of tetracycline resistance (MIC ≥ 8 μg/ml) associated with the presence of the tet(M)-determinant causes cross-resistance of mycoplasmas to other tetracycline antibiotics [5, 40]. Furthermore, it is possible that resistance of mycoplasmas to these drugs may be associated with mutations in the tetracycline-binding unit of 16S rRNA [41, 42]. Mycoplasma strains characterized by high tetracycline resistance were also obtained *in vitro* by stepwise selection in media containing gradually increased concentrations of antibiotics [5,

Table 1. Resistance to antibiotics (tetracyclines, fluoroquinolones, and macrolides) in mycoplasma associated with target gene mutations [5].

| Mycoplasma | Antibiotic class | Resistance | | Mutations – positions | MIC range in resistant isolates, μg/ml |
|---|---|---|---|---|---|
| | | *in vitro* | *in vivo* | | |
| *M. pneumoniae* | MLSK[a] | + | + | 23S rRNA – 2611, 2058, 2059, 2062[b] | 64 -> 256 (erythromycin) |
| | Tetracyclines | + | - | 16S rRNA – 968, 1193 (only *in vitro*) | 2 (tetracycline) |
| | Fluoroquinolones | + | - | QRDR[c] *gyr*A – 83[d]; *gyr*B – 426, 447, 466; *par*C – 78, 80, 84; *parE* – 439 | 2–16 (levofloxacin), 8–128 (ciprofloxacin) |
| *M. hominis* | MLSK | + | + | 23S rRNA – 2610, 2611, 2057, 2059, 2062 | 16–64 (clindamycin) |
| | Tetracyclines | + | + | tet(M)-mediated protection of ribosome; 16S rRNA – 346, 965, 966, 967, 1054 (only *in vitro*) | 8 -> 64 (tetracycline), 2–8 (tetracycline) |
| | Fluoroquinolones | + | + | QRDR *gyr*A – 82, 83, 87, 93; *gyr*B – 450, 453; *par*C – 73, 80; *parE* – 420, 441, 460; Drug efflux (only *in vitro*, enchances MIC of ciprofloxacin and norfloxacin) | 2–32 (levofloxacin), 4–8 (ciprofloxacin) |
| *M. genitalium* | MLSK | - | + | 23S rRNA – 2058, 2059; ribosomal protein L4 | 16 -> 64 (erythromycin) |
| | Tetracyclines | - | - | Resistance genes are not determined | ND[f] |
| | Fluoroquinolones | - | + | QRDR *gyr*A – 83, 87, 96; *gyr*B – 447, 466, *par*C – 78, 79, 80, 84, 94, 100; *par*E – 419, 461 | ND |
| *Ureaplasma spp.* | MLSK | + | + | Ribosomal protein L4; 23S rRNA – 2056, 2057, 2058. Methylation of rRNA by ermB[e]. Drug efflux mediated by *msr*A, *msr*B, or *msr*D products | 64- > 128 (erythromycin) |
| | Tetracyclines | + | + | tet(M) mediated protection of ribosomes | 2 -> 32 |
| | Fluoroquinolones | + | + | QRDR *gyr*A – 83, 95; *gyr*B – 119; *par*C – 80, 84, 123, 134; *par*E – 151, 249, 274 | 4–32 (levofloxacin) |
| *M. hyorhinis* | MLSK | + | + | 23S rRNA – 2059 (*in vivo*); 23S rRNA – 2059 (*in vitro*); 23S rRNA – 2597, 2611; 23S rRNA – 2597, 2611 | 10–100 (tylosin), 25- >100 (lincomycin) > 100 (tylosin) 50 (lincomycin) 100 (tylosn), 50 (lincomycin) |
| | Tetracyclines | - | + | ND | 12.5 (chlortetracycline) |
| | Fluoroquinolones | - | + | ND | 1–4 (enrofloxacin) |
| *M. hyopneumoniae* | MLSK | - | + | 23S rRNA – 2058 | > 64 (lincomycin) |
| | Tetracyclines | + | + | ND | 12.5->100 (chlortetracycline) |
| | Fluoroquinolones | + | + | QRDR *gyr*A – 83; *par*C (*in vivo*) – 80, 84, 116 | 0.25- >1 (enrofloxacin) |
| *M. bovis* | MLSK | + | + | 23S rRNA – 748, 2058 (*in vitro*) 23S rRNA – 748, 752, 2058, 2059 (*in vivo*); Ribosomal proteins L4 and L22 | >1024 (tylosin), >256 (tilmicosin) 8–1024 (tylosin), 32 – >256 (tilmicosin) |
| | Tetracyclines | + | + | ND | >32 (oxytetracycline) |
| | Fluoroquinolones | + | + | QRDR *gyr*A – 81, 83; *par*C – 78, 80, 81, 84 | 2.5–32 (enrofloxacin) |
| *M. gallisepticum* | MLSK | + | + | 23S rRNA – 2058, 2059 (*in vivo*); 23S rRNA – 2058, 2503 (*in vitro*) | 0.63–5 (tylosin), 1.25-> 10 (tilmicosin) 256–512 (tilmicosin), 256->512 (erythromycin) |
| | Tetracyclines | + | + | ND | 5 ->16 (oxytetracycline) |
| | Fluoroquinolones | + | + | QRDR *gyr*A – 81, 83, 84, 87; *gyr*B – 426, 464, 465; *par*C – 64, 80, 81, 84; *par*E (*in vitro*) – 420, 463, 467 | 1–32 (enrofloxacin) 1–10 (enrofloxacin) |

[a]MLSK: macrolides, lincosamides, streptogramines, and ketolides.
[b]E. coli numbering system (nucleotide sequence).
[c]QRDR: quinolone resistance determining region
[d]E. coli numbering system (amino acid sequence).
[e]*erm* and efflux macrolide genes were found only in one study [29] and were not detected in the others.
[f]ND – not determined

42]. However, the mechanisms of antibiotic resistance could not be determined in these cases.

Macrolide antibiotics are widely used to treat mycoplasmal infections in children (primarily respiratory infections caused by *Mycoplasma pneumonia* and neonatal infections associated with *Ureaplasma spp.),* as well as to suppress mycoplasmoses in animals [5, 43–47]. These antibiotics are often administered in cases where tetracyclines and fluoroquinolones cannot be used.

The antibacterial activity of macrolides is based on the reversible binding of these antibiotics to the 50S ribosomal subunit (including 23S rRNA and some ribosomal proteins, e.g. L4, L22), inducing separation of peptidyl-tRNA from the ribosome, and thus blockage of the synthesis of the peptide chain [48]. *There are three paths of development of macrolide resistance in classical bacteria*: target modification (in particular, structural changes in the 50S ribosomal subunit), change in drug efflux, and enzymatic inactivation of the antibiotic [48, 49].

*Development of macrolide resistance in mycoplasmas* is believed to be associated with inhibition of antibiotic efflux into the cell, as well as structural changes in the 50S ribosomal subunit [5]. In some cases, macrolide resistance in mycoplasmas is associated with changes in the central loop of domain V of 23S rRNA [5, 50]. Mutation in the corresponding gene area leads to increased resistance of certain mycoplasma species to several antibiotics of this group and reduced or lost resistance to others.

Fluoroquinolones are the most popular group of drugs used to inhibit mycoplasma infections and contamination of cell cultures [4, 5, 28]. This is due to the fact that mycoplasma infections often occur in immunodeficient patients and, as a rule, are complex. In such cases, the use of microbicides is recommended. The fluoroquinolone drug ciprofloxacin is a widely used representative of this group [51–53].

The molecular mechanisms of the bactericidal action of fluoroquinolones are based on binding to DNA gyrase and/or DNA topoisomerase IV, which leads to inhibition of bacterial DNA replication [49, 54]. *The main mechanisms of fluoroquinolone resistance of classical bacteria* is associated with target modifications caused by mutations in the QRDR (quinolone resistance-determining region) region of the target genes *gyr*A (DNA gyrase subunit A), *gyr*B (DNA gyrase subunit B), *par*C (topoisomerase IV subunit A), *par*E (topoisomerase IV subunit B), as well as with reduced drug accumulation in the cell (due to active efflux or suppression of influx) and acquired-resistance determinants by horizontal gene transfer [55].

*Development of fluoroquinolone resistance by mycoplasmas* is usually associated with mutations in the QRDR region of the target genes (DNA gyrase and topoisomerase IV). Depending on the antibiotic, significant mutations can occur in the genes of certain enzymes [5]. For example, development of *in vitro* resistance to pefloxacin, ofloxacin, ciprofloxacin, and trovafloxacin in *Mycoplasma hominis* is associated with mutations in the topoisomerase IV gene, while resistance to sparfloxacin occurs due to mutations in the DNA gyrase gene [5, 41, 56]. Fluoroquinolone-resistant clinical isolates of mycoplasma usually demonstrate cross-resistance to all drugs of this group. The resistance level often correlates with the number of mutations and their location [5, 57]. However, a long series of observations of the adaptation to fluoroquinolones in mycoplasmas has shown that displacement of cells lacking the QRDR-mutation from the culture occurs only when bacteria are cultured in media containing high concentrations of ciprofloxacin [58]. With low concentrations of ciprofloxacin, the key role is apparently played by other mechanisms, such as cellular efflux. This type of adaptation to fluoroquinolones, which was identified in a number of bacteria, occurs by means of endogenous ABC-type pumps associated with multidrug resistance (MDR). Increased expression of corresponding genes can determine the MDR-phenotype. ABC-type genes annotated as "suspected MDR genes" were detected in the genomes of certain mycoplasmas [22–24]. According to the results of quantitative competitive RT-PCR, these genes are constitutively expressed in the parental strains, while in the strains with the MDR-phenotype their expression level is increased [18]. However, rapid adaptation of various mycoplasmas to fluoroquinolones still cannot be explained by these factors.

Efforts to figure out the causes of increased fluoroquinolone resistance by microorganisms, which are currently being reported all over the world [56, 59, 60], have led to the assumption that, in addition to these mechanisms, there are other ways that determine the possibility of rapid bacterial adaptation to antibiotics in microbial communities [55]. This assumption is based on the results of both experimental studies and monitoring data in different countries. A very rapid increase in fluoroquinolone resistance is observed in agricultural animals, although these drugs were introduced in veterinary practice only two decades ago [5, 61–63].

Since Mollicutes class representatives are believed to be tachytelic organisms, it is assumed that their rapid adaptation to antimicrobial agents is caused by frequent mutation events, and that changes in the genes of the target proteins are significant [19, 64, 65]. However, according to the results of a complete nucleotide sequence analysis of genes of the *gyrA, gyrB, parC,* and *parE* strains of *Ureaplasma parvum* and *U. urealyti-*

*cum, a* significant portion of nucleotide substitutions in these mycoplasmic genes represents a specific polymorphism and does not affect antibiotic sensitivity [66]. This finding casts doubt on our knowledge on the mutational mechanisms of antibiotic resistance in mycoplasmas (and other bacteria) and calls for verification of these data using new approaches. Meanwhile, data demonstrating the active role of extracellular vesicles in bacterial adaptation to stress conditions, including antibiotics, have been recently published [3, 67–72]. Vesicles produced by cells contain various compounds and are involved in intercellular interactions in prokaryotes and eukaryotes [69, 73–75]. As early as in 1996, it was established that vesicles of gram-negative bacteria are involved in antibiotic transportation and antibiotic resistance control in bacterial populations [76]. However, the role of vesicles in the bacterial response to antimicrobial agents is only now being extensively studied in connection with the "universality" of vesicular transport, which was esstablished in all organisms, including the smallest prokaryotes, and the development of high-resolution analysis techniques [3, 6–9, 69–71, 73, 74, 76–80].

Active participation of extracellular vesicles in the development of bacterial resistance to fluoroquinolones was first exemplified with *Acholeplasma laidlawii,* mycoplasma infecting humans, animals, plants, and the main contaminant of cell cultures [71, 81]. *A.laidlawii* strains that differed in their susceptibility to ciprofloxacin were obtained by stepwise selection. It was found that vesicles produced by mycoplasma cells growing in a medium with ciprofloxacin mediate the cellular efflux of this drug, have bacteriostatic action against the antibiotic-sensitive *Staphylococcus aureus* strain, and transport the mutant genes of fluoroquinolone target proteins. Differential expression of ABC-transporter genes, which in some bacteria are involved in active efflux of antibiotics and the formation of multi-drug resistance, recorded in response to ciprofloxacin is indicative of the fact that rapid efflux of ciprofloxacin from mycoplasma cells (including through vesicles) can be also associated with modulation of the ABC-transporter system.

Detection of genetic material in vesicles also suggests that they participate in horizontal gene transfer [8, 81–83]. The transport of fluoroquinolone target genes mediated by *A. laidlawii* vesicles may contribute to the rapid expansion of mutant genes in a bacterial population [71, 81]. The possibility of such events is exemplified by *Acinetobacter baumannii*. The extracellular vesicles of this bacterium facilitate the transfer of the *OXA-24* gene, which determines resistance to carbapenems [84]. Thus, transfer of antibiotic resistance factors mediated by the vesicles of certain bacteria may contribute to the survival of various bacteria in a microbial community. An example of such cooperation was illustrated in a *S. aureus* model, where a vesicle-mediated spread of β-lactamase from these bacteria in microorganism populations resulted in the survival of gram-negative and gram-positive bacteria sensitive to ampicillin on an ampicillin-containing medium [78]. There is clear evidence of the participation of extracellular vesicles in bacterial adaptation to various stress conditions, including antimicrobials. However, it is obvious that comprehensive systematic studies using high-resolution techniques are required in order to uncover the role of vesicular components in the development of bacterial resistance to antibiotics

The development of post-genomic technologies has opened up entirely new possibilities to determine resistomes, the combination of genes and their products involved in the formation of antimicrobial resistance. Information about the resistomes of some bacteria to a number of drugs is now available [85–104]. Such information was recently ,obtained for *A.laidlawii* [105]. The information is based on the analysis of complete *A .laidlawii* genomes, as well as the cellular and vesicular proteomes of strains differing in their sensitivity to ciprofloxacin, i.e. the laboratory strain PG8 (MIC 0.5 μg/ml) and the ciprofloxacin-resistant $PG8R_{10}$ strain (MIC 20 μg/ml) derived from the latter by stepwise selection.

A comparative analysis of the nucleotide sequences of *A. laidlawii* and *PG8* and *A. laidlawii* $PG8R_{10}$ in the genome of a ciprofloxacin-resistant strain revealed multiple mutations (insertions, deletions, and single nucleotide polymorphism (SNP)) localized in fluoroquinolone target genes (DNA gyrase and DNA topoisomerase), as well as in many other genes whose products participate in various cellular processes and bacterial pathogenicity. A total of 255 mutations in 188 genes were found in the *A. laidlawii* $PG8R_{10}$ genome (*Fig.1).* Some of these mutations had been previously identified in other microorganisms in connection with the development of resistance to particular antibiotics (for example, daptomycin resistance in *S. aureus* and multidrug resistance to ciprofloxacin, imipenem, amikacin, minocycline, levofloxacin, piperacillin, tazobactam, ceftazidime, cefotaxime, cefepime, cefoperazone, sulbactam, and meropenem in *A. baumannii* [95, 102]).

A proteomic analysis of *A. laidlawii* PG8 and $PG8R_{10}$ cells resulted in the identification of proteins whose proportion differed significantly in these strains. A total of 64 such proteins were identified, and only four of them proved to be the products of mutant genes (ACL_0380, ACL_0418, ACL_0435, ACL_0436). Many of these proteins are involved in fundamental cellular processes (energy production, translation, transcription, replication, membrane biogenesis, protein folding,

Table 2. Proteins identified in the extracellular vesicles of *A. laidlawii* $PG8R_{10}$

| No | Protein (gene) | NCBI[1] | COG[2] | score[3] | n[4] | %[5] |
|---|---|---|---|---|---|---|
| 1 | Glycine cleavage system P-protein subunit 1 (ACL_1410) | 162447261 | E | 18 | 2 | 12.1 |
| 2 | Enolase (eno) | 162447267 | G | 662 | 6 | 22.7 |
| 3 | Phosphoglycerate kinase (pgk) | 162448052 | G | 26 | 2 | 25.3 |
| 4 | S-adenosylmethionine synthetase (*metK1*) | 162447194 | H | 23 | 2 | 15 |
| 5 | 50S ribosomal protein L17 (*rplQ*) | 162446985 | J | 300 | 2 | 20.2 |
| 6 | Methionyl-tRNA synthetase (*metG*) | 162447002 | J | 19 | 2 | 13.4 |
| 7 | Elongation factor Tu (*tuf*) | 162447058 | J | 113 | 3 | 23.3 |
| 8 | Methionyl-tRNA formyltransferase (*fmt*) | 162447191 | J | 17 | 2 | 23 |
| 9 | TrmA family RNA methyltransferase (ACL_0513) | 162447375 | J | 21 | 2 | 8.9 |
| 10 | Ribosome recycling factor (frr) | 162447997 | J | 75 | 2 | 40.8 |
| 11 | DNA-directed RNA polymerase subunit beta (*rpoB*) | 162447041 | K | 17 | 2 | 24.7 |
| 12 | UDP glucose pyrophosphorylase (*galU*) | 162447697 | M | 17 | 2 | 32.9 |
| 13 | ABC transporter substrate-binding protein (ACL_0720) | 162447580 | P | 31 | 2 | 6.5 |
| 14 | Acyl carrier protein (*acpP*) | 162447111 | Q | 131 | 2 | 42.1 |
| 15 | Peptidase U35 (ACL_0611) | 162447472 | R | 47 | 2 | 35.4 |
| 16 | ComEC-like compentence protein (ACL_0895) | 162447752 | R | 295 | 2 | 21.2 |
| 17 | Hypothetical protein (ACL_0450) | 162447314 | - | 22 | 2 | 10.5 |

[1] Protein identification number in the NCBI database.
[2] Proteins classification into functional categories is shown according to COG (E – amino acid transport and metabolism, G – carbohydrate transport and metabolism, H – coenzyme transport and metabolism, J – translation, ribosomal structure and biogenesis, K – transcription, M – cell wall/membrane/envelope biogenesis, P – inorganic ion transport and metabolism, Q – secondary metabolites biosynthesis, transport and catabolism, R – general function prediction only, "-" – not in COG).
■ – bacterial virulence factors
[3] Reliability of protein search in NCBI database using the Mascot software.
[4] the number of various amino acid sequences of peptides which were used to identify the protein.
[5] Percent of amino acid sequence coverage.

transport and metabolism of amino acids, nucleotides, carbohydrates, lipids, inorganic ions, signal transduction, and defense mechanisms) and bacterial pathogenicity; some of them are involved in the development of antibiotic resistance in other bacteria (for example, to carbapenems in *A. baumannii* and to oxacillin in *S. aureus* [106, 107]).

We have found significant differences in the proteomic profile of extracellular vesicles in strains that differ in susceptibility to ciprofloxacin (*Table* 2). Thus, 97 proteins were identified in *A. laidlawii* PG8 vesicles and 17 proteins were identified in *A. laidlawii* $PG8R_{10}$ vesicles; 13 of them are absent in parental strain vesicles [105]. Further, the metallo-β-lactamase protein involved in the hydrolysis of β-lactam antibiotics was found in the vesicles of *A. laidlawii* PG8. Since the action of β-lactam antibiotics is targeted at the bacterial cell wall, which is absent in Mollicutes, the role of this enzyme in *A. laidlawii* PG8 remains unknown. It is possible that *A. laidlawii* PG8, similarly to *S. aureus*, may assist other bacteria having cell walls and necessary for the survival of these mycoplasmas in microbiocenosis in adaptation to β-lactam antibiotics [6].

The contribution of each protein and gene of mycoplasmas, reacting to stress, to the development of ciprofloxacin resistance should be elucidated in the future. However, it is obvious that multiple changes in genomic profiles, as well as the cellular and vesicular proteome, in the ciprofloxacin-resistant *A. laidlawii* strain can determine significant restructuring of bio-

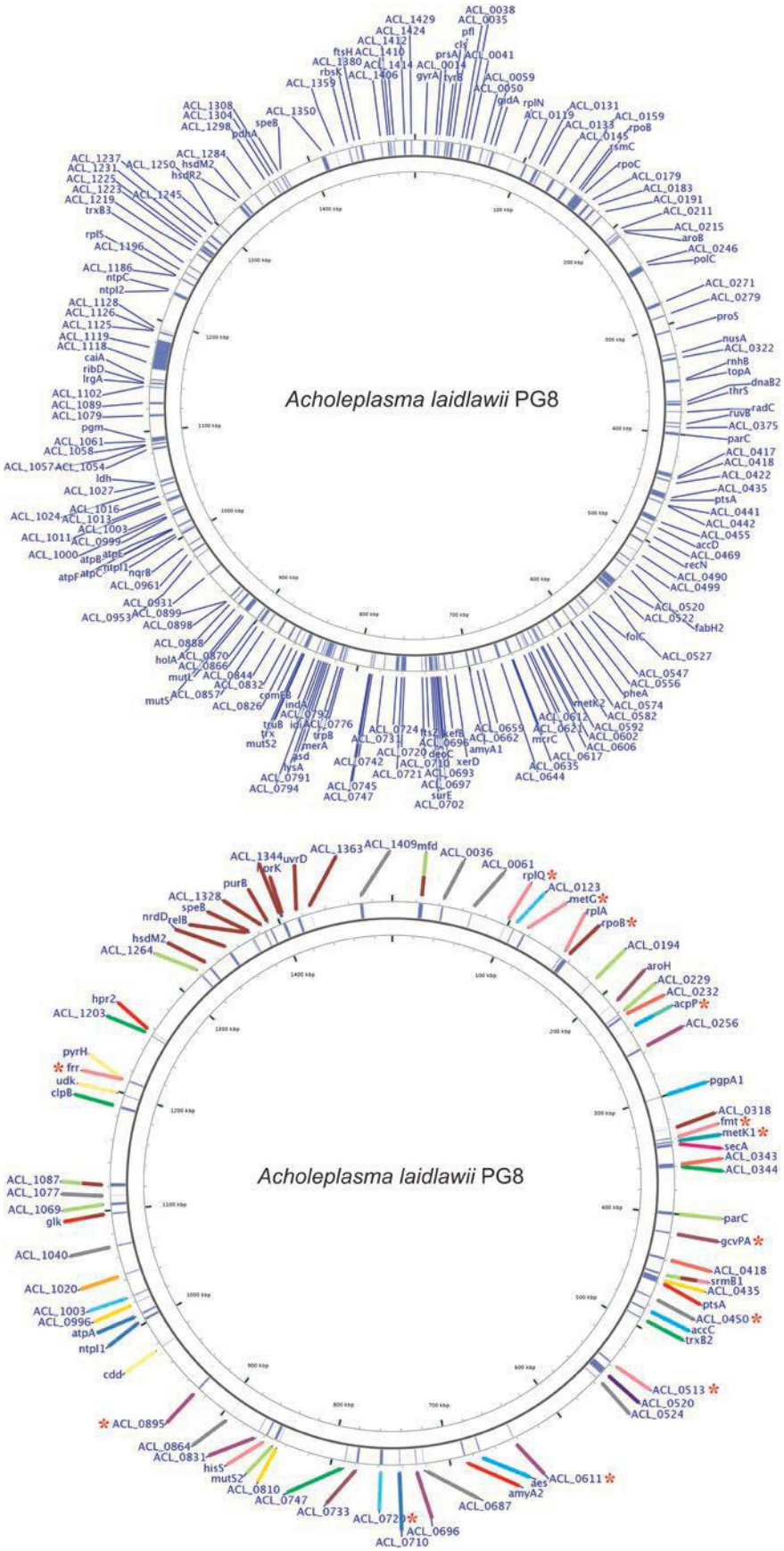


Fig. 1. Localization of genes which differ in *A.laidlawii* PG8 and *A.laidlawii* $PG8R_{10}$ in their primary structure (A) and genes for proteins differentially expressed in the respective strains (B) on the mycoplasma genome map. * – genes for proteins identified only in the extracellular vesicles derived from *A.laidlawii* $PG8R_{10}$. The functional categories were decided according to COG:
■ – [C] energy production and conversion, ■ – [E] amino acid transport and metabolism, ■ – [F] nucleotide transport and metabolism, ■ – [G] carbohydrate transport and metabolism, ■ – [H] coenzyme transport and metabolism, ■ – [I] lipid transport and metabolism, ■ – [J] translation, ribosomal structure and biogenesis, ■ – [K] transcription, ■ – [L] replication, recombination and repair, ■ – [M] cell wall/membrane/envelope biogenesis, ■ – [N] cell motility, ■ – [O] posttranslational modification, protein turnover, chaperones, ■ – [P] inorganic ion transport and metabolism, ■ – [Q] secondary metabolites biosynthesis, transport and catabolism, ■ – [R] general function prediction only, ■ – [S] function unknown, ■ – [T] signal transduction mechanisms, ■ – [U] intracellular trafficking, secretion, and vesicular transport, ■ – [V] defense mechanisms, ■ – [-] not in COG.

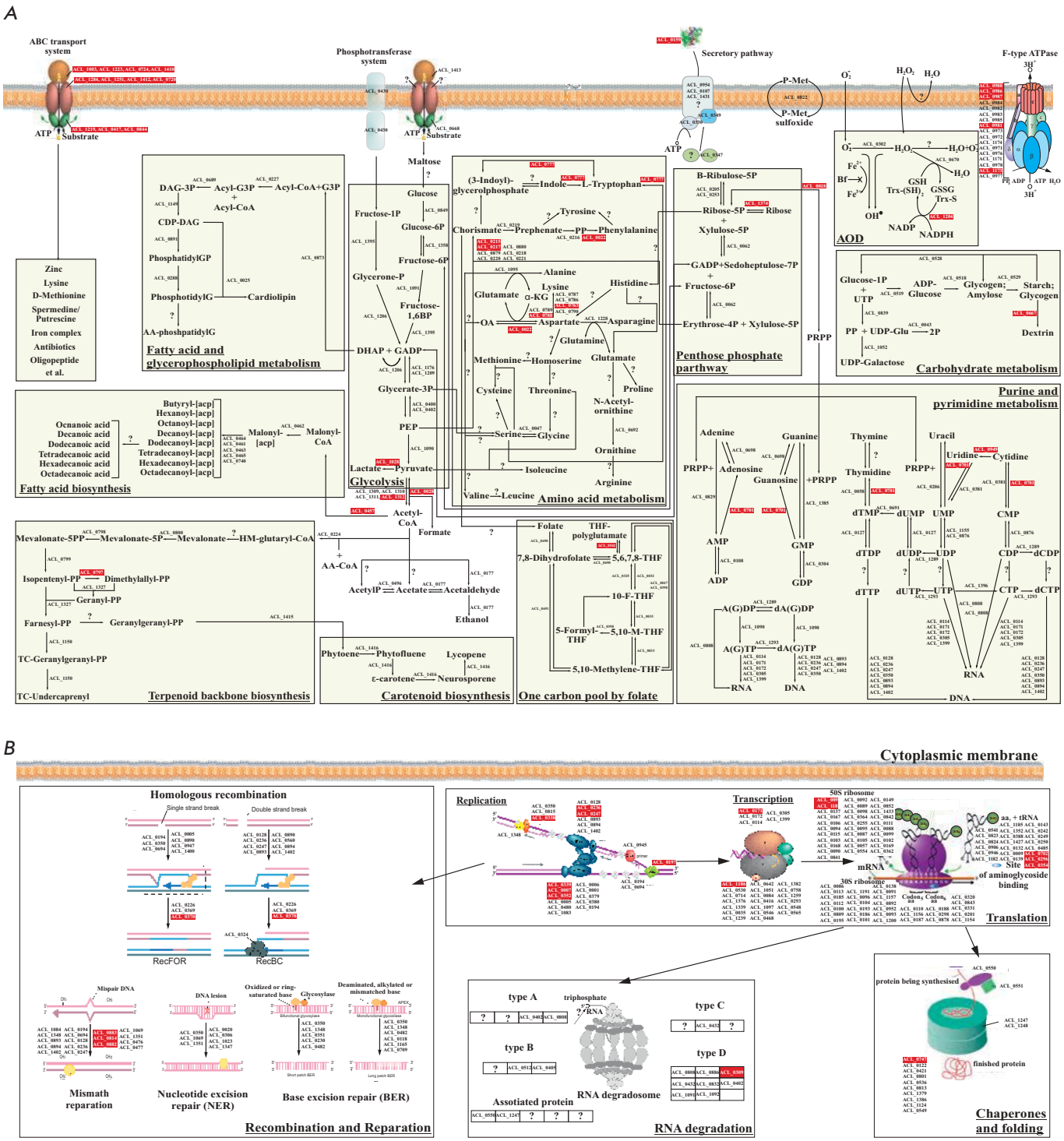


Fig. 2. The schemes of metabolic pathways (A) and cellular processes (B) in *Acholeplasma laidlawii* PG8 (according to [108], NCBI (accession number NC_010163) and KEGG). ■ - products of genes in which non-synonymous SNPs and indels were detected in the case of *Acholeplasma laidlawii* PG8R$_{10}$.
PTS – phosphotransferase system; Fructose-1P – Fructose 1-phosphate; Glucose-6P – Glucose 6-phosphate; Fructose-6P – Fructose 6-phosphate; Fructose-1,6BP – Fructose 1,6-bisphosphate; DHAP – Dihydroxyacetone phosphate; GA3P – Glyceraldehyde 3-phosphate; 3Pglycerate – glycerate 3-phosphate; PEP – phosphoenolpyruvate; D- Ribulose-5P – D- Ribulose 5-phosphate; Ribose-5P – Ribose 5-phosphate; Xylulose-5P – Xylulose 5-phosphate; Sedoheptulose-7P – Sedoheptulose 7-phosphate; Erythrose-4P – Erythrose 4-phosphate; Glucose-1P – Glucose

1-phosphate; ADP-Gluc – Adenosine diphosphate glucose; UDP-Gluc – Uridine diphosphate glucose; UDP-Gal – Uridine diphosphate galactose; Acetyl-CoA – Acetyl coenzyme A; AcetylP – Acetyl phosphate; Malonyl-CoA – Malonyl coenzyme A; Malonyl-ACP – malonyl:acyl carrier protein; Butyryl-ACP - Butyryl:acyl carrier protein; Hexanoyl -ACP – Hexanoyl:acyl carrier protein; Octanoyl-ACP – Octanoyl:acyl carrier protein; Decanoyl-ACP – Decanoyl:acyl carrier protein; Dodecanoyl-ACP – Dodecanoyl:acyl carrier protein; Tetradecanoyl-ACP – Tetradecanoyl:acyl carrier protein; Hexadecanoyl-ACP – Hexadecanoyl:acyl carrier protein; Octadecanoyl-ACP – Octadecanoyl:acyl carrier protein; G-3P – Glycerol 3-phosphate;Acyl-CoA – Acyl coenzyme A; Acyl-G-3P – Acylglycerol-3-phosphate; DAG-3P – Diacylglycerol-3-phosphate; CDP-DAG – Cytidinediphosphate-diacylglycerol; Phosphatidyl-GP – Phosphatidylglycerol phosphate; Phosphatidyl-G – Phosphatidylglycerol; AA-CoA – Acetoacetyl coenzyme A; HM-glutaryl-CoA – 3-hydroxy-3-methylglutaryl-coenzyme A; Mevalonate-5P – Mevalonate-5-phosphate; Mevalonate-5PP – Mevalonate-5-pyrophosphate; Isopentenyl-PP – Isopentenyl pyrophosphate; Geranyl-PP – Geranyl pyrophosphate; Farnesyl-PP – Farnesyl pyrophosphate; TC-Geranylgeranyl-PP – Di-trans, poly-cis-geranylgeranyl pyrophosphate; TC-undecaprenyl-PP – Di-trans, poly-cis-undecaprenyl-pyrophosphate; Geranylgeranyl-PP – Geranylgeranyl pyrophosphate; 5, 6, 7, 8-THF – 5, 6, 7, 8-tetrahydrofolate; 5,10-M-THF – 5,10-methenyltetrahydrofolate; 10-F-THF – 10-formyltetrahydrofolate; PP – Phenylpyruvate; α-KG – α-Ketoglutaric acid; OA – Oxaloacetate; 5PRPP – 5- Phosphoribosyl pyrophosphate; AMP – Adenosine monophosphate; ADP – Adenosine diphosphate; ATP – Adenosine triphosphate; dADP – Deoxyadenosine diphosphate; dATP – Deoxyadenosine triphosphate; GMP – Guanosine monophosphate; GDP – Guanosine diphosphate; GTP – Guanosine triphosphate; dGDP – Deoxyguanosine diphosphate; dGTP – Deoxyguanosine triphosphate; dTMP – Deoxythymidine monophosphate; dTDP – Deoxythymidine diphosphate; dTDP – Deoxythymidine triphosphate; dUMP – Deoxyuridine monophosphate; dUDP – Deoxyuridine diphosphate; dUTP – Deoxyuridine triphosphate; UMP –Uridine monophosphate; UDP – Uridine diphosphate; UTP – Uridine triphosphate; CMP – Cytidine monophosphate; CDP – Cytidine diphosphate; CTP – Cytidine triphosphate; dCMP – Deoxycytidine monophosphate; dCDP – Deoxycytidine diphosphate; dCTP – Deoxycytidine triphosphate; RNA – Ribonucleic acid; DNA – Deoxyribonucleic acid; mRNA – Messenger ribonucleic acid; tRNA – Transfer ribonucleic acid; A – Adenine; G – Guanine; C – Cytosine; U – Uracil; $O2^{-}$– Superoxide; H2O2 – Hydrogen peroxide; H2O – Water; GSH – Reduced glutathione; GSSG – Oxidized glutathione; Trx-S2 – Oxidized thioredoxin; Trx-(SH)2 – Reduced thioredoxin; NADPH – Nicotinamide adenine dinucleotide phosphate reduced; NADP – Nicotinamide adenine dinucleotide phosphate; PPi – Pyrophosphate inorganic; Pi – Phosphate inorganic; H+ – Proton; P-Met – Methionine; Fe – Iron.

chemical processes in mycoplasma cells *(Fig. 2)*. These data were obtained for *Pseudomonas aeruginosa* in connection with the development of resistance to certain antibiotics, including ciprofloxacin [87, 96, 109]. The development of resistance to antimicrobials in various bacterial species proved to be associated with changes not only in the targets of these drugs, but also in many genes and proteins involved in the processes of energy production, transport, and protective mechanisms, as well as in virulence. These results require special attention from researchers involved in the development of control means for pathogenic bacteria and the search for new antimicrobial targets (and virulence factors are possible candidates for this role).

The study of the adaptation of microorganisms to antimicrobial agents using omics technologies is in its infancy. However, the results suggest that the formation of bacterial resistance to antibiotics is, apparently, made possible by more complex mechanisms than has previously been thought. The development of resistance proves to be associated with significant changes in the genomic, transcriptomic, proteomic, and secretomic profiles of microorganisms, which can determine significant restructuring in cellular processes and pathogenicity. Resistome elements that are similar in different bacteria may be indicative of the existence of universal modules regulating cellular reprogramming and ensuring survival in stress conditions. Identification and elucidation of their functional principles is crucial in understanding the "logic of life" of mycoplasma, the rapid bacterial adaptation to stress in microbiocenosis, and finding ways to solve the problem of how to control mycoplasma infection and contamination of cell cultures. Large-scale studies of microorganisms in axenic cultures, as well as in associates in various environments, based on high-tech methodic platforms using meta-omics approaches are required to accumulate the corresponding information.

*This work was carried out as part of the competitiveness facilitation program at Kazan (Volga Region) Federal University of the Ministry of Education and Science of the Russian Federation. This study was performed using the equipment of the Interdisciplinary Collective Use Center of the Kazan Federal University Center with state financial support from the Ministry of Education and Science of the Russian Federation (ID RFMEFI59414X0003), as well as the Russian Foundation for Basic Research (grant number 14-04-00883a, 15-44-02594).*

REFERENCES


1. Nikfarjam L., Farzaneh P. // Cell J. (Yakhteh). 2012. V. 13. P. 203–212.
2. Rottem S., Kornspan J.D., Kosower N.S. Biomedical Tissue Culture. InTech, 2012. P. 248. http://www.intechopen.com/books/biomedical-tissue-culture
3. Chernov V.M., Chernova O.A., Sanchez-Vega J.T., Kolpakov A.I., Il'inskaya O.N. // Acta Naturae. 2014. V. 6. No 3. P. 41–51.
4. Uphoff C.C., Drexler H.G. // Curr. Protoc. Mol. Biol. 2014. V. 106. P. 28.5.1–28.5.12.
5. Waites K.B., Lysnyansky I., Bebear C.M. Emerging antimicrobial resistance in mycoplasmas of humans and animals. In: Mollicutes: molecular biology and pathogenesis. UK: Caister Acad. Press, 2014. P. 350.
6. Muzykantov A.A., Baranova N.B., Medvedeva E.S., Grigor'eva T.Y., Chernova O.A., Chernov V.M. // Rep. Biochem. Biophys. 2014. V. 455. № 1. P. 43–48.
7. Chernov V.M., Chernova O.A., Medvedeva E.S., Mouzykantov A.A., Ponomareva A.A., Shaymardanova G.F., Gorshkov O.V., Trushin M.V. // J. Proteomics. 2011. V. 4. P. 2920–2936.
8. Chernov V.M., Chernova O.A., Mouzykantov A.A., Efimova I.R., Shaymardanova G.F., Medvedeva E.S., Trushin M.V. // ScientificWorldJournal. 2011. V. 11. P. 1120–1130.
9. Chernov V.M., Chernova O.A., Mouzykantov A.A., Baranova N.B., Gorshkov O.V., Trushin M.V., Nesterova T.N., Ponomareva A.A. // ScientificWorldJournal. 2012. Article ID 315474. P. 6.
10. Vanyushkina A.A., Fisunov G.Y., Gorbachev A.Y., Kamashev D.E., Govorun V.M. // PLoS One. 2014. V. 9(3). e89312.
11. Mazin P.V., Fisunov G.Y., Gorbachev A.Y., Kapitskaya K.Y., Altukhov I.A., Semashko T.A., Alexeev D.G., Govorun V.M. // Nucl. Acids Res. 2014. V. 42(21). P. 13254–13268.
12. Citti C., Blanchard A. // Trends Microbiol. 2013. V. 21. P. 196–203.
13. Güell O., Sagués F., Serrano M.Á. // Sci. Rep. 2012. V. 2. P. 621.
14. Lazarev V.N. // Acta Naturae. 2009. V. 1. № 1. P. 121–123.
15. Béven L., Wróblewski H. // Res. Microbiol. 1997. V. 148. № 2. P. 163–175.
16. Borth W.B., Jones V.P., Ullman D.E., Hu J.S. // Antimicrob. Agents Chemother. 2001. V. 45. № 6. P. 1894–1895.
17. Béven L., Castano S., Dufourcq J., Wieslander A., Wróblewski H. // Eur. J. Biochem. 2003. V. 270. № 10. P. 2207–2217.
18. Lazarev V.N., Stipkovits L., Biro J., Miklodi D., Shkarupeta M.M., Titova G.A., Akopian T.A., Govorun V.M. // Microbes Infect. 2004. V. 6. № 6. P. 536–541.
19. Fehri L.F, Sirand-Pugnet P., Gourgues G., Jan G., Wróblewski H., Blanchard A. // Antimicrob. Agents Chemother. 2005. V. 49. № 10. P. 4154–4165.
20. Park H.J., Kang K.M., Dybvig K., Lee B.L., Jung Y.W., Lee I.H. // FEBS Lett. 2013. V. 587. № 20. P. 3321–3326.
21. Shelton C.L., Raffel F.K., Beatty W.L., Johnson S.M., Mason K.M. // PLoS Pathog. 2011. V. 7. e1002360.
22. van Veen H.W., Konings W.N. // Biochim. Biophys. Acta. 1998. V. 1365. P. 31–36.
23. Paulsen I.T., Nguyen L., Sliwinski M.K., Rabus R., Saier M.H. // J. Mol. Biol. 2000. V. 301. P. 75–100.
24. Raherison S., Gonzalez P., Renaudin H., Charron A., Bébéar C., Bébéar C.M. // Antimicrob. Agents Chemother. 2005. V. 49. P. 421–424.
25. Piddock L.J. // Clin. Microbiol. Rev. 2006. V. 19. P. 382–402.
26. Martinez J.L., Sánchez M.B., Martínez-Solano L., Hernandez A., Garmendia L., Fajardo A., Alvarez-Ortega C. // FEMS Microbiol. Rev. 2009. V. 33. P. 430–449.
27. Pereyre S., Gonzalez P., De Barbeyrac B., Darnige A., Renaudin H., Charron A., Raherison S., Bébéar C., Bébéar C.M. // Antimicrob. Agents Chemother. 2002. V. 46. P. 3142–3150.
28. Antunes N.T., Assunção P., Poveda J.B., Tavío M.M. // Vet. J. 2015. V. 204. P. 327–332.
29. Lu C., Ye T., Zhu G., Feng P., Ma H., Lu R., Lai W. // Curr. Microbiol. 2010. V. 61. P. 44–49.
30. Duffy L.B., Crabb D., Searcey K., Kempf M.C., Duffy L. // J. Antimicrob. Chemother. 2000. V. 45. P. 29–33.
31. Bartlett J.G. // Clin. Infect. Dis. 2008. V. 47. Suppl 3. P. S232–S236.
32. Nguyen F., Starosta A.L., Arenz S., Sohmen D., Dönhöfer A., Wilson D.N. // Biol. Chem. 2014. V. 395. P. 559–575.
33. Chopra I., Roberts M. // Microbiol. Mol. Biol. Rev. 2001. V. 65. № 2. P. 232–260.
34. Thaker M., Spanogiannopoulos P., Wright G.D. // Cell Mol. Life Sci. 2010. V. 67. P. 419–431.
35. Dai M., Lu J., Wang Y., Liu Z., Yuan Z. // J. Microbiol. 2012. V. 50. № 5. P. 807–812.
36. Sullivan B.A., Gentry T., Karthikeyan R. // J. Appl. Microbiol. 2013. V. 115. P. 774–785.
37. Pinto T.C., Costa N.S., Corrêa A.B., de Oliveira I.C., de Mattos M.C., Rosado A.S., Benchetrit L.C. // Braz. J. Microbiol. 2014. V. 45. № 3. P. 785–789.
38. Jahan M., Zhanel G.G., Sparling R., Holley R.A. // Int. J. Food Microbiol. 2015. V. 199. P. 78–85.
39. Taraskina A.E., Savicheva A.M., Akopian T.A., Soroka A.E., Momynaliev K.T., Govorun V.M. // Bull. Exp. Biol. Med. 2002. V. 134. № 1. P. 60–63.
40. Shen X., Yang H., Yu S., Yao K., Wang Y., Yuan L., Yang Y. // Microb. Drug Resist. 2008. V. 14. P. 155–161.
41. Bebear C.M., Kempf I. Mycoplasmas: molecular biology pathogenicity and strategies for control. UK: Horizon Bioscience, 2005. P. 535–569.
42. Dégrange S., Renaudin H., Charron A., Pereyre S., Bébéar C., Bébéar C.M. // J. Antimicrob. Chemother. 2008. V. 61. № 6. P. 1390–1392.
43. Schelonka R.L., Waites K.B. // Semin. Perinatol. 2007. V. 31. P. 2–9.
44. Lerner U., Amrama E., Ayling R.D., Mikula I., Gerchman I., Harrus S., Teff D., Yogev D., Lysnyansky I. // Vet. Microbiol. 2013. V. 168. P. 365–371.
45. Meyer Sauteur P.M., van Rossum A.M., Vink C. // Curr. Opin. Infect. Dis. 2014. V. 27. P. 220–227.
46. Spuesens E.B., Meyer Sauteur P.M., Vink C., van Rossum A.M. // J. Infect. 2014. V. 69. Suppl 1. P. S42–S46.
47. Gautier-Bouchardon A.V., Ferré S., Le Grand D., Paoli A., Gay E., Poumarat F. // PLoS One. 2014. V. 9. e87672.
48. Leclercq R. // Clin. Infect. Dis. 2002. V. 34. № 4. P. 482–492.
49. Alekshun M.N., Levy S.B. // Cell. 2007. V. 128. № 6. P. 1037–1050.
50. Lysnyansky I., Gerchman I., Flaminio B., Catania S. // Microb. Drug Resist. 2015. V. 3. [Epub ahead of print].
51. Paterna A., Sánchez A., Gómez-Martín A., Corrales J.C., De la Fe C., Contreras A., Amores J. // J. Dairy Sci. 2013. V. 96. № 11. P. 7073–7076.
52. Wang Q.Y., Li R.H., Zheng L.Q., Shang X.H. // J. Microbiol. Immunol. Infect. 2014. pii: S1684-1182(14)00118-2.
53. Couldwell D.L., Lewis D.A. // Infect. Drug Resist. 2015. V. 8. P. 147–161.
54. Fàbrega A., Madurga S., Giralt E., Vila J. // Microb. Biotechnol. 2009. V. 2. P. 40–61.

55. Redgrave L.S., Sutton S.B., Webber M.A., Piddock L.J.V. // Trends Microbiol. 2014. V. 22. P. 438–445.
56. Meng D.-Y., Sun C.-J., Yu J.-B., Ma J., Xue W.-C. // Braz. J. Microbiol. 2014. V. 45. P. 239–242.
57. Bébéar C.M., de Barbeyrac B., Pereyre S., Renaudin H., Clerc M., Bébéar C. // Clin. Microbiol. Infect. 2008. V. 14. P. 801–805.
58. Govorun V.M., Gushchin A.E., Ladygina V.G., Abramycheva N.Yu., Topol Yu.Yu. // Mol. Gen. Mikrobiol. Virusol. 1998. V. 3. P. 16–19.
59. Li L., Weimin S., Zhang K., Tang X., Guo N., Shen F., Xing M., Liua L., Yuan P., Shi Q., Liang J., Yu L. // Iranian J. Pharm. Res. 2012. V. 11. P. 1111–1119.
60. Kikuchi M., Ito S., Yasuda M., Tsuchiya T., Hatazaki K., Takanashi M., Ezaki T., Deguchi T. // J. Antimicrob. Chemother. 2014. V. 69. P. 2376–2382.
61. Engberg J., Aarestrup F.M., Taylor D.E., Gerner-Smidt P., Nachamkin I. // Emerging Infect. Dis. 2001. V. 7. № 1. P. 24–34.
62. de Jong A., Stephan B., Silley P. // J. Appl. Microbiol. 2011. V. 112. P. 239–245.
63. Kong L.-C., Gao D., Gao Y.-H., Liu S.-M., Ma H.-X. // J. Vet. Med. Sci. 2014. V. 76. № 12. P. 1655–1657.
64. Dybvig K., Voelker L.L. // Annu. Rev. Microbiol. 1996. V. 50. P. 25–57.
65. Delaney N.F., Balenger S., Bonneaud C., Marx C.J., Hill G.E., Ferguson-Noe N., Tsai P., Rodrigo A., Edwards S.V. // PLoS Genet. 2012. V. 8(2). e1002511.
66. Beeton M.L., Chalker V.J., Kotecha S., Spiller O.B. // Antimicrob. Agents Chemother. 2009. V. 64. P. 529–538.
67. Manning A.J., Kuehn M.J. // BMC Microbiol. 2011. V. 11. P. 258.
68. Schrempf H., Koebsch I., Walter S., Engelhardt H., Meschke H. // Microb. Biotechnol. 2011. V. 4. P. 286–299.
69. Schertzer J.W., Whiteley M. // J. Mol. Microbiol. Biotechnol. 2013. V. 23. P. 118–130.
70. Kulkarni H.M., Swamy Ch.V.B., Jagannadham M.V. // J. Proteome Res. 2014. V. 13. P. 1345–1358.
71. Medvedeva E.S., Baranova N.B., Mouzykantov A.A., Grigorieva T.Y., Davydova M.N., Trushin M.V., Chernova O.A., Chernov V.M. // ScientificWorldJournal. 2014. Article ID 150615.
72. Chattopadhyay M.K., Jagannadham M.V. // Front. Microbiol. 2015. V. 6. P. 758.
73. Kulp A., Kuehn M.J. // Annu. Rev. Microbiol. 2010. V. 64. P. 163–184.
74. Deatherage B.L., Cookson B.T. // Infect. Immun. 2012. V. 80. P. 1948–1957.
75. Kim J.H., Lee J., Park J., Gho Y.S. // Semin. Cell. Dev. Biol. 2015. V. 40. P. 97–104.
76. Kadurugamuwa J.L., Beveridge T.J. // J. Bacteriol. 1996. V. 178. P. 2767–2774.
77. Manning A.J., Kuehn M.J. // J. Mol. Microbiol. Biotechnol. 2013. V. 23. P. 131–141.
78. Lee J., Lee E.Y., Kim S.H., Kim D.K., Park K.S., Kim K.P., Kim Y.K., Roh T.Y., Gho Y.S. // Antimicrob. Agents Chemother. 2013. V. 57. P. 2589–2595.
79. Bonnington K.E., Kuehn M.J. // Biochim. Biophys. Acta. 2014. V. 1843. P. 1612–1619.
80. Park A.J., Suretteand M.D., Khursigara C.M. // Front. Microbiol. 2014. V. 5. P. 464.
81. Medvedeva E.S., Baranova N.B., Muzykantov A.A., Grigor'eva T.Yu., Davydova M.N., Chernova O.A., Chernov V.M. // Rep. Biochem. Biophys. 2014. V. 454. № 1. P. 34–37.
82. Mashburn-Warren L., Howe J., Brandenburg K., Whiteley M. // J. Bacteriol. 2009. V. 191. P. 3411–3414.
83. Vidakovics M.L., Jendholm J., Mörgelin M., Månsson A., Larsson C., Cardell L.O., Riesbeck K. // PLoS Pathog. 2010. V. 6. e1000724.
84. Rumbo C., Fernández-Moreira E., Merino M., Poza M., Mendez J.A., Soares N.C., Mosquera A., Chaves F., Bou G. // Antimicrob. Agents Chemother. 2011. V. 55. P. 3084–3090.
85. D'Costa V.M., McGrann K.M., Hughes D.W., Wright G.D. // Science. 2006. V. 311. № 5759. P. 374–377.
86. Wright G.D. // Handb. Exp. Pharmacol. 2012. V. 211. P. 13–30.
87. Cox G., Wright G.D. // Int. J. Med. Microbiol. 2013. V. 303. P. 287–292.
88. Gillings M.R. // Front. Microbiol. 2013. V. 4. P. 4.
89. Perry J.A., Westman E.L., Wright G.D. // Curr. Opin. Microbiol. 2014. V. 21. P. 45–50.
90. Breidenstein E.B.M., Khaira B.K., Wiegand I., Overhage J., Hancock R.E.W. // Antimicrob. Agents Chemother. 2008. V. 52. № 12. P. 4486–4491.
91. Fajardo A., Martínez-Martín N., Mercadillo M., Galán J.C., Ghysels B., Matthijs S., Cornelis P., Wiehlmann L., Tümmler B., Baquero F., et al. // PLoS One. 2008. V. 3. e1619.
92. Girgis H.S., Hottes A.K., Tavazoie S. // PLoS One. 2009. V. 4. e5629.
93. Alvarez-Ortega C., Wiegand I., Olivares J., Hancock R.E., Martínez J.L. // Antimicrob. Agents Chemother. 2010. V. 54. № 10. P. 4159–4167.
94. Poirel L., Bonnin R.A., Nordmann P. // Antimicrob. Agents Chemother. 2011. V. 55. P. 4224–4229.
95. Peleg A.Y., Miyakis S., Ward D.V., Earl A.M., Rubio A., Cameron D.R., Pillai S., Moellering Jr. R.C., Eliopoulos G.M. // PLoS One. 2012. V. 7. e28316.
96. Su H.-C., Khatun J., Kanavy D.M., Giddings M.C. // Microbial. Drug Resistance. 2013. V. 19. P. 428–436.
97. Tan S.Y., Chua S.L., Liu Y., Høiby N., Andersen L.P., Givskov M., Song Z., Yang L. // Genome Biol. Evol. 2013. V. 5. P. 807–818.
98. Hu Y., Zhu Y., Ma Y., Liu F., Lu N., Yang X., Luan C., Yi Y., Zhu B. // Antimicrob. Agents Chemother. 2015. V. 59. P. 1152–1161.
99. Sánchez M.B. // Front. Microbiol. 2015. V. 6. P. 658.
100. Ilina E.N., Shitikov E.A., Ikryannikova L.N., Alekseev D.G., Kamashev D.E., Malakhova M.V., Parfenova T.V., Afanas'ev M.V., Ischenko D.S., Bazaleev N.A., et al. // PLoS One. 2013. V. 8. e56577.
101. Zhu L., Yan Z., Zhang Z., Zhou Q., Zhou J., Wakeland E.K., Fang X., Xuan Z., Shen D., Li Q.Z. // PLoS One. 2013. V. 8. e66584.
102. Petty N.K., Ben Zakour N.L., Stanton-Cook M., Skippington E., Totsika M., Forde B.M., Phan M.D., Gomes Moriel D., Peters K.M., Davies M., et al. // Proc. Natl. Acad. Sci. USA. 2014. V. 111. P. 5694–5699.
103. Coldham N.G., Randall L.P., Piddock L.J., Woodward M.J. // J. Antimicrob. Chemother. 2006. V. 58. № 6. P. 1145–1153.
104. Madeira A., Santos P.M., Coutinho C.P., Pinto-de-Oliveira A., Sá-Correia I. // Proteomics. 2011. V. 11. P. 1313–1328.
105. Medvedeva E.S., Davydova M.N., Muzykantov A.A., Baranova N.B., Grigor'eva T.Yu., Sinyagina M.N., Bulygina E.A., Chernova O.A., Chernov V.M. // Rep. Biochem. Biophys. 2016 V. 466. № 1. P. 23–27.
106. Tiwari V., Vashistt J., Kapil A., Moganty R.R. // PLoS One. 2012. V. 7. e39451.
107. Liu X., Hu Y., Pai P.J., Chen D., Lam H. // J. Proteome Res. 2014. V. 13. № 3. P. 1223–1233.
108. Himmelreich R., Hilbert H., Plagens H., Pirkl E., Li B.C., Herrmann R. // Nucl. Acids Res. 1996. V. 24. P. 4420–4449.
109. Perry J.A., Wright G.D. // Bioessays. 2014. V. 36. P. 1179–1184.

# Modeling of the Binding of Peptide Blockers to Voltage-Gated Potassium Channels: Approaches and Evidence

V. N. Novoseletsky[1]*, A. D. Volyntseva[1], K. V. Shaitan[1], M. P. Kirpichnikov[1,2], A. V. Feofanov[1,2]
[1]M.V.Lomonosov Moscow State University, Faculty of Biology, Leninskie Gory 1, bldg. 12, 119992, Moscow, Russia
[2]Shemyakin-Ovchinnikov Institute of Bioorganic Chemistry, Russian Academy of Sciences, Miklukho-Maklaya str. 16/10, 117997, Moscow, Russia
*Email: valeryns@gmail.com
Received: 06.07.2015


**ABSTRACT** **Modeling of the structure of voltage-gated potassium ($K_V$) channels bound to peptide blockers aims to identify the key amino acid residues dictating affinity and provide insights into the toxin-channel interface. Computational approaches open up possibilities for *in silico* rational design of selective blockers, new molecular tools to study the cellular distribution and functional roles of potassium channels. It is anticipated that optimized blockers will advance the development of drugs that reduce over activation of potassium channels and attenuate the associated malfunction. Starting with an overview of the recent advances in computational simulation strategies to predict the bound state orientations of peptide pore blockers relative to $K_V$-channels, we go on to review algorithms for the analysis of intermolecular interactions, and then take a look at the results of their application.**
**KEYWORDS** **blockers, potassium channels , molecular modeling, complex structure .**
**ABBREVIATIONS** **BD – Brownian dynamics, MD – molecular dynamics, PMF – the potential of mean force, X-ray – x-ray analysis, RMSD – root mean square deviation, SF - selectivity filter, NMR – nuclear magnetic resonance, αKTx – a family of channel blocker toxins from scorpion venom, $K_V$channels – voltage-gated potassium channels, MM-PBSA - molecular mechanics/Poisson-Boltzmann surface area, VSD – voltage-sensor domain**

## INTRODUCTION

Potassium ($K^+$) channels are pore-forming transmembrane proteins known to mediate cell functions via selectively allowing potassium fluxes across the cell membrane. Potassium channels are ubiquitously expressed in all cell types, contributing to the maintenance of the resting membrane potential, the regulation of cardiac and nerve excitability, the release of neurotransmitters, the contraction of muscles, and the secretion of hormones [1, 2]. Potassium channels play an important role in the diagnosis and treatment of different pathologies [3–6].

The group of human potassium channels includes $Ca^{2+}$-activated channels ($K_{Ca}$), inwardly rectifying channels ($K_{IR}$), and two-pore domain ($K_{2p}$) and voltage-gated ($K_V$) channels. The latter form the largest family that comprises 12 subfamilies, such as Shaker/$K_V$1 (KCNA), Shab/$K_V$2 (KCNB), Shaw/$K_V$3 (KCNC), etc. They share structural similarities (except $K_V$4–$K_V$9) and exist as homotetrameric proteins with a four-fold axis of symmetry. The mechanisms by which $K_V$-channels are activated have been reviewed in reference [7].

Dysfunctional $K_V$-channel activity is implicated in the etiology of a number of human diseases. The pharmacological targeting of ion channels offers abundant opportunity for treatment. For example, these disorders have negative consequences on membrane excitability, as well as cardiac and nerve function [8]. Episodic ataxia type 1, an autosomal dominant neurological disorder, is caused by a mutation of the KCNA1 gene encoding the voltage-gated $K^+$ channel $K_V$1.1, which substitutes valine for leucine at position 408 [9]. Genetic studies have also identified mutations in KCNQ2 and KCNQ3 encoding the voltage-gated $K^+$ channels $K_V$7.2 and Kv7.3, which lead to benign familial neonatal seizures [10]. Gene expression profiles across various stages of Alzheimer's disease progression showed that $K_V$3.4 overexpression (KCNC4) and $K_V$3.1 dysfunction (KCNC1) alter the ion currents in neurons and, consequently, synaptic activity, resulting in neurodegenerative sequelae [11]. Voltage-gated $K^+$ channel defects ($K_V$7.1 (KCNQ1), $K_V$11.1 (KCNH2), KCNE1, KCNE2) have been associated with the long Q-T interval syndrome [12]. The Brugada syndrome is a genetic heart

disorder resulting from mutations in the KCND3 gene encoding the $K_V$4.3 channel [13]. Studies with patients suffering from acute coronary insufficiency identified mutations in the $K_V$1.3 encoded gene [14]. $K_V$1.3 inhibitors suppress the proliferation of T-lymphocytes (particularly, effector memory T cells), relieving symptoms of multiple sclerosis, type 1 diabetes, rheumatoid arthritis, psoriasis, and bronchial asthma [15]. The $K_V$2.1 channel was therapeutically targeted to mitigate type 2 diabetes [16]. Various snake, scorpion, spider, cone snail, and sea anemone toxins can readily modulate channel gating. These peptide toxins are classified in terms of their mechanism of action: (i) pore blockers binding to and plugging the external mouth of the channel (scorpion and sea anemone toxins); (ii) – peptides interacting with the VSD-domain, locking the channel in the resting state (tarantula venom peptides).

Until recently, only a few crystal structures of $K_V$-channels in complex with pore-blocking toxins had been solved [17, 18]. However, the lack of experimental data can be compensated through the use of molecular modeling tools.

Peptide blockers may have strong affinity (dissociation constants in the pico- and nanomolar range) for several closely related members of the $K_V$-channel family. To this end, the pharmacological potential of toxins is exploited to increase selectivity via structure optimization. One such example is ShK-186, a synthetic analog of the sea anemone peptide, which blocks the potential-gated $K_V$1.3 channel in the picomolar range. It is currently under investigation in phase 1B clinical trials as a therapeutic for autoimmune diseases [19]. Another feature of selective toxins is their potential use for ion channel discovery, ion channel distribution, and identification of a role for a channel in pathologies. Major efforts to address these issues are based on molecular modeling.

We will begin this review by summarizing published research on the molecular modeling of the interactions between $K_V$-channels and pore blockers, including docking and binding energy calculations. A general overview of theory and approaches in modeling of ion channels, as well as a summary of the literature on the use of molecular modeling of ion channels outside the family of $K_V$-channels, is beyond the scope of this review, and the reader is referred to the recent comprehensive publication by Gordon *et al* [20].

## THE STRUCTURE OF $K_V$-CHANNELS AND PEPTIDE PORE BLOCKERS IN FREE AND COMPLEX FORMS

X-ray crystallography, nuclear magnetic resonance spectroscopy (NMR), and electron microscopy offer unique advantages for determining the molecular architecture of potassium channels bound to toxins. To date, numerous structures of peptide pore blockers, 12 potassium channels in free form [21] and two in complex with charybdotoxin have been solved and reported. Analysis of the atomic structure of K+ channels in

Table 1. Important peptide blockers of $K_V$-channels with experimentally determined structures

| Name | Abbreviation | Subfamily | Pdb code (reference) | Target channels |
|---|---|---|---|---|
| Charybdotoxin | ChTx | α -KTx 1.1 | 2CRD [23] | Kv1.1, 1.2, 1.3, 1.6 $K_{Ca}$1.1, 3.1 |
| | Lq2 | α -KTx 1.2 | 1LIR [24] | $K_V$, $K_{Ca}$, $K_{IR}$ |
| Noxiustoxin | NTX | α -KTx 2.1 | 1SXM [25] | $K_V$1.2, 1.3 |
| Margatoxin | MgTx | α -KTx 2.2 | 1MTX [26] | $K_V$1.1, 1.2, 1.3 |
| Chongotoxin | HgTx | α -KTx 2.5 | 1HLY [27] | $K_V$1.2, 1.3 |
| Kaliotoxin | KTx | α -KTx 3.1 | 1XSW [28] | $K_V$1.1, 1.2, 1.3, 1.6 $K_{Ca}$3.1 |
| Agitoxin | AgTx2 | α -KTx 3.2 | 1AGT [29] | $K_V$1.1, 1.2, 1.3, 1.6 |
| | BmKTx | α -KTx 3.6 | 1BKT [30] | $K_V$1.3 |
| | OSK1 | α -KTx 3.7 | 1SCO [31] | $K_V$1.1, 1.2, 1.3, $K_{Ca}$3.1 |
| | Pi1 | α -KTx 6.1 | 1WZ5 [32] | $K_V$1.2 |
| Maurotoxin | MTX | α -KTx 6.2 | 1TXM [33] | $K_V$1.1, 1.2, 1.3, $K_{Ca}$3.1 |
| | HsTx1 | α -KTx 6.3 | 1QUZ [34] | $K_V$1.1, 1.3, $K_{Ca}$3.1 |
| | Pi4 | α -KTx 6.4 | 1N8M [35] | $K_V$1.2 |
| | BmP01 | α -KTx 7.2 | 1WM7 [36] | $K_V$1.3 |
| Cobatoxin | CoTx1 | α -KTx 10.1 | 1PJV [37] | $K_V$1.2 |
| | Vm24 | α -KTx 23.1 | 2K9O [38] | $K_V$1.3 |
| | ShK | | 1ROO [39] | $K_V$1.1, 1.3, 1.6, 3.2, $K_{Ca}$3.1 |
| Dendrotoxin-K | DTX-K | | 1DTK [40] | Kv1.1 |

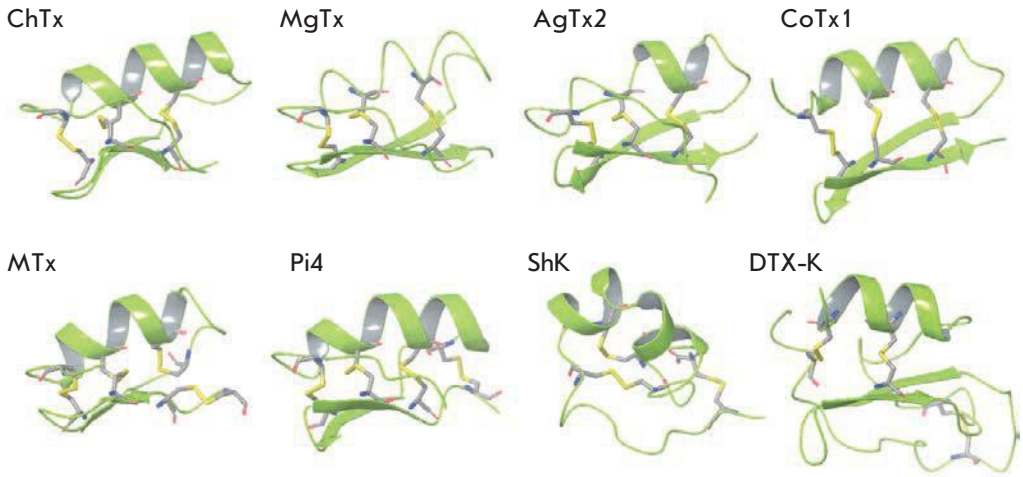


Fig. 1. Structures of charybdotoxin (ChTx), margatoxin (MgTx), agitoxin-2 (AgTx2), cobatoxine-1 (CoTx1), maurotoxin (MTx), toxin Pi4, ShK toxin, and dendrotoxin DTX-K in a ribbon representation. The cysteine residues that form disulfide bridges are shown in rods

bound and free states has been hampered by technical difficulties with extraction, purification, and crystallization of membrane proteins. These challenges add value to each resolved structure that provides structural details of the activation mechanisms, function, and interaction-induced changes [22].

## STRUTURAL CHARACTERIZATION OF PORE-BLOCKING PEPTIDES THAT BLOCK K+ CHANNELS

Most potassium channel blockers found in scorpion venoms belong to the α-KTx family. The sea anemone toxin ShK and dendrotoxins from mamba snake venom (α-DTX, DTX-I, DTX-K, δ-DTX) are also among the $K_V$-channels blockers. Certain peptides can block both the $K_V$- and $K_{Ca}$-channels (*Table 1*). NMR measurements and, to some extent, X-ray analysis have helped understand the structures of many pore blockers (*Table 1*), laying the groundwork for subsequent interface analysis.

Alpha-KTx peptides (more than 50 NMR structures available) adopt a common alpha/beta scaffold (*Fig. 1, 2*), comprising an α-helix and two or three β-sheets. The structural differences lie in the sequence length (ranging from 29 to 40 residues) and amino acid composition (*Fig. 2*) affecting the alpha helical and beta structural regions.

Alpha-KTx peptides contain three or four disulfide bonds which hold the conformation in a rigid state. The number of disulfide bonds is fixed within each subfamily, except for the α-KTx6 subfamily, whereby disulfide bond formation is favored between cysteine residues 1 and 5, 2 and 6, 3 and 7, 4 and 8, as is in Pi4 toxin (*Fig. 1, 2*). By contrast, maurotoxin (*Fig. 1, 2*) and spinotoxin (α-KTx6.13) contain disulfide bonds between cysteine residues at positions 1 and 5, 2 and 6, 3 and 4, 7 and 8. Structural studies suggest more than one disulfide

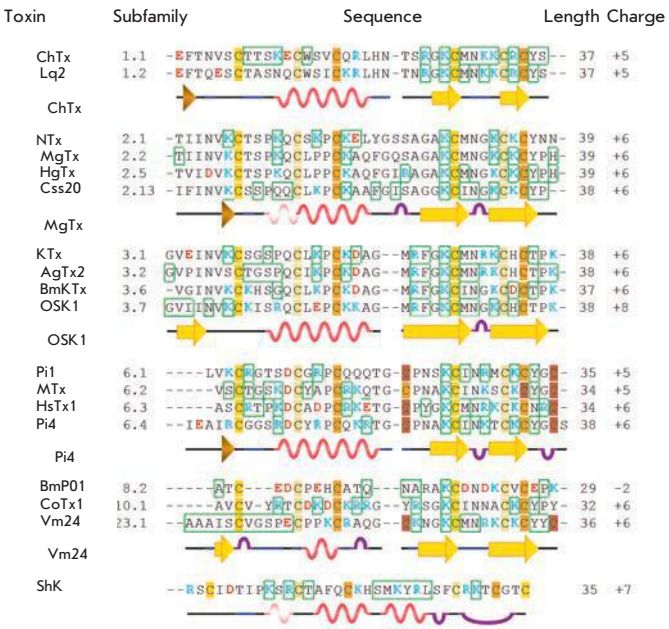


Fig. 2. Alignment of the amino acid sequences of toxins blocking $K_V$-channels. Residues that form contacts with a variety of channels according to the simulation are marked with green boxes. Cys residues are highlighted in yellow and shades of brown (residues forming disulfide bridges are shown with the same color), positively and negatively charged residues are in blue and red, respectively. The secondary structure of several toxins is shown (according to PDB identifiers, Table 1). Beta-strands are represented in yellow arrows, alpha-helices in bright wavy lines, 3/10-helices in pale wavy lines, turns in purple arcs, and curves in blue lines. Unstructured areas are shown in black lines

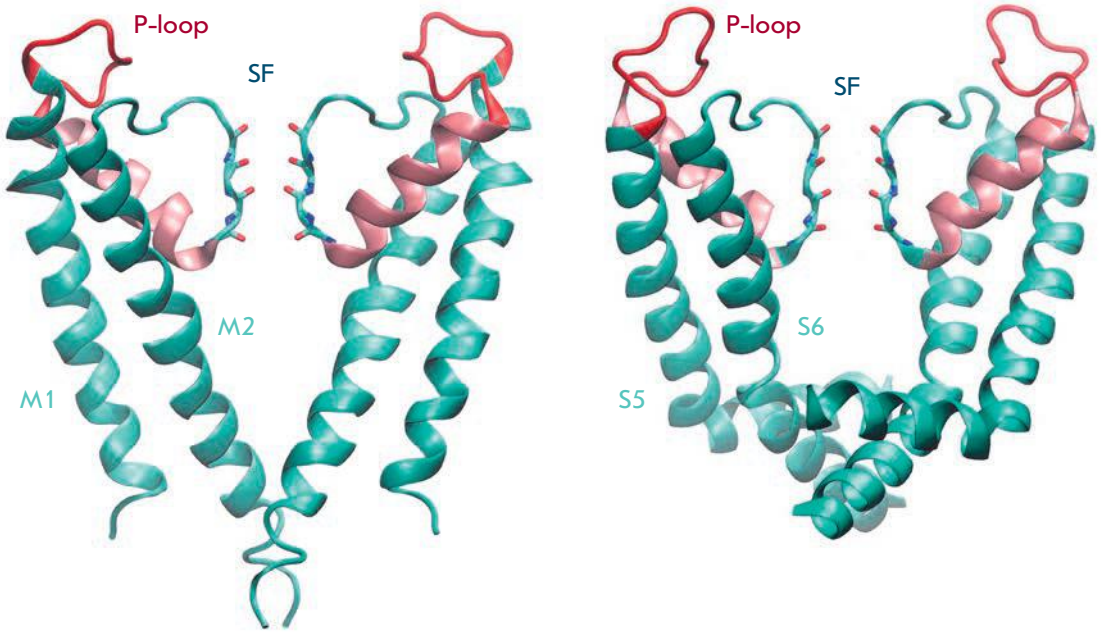


Fig. 3. Crystallographic structure of the KcsA channel (pdb code 1BL8) (left) and the pore domain of the $K_V1.2$ channel (pdb code 2A79) (right) in a ribbon representation. For clarity, only two α-subunits out of four are shown. The P-loops are shown in red; P-helices, in pink. Backbone oxygen atoms of the residues forming the SF are shown. Potassium ions are not shown

Table 2. Structures of $K_V$-channels alone and in complex with charybdotoxin used in homology modeling studies

| Description | pdb-code (resolution, Å) (reference) | Reporting studies |
|---|---|---|
| KcsA channel | 1BL8 (3.20 Å) [54] | [55] |
| $K_V$AP channel | 1ORQ (3.20 Å) [56] | [57] |
| $K_V1.2$ channel | 2A79 (2.90 Å) [43] | [58, 59] |
| | 3LUT (2.90 Å) [44] | [60–62] |
| Chimaeric $K_V1.2$-2.1 channel | 2R9R (2.40 Å) [45] | [63–68] |
| Mutant KcsA in complex with ChTx | 2A9H# [17] | [69, 70] |
| $K_V1.2$-2.1 in complex with ChTx | 4JTA (2.50 Å) [18] | [71] |

# The structure was solved by NMR in contrast to the other structures solved by X-ray crystallography.

bonding pattern without changing the overall conformation in light of the fact that sulphur atoms in cysteines at 3, 4, 7 and 8 are in close proximity to one another [41].

At neutral pH, α-KTx toxins carry an overall positive charge that varies between +2 to +8, whereas negatively charged residues are more clustered in the N-terminal half of the peptide (*Fig. 2*). An exception is α-KTx8 toxins, in particular, BmP01 [41] with a net charge of −2 (*Table 1*, *Fig. 2*), a peptide with activity toward Kv1.3 channels [42].

ShK and DTX-K dendrotoxin peptides are closely related in terms of sequence length and disulfide bonding pattern to scorpion venom toxins but differ in structure (*Fig. 1, 2*).

## EXPERIMENTALLY SOLVED STRUCTURES OF POTASSIUM CHANNELS

The KcsA prokaryotic potassium ion channel was among the first to be structurally resolved by X-ray crystallography (*Table 2*). The pore forms a cone-like structure composed of four α-subunits. Each subunit is made up of two transmembrane α-helices M1 and M2 and the pore region P, which can be divided into a P-loop, a P-helix, and a selectivity filter (SF, *Fig. 3*). SF is formed by oxygen atoms of amino acid residues comprising a TVGYG motif (in some ion channels TIGYG or SVGFG) characteristic of potassium channels. The overall length is 12 Å, and the cavity can only accommodate K+ ions. Although KcsA is not voltage-gated,

the TVGYG motif in the filter region seems to be conserved in eukaryotic $K_V$-channels (*Fig. 4*).

A total of 60 possible states of KcsA have been identified, which include open or closed conformation, in complex with low-molecular-weight ligands, with ions at the ion binding sites in the selectivity filter ($K^+$, $Cs^+$, $Rb^+$, $Tl^+$), including mutation-induced conformations that mimic the structural features of the pore regions of eukaryotic potassium channels. The atom coordinates of the P-loop and the docking position of pore blockers remain unaltered across all conformational states.

Another prokaryotic potassium channel with a refined X-ray structure is the archeal voltage-gated $K_V$AP channel (*Table 2*). The archeal channel differs from KcsA in a more complex structure of α-subunits containing six helices (S1–S6). The helices S5 and S6 of four α-subunits, like the M1 and M2 helices of the KcsA channel, are arranged to form a cone-shaped structure with a pore, while S1–S4 helices make up a voltage-sensor domain (VSD-domain).

Only a few eukaryotic potassium channels have so far been described (*Table 2*). Among the first was the $K_V$1.2 channel [43], later refined to a higher atomic resolution [44]. As is the case with $K_V$AP, the α-subunits of $K_V$1.2 are each composed of six helices (S1–S6) lining the central pore (S5–S6) and the VSD-domain (S1–S4). The $K_V$1.2 refined structure clearly shows the spatial arrangement of the loops S1–S2, S2–S3 and S3–S4 which connect the helices of the VSD-domain and side chains of residues in the helices S2, S4, and the loop S5–P. A crystallographic analysis of $K_V$1.2 revealed structural homology to the pore domains of both $K_V$AP and KcsA (*Fig. 4*). Despite a shared homology of 65%, the structure and adjacent sequence of the selectivity filter demonstrate a high conservation (the root mean-square deviations of the Cα carbon atoms positions for residues 65–85 in KcsA from their positions in the $K_V$1.2 are within 0.8 Å). However, the pore domains of $K_V$1.2 and KcsA slightly differ in length and conformation of the P-loops and cytoplasmic side of the transmembrane helices (*Fig. 3*). A comparative crystallographic analysis of the $K_V$1.2 channel showed that the P-loop conformation seems to be flexible: the most common conformation found in structures with PDB IDs 2A79 and 3LNM and a unique conformation assigned under PDB ID 3LUT.

Although the pore domains of $K_V$1.2 and $K_V$AP are structurally related, the spatial organization of VSD-domains exhibits dramatic variations. It is likely that these differences are brought about by changes in the structure during extraction and crystallization of $K_V$AP [43].

Yet, the structures of other eukaryotic $K_V$-channels remain to be determined, but based on the high level of homology the structure of their pore domains is anticipated to be similar to that of $K_V$1.2.

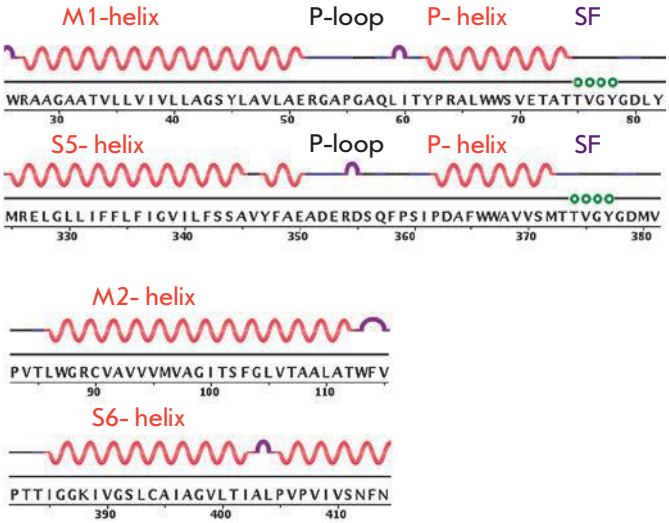


Fig. 4. Comparison of the primary and secondary structures of the KcsA channel (pdb code 1BL8) and the pore domain of the $K_V$1.2 channel (pdb code 2A79). Circles indicate residues that are in contact with the K+ ions in the SF (a fragment of the motif TVGYG). The secondary structure is presented as in *Fig. 2*.

## RESOLVED STRUCTURES OF PATASSIUM CHANNELS IN COMPLEX WITH PEPTIDE BLOCKERS

The first crystal structure of an ion potassium channel bound to a pore-blocking peptide was solved by NMR for a surrogate KcsA ion channel and charybdotoxin (*Table 2*) utilizing structural knowledge of pore channels and blockers [17]. The wild-type KcsA, insensitive to eukaryotic potassium channel blockers, was modified by mutating three residues (Q58A, T61S, R64D). These mutations enhanced structural similarity to eukaryotic Shaker $K_V$ channels and increased affinity for charybdotoxin. Another three mutations (F103Y, T107F, L110V) were introduced to the central region to increase homology to human $K_V$11.1. A NMR spectral analysis showed that charybdotoxin binding induces conformational changes in the channel structure, whereas the M1 and M2 helices remain unperturbed. Following binding, the toxin backbone remains rigid. There is evidence defining a blocking mechanism for K27 charybdotoxin at the toxin-pore interface.

Recently, Banerjee *et al* reported on the structure of a chimaeric $K_V$1.2–2.1 channel in complex with charybdotoxin resolved by X-ray crystallography (Table 2, *Fig. 5*). The voltage-sensor paddle (the S3b–S4 loop segment) of $K_V$1.2 was replaced by the voltage-sensor paddle of $K_V$2.1 as described previously [45]. The crys-

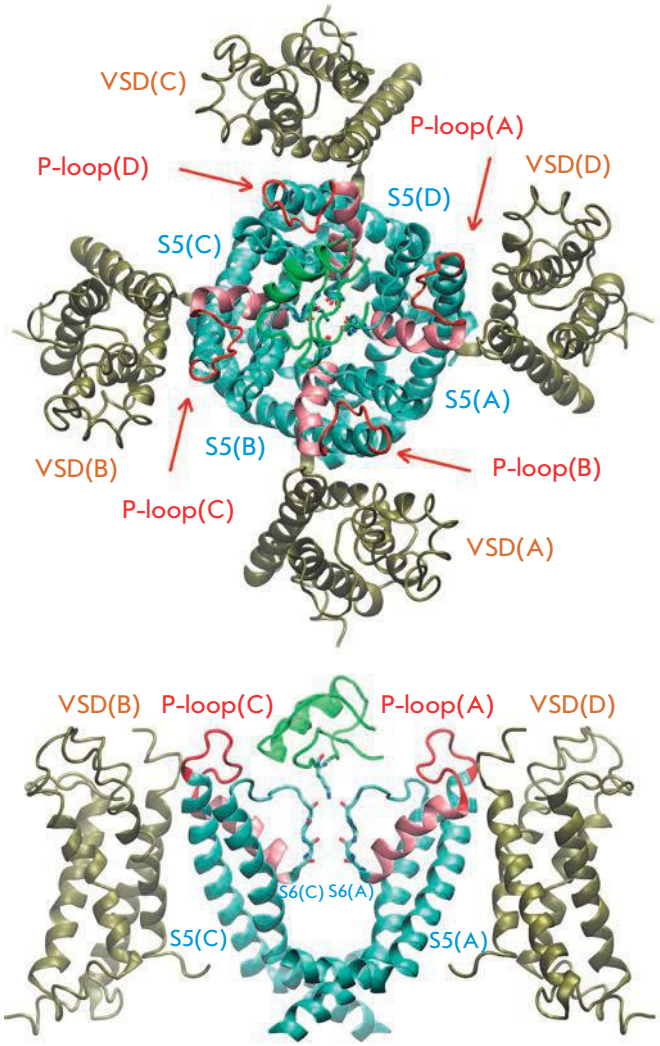


Fig. 5. Crystallographic structure of charybdotoxin in complex with the chimaeric $K_V$1.2-2.1 channel (PDB code 4JTA) is shown in a ribbon representation (top view and side view). For clarity, only two α-subunits are shown. The voltage-sensitive domain (VSD) is shown in olive green. The toxin is shown in bright green, and its residue K27 projecting into the pore is shown in a rod representation. The other designations are the same as in *Fig. 3*. The letters A, B, C, and D denote the subunits of the channel.

tal structure demonstrated that the chimaeric channel does not undergo conformational changes upon toxin binding [18].

Studies of the structures of pore-blocking toxins such as charybdotoxin in complex with Kv channels (mutated KcsA and chimaeric $K_V$1.2–2.1) reveal that the binding involves most of the interactions between amino acid residues of the toxin molecule and the channel loops. Importantly, the P-loops exhibit the widest variation across domains in $K_V$-channels and it is highly likely that it is this variation that accounts for the varying degrees of toxin affinity to the target channels.

## HOMOLOGY MODELING OF POTASSIUM CHANNELS AND THEIR COMPLEXES

In the case when only a few potassium channels have atomic resolution models in free form and in complex with pore blockers, homology modeling happens to contribute to the construction of a structure of target $K_V$-channels and their complexes. This approach [46] relies on modeling a three-dimensional structure of the target protein using an experimentally determined structure of a related protein (the template). The steps in homology modeling are the following [47]:

Template identification: search for homologous proteins with elucidated structures, for example, using BLAST [48] or FASTA [49];

Target-template amino acid sequence alignment, for example, using CLUSTALW [50]; and

Model generation by threading the sequence on the template sequence, replacing residues and building missing parts, for example, using the Modeller software [51].

Fortunately, the Swiss-model online server [52] can run all three steps in automated mode.

An important requirement for model generation is that the sequences should have more than 20–30% sequence identity [53]. The pore domains of potassium channels readily meet this criterion: the sequence identity of these domains of $K_V$-channels share over 80%, with most of the variability located in the small pore loop. The atomic resolution of $K_V$1.2–2.1 bound to charybdotoxin [18] is in good agreement with other experimental findings, which indicates that the VSD-domain is not involved in the binding. For this reason, modeling of complex structures of pore blockers with $K_V$-channels is only focused on pore domains.

The sequence homology of the pore domains of $K_V$-channels and the prokaryotic KcsA channel is approximately 30%, thus making KcsA, together with other structures, an optimal template for modeling studies [55, 69, 70, 72] (Table. 2). This is justified by experimental measurements demonstrating that chimaeric KcsA-Kv1.x channels (KcsA, in which the P-loop is replaced by the P-loop of Kv1.x, x = 1, 2, 3, 6) retain affinity, characteristic of Kv1.x channels [73–75].

Homology modeling is used in conjunction with Brownian dynamics (BD), molecular docking, and molecular dynamics (MD) simulations.

## BROWNIAN DYNAMICS

A Brownian dynamics is a case of stochastic dynamics treating the movement of molecules as solid bodies under the influence of external perturbations and friction

forces which simulate the interaction with solvent molecules and random forces. BD has been widely used for simulating ion transport [76, 77] and, to some extent, binding of toxins to ion channels [78, 79]. It is assumed that channels and blockers have rigid structures, the solvent is implicit, and the cell membrane is represented as an idealized dielectric slab [20]. Brownian dynamics simulations with these key assumptions allow one to decrease computational costs and speed up the overall process for macroscopic effects to be detected [80].

Using Brownian dynamics simulations, the predicted structure of Lq2 toxin (*Table 1*) bound to mutated KcsA revealed the key amino acids of the toxin responsible for binding [78]. Since this model assumes that the blocker and channels have rigid structures, the conformational flexibility of the blocker was simulated based on all 22 structure variants available for Lq2 in the PDB-file. One variant yielded a model consistent with experimental observations. The channel flexibility was excluded from the analysis.

Structural insights into conformational flexibility in Brownian dynamics simulations could be gained by incorporating MD to the protein structures, as was successfully applied to $K_V1.3$ in complex with agitotoxin, charybdotoxin, kaliotoxin, margatotoxin, and noxiustoxin [79]. Electrostatic energy calculations in complexes have been shown to tightly correlate with logarithms of dissociation constants ($R^2 = 0.60$). However, this was not true for kaliotoxin, which can be explained by an inappropriate structure (PBD ID 1KTX), showing poor structural alignment with agitotoxin and OSK1. Refined kaliotoxin structures (PBD ID 1XSW, 3ODV) do not have this drawback.

## MOLECULAR DOCKING

Molecular docking is a computational technique that predicts the preferred orientation and conformation of a ligand that binds to a target binding site. Toxins in complex with potassium channels have been widely explored in molecular docking studies [38, 62, 80].

In a protein-protein docking algorithm, one molecule is fixed in space and the other is translated and rotated around, exploring possible orientations and conformations. The quality of each possible fit is calculated by a scoring function that takes into consideration complementarity, electrostatic interactions, van der Waals repulsion, desolvation energy, internal energy strain (deformation of valence bonds), hydrogen bonding, and aromatic group interactions.

Molecular docking is carried out using a suite of docking tools, such as AutoDock (http://autodock.scripps.edu/) [81], RosettaDock [82], BiGGER [83], HADDOCK (http://haddock.science.uu.nl/) [84], or ZDOCK (http://zdock.umassmed.edu/) [85]. The latter three software are the most common for channel blocker complexes simulations [37, 86, 87].

A distinctive feature of HADDOCK is that it performs docking of large and flexible peptide ligands. This software was used to develop a comparative docking protocol predicting the selectivity profiles of α-KTx toxins [87]. Channel-toxins interactions were successfully modeled using this protocol. However, the HADDOCK scoring function failed to accurately predict affinity scores, which impedes correct ranking.

Molecular docking can be employed to investigate the conformational flexibility of toxins. Corzo *et al* attempted *in silico* modeling of the interactions of Css20, a novel voltage-dependent K+-channel blocker, with potassium channels [58]. A total of over 1,000,000 structures were generated, of which the 2,000 best ranking complexes were visually inspected. Unfortunately, this approach is computationally laborious and has insufficient scoring functions, which generate multiple top scoring hits, among which the best scoring pose is ranked inaccurately. A possible solution to this problem is small-scale screening, followed by molecular dynamics simulations and determination of binding constants through free energy calculations [20].

## MOLECULAR DYNAMICS

In molecular dynamics simulations, the temporal evolution of interacting atoms or particles is determined by numerically solving the equations of motion. The accuracy of MD algorithms depends on force fields: i.e., potential energy functions and parameters deduced from experimental data and quantum-mechanical measurements. Current generation force fields provide energy estimates with remarkable accuracy [88]. Full-atomic force fields such as OPLS-AA and CHARMM variants take into account all atoms in the system. Alternatively, force fields with united atoms like GROMOS and OPLS-UA treat heavy nonpolar atoms (carbon, sulphur) and related hydrogen atoms as single interaction entities [89].

The NAMD software package [90], together with CHARMM [91], including variants such as CHARMM22, CHARMM27 and CHARMM36, has been the most commonly used for $K_V$-channel modeling (Table. 3). The CHARMM27 force field is optimized for DNA, RNA and lipids, and in combination with CHARMM22, for DNA-protein interactions. Although CHARMM27 seems to be not intended to simulate protein-protein interactions, the free energy binding estimates generated by this software are in good agreement with experimental observations [60, 66, 92], (*Table 3*). Unlike CHARMM22, CHARMM36 has been extended to incorporate optimized parameters for the conformational space upon protein folding, protein as-

Table 3. Comparison of computed ($\Delta G_{calc}$) and empirical ($\Delta G_{exp}$) free energy values for $K_V$-channels bound to pore blocking peptides

| Channel (pdb-code of template) | Toxinн (pdb-code of structure or template) | MD force field | $\Delta G_{calc}$, kcal/mol | $\Delta G_{exp}$, kcal/mol | reference |
|---|---|---|---|---|---|
| $K_V$1.1 (2R9R) | HsTx1 (1QUZ) | NAMD, CHARMM36 | -10.1 ± 0.6 | -11.1 ± 0.1 | [68] |
| | ShK (1ROO) | NAMD, CHARMM22 | -14.3 ± 1.1 | -14.7 ± 0.1 | [63] |
| | ShK-K-amide (1ROO) | NAMD, CHARMM22 | -11.8 ± 1 | -12.3 ± 0.1 | [64] |
| | ShK-K18A (1ROO) | NAMD, CHARMM27 | -11.7 ± 0.7 | -11.3 ± 0.1 | [66] |
| $K_V$1.2 (2R9R) | HsTx1 (1QUZ) | NAMD, CHARMM36 | -8.9 ± 0.6 | -9.5 ± 0.1 | [68] |
| | ShK (1ROO) | NAMD, CHARMM22 | -10.1 ± 1.1 | -11 ± 0.1 | [63] |
| | MTx (1TXM) | NAMD, CHARMM36 | -12.6 | -12.6 | [92] |
| $K_V$1.3 (3LUT) | ChTx (2A9H) | NAMD, CHARMM27 | -10.4 | -12.5 | [60] |
| | MgTx (1MTX) | NAMD, CHARMM36 | -11.5 | -13.9 | [62] |
| $K_V$1.3 (2A79) | ChTx (2CRD) | GROMACS, OPLS-AA | -26 ± 1 | -11.4 ± 0.2 | [59] |
| $K_V$1.3 (2R9R) | HsTx1 (1QUZ) | NAMD, CHARMM36 | -14.0 ± 0.6 | -14.9 ± 0.2 | [68] |

sembly into complexes, and the relevant conformational changes [93].

Current MD simulations allow one to investigate toxin-channel complex interactions with the lipid membranes which affect the predicted structure of a toxin bound to the VSD-domain of a channel [94]. The lipid bilayer *per se* is not relevant for modeling complexes of pore-blocking peptides [55]. This is in good agreement with experimental data and calculations of complex formation free energies optimized by a MD analysis [95, 96]. Discarding the lipid-protein interactions helps reduce the computational burden and allows one to extend MD trajectories and the computational space. Another approach to addressing computational challenges is the use of an implicit solvent model, in particular, a generalized Born solvation model. Regardless of the solvation model utilized, MD simulations are carried out in the range of 15–20 [68, 92] to 40–50 ns trajectories [62, 97].

In certain cases, complex formation is examined using steered MD. These simulations are based on the pulling of a number of toxin residues to the corresponding residues of the channel, provided that these pairs of residues are key determinants in the complexation. The advantage of this method is that it considers experimental data on the interacting residues, the contacts of which are assumed more accurate. Steered MD has been well used in studies on a $K_V$1.2 channel complex with maurotoxin [92] and a $K_V$1.3 channel complex with margatoxin and chongotoxin [62].

## ENERGY CALCULATIONS OF CHANNEL-TOXIN COMPLEXES

The quality of predicted protein structures is validated by the free-energy change ΔG. These calculations are of paramount importance for determining the energetic favorability of a given biochemical reaction, as well as ligand binding to receptors and downstream conformational changes [98].

Binding free energies of ligand binding to potassium channels are determined by the potential of mean force calculations using an umbrella sampling scheme for conformational states [99]. This technique predicts ΔG values that are consistent with experimental data (*Table 3*), thus suggesting the high accuracy of predictions made by a numeric model and utility for constructing peptide blockers with the desired properties. Khabiri *et al* [59] obtained ΔG values which were at least two-fold lower than the calculated ones due to the differences in the ionic strength in computational and experimental conditions. Alternatively, the discrepancy may be explained by the lower accuracy of the OPLS-AA force field versus CHARMM variants (Table. 3).

Another, but less commonly used, approach to free energy estimation is MM-PBSA (molecular mechanics/Poisson–Boltzmann surface area), which combines the molecular mechanics potential energy in vacuum and the Poisson–Boltzmann surface area method for calculating free energies of solvation. The MM-PBSA method is incorporated in AMBER [100] and GROMACS [101] and is qualitatively consistent with experimental measurements in the case of free energies of toxin binding to channels [102].

## THE USAGE OF MOLECULAR MODELING TECHNIQUES

Modeling of the structures of $K_V$-channels in complex with naturally occurring and chemically designed peptide blockers provides valuable insights into structural and interactional properties, key atoms between the

two docked structures, and could aid in understanding the observed potency and range of activities for pore blockers of interest.

Experimental findings on the binding of intact and mutant Pi1 to $K_V$1.2 were explained when these complexes were homology modeled using maurotoxin (*Table 1*) and KcsA template structures [86]. After a series of docking calculations, the peptide residues R5, R12, R28, and K31 were found to contribute in stabilizing the complex.

A similar approach was followed in conducting a structural characterization of the interface of $K_V$1.2 in complex with cobatoxin (*Table 1*) and its synthetic analog ACoTX1, which contains T7P and D9Q substitutions [37]. The inspection revealed that the orientation of the dipole moment does not much contribute to its selectivity, leading to a conclusion that molecular modeling is particularly important in screening for toxin analogs with high affinity and/or selectivity.

Notably, docking experiments clarified the remarkable selectivity of Vm24 and its analogs towards $K_V$1.3 [38]. These selectivity factors were assigned to tight contacts between the N-terminal portion of Vm24 and the channel molecule, which is not the case for other α-KTx family toxins (*Fig. 2*).

Jin *et al* [55] explored the space of possible poses of ShK in complex with $K_V$1.3 by combining molecular docking and molecular dynamics methods and discovered two favorable interaction states. In the first pose, the channel selectivity filter was occluded with the K22 residue; in the other, with the R24 residue. MM-PBSA calculations of ΔΔG upon substitutions to Ala changes in the peptide molecule, together with empirical data on complex dissociation constants, favored the second model with the R24 residue.

The mutant cycle analysis has emerged as a valuable tool for the study of toxin-channel complexes. This approach was first applied to characterize Shaker channel binding sites relative to the agitoxin 2 structure [103]. It is logically clear that substituting residues in the structures of a toxin and a channel will affect the dissociation constant if the targeted residues are key to binding that can be defined by the coupling coefficient. Knowledge of the details of the key contacts between the toxin and channel allows one to model complex structures in docking simulations. Owing to algorithm advances in free energy calculations, mutant cycle analysis has become a well established approach commonly used in docking studies [55, 57, 95, 102, 104].

Yi *et al* [105] reported on a specific binding of maurotoxin to the Kv1.2 channel explored by molecular dynamics and molecular docking screening. Calculation of the binding free energy by MM-PBSA upon substitutions of Ala residues based on experimental findings identified the most plausible candidate structure with the key residues located at positions K23, I25, and Y32 in the toxin and R254, F359, P360, D379, V381, and T383 in the channel.

Molecular modeling of the spatial structures of ADWX-1 in complex with $K_V$1.1 and $K_V$1.3 [106] revealed three favorable pore loop conformations in complex with pore blockers: open, half-open/half-closed, and closed. In the open conformation of pore loops, the peptide interacts with the residues outside the selectivity filter and the pore loop has no effect on the toxin channel interface. This is how, in accord with reference [105], the maurotoxin peptide seems to bind to the $K_V$1.2 channel. When the pore loop conformation is half-open/half-closed, the loops play a minor role in stabilizing the interaction, as previously shown for ADWX-1 in complex with $K_V$1.1 and $K_V$1.3. In the closed structure, the binding interface is formed by both the pore loops and the region around the selectivity filter, driving affinity and selectivity for toxin binding.

It has been recently shown [60] that the contribution of electrostatic interactions dominates over the contribution of van der Waals forces in complexes of charybdotoxin, OSK1, and ShK with $K_V$1.3. The critical amino acid residues dictating the toxin orientation were lysine and arginine: K27 and R25 in charybdotoxin, K27 and R24 in OSK1, K22, and R11 in ShK (*Fig. 2*). Binding energy values calculated by mean force potentials were found to be in agreement with published experimental studies (*Table 3*). Unfortunately, providing high accuracy imposes a computational burden, which limits the application of numerical modeling of binding energies and highlights the need for improved computational efficiency. Of note, the findings reported by Jin *et al* and Chen *et al* on ShK in complex with Kv1.3 are not consistent [55, 62] and require further clarification.

MD screening for toxin-induced conformational changes in the chimaeric KcsA-$K_V$1.3 channel in complex with kaliotoxin [72] led to a model in which the Y78 residue of the toxin and D80 residue of the channel changed positions following interface formation. The simulation was validated using NMR measurements.

The nascent research efforts to study potassium channel blockers led to an idea [107], which matured and expanded afterwards, that the ability of toxins from different species to target $K_V$-channels is attributed to the presence of the functional dyad: a lysine residue that recognizes the selectivity filter and a hydrophobic residue (Tyr, Phe or Leu) 6–7 Å away from SF. With advances in computational techniques, including molecular modeling, the specificity for $K_V$-channel binding was shown to depend on other amino

acid residues. The extent to which the functional dyad contributes to the binding energy also varies depending on toxin fold and other amino acid resides [108]. Molecular modeling data clearly demonstrate that the toxin-channel interface is caused by contacts between multiple residues. This network of binding interactions differs not only among groups and subfamilies, but even among highly homologous peptides.

Improved selectivity of $K_V$-channel blockers has been the focus of pharmacological studies, because naturally occurring toxins have the peculiarity of possessing affinity for a range of channel types. The identification of the differences between interacting resides of the toxin and channel, as determined by molecular modeling, offers much opportunity for site-directed mutagenesis to modulate toxin binding to a given channel.

The Css20 toxin acts on $K_V$1.2 and $K_V$1.3 versus $K_V$1.1 and $K_V$1.4 [58]. Molecular modeling showed that the key amino acid residues of $K_V$1.2 and $K_V$1.3, which are in contact with Css20, are located around the selectivity filter and in the P-loop (7 out of 8 residues differ among the channels). The K28 residue was found to be crucial for binding $K_V$1.2 and $K_V$1.3, and the Q11, I30, K33, and Y37 residues form favorable contacts with only $K_V$1.2. In addition, new contacts may arise with $K_V$1.2 upon substitution of A19 and A20 for the positively charged Arg or Lys. It is suggested that tailored mutations can enhance the selectivity of Css20 analogs for $K_V$1.2 and $K_V$1.3.

The same approach based on MD and the potentials of the mean force was applied to the bound complex OSK1 and $K_V$1.1– $K_V$1.3 channels in the search for amino acid substitutions increasing the activity of the peptide [65]. The authors revealed that K9S and S11R could lead to enhanced potency in blocking Kv1.3 with decreased activity toward $K_V$1.1 and $K_V$1.2. The mutant OSK was 10,000-fold more specific for Kv1.3 than for Kv1.1 and Kv1.2. The potency of OSK1 for Kv1.3 was increased by 100-fold.

In a site-directed mutagenesis study, Han *et al* [102] introduced the G11R, I28T, and D33H substitutions into the BmKTX peptide to obtain a highly potent $K_V$1.3-blocking peptide, named ADWX-1 [102]. The functional residues of ADWX-1 in complex with $K_V$1.3 were identified using a structural model of the ADWX-1-Kv1.3 complex constructed by molecular modeling. Energy binding estimates for ADWX-1 and its variants (R23A, F24A, K26A, N29A, T35A) established an important role for positively charged residues in recognizing $K_V$1.3. In addition, the R23A and F24A substitutions provide steric hindrance to the contact of the key K26 residue with the channel pore. The experimentally determined affinity of ADWX-1 for $K_V$1.3 was increased by 100-fold relative to the native BmKTX peptide. The selectivity of ADWX-1 toward Kv1.3 was increased by 340-fold and $> 10^5$ -fold versus $K_V$1.1 and $K_V$1.2.

## CONCLUSION

Over 30 wide-scale studies utilizing computational simulations have been carried out to provide insights into the structure of potassium channels alone and in complex with toxins. *In silico* approaches contributed to the elucidation of toxin-channel interactions, revealed important molecular clues on the mechanisms of selectivity and affinity of toxins, and laid the basis for a rational design of pore-blocking peptides with tailored properties.

The most commonly used modeling approach to resolving toxin-channel structures involves homology modeling, molecular docking, and molecular dynamics techniques, which could be combined with MM-PBSA free energy computations or the potentials of the mean force. Each algorithm is executed in a defined computational context of parameters depending on an investigator's preferences and experimental design. Currently, there is a clear trend away from Brownian dynamics and implicit solvation approaches to simulations in explicit water. MM-PBSA free energy computations are discarded in favor of the potentials of the mean force.

Further improvement in molecular modeling algorithms requires the availability of high-resolution structures of channels from major families and/or toxin-channel complexes. However, the accuracy of the modeling depends on force fields, high throughput docking algorithms, and free-energy calculations to determine the binding free energies of toxins.

Due to their biological and medical significance, potassium channels offer great promise to encourage novel computational approaches that will minimize the computational burden and cost.

*This work was supported by the Russian Scientific Foundation, grant № 14-14-00239.*

REFERENCES

1. Wulff H., Zhorov B.S. // Chem. Rev. 2008. V. 108. № 5. P. 1744–1773.
2. Haddy F.J., Vanhoutte P.M., Feletou M. // Am. J. Physiol. Regul. Integr. Comp. Physiol. 2006.V. 290. № 3. P. R546–R552.
3. Tian C., Zhu R., Zhu L., Qiu T., Cao Z., Kang T. // Chem. Biol. Drug Des. 2014. V. 83. № 1. P. 1–26.
4. Maljevic S., Lerche H. // J. Neurol. 2013. V. 260. № 9. P. 2201–2211.
5. Castle N. // Expert Opin. Ther. Pat. 2010. V. 20. № 11. P. 1471–1503.

6. Huang X., Jan L.Y. // J. Cell Biol. 2014. V. 206. № 2. P. 151–162.
7. Grizel A.V, Glukhov G.S., Sokolova O.S. // Acta Naturae. 2014. V. 6. № 23. P. 10–26.
8. Shieh C.C., Coghlan M., Sullivan J.P., Gopalakrishnan M. // Pharmacol. Rev. 2000. V. 52. P. 557–594.
9. Jan L.Y., Jan Y.N. // J. Physiol. 2012. V. 590(Pt 11). P. 2591–2599.
10. Volkers L., Rook M.B., Das J.H., Verbeek N.E., Groenewegen W.A., van Kempen M.J., Lindhout D., Koeleman B.P. // Neurosci. Lett. 2009. V. 462. № 1. P. 24–29.
11. Angulo E., Noé V., Casadó V., Mallol J., Gomez-Isla T., Lluis C., Ferrer I., Ciudad C.J., Franco R.J. // Neurochem. 2004. V. 91. № 3. P. 547–557.
12. Martin C.A., Matthews G.D., Huang C.L. // Heart. 2012. V. 98. № 7. P. 536–543.
13. Giudicessi J.R., Ye D., Kritzberger C.J., Nesterenko V.V., Tester D.J., Antzelevitch C., Ackerman M.J. // Hum. Mutat. 2012. V. 33. № 6. P. 989–997.
14. Xu R., Cao M., Wu X., Wang X., Ruan L., Quan X., Lü C., He W., Zhang C. // Clin. Immunol. 2012. V. 142. № 2. P. 209–217.
15. Chhabra S., Chang S.C., Nguyen H.M., Huq R., Tanner M.R., Londono L.M., Estrada R., Dhawan V., Chauhan S., Upadhyay S.K., et al. // FASEB J. 2014. V. 28. P. 3952–3964.
16. Zhuang G.Q., Wu W., Liu F., Ma J.L., Luo Y.X., Xiao Z.X., Liu Y., Wang W., He Y. // Biochem. Biophys. Res. Commun. 2009. V. 379. № 4. P. 812–816.
17. Yu L., Sun C., Song D., Shen J., Xu N., Gunasekera A., Hajduk P.J., Olejniczak E.T. // Biochemistry. 2005. V. 44. № 48. P. 15834–15841.
18. Banerjee A., Lee A., Campbell E., Mackinnon R. // Elife. 2013. V. 2013. № 2. P. 1–22.
19. Chi V., Pennington M.W., Norton R.S., Tarcha E.J., Londono L.M., Sims-Fahey B., Upadhyay S.K., Lakey J.T., Iadonato S., Wulff H., et al. // Toxicon. 2012. V. 59. № 4. P. 529–546.
20. Gordon D., Chen R., Chung S.-H. // Physiol. Rev. 2013. V. 93. № 2. P. 767–802.
21. Kuang Q., Purhonen P., Hebert H. // Cell. Mol. Life Sci. 2015. V. 72. P. 3677–3693.
22. MacKinnon R. // FEBS Lett. 2003. V. 555. № 1. P. 62–65.
23. Bontems F., Gilquin B., Roumestand C., Ménez A., Toma F. // Biochemistry. 1992. V. 31. № 34. P. 7756–7764.
24. Renisio J.G., Lu Z., Blanc E., Jin W., Lewis J.H., Bornet O., Darbon H. // Proteins Struct. Funct. Genet. 1999. V. 34. № 4. P. 417–426.
25. Dauplais M., Gilquin B., Possani L.D., Gurrola-Briones G., Roumestand C., Ménez A. // Biochemistry. 1995. V. 34. № 51. P. 16563–16573.
26. Johnson B.A., Stevens S.P., Williamson J.M. // Biochemistry. 1994. V. 33. № 50. P. 15061–15070.
27. Pragl B., Koschak A., Trieb M., Obermair G., Kaufmann W.A., Gerster U., Blanc E., Hahn C., Prinz H., Schütz G., et al. // Bioconjug. Chem. 2002. V. 13. № 3. P. 416–425.
28. Lange A., Becker S., Seidel K., Giller K., Pongs O., Baldus M. // Angew. Chem. Int. 2005. V. 44. № 14. P. 2089–2092.
29. Krezel A.M., Kasibhatla C., Hidalgo P., MacKinnon R., Wagner G. // Protein Sci. 1995. V. 4. № 8. P. 1478–1489.
30. Renisio J.G., Romi-Lebrun R., Blanc E., Bornet O., Nakajima T., Darbon H. // Proteins Struct. Funct. Genet. 2000. V. 38. № 1. P. 70–78.
31. Jaravine V.A., Nolde D.E., Reibarkh M.J., Korolkova Y.V., Kozlov S.A., Pluzhnikov K.A., Grishin E.V., Arseniev A.S. // Biochemistry. 1997. V. 36. № 6. P. 1223–1232.
32. Carrega L., Mosbah A., Ferrat G., Beeton C., Andreotti N., Mansuelle P., Darbon H., De Waard M., Sabatier J.M. // Proteins Struct. Funct. Genet. 2005. V. 61. № 4. P. 1010–1023.
33. Blanc E., Sabatier J.M., Kharrat R., Meunier S., el Ayeb M., Van Rietschoten J., Darbon H. // Proteins Struct. Funct. Genet. 1997. V. 29. № 3. P. 321–333.
34. Savarin P., Romi-Lebrun R., Zinn-Justin S., Lebrun B., Nakajima T., Gilquin B., Menez A. // Protein Sci. 1999. V. 8. № 12. P. 2672–2685.
35. Guijarro J.I., M'Barek S., Gómez-Lagunas F., Garnier D., Rochat H., Sabatier J.M., Possani L., Delepierre M. // Protein Sci. 2003. V. 12. № 9. P. 1844–1854.
36. Wu G., Li Y., Wei D., He F., Jiang S., Hu G., Wu H. // Biochem. Biophys. Res. Commun. 2000. V. 276. № 3. P. 1148–1154.
37. Jouirou B., Mosbah A., Visan V., Grissmer S., M'Barek S., Fajloun Z., van Rietschoten J., Devaux C., Rochat H., Lippens G., et al. // Biochem. J. 2004. V. 377. Pt 1. P. 37–49.
38. Gurrola G.B., Hernández-López R.A., Rodríguez de la Vega R.C., Varga Z., Batista C.V., Salas-Castillo S.P., Panyi G., del Río-Portilla F., Possani L.D. // Biochemistry. 2012. V. 51. № 19. P. 4049–4061.
39. Tudor J.E., Pallaghy P.K., Pennington M.W., Norton R.S. // Nat. Struct. Biol. 1996. V. 3. № 4. P. 317–320.
40. Berndt K.D., Güntert P., Wüthrich K. // J. Mol. Biol. 1993. V. 234. № 3. P. 735–750.
41. Romi-Lebrun R., Martin-Eauclaire M.F., Escoubas P., Wu F.Q., Lebrun B., Hisada M., Nakajima T. // Eur. J. Biochem. 1997. V. 245. № 2. P. 457–464.
42. Zhu S., Peigneur S., Gao B., Luo L., Jin D., Zhao Y., Tytgat J. // Mol. Cell. Proteomics. 2011. V. 10. № 2. P. M110.002832.
43. Long S.B., Campbell E.B., Mackinnon R. // Science. 2005. V. 309. № 5736. P. 897–903.
44. Chen X., Wang Q., Ni F., Ma J. // Proc. Natl. Acad. Sci. USA. 2010. V. 107. № 25. P. 11352–11357.
45. Long S.B., Tao X., Campbell E.B., MacKinnon R. // Nature. 2007. V. 450. № 7168. P. 376–382.
46. Giorgetti A., Carloni P. // Curr. Opin. Chem. Biol. 2003. V. 7. № 1. P. 150–156.
47. Cavasotto C.N., Phatak S.S. // Drug Discovery Today. 2009. V. 14. № 13–14. P. 676–683.
48. Altschul S.F., Gish W., Miller W., Myers E.W., Lipman D.J. // J. Mol. Biol. 1990. V. 215. № 3. P. 403–410.
49. Pearson W.R. // Methods Enzymol. 1990. V. 183. P. 63–98.
50. Larkin M.A., Blackshields G., Brown N.P., Chenna R., McGettigan P.A., McWilliam H., Valentin F., Wallace I.M., Wilm A., Lopez R., et al. // Bioinformatics. 2007. V. 23. № 21. P. 2947–2948.
51. Sali A., Blundell T.L. // J. Mol. Biol. 1993. V. 234. № 3. P. 779–815.
52. Schwede T., Kopp J., Guex N., Peitsch M.C. // Nucl. Acids Res. 2003. V. 31. № 13. P. 3381–3385.
53. Baker D., Sali A. // Science. 2001. V. 294. № 5540. P. 93–96.
54. Doyle D.A., Morais Cabral J., Pfuetzner R.A., Kuo A., Gulbis J.M., Cohen S.L., Chait B.T., MacKinnon R. // Science. 1998. V. 280. № 5360. P. 69–77.
55. Jin L., Wu Y. // J. Chem. Inf. Model. 2007. V. 47. № 5. P. 1967–1972.
56. Jiang Y., Lee A., Chen J., Ruta V., Cadene M., Chait B.T., MacKinnon R. // Nature. 2003. V. 423. № 423(6935). P. 33–41.
57. Visan V., Fajloun Z., Sabatier J.M., Grissmer S. // Mol. Pharmacol. 2004. V. 66. № 5. P. 1103–1112.
58. Corzo G., Papp F., Varga Z., Barraza O., Espino-Solis P.G., Rodríguez de la Vega R.C., Gaspar R., Panyi G., Possani L.D. // Biochem. Pharmacol. 2008. V. 76. № 9. P. 1142–1154.

59. Khabiri M., Nikouee A., Cwiklik L., Grissmer S., Ettrich R. // J. Phys. Chem. B. 2011. V. 115. № 39. P. 11490–11500.
60. Chen R., Robinson A., Gordon D., Chung S.H. // Biophys. J. Biophys. Soc. 2011. V. 101. № 11. P. 2652–2660.
61. Chen R., Chung S.-H. // Biophys. J. Biophys. Soc. 2013. V. 105. № 8. P. 1829–1837.
62. Chen R., Chung S.-H. // Toxins (Basel). 2014. V. 6. № 7. P. 2149–2161.
63. Rashid M.H., Kuyucak S. // J. Phys. Chem. B. 2012. V. 116. № 16. P. 4812–4822.
64. Pennington M.W., Rashid M.H., Tajhya R.B., Beeton C., Kuyucak S., Norton R.S. // FEBS Lett. 2012. V. 586. № 22. P. 3996–4001.
65. Chen R., Chung S.H. // Biochemistry. 2012. V. 51. № 9. P. 1976–1982.
66. Rashid M.H., Heinzelmann G., Huq R., Tajhya R.B., Chang S.C., Chhabra S., Pennington M.W., Beeton C., Norton R.S., Kuyucak S. // PLoS One. 2013. V. 8. № 11. P. e78712.
67. Rashid M.H., Huq R., Tanner M.R., Chhabra S., Khoo K.K., Estrada R., Dhawan V., Chauhan S., Pennington M.W., Beeton C., et al. // Sci. Rep. 2014. V. 4. P. 4509.
68. Rashid M.H., Kuyucak S. // J. Phys. Chem. B. 2014. V. 118. № 3. P. 707–716.
69. Chen P.C., Kuyucak S. // Biophys. J. Biophys. Soc. 2009. V. 96. № 7. P. 2577–2588.
70. Chen P.C., Kuyucak S. // Biophys. J. Biophys. Soc. 2011. V. 100. № 10. P. 2466–2474.
71. Kohl B., Rothenberg I., Ali S.A., Alam M., Seebohm G., Kalbacher H., Voelter W., Stoll R. // Toxicon. 2015. V. 101. P. 70–78.
72. Zachariae U., Schneider R., Velisetty P., Lange A., Seeliger D., Wacker S.J., Karimi-Nejad Y., Vriend G., Becker S., Pongs O., et al. // Structure. 2008. V. 16. № 5. P. 747–754.
73. Legros C., Pollmann V., Knaus H.G., Farrell A.M., Darbon H., Bougis P.E., Martin-Eauclaire M.F., Pongs O. // J. Biol. Chem. 2000. V. 275. № 22. P. 16918–16924.
74. Kudryashova K.S., Nekrasova O.V., Kuzmenkov A.I., Vassilevski A.A., Ignatova A.A., Korolkova Y.V., Grishin E.V., Kirpichnikov M.P., Feofanov A.V. // Anal. Bioanal. Chem. 2013. V. 405. № 7. P. 2379–2389.
75. Kuzmenkov A.I., Vassilevski A.A., Kudryashova K.S., Nekrasova O.V., Peigneur S., Tytgat J., Feofanov A.V., Kirpichnikov M.P., Grishin E.V. // J. Biol. Chem. 2015. V. 290. № 19. P. 12195–12209.
76. Turchenkov D.A., Bystrov V.S. // J. Phys. Chem. B. 2014. V. 118. № 31. P. 9119–9127.
77. Kurczynska M., Kotulska M. // Acta Bioeng. Biomech. 2014. V. 16. № 4. P. 107–116.
78. Cui M., Shen J., Briggs J.M., Luo X., Tan X., Jiang H., Chen K., Ji R. // Biophys. J. 2001. V. 80. № 4. P. 1659–1669.
79. Yu K., Fu W., Liu H., Luo X., Chen K.X., Ding J., Shen J., Jiang H. // Biophys. J. 2004. V. 86. № 6. P. 3542–3555.
80. Chung S.-H., Kuyucak S. // Eur. Biophys. J. 2002. V. 31. № 4. P. 283–293.
81. Morris G.M., Goodsell D.S., Halliday R.S., Huey R., Hart W.E., Belew R.K., Olson A.J. // J. Comput. Chem. 1998. V. 19. № 14. P. 1639–1662.
82. Gray J.J., Moughon S., Wang C., Schueler-Furman O., Kuhlman B., Rohl C.A., Baker D. // J. Mol. Biol. 2003. V. 331. № 1. P. 281–299.
83. Palma P.N., Krippahl L., Wampler J.E., Moura J.J. // Proteins. 2000. V. 39. № 4. P. 372–384.
84. Dominguez C., Boelens R., Bonvin A.M. // J. Am. Chem. Soc. 2003. V. 125. № 7. P. 1731–1737.
85. Pierce B.G., Wiehe K., Hwang H., Kim B.H., Vreven T., Weng Z. // Bioinformatics. 2014. V. 30. № 12. P. 1771–1773.
86. Mouhat S., Mosbah A., Visan V., Wulff H., Delepierre M., Darbon H., Grissmer S., De Waard M., Sabatier J.M. // Biochem. J. 2004. V. 377. Pt 1. P. 25–36.
87. Chen P.C., Kuyucak S. // Toxins. 2012. V. 4. № 2. P. 110–138.
88. Orozco M. // Chem. Soc. Rev. 2014. V. 43. № 14. P. 5051–5066.
89. Tang X., Koenig P.H., Larson R.G. // J. Phys. Chem. B. 2014. V. 118. № 14. P. 3864–3880.
90. Phillips J.C., Braun R., Wang W., Gumbart J., Tajkhorshid E., Villa E., Chipot C., Skeel R.D., Kalé L., Schulten K. // J. Comput. Chem. 2005. V. 26. № 16. P. 1781–1802.
91. Brooks B.R., Bruccoleri R.E., Olafson B.D., States D.J., Swaminathan S., Karplus M. // J. Comput. Chem. 1983. V. 4. № 2. P. 187–217.
92. Chen R., Chung S.H. // PLoS One. 2012. V. 7. № 10. P. 1–8.
93. Best R.B., Zhu X., Shim J., Lopes P.E., Mittal J., Feig M., Mackerell A.D. Jr. // J. Chem. Theory Comput. 2012. V. 8. № 9. P. 3257–3273.
94. Bemporad D., Sands Z.A., Wee C.L., Grottesi A., Sansom M.S. // Biochemistry. 2006. V. 45. № 39. P. 1844–1855.
95. Eriksson M.A.L., Roux B. // Biophys. J. 2002. V. 83. № 5. P. 2595–2609.
96. Wu Y., Cao Z., Yi H., Jiang D., Mao X., Liu H., Li W. // Biophys. J. 2004. V. 87. № 1. P. 105–112.
97. Almeida D.D., Torres T.M., Barbosa E.G., Lima J.P., de Freitas Fernandes-Pedrosa M. // Biochem. Biophys. Res. Commun. 2013. V. 430. № 1. P. 113–118.
98. Knight J.L., Brooks C.L. // J. Comput. Chem. 2009. V. 30. № 11. P. 1692–1700.
99. Torrie G.M., Valleau J.P. // J. Comput. Phys. 1977. V. 23. № 2. P. 187–199.
100. Salomon-Ferrer R., Case D.A., Walker R.C. // Wiley Interdiscip. Rev. Comput. Mol. Sci. 2013. V. 3. № 2. P. 198–210.
101. Kumari R., Kumar R., Lynn A. // J. Chem. Inf. Model. 2014. V. 54. № 7. P. 1951–1962.
102. Han S., Yi H., Yin S.J., Chen Z.Y., Liu H., Cao Z.J., Wu Y.L., Li W.X. // J. Biol. Chem. 2008. V. 283. № 27. P. 19058–19065.
103. Hidalgo P., Mackinnon R. // Science. 1994. V. 268. № 5208. P. 307–310.
104. Jin L., Wu Y. // J. Mol. Recognit. 2011. V. 24. № 1. P. 101–107.
105. Yi H., Qiu S., Cao Z., Wu Y., Li W. // Proteins Struct. Funct. Genet. 2008. V. 70. № 3. P. 844–854.
106. Yin S.J., Jiang L., Yi H., Han S., Yang D.W., Liu M.L., Liu H., Cao Z.J., Wu Y.L., Li W.X. // J. Proteome Res. 2008. V. 7. № 11. P. 4890–4897.
107. Dauplais M., Lecoq A., Song J., Cotton J., Jamin N., Gilquin B., Roumestand C., Vita C., de Medeiros C.L., Rowan E.G., et al. // J. Biol. Chem. 1997. V. 272. № 7. P. 4302–4309.
108. Mouhat S., De Waard M., Sabatier J.M. // J. Pept. Sci. 2005. V. 11. № 2. P. 65–68.

# Lipid Transfer Proteins As Components of the Plant Innate Immune System: Structure, Functions, and Applications

E. I. Finkina, D. N. Melnikova, I. V. Bogdanov, T. V. Ovchinnikova*
Shemyakin and Ovchinnikov Institute of Bioorganic Chemistry, Miklukho-Maklaya Str. 16/10, 117997, Moscow, Russia
*E-mail: ovch@ibch.ru
Received 05.08.2015


**ABSTRACT** **Among a variety of molecular factors of the plant innate immune system, small proteins that transfer lipids and exhibit a broad spectrum of biological activities are of particular interest. These are lipid transfer proteins (LTPs). LTPs are interesting to researchers for three main features. The first feature is the ability of plant LTPs to bind and transfer lipids, whereby these proteins got their name and were combined into one class. The second feature is that LTPs are defense proteins that are components of plant innate immunity. The third feature is that LTPs constitute one of the most clinically important classes of plant allergens. In this review, we summarize the available data on the plant LTP structure, biological properties, diversity of functions, mechanisms of action, and practical applications, emphasizing their role in plant physiology and their significance in human life.**
**KEYWORDS** **allergens, antimicrobial activity, cross reactivity, plant lipid transfer proteins, lipid binding and transfer, plant defense.**
**ABBREVIATIONS** **LTP – lipid transfer protein; FA – fatty acid; PC – phosphatidylcholine; PI – phosphatidylinositol; PG – phosphatidylglycerol; PRP – pathogenesis-related protein; AMP – antimicrobial peptide; PAMP – pathogen associated molecular pattern; DAMP – damage associated molecular pattern; GPI anchor – glycosylphosphatidylinositol anchor; ROS – reactive oxygen species; SAR – systemic acquired resistance; HR – hypersensitive response; ASIT – allergen-specific immunotherapy.**

## INTRODUCTION

Lipids and their derivatives are involved in a variety of processes, including membrane biogenesis, cell differentiation, intercellular and intracellular signaling, and formation of water-repellent and thermal insulation covers protecting plants from adverse environmental factors; they also function as a storage and source of energy. The proteins involved in the intra- and extracellular transport of lipids play an important role in the lipid metabolism of pro- and eukaryotic cells. In plants, several classes of proteins capable of binding and transferring lipids and their derivatives have been identified: acyl-CoA-binding proteins; glycolipid-transfer proteins; sterol carrier proteins; homologues of the major pollen allergen of birch (*Betula verrucosa*), which is listed in the IUIS allergen database under the name Bet v 1; fatty acid binding proteins; puroindolines; and lipid transfer proteins.

Comparison of the amino acid sequences of the proteins of the listed classes demonstrated no significant structural homology among them. These proteins have an intra- or extracellular localization, relatively low molecular weight (7–30 kDa), a high isoelectric point (pI ~ 9–11), and a compact structure stabilized by disulfide bonds. A common feature of the spatial structure of lipid transfer proteins is a hydrophobic cavity accommodating a ligand-binding site. These proteins reversibly bind lipids and deliver them to their destination. Proteins of some classes have highly specific ligands, while other proteins bind and transfer a wide range of lipids.

LTPs belong to the most functionally important classes of plant proteins that bind and transfer lipids. These proteins were discovered in 1970 and were originally named phospholipid exchange proteins [1], but later they were renamed phospholipid transfer proteins [2]. Further studies showed that not only phospholipids, but other hydrophobic molecules as well may be ligands of such proteins, and, therefore, LTPs were given their present name – non-specific lipid transfer proteins [3].

## STRUCTURAL CHARACTERIZATION OF PLANT LTPS

On the basis of structural organization features, plant LTPs are divided into two subclasses: LTP1s with a molecular weight of 9–10 kDa and LTP2s with a mo-

Comparative characterization of two plant LTP subclasses

| Characteristic | LTP1 | LTP2 |
|---|---|---|
| **MW, kDa** | 9–10 | 6–7 |
| **Number of amino acids (a.a.)** | 90–95 | 65–70 |
| **Conserveda. a.** | C, G, P, R, Y(F) | C, Q, P, Y(F) |
| **–$C^{V}XC^{VI}$– motif** | X – a hydrophilic amino acid residue (usually N) exposed on the protein surface | X – a hydrophobic amino acid residue (usually F) buried inside the protein molecule |
| **Disulfide bond arrangement** | $C^{I}$–$C^{VI}$, $C^{II}$–$C^{III}$, $C^{IV}$–$C^{VII}$, $C^{V}$–$C^{VIII}$ | $C^{I}$–$C^{V}$, $C^{II}$–$C^{III}$, $C^{IV}$–$C^{VII}$, $C^{VI}$–$C^{VIII}$ |
| **Spatial structure** | 4 α-helices, a $3_{10}$-helix fragment, and an unstructured C-terminal loop | 3 α-helices and a region containing a single helix-turn-helix |
| **Hydrophobic cavity** | A tunnel with large and small entrances that is formed by H1, H2, and H3 helices arranged parallel to each other | A triangular hollow box; H1 and H2 helices are arranged parallel to each other; the H3 helix forms an angle of 90° with H2 |
| **Sterol-binding ability** | No | Yes |
| **Amino acid residues interacting with a ligand** | Arg44 and Tyr79 (numeration for rice LTP1) | Phe36, Tyr45, and Tyr48 (numeration for rice LTP2) |
| **Signal peptide, a.a.** | 21–27 | 27–35 |
| **Localization** | Cutin-coated organs (leaves, stems, flowers) | Suberin-coated organs (subterraneous organs) |
| **Potential function** | Cutin biosynthesis | Suberin biosynthesis |
| **Activation of immune response** | Elicitors in a complex with jasmonic acid | Elicitors in a complex with sterol |
| **Allergens listed in IUIS** | LTP1s of 42 plants (excluding iso-allergens and variants) | Tomato Sola l 6, celery Api g 6, peanut Ara h 16 |

lecular weight of about 7 kDa (*Table*). Amino acid sequence homology among representatives of the two subclasses is less than 30% (*Fig. 1*). All LTPs are basic proteins (pI ~9–10). The vast majority of LTPs contain eight conserved cysteine residues (..$C^{I}$...$C^{II}$...$C^{III}C^{IV}$... $C^{V}XC^{VI}$...$C^{VII}$...$C^{VIII}$..) forming four disulfide bonds that stabilize their structure and, thereby, underlie the resistance of LTPs to high temperatures and proteolytic enzymes. Some proteins from this class retain their native conformation and biological activity even after incubation at a temperature of about 100°C [4]. The LTP spatial structure is mainly composed of α-helical regions. Hydrophobic amino acid residues in LTPs are buried inside a molecule and are not in contact with each other, forming an internal protein cavity comprising a potential binding site for hydrophobic and amphiphilic molecules, such as lipids.

LTP1s consist of 90–95 amino acid residues and have disulfide bonds formed in the following order: $C^{I}$–$C^{VI}$, $C^{II}$–$C^{III}$, $C^{IV}$–$C^{VII}$, and $C^{V}$–$C^{VIII}$ (*Fig. 1A, 2A*). The fragment –$C^{V}XC^{VI}$– in the LTP1 structure contains a hydrophilic amino acid (usually asparagine) whose side chain is exposed on the surface of a molecule. The spatial structure of these proteins consists of four α-helices, a $3_{10}$-helix fragment, and an extended unstructured C-terminal region (*Fig. 2A*) [5, 6]. In the structure of some LTP1s, e.g., proteins isolated from maize (*Zea mays*) and tobacco (*Nicotiana tabacum*), the H1 and H4 helices are interrupted by proline residues into two fragments (H1a/H1b and H4a/H4b, respectively). The LTP1 hydrophobic cavity is shaped as an elongated tunnel formed by H1, H2, and H3 helices arranged parallel to each other. The hydrophobic nature of the tunnel surface is determined by the side chains of amino acid residues, including Ile, Val, Leu, and Ala; however, hydrophilic amino acid residues (Arg, Lys, Ser) are also involved in the cavity formation [7]. The tunnel in LTP1s has two entrances that differ in size. In most LTP1s, a basic residue – Arg44 – (position numbering relative to LTP1 of rice (*Oryza sativa*)) is located near the larger entrance and is involved in the interaction with polar lipid heads [8]. In rice LTP1, this interaction involves another basic residue, Lys35. In addition to cysteine residues, most LTP1s contain conserved glycine and proline residues that enable interhelical turns; two tyrosine residues, one of which is located in the N-terminal region, outside of the α-helix, and a second located in the C-terminal region, near the larger entrance to the hydrophobic tunnel and involved in the interaction with hydrophobic ligands [7, 9].

LTP2s consisting of 65–70 amino acid residues have been less studied than LTP1s. The –$C^{V}XC^{VI}$– fragment

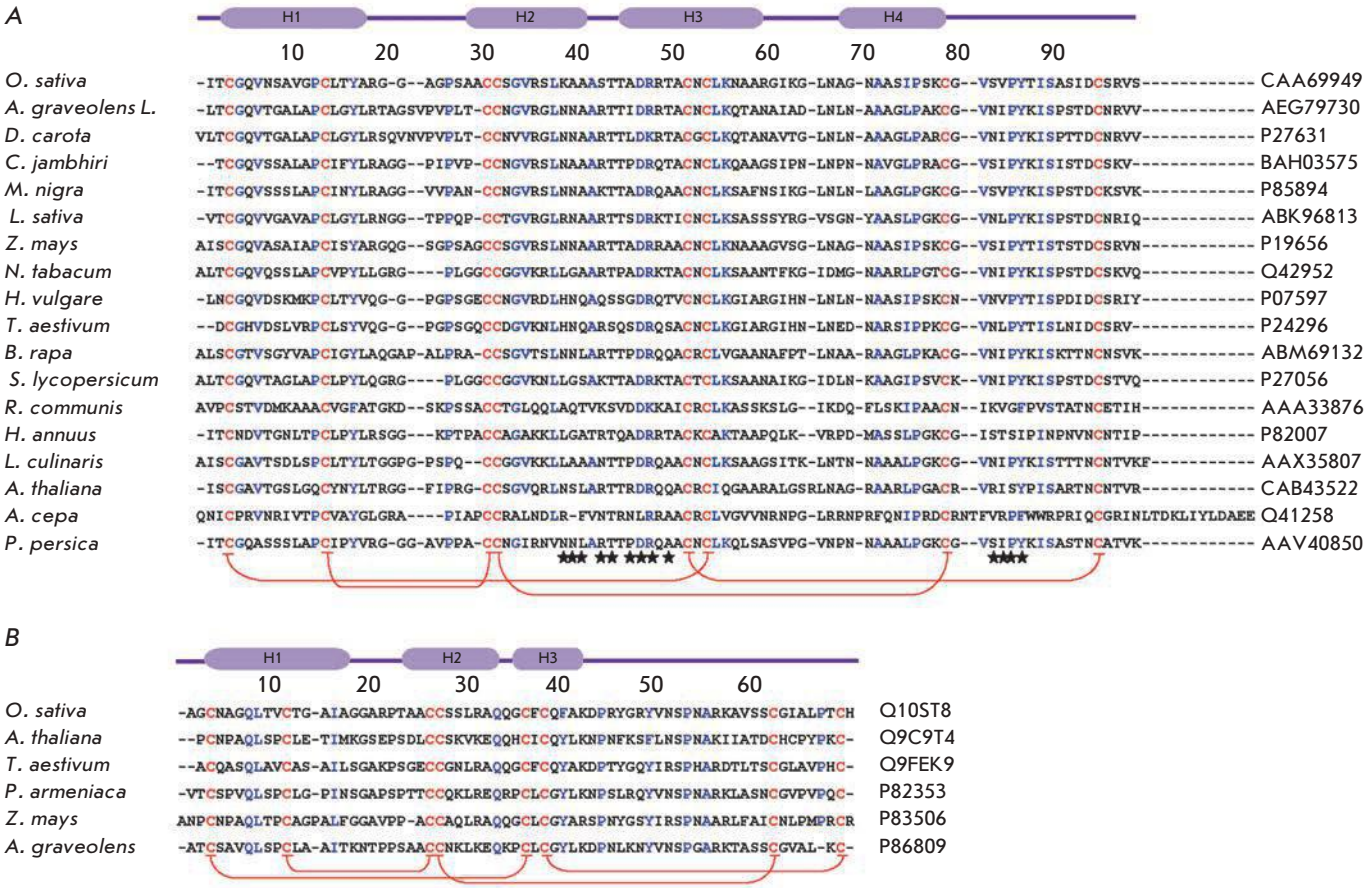


Fig. 1. Comparison of the amino acid sequences of LTP1s (A) and LTP2s (B). Conserved cysteine residues are shown in red; amino acid residues typical of most subclass representatives are shown in blue. Disulfide bond arrangement is denoted by brackets. The localization of α-helices in the rice LTP1 (PDB ID: 1RZL) [5] and LTP2 (PDB ID: 1L6H) structures [10] is shown on the top of the panels. The asterisks denote the amino acid residues involved in the conformational epitopes of Pru p 3 (GenBank:AAV40850) [98].

of LTP2s usually contains phenylalanine as the central residue, which points inward the molecule. LTP2s have a different organization of disulfide bonds: $C^{I}$–$C^{V}$, $C^{II}$–$C^{III}$, $C^{IV}$–$C^{VII}$, $C^{VI}$–$C^{VIII}$ (*Fig. 1B, 2B*) [10]. The spatial structure of proteins of this subclass includes three α-helices and a region containing single helical coils (*Fig. 2B*). In the LTP2 structure, the H1 and H2 helices are arranged parallel to each other and the H3 helix forms an angle of 90° with respect to H2. The shape of the LTP2 hydrophobic cavity resembles a triangular hollow box, with side chains of the Ala, Ile, Leu, Phe, and Val residues situated within. The volume of the triangular LTP2 box is smaller than that of the LTP1 hydrophobic cavity, but pronounced flexibility of the former allows proteins of this subclass to bind large ligands with a rigid structure, such as sterols [10–12]. Side chains of Phe39, Tyr45, and Tyr48 (numbering relative to rice LTP2) are rotated inside the cavity and in contact with a lipid ligand [13]. In addition to cysteine residues, the LTP2 structure comprises conserved Gln, Tyr, and Pro residues.

The hydrophobic cavity volume in both LTP subclasses can vary considerably. For example, the hydrophobic cavity volume of rice LTP1 is 249 Å$^3$, but the cavity volume increases to 1,354 Å$^3$ when the protein binds palmitic acid. This flexibility of LTP molecules may be the cause of their low specificity to a lipid ligand.

## LIPID BINDING AND TRANSFER

The presence of a hydrophobic cavity in the structure of LTP molecules enables these proteins to bind and transfer a variety of ligands. The LTP-ligand complex formation *in vitro* depends on the hydrophobic cavity size, the amino acid residues constituting the cavity, the spatial structure of the ligand, as well as experimental conditions (pH, buffer composition, temperature). LTPs isolated from various plant sources have

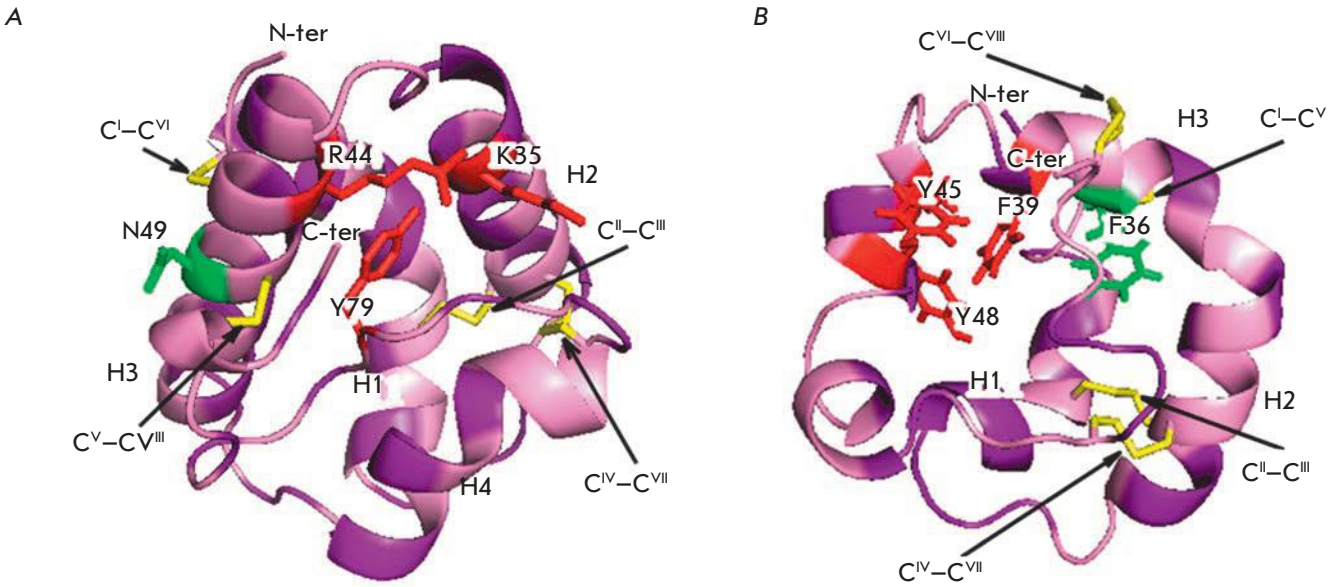


Fig. 2. The spatial structures of (A) LTP1 (PDB ID: 1RZL) and (B) LTB2 (PDB ID: 1L6H) from rice in a ribbon representation. Identification numbers of α-helices (H1–H4) are specified. Hydrophobic amino acid residues are shown in purple; residues interacting with lipid ligands are shown in red [5, 10]; disulfide bonds are marked in yellow; the central residue in the $-C^{V}XC^{VI}-$ fragment, directed either outward or inward the protein molecule, is shown in green.

been shown to be capable of binding lipids. However, it should be noted that there are exceptions to this rule. For example, a protein from onion (*Allium cepa*) seeds, termed Ace-AMP1, has a pronounced homology with plant LTPs but does not interact with lipids, perhaps because of the absence of a one-whole cavity in the protein molecule [14].

Various LTPs bind a wide range of ligands, including fatty acids (FAs) with a $C_{10}$–$C_{18}$ chain length, acyl derivatives of coenzyme A (CoA), phospho- and galactolipids, prostaglandin B2, sterols, molecules of organic solvents, and some drugs [15, 16]. Although LTPs lack marked specificity to ligands, these proteins form the most stable complexes with FAs containing from 16 to 18 carbon atoms. LTPs do not form stable complexes with molecules with a chain length longer than $C_{20}$ due to the spatial constraints imposed by the hydrophobic cavity size [17]. Furthermore, the complex stability has been shown to be affected by the number of double bonds in FA molecules and their configuration. LTPs form the most stable complexes with various unsaturated FAs with one or two double bonds in the *cis*-configuration [18], two of which, the linoleic and oleic acids, are precursors of cutin and suberin monomers.

Unlike LTP2s, LTP1s do not bind sterols. The ligand orientation in the LTP1 hydrophobic cavity was found to be different, depending on the spatial arrangement of ligand and LTP1 molecules. For example, in complexes of maize LTP1 with 1-palmitoyl lysophosphatidylcholine [9] and wheat (*Triticuma estivum*) LTP1 with dimyristoyl phosphatidylglycerol [18], ligands in the protein cavity occur in the "forward" orientation; i.e., polar lipid heads are located near the larger entrance to the hydrophobic cavity. At the same time, the ligand in the complex of barley (*Hordeum vulgare*) LTP1 with palmitoyl CoA occurs in "reverse" orientation, its aliphatic chains are strongly bent, and the polar head points towards the smaller entrance to the cavity [19].

Plant LTP1s can bind one or two lysophospholipid molecules [20]. LTPs of this subclass are supposed to interact with ligands according to a cooperative binding model. If two ligand molecules occur in the hydrophobic cavity, their orientation and binding affinity for the protein are not identical. For example, two lyso-myristoyl phosphatidylcholine molecules bound to wheat LTP1 have a "head-to-tail" orientation in the hydrophobic cavity [19, 21]. It is suggested that the second binding site of LTP is activated only when the first site is already occupied by a ligand.

The calcium-calmodulin system was shown to be involved in the regulation of lipid binding to plant LTPs. Plant LTPs bind calmodulin regardless of the presence of calcium ions. In maize Zm-LTP and onion Ace-AMP1, a potential site for binding of calmodulin is situated in the middle portion of the LTP polypeptide chain (residues 46–60) and has a structure similar to

that of the basic amphiphilic α-helix (BAA) domain of calmodulin-binding proteins [22]. A distinctive feature of the BAA-like domain in plant LTPs is the absence of Trp that plays a crucial role in calcium-dependent binding of calmodulin. Maize Zm-LTP affinity for binding lipids is reduced in the presence of calmodulin. This is explained by the fact that the calmodulin binding site of the protein contains the Arg46 residue involved in the binding of lipids. At the same time, the calmodulin binding site in the bok choy (*Brassica rapa subsp. chinensis*) protein, termed BP-10, and arabidopsis (*Arabidopsis thaliana*) LTP1 is located in the C-terminal region (amino acid residues 69–81) and has no structural similarity with any of the known calmodulin binding sites [23]. The BP-10-calmodulin complex formation increases the efficiency of lipid binding. The cause of this effect is believed to be the residue Tyr81 located in the calmodulin binding site of the LTP protein and playing an important role in the interaction with a lipid ligand.

Plant LTPs not only bind lipids, but also transfer them between membranes in experiments *in vitro*. They transfer phospholipids, such as phosphatidylcholines (PCs), phosphatidylinositols (PIs), phosphatidylglycerols (PGs), their derivatives, as well as acyl-CoA [24–26]. Wheat LTPs were used to demonstrate that the lipid transfer activity of LTP2s is several times higher than that of LTP1s [27].

The lipid transfer mechanism involving LTPs remains unclear. Plant LTPs, like mammalian phosphatidylcholine-specific LTPs, are supposed to transfer lipids by the shuttle mechanism. A LTP-phospholipid complex interacts with the membrane, which results in phospholipid exchange between the complex and membrane [3].

To date, there is no direct evidence of involvement of plant LTPs in the binding and transfer of lipids *in vivo*. The only LTP-ligand complex found in plant cells is a covalent adduct of barley LTP1 and oxylipin that is formed by reacting the carboxyl group of Asp7 with the allene oxide in a 9(*S*),10-epoxy-10,12(*Z*)-octadecadienoic acid molecule [28, 29]. The reaction yields α-ketol-9-hydroxy-10-oxo-12(*Z*)-octadecenoic acid. It should be noted that the formation of this covalent complex, known as LTP1b, increases the hydrophobic cavity flexibility and the protein ability to transfer lipids.

Some LTPs are not only able to bind and transfer lipids but also to induce permeabilization of model membranes. For example, the sunflower (*Helianthus annuus*) protein termed Ha-AP10 damages liposomes consisting of PCs and PGs [30]. It is interesting to note the lack of a correlation between the lipid binding and lipid transfer activity and the LTP ability to damage membranes. For example, barley LTP binds a wide range of lipids but has little effect on the properties of model membranes [31]. Onion Ace-AMP1 does not bind lipids but induces permeabilization of bilayer vesicles consisting of anionic lipids [14].

## BIOSYNTHESIS AND LOCALIZATION

The LTP class belongs to a large family of pathogenesis-related proteins (PRPs). Induction of the synthesis of these proteins occurs upon exposure of a plant to abiotic and biotic stress factors and underlies one of the key defense mechanisms in plants. PRPs are present in all plant organs and accumulated in the vacuoles and apoplast, as well as in the primary and secondary cell walls. This localization is consistent with the defense function of PRPs that, along with antimicrobial peptides (AMPs), create a specific barrier to pathogen penetration [32].

The family of pathogenesis-related proteins includes, along with LTPs (PRP-14), proteins of 16 more classes: glucanases (PRP-2), chitinases (PRP-3, 4, 8), protease inhibitors (PRP-6), homologs of the major birch pollen allergen Bet v 1 (PRP-10), defensins (PRP-12), thionins (PRP-13), etc. [33]. Abiotic inducers of the PRP synthesis include UV radiation, osmotic shock, lack of moisture, low temperatures, and soil salinity. The PRP synthesis in an infected plant is induced by both primary and secondary elicitors: non-specific pathogen-associated molecular patterns (PAMPs) and damage-associated molecular patterns (DAMPs), as well as by specific effector proteins of pathogens. PRP synthesis inducers include phytohormones, such as ethylene, auxins, as well as abscisic, jasmonic, and salicylic acids. At certain stages of ontogeny, activation of synthesis and tissue-specific accumulation of PRPs also occur in the absence of stressors [34].

LTPs have been found in various plant organs: seeds, leaves, stems, roots, flowers, and fruits. Most often, LTPs occur in cuticle-covered epidermal cells but are also found in embryonic and vessel tissues. LTPs are synthesized in plant cells as preproteins containing a hydrophobic signal sequence (21–27 or 27–35 amino acid residues in LTP1s or LTP2s, respectively) and are secretory proteins with a predominantly extracellular localization [35, 36]. Some LTPs have an atypical intracellular localization. For example, LTP from castorbean (*Ricinus communis*) seeds was found in glyoxysomes [37]; LTP from cowpea (*Vigna unguiculata*) seeds was found in vacuoles [38]; Ca-LTP(1) from pepper (*Capsicum annuum*) seeds was found in vesicles [39]. Of particular interest is the question of how LTPs synthesized as preproteins without appropriate signal sequences occur in these cell organelles. Sunflower LTP, HaAP10, was found to be relocalized. In dry seeds, Ha-AP10 occurs in the apoplast; upon imbibition and germination of seeds, it relocalizes,

possibly by endocytosis, to the intracellular organelles involved in lipid metabolism [40].

In some plants, LTPs termed GPI-anchored lipid transfer proteins (LTPGs) were found. These proteins are synthesized as precursors containing, in addition to the N-terminal signal peptide, the C-terminal signal sequence. This sequence ensures the post-translational attachment of the glycosylphosphatidylinositol anchor (GPI) to the protein, through which LTPGs can be localized on the outer side of the cell membrane or secreted to the apoplast after GPI-anchor cleavage [41]. Another group of unusual LTPs with extracellular localization is constituted by the xylogen from zinnia (*Zinnia elegans*) and xylogen-like proteins of other plants [42]. The gene structure of xylogen-like proteins, which belong to a large family of arabinogalactan proteins (AGPs), contains a signal peptide, the LTP domain, several AGP domains, and the GPI anchor attachment signal. During maturation, these proteins undergo a series of post-translational modifications, including removal of the N-terminal signal peptide, GPI anchor attachment, proline hydroxylation, and O-glycosylation [42].

Plant LTPs are encoded by multigene families and, in the plant genome, are usually represented by a set of genes encoding different isoforms. Expression of genes of different LTP isoforms is characterized by pronounced tissue specificity and occurs at certain stages of ontogeny [36]. This may be related to the fact that different LTP isoforms have different functions [43]. Differential expression of genes of multiple LTP isoforms also occurs when a plant is exposed to a variety of abiotic and biotic environmental factors and may be considered as one of the defensive strategy elements under stress conditions [44]. Differential expression of isoform genes was shown for LTPs from sesame (*Sesam umindicum*) [45], arabidopsis [43, 46], pepper [47], castorbean [37], grape (*Vitis vinifera*) [48], Kashgar tamarisk (*Tamarix hispida*) [49], and tomato (*Lycopersicon pennellii*) [50].

## BIOLOGICAL ACTIVITY

As mentioned, LTPs constitute one of the classes of defense PRPs, many of which have antimicrobial and enzymatic activities or are enzyme inhibitors. Various representatives of the LTP class exhibit antibacterial, antifungal, antiviral, and antiproliferative activities, and inhibit some enzymes [36].

### Antimicrobial activity

Many LTPs have antimicrobial activity and inhibit the growth of pathogenic bacteria and fungi, such as *Clavibacter michiganensis*, *Pseudomonas solanacearum*, *P. syringae*, *Alternaria brassicola*, *Ascochyta pisi*, *Colletotrichum lindemuthianum*, *Fusarium solani*, *F. graminearum*, *F. culmorum*, *F. oxysporum*, *Botrytis cinerea*, *Sclerotinia sclerotiorum*, *Verticillium dahliae*, etc. LTPs from pepper and coffee (*Coffe acanephora*) are also active against human pathogenic fungal strains from the *Candida* genus [39, 51]. The antimicrobial activity of most plant LTPs is specific and exhibited against a particular spectrum of microorganisms. LTPs from onion [52], radish (*Raphanus sativus*) [52], and arabidopsis [53] have pronounced antimicrobial activity at micromolar concentrations. Most LTPs have a moderate or little effect on the growth of microorganisms; in some cases, this effect is absent. [54] The antimicrobial activity of plant LTPs decreases in high salt solutions and in the presence of calcium ions, which is a common feature of other classes of plant AMPs and PRPs [52]. Like plant defensins, LTPs are able to act in synergy with thionins [55] and have no toxic effects on plant cells and mammalian cells, including fibroblasts and red blood cells [30, 52].

Disruption of the disulfide bonds stabilizing the structure of plant LTPs leads to a loss of the ability of the proteins to inhibit the growth of microorganisms and bind lipids [56]. At the same time, the other amino acid residues that are necessary for exhibiting the antimicrobial activity remain unknown. The antimicrobial activity of rice LTP110 was shown to require the presence of the conserved residues Tyr17, Arg46, and Pro72 that play an important role in the stabilization of the protein structure in most LTP1s [57]. A study of wheat LTP isoforms demonstrated that difference in one amino acid residue only (Pro3Ser in TaLt10B6 and TaLt710H24 isoforms and Asn24Ser in TaLt10F9 and TaBs116G9 isoforms) significantly affects the antimicrobial activity of the proteins. It is assumed that the replacement of just one amino acid residue may result in a change in the LTP spatial structure and affect the positive charge distribution over the molecule surface [56].

To date, the antimicrobial activity of plant LTPs is found not to be related to their ability to interact with lipids. For example, eight wheat LTP isoforms were shown to have no correlation between the ability of the proteins to inhibit the growth of pathogenic microorganisms and to bind lipids [56]. Using onion Ace-AMP1 [52] and a mutant rice LTP isoform [57], it was also shown that this class of proteins may possess antimicrobial activity but not bind lipid molecules and vice versa.

Plant LTPs have not only fungistatic, but also fungicidal activity and, like other AMPs, are able to induce permeabilization of the model membranes [30] and cell membranes of pathogenic fungi [30, 56]. For example, LTPs from onion [14], sunflower [30], and, to a lesser

extent, barley [31] are able to induce permeabilization of liposomes consisting of anionic phospholipids only or a mixture of anionic and neutral phospholipids, causing fluorescent dye leakage from liposomes. However, it should be noted that this effect is much weaker than that in other plant AMPs and observed only in low-ionic-strength solutions.

The mechanism of antimicrobial action of representatives of the LTP class remains unclear. Nevertheless, the cell membrane is considered as a potential target for LTP antimicrobial action. Plant LTPs, like other cationic membrane-active AMPs, are supposed to bind to the cell membrane of the phytopathogen through electrostatic interactions and cause destabilization and permeabilization of the membrane. The weaker antimicrobial activity of LTP isoforms containing a smaller number of basic amino acids is explained by the attenuation of the electrostatic interaction with the cell membrane of the phytopathogen [56]. A potential cause of the selective toxicity of plant LTPs is believed to be the differences in the lipid composition of the cell membranes of bacteria, fungi, plants, and mammals.

### Antiviral and antiproliferative activities

LTPs from Chinese daffodil (*Narcissus tazetta*) and cole seed (*Brassica campestris*) were shown to have antiviral activity and the ability to inhibit the proliferation of human tumor cells. In *in vitro* experiments, *N.tazetta* LTP, designated as NTP, significantly inhibited plaque formation of the respiratory syncytial virus (RSV), the cytopathic effect of the influenza A virus (H1N1), and the proliferation of the human acutepromyelocytic leukemia cell (HL-60). *B. campestris* LTP inhibit the activity of HIV-1 reverse transcriptase and the proliferation of hepatoma HepG2 and breast cancer MCF7 cells. To date, the mechanism of LTP anti-tumor activity has not been determined [58, 59].

### Inhibition of enzyme activity

Some members of the LTP class, like protease inhibitors (PRP-6) and certain defensins (PRP-12) [60, 61], can inhibit the activity of proteolytic enzymes and α-amylases. For example, barley seed LTPs of both subclasses were found to inhibit cysteine endoproteases [62]. Also, LTP1 from the *Ginkgo biloba* seed inhibits cysteine (papain), aspartate (pepsin), and serine (trypsin) proteases [63]. LTP1 from seeds of coffee and pepper inhibit the activity of human α-amylase [39, 51]. LTPs capable of inhibiting the activity of their own and foreign enzymes are believed to be involved both in the development and germination of seeds and in the protection of plants against insects and herbivores.

## POTENTIAL LTP FUNCTIONS

LTPs are known to play an important role in plants. Knockout of the genes encoding these proteins leads to disruption of the vegetative and reproductive development of plants and a decrease in their resistance to infections [43, 64, 65]. The results of a study of the inhibition of LTP gene expression support a number of assumptions about the possible involvement of proteins from this class in the adaptation of plants to stress, lipid metabolism, embryogenesis, growth and reproduction of plants, symbiosis, and other processes. Many of these functions are believed to be associated with the LTP ability to bind and transfer lipid molecules (*Fig. 3*).

### Involvement in lipid metabolism

Because plant LTPs are capable of binding and transferring lipids, these proteins are believed to be involved in a variety of processes that are accompanied by changes in lipid composition. Extracellular LTPs are supposed to participate in the formation of a protective cuticle layer whose monomeric components are formed in epidermal cells and delivered to the biosynthesis site. Activation of biosynthesis of the cuticle, which plays an important role in maintaining the water balance and protection of plants from penetration by pathogens, occurs under the action of a variety of stress factors and is one of the defense mechanisms in plants. There is no direct evidence of LTP involvement in this process. However, plant LTPs were shown to occur at high concentrations in epidermal tissues and of being capable of binding the fatty acids required for the synthesis of cutin and suberin. Furthermore, induction of LTP synthesis is accompanied by thickening of the cuticle layer [66] and knockout of LTP genes leads to changes in the lipid composition and density of the cuticle layer [67]. Two potential mechanisms of cuticle component delivery with involvement of LTPs were suggested. According to the first of them, LTPs enter the cell by receptor-mediated endocytosis and are loaded by the fusion of vesicles containing LTP and cutin monomers. The second mechanism suggests shuttling of LTPs between the cell membrane and the cell wall of plants and the existence of a carrier molecule acting on the inner side of the cell membrane [68]. An interesting fact is that LTP1s are present in organs covered by a cutin layer (leaves, stems, flowers), while LTP2s occur in suberin-covered subterranean organs. This argues for a differential involvement of proteins of the first and second subclasses in the cutin and suberin layer formation [35]. LTPGs having a GPI anchor were demonstrated to be possibly involved in the biosynthesis and accumulation of suberin [41].

LTPs found in various intracellular organelles are presumably involved in the mobilization of lipids

through their transfer, e.g., during seed germination. For example, castorbean LTP found in glyoxysomes binds both free FAs and acyl-CoA. This protein also increases the activity of acyl-CoA oxidase involved in the β-oxidation of FAs [37]. Sunflower LTP Ha-AP10 entering the cell during seed germination is supposed to transfer FAs, liberated by cleavage of triacylglycerols, to glyoxysomes for further β-oxidation [40].

Induction of the expression of genes encoding carrot (*Daucus carota*) LTP was demonstrated to occur at the early stages of embryogenesis when degradation of some lipids and biosynthesis of others, as well as the protective lipid layer formation around the embryo, takes place [69]. The role of this protein in embryogenesis is presumably to participate in these processes via the transfer of relevant lipid molecules.

## Involvement in fertilization of flowering plants

Plant LTPs are believed to play an important role in the reproduction of flowering plants. For example, lily (*Lilium longiflorum*) LTP1 is a component necessary for pollen adhesion and formation and growth of the pollen tube [70]. LTP1 is supposed to be capable of acting directly as an adhesive component or as a carrier of the hydrophobic adhesive component. Also, one of the isoforms of a lipid transfer protein from arabidopsis, LTP5, was shown to be involved in the growth of the pollen tube and seed formation [64].

The role of rice LTP OsC6 in postmeiotic pollen development has been determined. This protein was found to be present in anther tissue and to be capable of binding FAs. OsC6 is supposed to be involved in the formation of lipid orbicles and pollen exine through transfer of essential lipids from tapetum cells to microspores [65].

## Involvement in protection and adaptation of plants under stress conditions

The belief that LTPs are involved in the protection and adaptation of plants to stress is mainly based on the fact of a stress-induced synthesis of these proteins. For example, the synthesis of LTPs, as well as that of

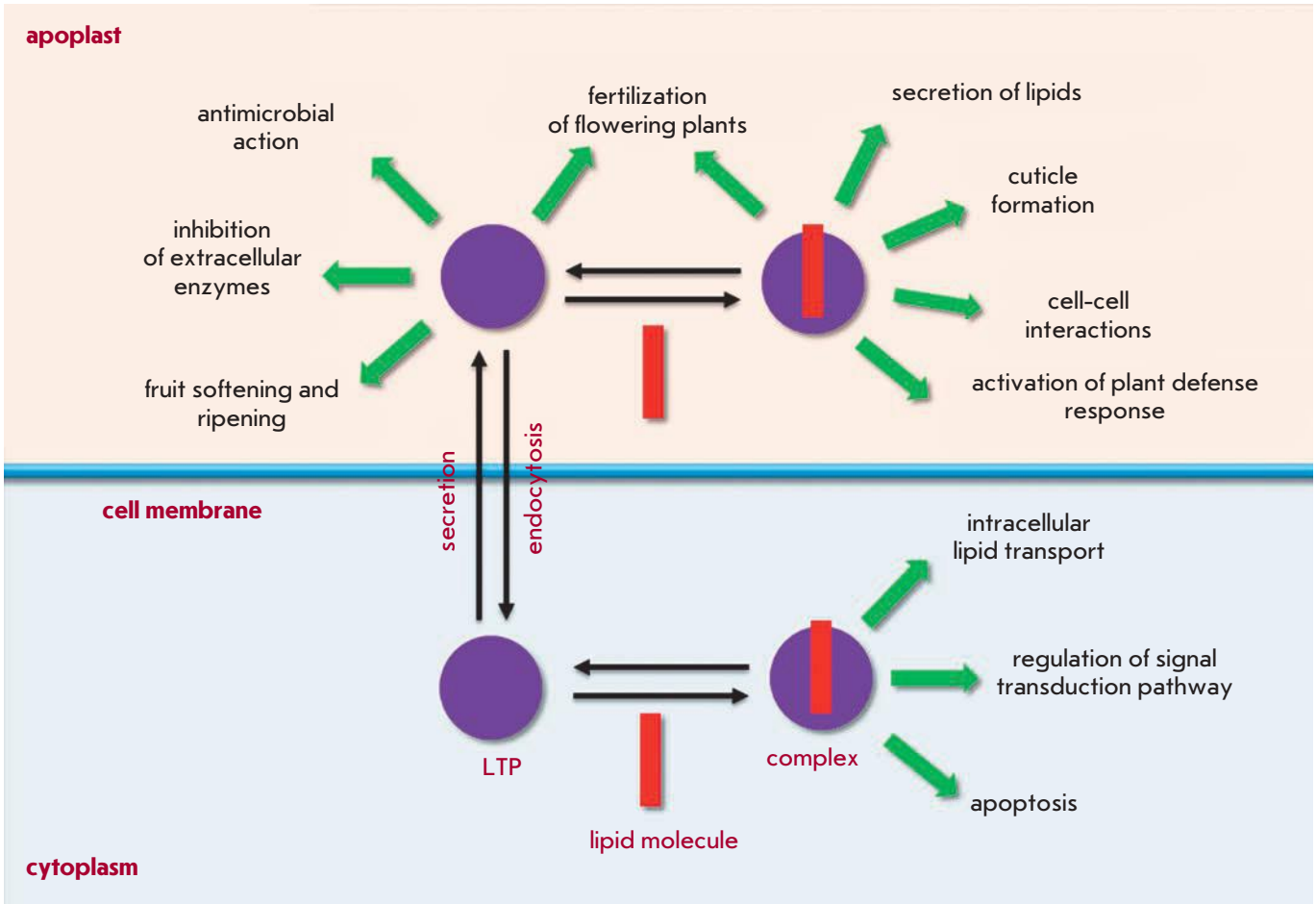


Fig. 3. Potential LTP functions in plants

other PRPs, is induced by wounding, moisture deficit, low temperatures, soil salinity, infections, and chemical agents [43, 45, 47, 50, 71, 72]. Induction of the expression of LTP genes under stress conditions may be associated with the presence of regulatory elements, which are also typical of other PRPs, in the promoter region of LTP genes. The regulation of LTP gene expression involves phytohormones, such as abscisic and salicylic acids, ethylene, and methyl jasmonate [36].

One of the possible causes behind the induction of LTP gene expression under stress conditions is believed to be the involvement of these proteins in the biosynthesis of the cuticle layer [50]. The protective function of LTPs in plants is related to their antimicrobial activity, cryoprotective action, and their ability to inhibit exogenous enzymes, as well as to their possible involvement in the secretion of other components of the plant immune system.

The glandular hairs (trichomes) of plants produce essential oils that are involved in metabolism, protect plants against pests and overheating, have a wound-healing effect, and attract insects. Tobacco (*N. tabacum*) NtLTP1 was found to be specifically expressed in long glandular trichomes and to be involved in the secretion, from trichome heads, of essential oil components (diterpenes, aliphatic hydrocarbons, and aromatic acids) that are plant protective factors [73]. LTP gene transcripts were also found in the glandular hairs of other plants, such as pepper mint (*Mentha piperita*), alfalfa (*Medicago sativa*), sweet wormwood (*Artemisia annua*), hop (*Humulus lupulus*), Greek sage (*Salvia fruticosa*), and tomato [73].

The resistance of plants to cold is known to be associated with stabilization of cell membranes and prevention of a protein solubility reduction at lower temperatures. WAX9 proteins that have a high degree of amino acid sequence homology with LTPs were identified in the leaves of a cold-acclimated cabbage (*Brassica oleracea*). These proteins cannot bind lipids, but, like β-1,3-glucanases, osmotins, and lectins, they are able to stabilize thylakoid membranes in cold conditions [72]. The mechanism of cryoprotective action of these proteins is supposed to be associated with a decrease in the fluidity of membrane lipids upon interaction between LTPs and the thylakoid membrane [74].

### Involvement in activation and regulation of signaling cascades

LTPs are supposed to be involved in the activation and regulation of various signaling pathways in plants through the formation of complexes with various lipid molecules. Oxylipins are one of the classes of signal mediators in plants. Oxylipins are produced from unsaturated FAs under the action of reactive oxygen species (ROS) or enzymes and are involved in the regulation of the growth and development of plants, as well as in triggering defense responses to stress conditions. In addition, oxylipins regulate the processes of neutralization of the toxic components formed during stress. As mentioned, barley LTP1, during seed germination, forms covalent complexes with oxylipin of 9(*S*),10-epoxy-10,12(*Z*)-octadecadienoic acid containing an unstable allene oxide resulting from the sequential action of lipoxygenase and allene oxide synthase [28, 29]. This interaction may indicate a joint involvement of LTPs and oxylipins in the regulation of the signaling pathways that trigger the mechanism preventing damage to plant cells under stress conditions [29].

LTPs bound to lipid molecules act as endogenous elicitors interacting with specific receptors on the cell membrane of plant cells and providing for the development of an immune response to infection (*Fig. 4*). For example, rice and tobacco LTPs were shown to be capable of interacting with elicitin receptors [21, 75, 76]. Elicitins are well-studied plant PAMPs that have a molecular weight of about 10 kDa and are produced by phytopathogenic oomycetes (*Phytophthora* and *Pythium*) parasitizing on higher plants. These proteins, due to a hydrophobic cavity in their structure, can bind sterols and provide phytopathogenic microorganisms with essential plant-derived lipids. All elicitins have a α-helical structure stabilized by three disulfide bonds; sterol-associated elicitins are recognized by the plant by means of receptor-like kinases located on the cell membrane. The recognition entails activation of plant defense mechanisms, such as the production of phytoalexins and ROS, as well as the development of a hypersensitive response (HR) and systemic-acquired resistance (SAR) [77, 78]. The amino acid sequences of LTPs and elicitins have a low degree of homology, whereas the spatial structures of the proteins have a pronounced similarity [79]. Lipid bound plant LTPs act as agonists of elicitins and DAMP, bind to elicitin receptors, and trigger an immune response. An interesting fact indicating the possibility of different pathways for the activation of a plant defense response involving representatives of the two LTP subclasses is the difference in the structure of a hydrophobic ligand. Sterols act as this ligand for LTP2s [75], while jasmonic acid is the ligand for LTP1s that have a less flexible hydrophobic cavity [21, 76].

An unusual LTP2 representative from arabidopsis – termed DIR1 – that has an isoelectric point in the acidic pH range plays the key role in SAR development [80]. During plant infection, the protein is supposed to bind to the lipid molecules (oxylipins, fatty acids, or monoacyl phospholipids) produced by lipases secreted by the pathogen. Then, the formed complex interacts with a

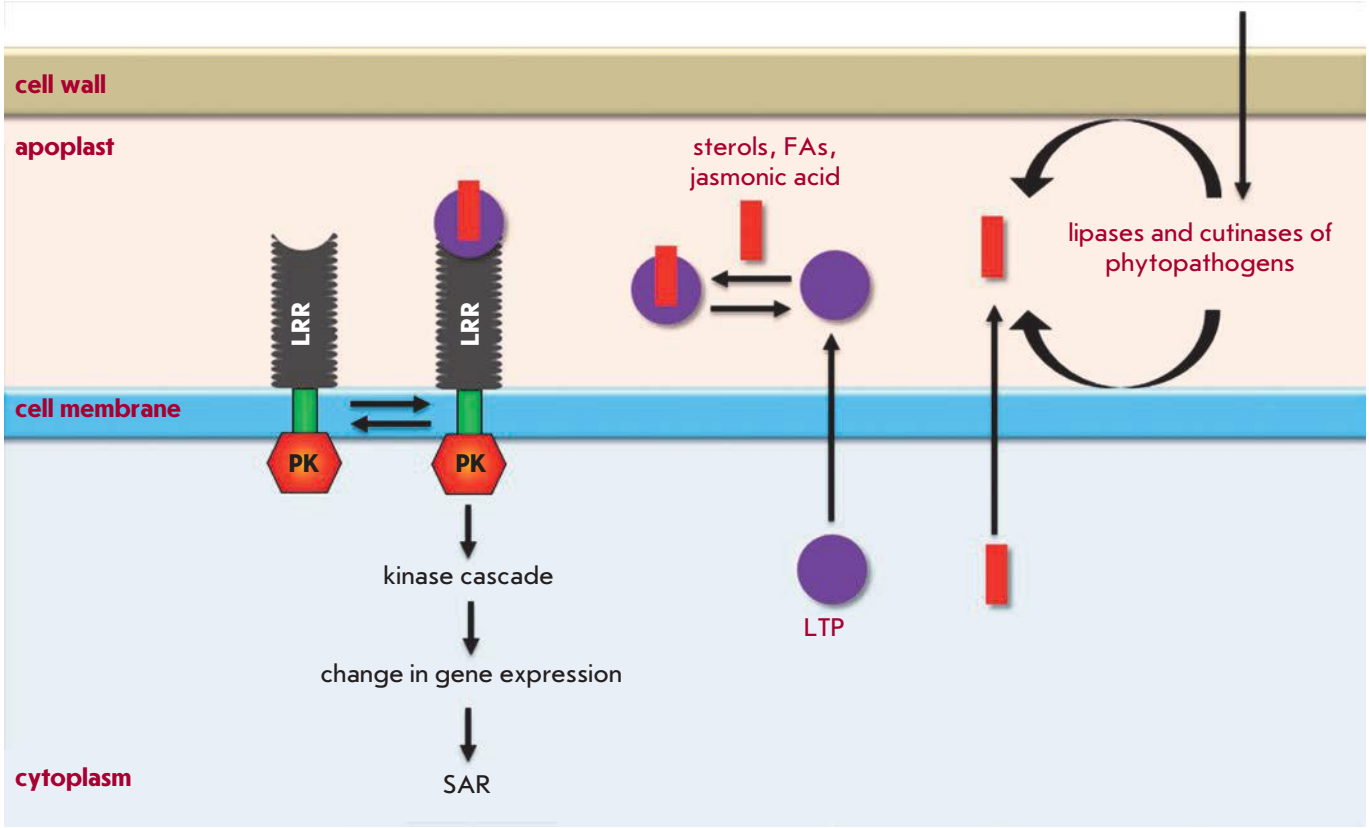


Fig. 4. A potential mechanism of LTP involvement in plant immune response. LTPs are secreted to the apoplast and bind to lipid molecules that are either secreted by the plant (e.g., jasmonic acid) or form under the action of enzymes secreted by phytopathogenic microorganisms. Lipid-bound LTPs interact with receptors, such as receptor-like serine/threonine protein kinases, located on the cell membrane that contain the extracellular leucine-rich repeat domain (LRR), transmembrane, and cytoplasmic protein kinase (PK) domains. This interaction may cause signal transduction mediated by versatile second messengers and a cascade of mitogen-activated protein kinases; activation of several transcription factors; induction of the synthesis of protective factors, including AMPs and PRPs (possibly, LTP isoforms with a pronounced antimicrobial activity); and, finally, SAR.

hypothetical receptor, triggering a signaling cascade that leads to SAR development [81].

Zinnia xylogen containing the GPI anchor and binding plant sterols was found to promote the differentiation of uncommitted cells into tracheary elements and, probably, to be involved in cell-cell interactions and signal transduction. It is thought that xylogen-like proteins of other plants, whose LTP domains are highly similar to those of LTP2s, may also be involved in cell-cell interactions and signal transduction, functioning in a complex with a lipid molecule [42].

## Involvement in apoptosis

Possible LTP involvement in apoptosis was assumed based on the similarity between maize LTP and the mammalian pro-apoptotic protein Bid that also has an internal cavity and binds and transfers lipids [82]. Bid occurs in the cytosol and, in the presence of lysophospholipids generated during programmed cell death, affects mitochondria, causing the release of apoptogenic factors, including cytochrome *c*. In the presence of lysophospholipids, maize LTP also causes the release of cytochrome *c* from mitochondria. A possible mechanism of the destabilizing action of both proteins includes transfer of lysophospholipids to the outer mitochondrial membrane. The lysophospholipids modify the membrane properties, thereby facilitating the action of other pro-apoptotic proteins [83].

## Involvement in symbiosis

Symbiotic rhizobacteria are known to be able to stimulate the growth of plants and protect them from soil phytopathogens, causing the development of the so-called induced systemic resistance (ISR) that is phenotypically and functionally similar to SAR [84]. Alfalfa LTP MtN5 was shown to play an important role in the development of symbiotic relationships between a plant and nodule bacteria. Namely, the protein is in-

volved in processes of bacteria penetration into root tissues and nodule formation [85]. The MtN5 function is supposed to maintain the balance between bacterial invasion and prevention of infection [86].

### Involvement in fruit ripening

Tomato LTP was shown to be capable of forming complexes with polygalacturonase, which is the most significant pectin-degrading enzyme. Upon complex formation, tomato LTP enhances the hydrolytic activity of the enzyme and may be involved in the regulation of fruit softening and ripening [87].

## LTPs AS ALLERGENS

LTPs are antigens involved in the development of allergic reactions of varying severity to pollen, plant foods, and latex. The structure of these proteins, stabilized by disulfide bonds, is responsible for their high resistance to cleavage by digestive enzymes and enables the proteins to reach the human intestine in native immunogenic form and to cause sensitization [88]. The allergenic capacity of LTPs in various processed foods (juices, jams, beer, wine, etc) is explained by their highly stable structure that is practically unsusceptible to thermal denaturation, as well as chemical and enzymatic degradation [89]. It should be noted that the defined allergens are mostly members of the first subclass of plant LTPs. For example, the IUIS allergen database now contains only three LTP2s (tomato, peanut, and celery) and 42 LTP1s from various plants, apart from their isoforms. The high structural homology of LTP1s underpins the development of cross-allergic reactions.

LTP1s, which are widely distributed in the plant kingdom, are the main allergens isolated from fruits and grains (peach (*Prunus persica*) Pru p 3, cherry (*P. avium*) Pru av 3, apple (*Malus domestica*) Mal d 3, plum (*P. domestica*) Pru d 3, orange (*Citrus sinensis*) Cit s 3, grape Vit v 1, strawberry (*Fragaria ananassa*) Fra a 3), nuts (hazelnut (*Corylus avellana*) Cor a 8, walnut (*Juglans regia*) Jug r 3, chestnut (*Castanea sativa*) Cas s 8), vegetables (asparagus (*Asparagus officinalis*) Aspa o 1, lettuce (*Lactuca sativa*) Lec s 1, cabbage Bra o 3, tomato (*Lycopersicone sculentum*) Lyc e 3, celery (*Apium graveolens*) Api g 2), cereals (maize Zea m 14, rice Ory s 14, wheat Tri a 14, barley Hor v 14), and legumes (peanut (*Arachis hypogaea*) Ara h 9, lentil Len c 3, bean Pha v 3) [90–92]. It is important to note that LTPs are accumulated mainly in the skin of fruits, not in their pulp [93], which may be the cause of anaphylactic reactions in humans upon dermal contact with fruits [94]. A significant contribution to primary sensitization is also made by pollen allergens of the LTP class: Jewish pellitory (*Parietaria judaica*) Par j 2, olive (*Olea europaea*) Ole e 7, plane tree (*Platan usacerifolia*) Pla a 3, mugwort(*Artemisia vulgaris*) Art v 3, etc. [95]. Interestingly, LTPs from fruits of *Rosaceae* family plants were also found in the pollen of these trees [96]. Peach Pru p 3 is believed to be the main LTP allergen that plays the major role in sensitization and is recognized by immunoglobulin E (IgE) in most individuals with allergies [97, 98].

In recent years, numerous studies have been conducted to elucidate the causes of high plant LTP1 allergenicity and development of cross-induced allergic reactions. For example, IgE-binding B-cell epitopes of Pru p 3 were identified. These are positively charged moieties on the protein surface that are associated with the amino acid residues 11–25, 31–45, and 71–80 (*Fig. 1A*) [99]. The identified antigenic determinants are highly homologous among various allergenic LTP1s. The key role in the interaction between Pru p 3 and IgE was found to be played by the residues Arg39, Thr40, and Arg44 that are typical of most allergenic LTP1s [100]. A polypeptide chain fragment comprising the amino acid residues 61–80 acts as a T-cell epitope of Pru p 3 [101]. Also, the development of a T-cell response to Pru p 3 was shown to be accompanied by increased expression of integrin α4β7 that provides lymphocyte migration to the intestinal wall where the primary lymphocyte activation occurs [102].

## EVOLUTION OF GENES

LTP genes are ubiquitous in higher plant genomes: from the most primitive bryophytes to tracheophytes, including ferns, lycopsids, angiosperms, and gymnosperms, but they are not found in lower plants, such as algae. In this regard, it is assumed that the LTPs involved in the protection of plants against various environmental stress factors could have developed during the emergence of terrestrial plants, i.e. about 400 million years ago [103].

As mentioned above, LTPs of one plant are usually encoded by tens of related genes forming a multigene family. The emergence of multiple LTP isoforms performing different functions in plants during evolution is believed to be associated with a number of successive duplications of an ancestral gene and subsequent mutations [104]. During evolution, most angiosperms are known to undergo one or more duplications of the whole genome. A phylogenetic analysis of multiple LTP isoforms of rice, wheat, and arabidopsis indicates that duplication of genes and chromosome fragments continues at the present time [105]. During evolution, mutations in duplicated LTP genes could lead to gene pseudogenization, subfunctionalization with preservation of some functions of the ancestral gene, or neofunctionalization, i.e. acquisition of totally new functions by the gene [106]. The last two possibilities might

lead to the appearance of new LTP isoforms with a different spectrum and degree of biological activity, as well as LTP-like proteins that significantly differ from members of the LTP class in structure and perform other functions.

## PRACTICAL APPLICATIONS

### LTPs as drug carriers

The LTP ability to bind and transfer lipids creates opportunities for possible use as ligand-binding proteins in developing drug and cosmetic agent delivery systems that protect from premature biodegradation or reduce side effects upon systemic application. The possibility of developing a LTP-based delivery system depends on a number of LTP properties: a) resistance to heat denaturation and protease action; b) the hydrophilic surface ensuring biocompatibility of a LTP-ligand complex and a reduced risk of side reactions; c) protection of a drug disposed within the LTP hydrophobic cavity from premature biodegradation; d) the small size of a LTP-ligand complex, ensuring its effective penetration into tissues; and e) increased affinity to and specificity for LTP-ligand complex formation, which may be achieved by modifying the protein amino acid sequence.

Several studies have demonstrated that plant LTPs form complexes not only with FAs and phospholipids, but also with other hydrophobic and amphiphilic ligands, including some drug substances. For example, wheat LTP1 forms complexes with prostaglandin B2 (PGB2). Upon interaction with LTP1, PGB2 was found to immerse completely into the hydrophobic cavity of the protein, becoming isolated from the environment [17]. Wheat LTP1 was shown to bind some components of the skin lipid layer (sphingosines, sphingomyelins, and cerebrosides), which are used in cosmetics. Thus, wheat LTP1 may be used in cosmetology as a skin lipids carrier. On the other hand, wheat LTP1 is able to bind drugs that are active against pathogens of leishmaniasis and HIV-1 and exhibit antineoplastic properties, but have serious side effects when administered systemically (e.g., edelfosine, ilmofosine, and their analogs). Using wheat LTP1 as a delivery vehicle may significantly reduce the toxicity of these drugs. Furthermore, wheat LTP1 is able to deliver antifungal agents, such as conazole BD56 and amphotericin B [16]. It should be noted that the protein binds all these substances with low affinity, which is a prerequisite for the transport and controlled release of the ligand.

Screening of maize LTP1 and rice LTP2 using the Comprehensive Medicinal Chemistry (CMC) database containing information about 7,300 biologically active compounds demonstrated that the proteins contain not one but two potential drug binding sites: one site occurs in the hydrophobic cavity, while the second site is situated on the hydrophilic surface of the protein molecule. In rice LTP2, the binding site for sterols, such as β-sitosterol or cholesterol, is located near the hydrophobic cavity; the binding site for triphenylmethane derivatives, such as diphenyl-4-pyridylmethane, occurs on the protein surface, near the C-terminal region [15].

### LTPs in the food industry

Surfactant properties of plant LTPs enable their use in the food industry as emulsion and foam stabilizers. Beer brewing is one of the food industry sectors where these LTP properties are widely used. The formation and stability of foam are known to be important beer quality indicators. Numerous studies demonstrate that LTPs are the major protein components of barley beer and play the key role in the formation and stabilization of beer foam [35, 75]. The main beer components include a barley LTP1 protein that binds lipids and, thereby, reduces their negative impact on the formation and stability of foam. In the brewing process, LTP1 glycosylation and acylation occur, which increases amphiphilicity and the surfactant properties of the protein [75]. LTP1b, a LTP1-9(*S*),10-epoxy-10,12(*Z*)-octadecadienoic acid covalent complex, forms during fermentation, which was mentioned above [107]. LTP1 and LTP1b are resistant to high temperatures and retain their structure and ability to interact with lipids upon heating during beer pasteurization. It should be noted that LTP1, unlike LTP1b, has antifungal activity, inhibits growth of yeast, and, therefore, can adversely affect the fermentation process. Therefore, LTP1b formation and the equilibrium between free and lipid-bound forms of LTP1 in beer are important for brewing high-quality barley beer.

### Generation of viable transgenic plants

Of high interest is the possibility of using LTPs for generating transgenic plants resistant to various abiotic and biotic stress factors. Transgenic plants carrying LTP genes possess enhanced resistance to phytopathogenic microorganisms [108], pests [73], high temperatures [109], soil salinity [108], drought [110], etc.

### LTPs in allergology

Another promising application for natural and recombinant plant LTPs is the development of modern test systems for component-resolved allergy diagnostics and vaccines for preventive allergen-specific immunotherapy (ASIT).

The main methods of allergy diagnostics include skin-provocative tests and elimination diet, together with enzyme immunoassay or immunofluorescent analysis aimed at assessing the total and specific IgE and

IgG antibodies levels. Classical allergy diagnostics uses crude allergen extracts yielding poorly reproducible, and sometimes even false, results due to the lack of a possibility to standardize them and fluctuations in the content of allergenic proteins and non-protein components. The current direction in allergy diagnostics development is based on the replacement of crude extracts by individual allergic components, which can be used to produce a molecular profile of the patient's sensitivity and to study cross-reactivity [111]. Modern microarray-based test systems designed for component-resolved diagnostics use several natural and recombinant pollen (mugwort Art v 3, plane tree Pla a 3, pellitory Par j 2, and olive Ole e 7) and food (peach Pru p 3, hazel Cor a 8, walnut Jug r 3, peanut Ara h 9, and wheat Tri a 14) allergenic LTPs.

A modern method for reducing the reactivity of an organism is allergen-specific immunotherapy (ASIT), where the patient is administered gradually increased allergen doses [112]. However, classical ASIT uses crude extracts or allergoids that have a low efficacy and a high risk of systemic allergic reactions. The most safe and promising ASIT approach involves the design and development of vaccines on the basis of individual natural and recombinant allergens and their hypoallergenic analogs. These analogs should have low allergenicity but quite high immunogenicity to avoid adverse allergic reactions and reduce the hypersensitivity for a long time [113]. Hypoallergenic forms are developed mainly using methods of rational design and site-directed mutagenesis by replacing amino acid residues constituting B-cell epitopes. To date, several hypoallergenic analogs of major pollen and food allergens from different classes are undergoing clinical trials [114]. So far, hypoallergenic forms of some plant LTPs have been produced: e.g., pellitory Par j 2 [115] and peach Pru p 3 [116]. However, there are no vaccines on the basis of hypoallergenic forms of plant LTPs among the drugs under clinical trials.

## CONCLUSION

LTPs are widespread in the plant kingdom and present in almost all plant tissues and organs, have intra- or extracellular localization, and play an important physiological role. LTPs encoded by a multigene family in plants are represented by a set of multiple isoforms differentially expressed in various tissues and organs under the influence of various stress environmental factors. In addition, various LTP-like proteins with very different structures and functional activities have been found in plants. The emergence of multiple isoforms of LTPs and LTP-like proteins during evolution is assumed to result from the need to expand the range of functions of these proteins.

The biological role of LTPs in plants is poorly understood. LTPs have been demonstrated to be involved in many processes, which might be largely associated with their ability to bind and transfer a variety of lipid molecules.

LTPs have been reliably ascertained to belong to molecular factors of the plant innate immune system. As components of the PRP family, LTPs belong to the plant defense system that enables them to adapt quickly and survive under stress conditions. The defense function of LTPs is associated with their antimicrobial activity and ability to inhibit foreign enzymes, involvement in the transfer of signaling mediators and protective and building lipids, as well as with their properties as endogenous elicitors whose complexes with lipids are recognized by specific receptors and trigger an immune response.

LTPs play an important role in human life. Their widespread occurrence and a similar spatial organization make these proteins one of the most important classes of cross-reactive plant allergens that are a frequent cause of allergic reactions of varying severity. Their surfactant and allergenic properties, as well as the LTP ability to bind and transfer hydrophobic ligands, make it possible to use these proteins in pharmacy for designing drug and cosmetic agent delivery systems; in allergology, for developing modern diagnostic test kits and vaccines for ASIT; in the food industry, for brewing high-quality beers; and in agriculture, for generating stress-resistant plants.

*This work was supported by the Russian Science Foundation (project No. 14-50-00131).*

REFERENCES

1. Abdelkader A.B., Mazliak P. // Eur. J. Biochem. 1970. V. 15. P. 250–262.
2. Vergnolle C., Arondel V., Jolliot A., Kader J. // Methods Enzymol. 1992. V. 209. P. 522–530.
3. Kader J.-C. // Annu. Rev. Plant. Physiol. Plant. Mol. Biol. 1996. V. 47. P. 627–654.
4. Perrocheau L., Bakan B., Boivin P., Marion D. // J. Agricult. Food Chem. 2006. V. 54. № 8. P. 3108–3113.
5. Lee J.Y., Min K., Cha H., Hwang D.H.S.K.Y., Suh S.W. // J. Mol. Biol. 1998. V. 276. P. 437–448.
6. Gizatullina A.K., Finkina E.I., Mineev K.S., Melnikova D.N., Bogdanov I.V., Telezhinskaya I.N., Balandin S.V., Shenkarev Z.O., Arseniev A.S., Ovchinnikova T.V. // Biochem. Biophys. Res. Commun. 2013. V. 439. № 4. P. 427–432.
7. Simorre J., Caille A., Dominique M., Didier M., Ptak M. // Biochemistry. 1991. V. 30. P. 11600–11608.
8. Yeasts T.H., Rose J.K.C. // Protein Sci. 2007. V. 17. P. 191–198.
9. Gomar J., Petit M.-C., Sodano P., Sy D., Marion D., Kader J.-C., Vovelle F., Ptak M. // Protein Sci. 1996. V. 5. № 4. P. 565–577.
10. Samuel D., Liu Y.J., Cheng C.S., Lyu P.C. // J. Biol. Chem. 2002. V. 277. P. 35267–35273.

11. Hoh F., Pons J.L., Gautier M.F., de Lamotte F., Dumas C. // ActaCrystallogr. D. Biol. Crystallogr. 2005. V. 61. P. 397–406.
12. Pons J.L., de Lamotte F., Gautier M.F., Delsuc M.A. // J. Biol. Chem. 2003. V. 278. P. 14249–14256.
13. Cheng C.S., Chen M.N., Lai Y.T., Chen T., Lin K.F., Liu Y.J., Lyu P.C. // Proteins. 2008. V. 70. № 3. P. 695–706.
14. Tassin S., BroekaertW.F., MarionD., AclandD.P., PtakM., VovelleF., SodanoP. // Biochem. 1998. V. 37. P. 3623–3637.
15. Cheng C.S., Chen M.N., Liu Y.J., Huang L.Y., Lin K.F., Lyu P.Ch. // Enzyme Microb. Technol. 2004. V. 35. P. 532–539.
16. Pato C., Borgne M., Baut G., Papec P., Marion D., Douliez J.-P. // Biochem. Pharmacol. 2001. V. 62. P. 555–560.
17. Tassin-Moindrot S., Caille A., Douliez J.P., Marion D., Vovelle F. // Eur. J. Biochem. 2000. V. 267. P. 1117–1124.
18. Douliez J.-P., Michon T., Marion D. // Biochim. Biophys. Acta. 2000. V. 1467. P. 65–72.
19. Charvolin D., Douliez J.-P., Marion D., Cohen-Addad C., Pebay-Peyroula E. // Eur. J. Biochem. 1999. V. 264. P. 562–568.
20. Cheng H., Cheng P., Peng P., Lyu P., Sun Y. // Protein Sci. 2004. V. 13. P. 2304–2315.
21. Buhot N., Gomès E., Milat M.L., Ponchet M., Marion D., Lequeu J., Delrot S., Coutos-Thévenot P., Blein J.P. // Mol. Biol. Cell. 2004. V. 15. № 11. P. 5047–5052.
22. Li C., Xie W., Bai W., Li Z., Zhao Y., Liu H. // FEBS J. 2008. V. 275. № 21. P. 5298–5308.
23. Wang Z., Xie W., Chi F., Li C. // FEBS Lett. 2005. V. 579. № 7. P. 1683–1687.
24. Guerbette F., Grosbois M., Jolliot-Croquin A. // Mol. Cell. Biochem. 1999. V. 192. P. 157–161.
25. Guerbette F., Grosbois M., Jolliot-Croquin A., Kader J.-C., Zachowski A. // Biochemistry. 1999. V. 38. P. 14131–14137.
26. Ostergaard J., Vergnolle C., Schoentgen F., Kader J.C. // Biochim. Biophys. Acta. 1993. V. 1170. P. 109–117.
27. Douliez J.-P., Pato C., Rabesona H., Molle D., Marion D. // Eur. J. Biochem. 2001. V. 268. P. 1400–1403.
28. Bakan B., Hamberg M., Larue V., Prangé T., Marion D., Lascombe M.B. // Biochem. Biophys. Res. Commun. 2009. V. 390. P. 780–785.
29. Bakan B., Hamberg M., Perrocheau L., Maume D., Rogniaux H., Tranquet O., Rondeau C., Blein J.P., Ponchet M., Marion D. // J. Biol. Chem. 2006. V. 281. № 51. P. 38981–38988.
30. Regente M.C., Giudici A.M., Villalaín J., de la Canal L. // Lett. Appl. Microbiol. 2005. V. 40. P. 183–189.
31. CaaveiroJ.M.M., MolinaA., González-MañasJ.M., Rodríguez-PalenzuelaP., García-OlmedoF., Goñi F.M. // FEBS Lett. 1997. V. 410. P. 338–342.
32. Hoffmann-Sommergruber K. // Biochem. Society Transactions. 2002. V. 30. P. 930–935.
33. van Loon L.C., Rep M., Pieterse C.M. // Annu. Rev. Phytopathol. 2006. V. 44. P. 135–162.
34. Edreva A. // Gen. Appl. Plant Physiol. 2005. V. 31. P. 105–124.
35. Douliez J., Michon T., Elmorjani K., Marion D. // J. Cereal Sci. 2000. V. 32. P. 1–20.
36. Carvalho A.O., Gomes V.M. // Peptides. 2007. V. 28. P. 1144–1153.
37. Tsuboi S., Osafune T., Tsugeki R., Nishimura M., Yamada M. // Biochem. 1992. V. 3. P. 500–508.
38. Carvalho A.O., Teodoro C.E.S., Da Cunha M., Okorokova-Facanha A.L., Okorokov L.A., Fernandes K.V.S.,Gomes V.M. // Physiol. Plant. 2004. V. 122. P. 328–336.
39. Diz M.S., Carvalho A.O., Ribeiro S.F., Da Cunha M., Beltramini L., Rodrigues R., Nascimento V.V., Machado O.L., Gomes V.M. // Physiol. Plant. 2011. V. 142. № 3. P. 233–246.
40. Pagnussat L., Burbach C., Baluska F., de la Canal L. // J. Exp. Bot. 2012. V. 63. № 18. P. 6555–6563.
41. Edstam M.M., Edqvist J. // Physiol Plant. 2014. V. 152. № 1.P. 32–42.
42. Kobayashi Y., Motose H., Iwamoto K., Fukuda H. // Plant Cell Physiol. 2011. V. 52. № 6.P. 1095–1106.
43. Chae K., Gonong B.J., Kim S.C., Kieslich C.A., Morikis D., Balasubramanian S., Lord E.M. // J. Exp. Bot. 2010. V. 61. № 15. P. 4277–4290.
44. Garcia-Olmedo F., Molina A., Segura A., Moreno M. // Trends in Microbiology. 1995. V. 3. № 2. P. 72–74.
45. Choi A.M., Lee S.B., Cho S.H., Hwang I., Hur C.-G., Suh M.C. // Plant Physiol. Biochem. 2008. V. 46. P. 127–139.
46. Thoma S., Hecht U., Kippers A., Botella J., De Vries S., Somerville C. // Plant Physiol. 1994. V. 105. P. 35–45.
47. Jung H.W., Kim W., Hwang B.K. // Plant Cell Environ. 2003. V. 26. № 6. P. 915–928.
48. Gomès E., Sagot E., Gaillard C., Laquitaine L., Poinssot B., Sanejouand Y.H., Delrot S., Coutos-Thévenot P. // Mol. Plant Microbe Interact. 2003. V. 16. № 5. P. 456–464.
49. Wang C., Yang C., Gao C., Wang Y. // Tree Physiol. 2009. V. 29. № 12.P. 1607–1619.
50. Trevino M.B., O'Conell M.A. // Plant Physiol. 1998. V. 116. P. 1461–1468.
51. Zottich U., Da Cunha M., Carvalho A.O., Dias G.B., Silva N.C., Santos I.S., do Nacimento V.V., Miguel E.C., Machado O.L., Gomes V.M. // Biochim. Biophys. Acta. 2011. V. 1810. № 4. P. 375–383.
52. Cammue B.P.A., Thevissen K., Hendriks M., Eggermont K., Goderis L.J., Proost P., Damme J.V., Osborn R.W., Guerbette F., Kader J., Broekaert W.F. // Plant Physiol. 1995. V. 109. P. 445–455.
53. Segura A., Moreno M., García-Olmedo F. // FEBS Lett. 1993. V. 332. № 3. P. 243–246.
54. Dubreil L., Gaborit T., Bouchet B., Gallant D.J., Broekaert W.F., Quillien L., Quillien L.,MarionD. // Plant Sci. 1998. V. 138. P. 121–135.
55. Molina A., Segura A., Garcia-Olmedo F. // FEBS. 1993. V. 316. P. 119–122.
56. Sun J.Y., Gaudet D.A., Lu Z.X., Frick M., Puchalski B., Laroche A. // Mol. Plant Microbe Interact. 2008. V. 21. № 3. P. 346–360.
57. Ge X., Chen J., Sun C., Cao K. // Prot. Eng. 2003. V. 16. P. 387–390.
58. Ooi L.S., Tian L., Su M., Ho W.S., Sun S.S., Chung H.Y., Wong H.N., Ooi V.E. // Peptides. 2008. V. 29. № 12. P. 2101–2109.
59. Lin P., Xia L., Wong J.H., Ng T.B., Ye X., Wang S., Shi X. // J. Pept. Sci. 2007. V. 13. № 10. P. 642–648.
60. Zhang N., Jonnes B.L., Tao H.P. // Cereal Chem. 1997. V. 74. № 2. P. 119–122.
61. Melo F.R., Rigden D.J., Franco O.L., Mello L.V., Ary M.B., Grossi de Sa M.F., Bloch C. // Proteins. 2002. V. 48. № 2. P. 311–319.
62. Jones B.L., Marinac L.A. // J. Agric. Food Chem. 2000. V. 48. P. 257–264.
63. Sawano Y., Hatano K., Miyakawa T., Komagata H., Miyauchi Y., Yamazaki H., Tanokura M. // Plant Physiol. 2008. V. 146. № 4.P. 1909–1919.
64. Chae K., Kieslich C., Morikis D., Kim S., Lord E.M. // Plant Cell. 2009. V. 21. P. 3902–3914.
65. Zhang D., Liang W., Yin C., Zong J., Gu F., Zhang D. // Plant Physiol. 2010. V. 154. № 1.P. 149–162.
66. Cameron K.D., Teece M.A., Smart L.B. // Plant Physiol. 2006. V. 140. P. 176–183.
67. Lee S.B., Go Y.S., Bae H.J., Park J.H., Cho S.H., Cho H.J.,

Lee D.S., Park O.K., Hwang I., Suh M.C. // Plant Physiol. 2009. V. 150. № 1. P. 42–54.
68. Kader J.-C. // Trends Plant Science. 1997. V. 2. № 2. P. 66–70.
69. Sterk P., Booij H., Schellekens G.A., van Kammen A., De Vries S.C. // Plant Cell. 1991. V. 3. P. 907–921.
70. Park S.Y., Jauh G.Y., Mollet J.C., Eckard K.J., Nothnagel E.A., Walling L.L., Lord E.M. // Plant Cell. 2000. V. 12. P. 151–163.
71. Ouvard O., Cellier F., Ferrare K., Tousch D., Lamaze T., Dupuis J.M., Casse-Delbart F. // Plant Mol. Biol. 1996. V. 31. P. 819–829.
72. Hincha D.K. // Phil. Trans. R. Soc. Lond. 2002. V. 357. P. 909–916.
73. Choi Y.E., Lim S., Kim H.J., Han J.Y., Lee M.H., Yang Y., Kim J.A., Kim Y.S. // Plant J. 2012. V. 70. № 3.P. 480–491.
74. Sror H.A., Tischendorf G., Sieg F., Schmitt J.M., Hincha D.K. //Cryobiology. 2003. V. 47. № 3.P. 191–203.
75. Cheng C.S., Samuel D., Liu Y.J., Shyu J.C., Lai S.M., Lin K.F., Lyu P.C. // Biochemistry. 2004. V. 43. P. 13628–13636.
76. Wang X., Wang H., Cao K., Ge X. // Mol. Biol. Rep. 2009. V. 36. P. 745–750.
77. Osman H., Vauthrin S., Mikes V., Milat M.L., Panabières F., Marais A., Brunie S., Maume B., Ponchet M., Blein J.P. // Mol. Biol. Cell. 2001. V. 12. P. 2825–2834.
78. Kim Y.T., Oh J., Kim K.H., Uhm J.Y., Lee B.M. // Mol. Biol. Rep. 2010. V. 37. № 2. P. 717–727.
79. Douliez N., Jacquemard A., Marion D., Tran V., Maume B., Milat M., Ponchet M., Mikes V., Kader J.-C., Blein J. // FEBS Lett. 2001. V. 509. № 1. P. 27–30.
80. Maldonado A.M., Doerner P., Dixon R.A., Lamb C.J., Cameron R.K. // Nature. 2002. V. 419. № 6905. P. 399–403.
81. Lascombe M.B., Bakan B., Buhot N., Marion D., Blein J.P., Larue V., Lamb C., Prangé T. // Protein Sci. 2008. V. 17. № 9. P. 1522–1530.
82. Degli Esposti M. // Biochim. Biophys. Acta. 2002. V. 1553. № 3. P. 331–340.
83. Crimi M., Astegno A., Zoccatelli G., Esposti M.D. // Arch. Biochem. Biophys. 2006. V. 445. № 1. P. 65–71.
84. Rudrappa T., Biedrzycki M.L., Kunjeti S.G., Donofrio N.M., Czymmek K.J., Paré P.W., Bais H.P. // Commun. Integr. Biol. 2010. V. 3. № 2. P. 130–138.
85. Pii Y., Astegno A., Peroni E., Zaccardelli M., Pandolfini T., Crimi M. // Mol. Plant Microbe Interact. 2009. V. 22. № 12. P. 1577–1587.
86. Pii Y., Molesini B., Pandolfini T. // Plant Signal Behav. 2013. V. 8. № 7. e24836.
87. Tomassen M.M., Barrett D.M., van der Valk H.C., Woltering E.J. // J. Exp. Bot. 2007. V. 58. № 5. P. 1151–1160.
88. Palacin A., Varelaw J., Quirce S., del Pozo V. // Clin. Exp. Allergy. 2009. V. 39. P. 1267–1276.
89. Salcedo G., Sanchez-Monge R., Diaz-Perales A., Garcia--Casado G., Barber D. // Clin. Exp. Allergy. 2004. V. 34. № 9. P. 1336–1341.
90. Hauser M., Roulias A., Ferreira F., Egger M. // Allergy Asthma Clin. Immunol. 2010. V. 6. № 1. P. 1–14.
91. Borges J.P., Barre A., Culerrier R., Granier C., Didier A., Rougé P // Biochem. Biophys. Res. Commun. 2008. V. 365. № 4. P. 685–690.
92. Akkerdaas J., Finkina E.I., Balandin S.V., Santos Magadán S., Knulst A., Fernandez- Rivas M., Asero R., van Ree R., Ovchinnikova T.V. // Int. Arch. Allergy Immunol. 2012. V. 157. P. 51–57.
93. Borges J.P., Jauneau A., Brule C., Culerrier R., Barre A., Didier A., Rougé P. // Plant Physiol. Biochem. 2006. V. 44. P. 535–542.
94. Fernandez-Rivas M., Gonzalez-Mancebo E., Rodriguez--Perez R., Benito C., Sanchez-Monge R., Salcedo G., Alonso M.D., Rosado A., Tejedor M.A., Vila C., et al. // J. Allergy Clin. Immunol. 2003. V. 112. P. 789–795.
95. Egger M., Hauser M., Mari A., Ferreira F., Gadermaier G. // Curr. Allergy Asthma Rep. 2010. V. 10. № 5. P. 326–335.
96. Marzban G., Mansfeld A., Herndl A., Jäger S., Stoyanova M. E., Hemmer W., Katinger H., Laimer M. // Aerobiologia. 2006. V. 22. P. 237–245.
97. Fernández-Rivas M., Bolhaar S., González-Mancebo E., Asero R., van Leeuwen A., Bohle B., Ma Y., Ebner C., Rigby N., Sancho A.I., et al. // J. Allergy Clin. Immunol. 2006. V. 118. P. 481–488.
98. Pacios L.F., Tordesillas L., Cuesta-Herranz J., Compes E., Sánchez-Monge R., Palacín A., Salcedo G., Díaz-Perales A. // Mol. Immunol. 2008. V. 45. № 8. P. 2269–2276.
99. García-Casado G., Pacios L.F., Díaz-Perales A., Sánche-z-Monge R., Lombardero M., García-Selles F.J., Polo F., Barber D., Salcedo G. // J. Allergy Clin. Immunol. 2003. V. 112. P. 599–605.
100. Salcedo G., Sanchez-Monge R., Barber D., Diaz-Perales A. // Biochim. Biophys. Acta. 2007. V. 1771. P. 781–791.
101.Tordesillas L., Cuesta-Herranz J., Gonzalez-Muñoz M., Pacios L.F., Compés E., Garcia-Carrasco B., Sanchez-Monge R., Salcedo G., Diaz-Perales A. // Mol. Immunol. 2009. V. 46. P. 722–728.
102. Schulten V., Radakovics A., Hartz C., Mari A., Vazquez--Cortes S., Fernandez-Rivas M., Lauer I., Jahn-Schmid B., Eiwegger T., Scheurer S., et al. // J. Allergy Clin. Immunol. 2009. V. 124. № 1. P. 100–107.
103. Edstam M.M., Viitanen L., Salminen T.A., Edqvist J. // Mol. Plant. 2011. V. 4. № 6. P. 947–964.
104. Boutrot F., Chantret N. Gautier M.-F. // BMC Genomics. 2008. V. 9. № 86. P. 1–19.
105. Jang C.S., Jung J.H., Yim W.C., Lee B.M., Seo Y.W., Kim W. // Mol. Cell. 2007. V. 24. № 2. P. 215–223.
106. Moore R.C., Purugganan M.D. // Curr. Opin. Plant Biol. 2005. V. 8. P. 122–128.
107. Nieuwoudt M., Lombard N., Rautenbach M. // Food Chem. 2014. V. 157. P. 559–567.
108. Safi H., Saibi W., Alaoui M.M., Hmyene A., Masmoudi K., Hanin M., Brini F. // Plant PhysiolBiochem. 2015. V. 89. P. 64–75.
109. Wang F., Zang X.S., Kabir M.R., Liu K.L., Liu Z.S., Ni Z.F., Yao Y.Y., Hu Z.R., Sun Q.X., Peng H.R. // Gene. 2014. V. 550. № 1.P. 18–26.
110. Guo C., Ge X., Ma H. // Plant Mol. Biol. 2013. V. 82. № 3.P. 239–253.
111. Van Winkle R.C., Chang C. // Clin. Rev. Allergy Immunol. 2014. V. 46. № 3. P. 211–224.
112. Bidad K., Nicknam M.H., Farid R. // Iran J. Allergy Asthma Immunol. 2011. V. 10. № 1. P. 1–9.
113. Mutschlechner S., Deifl S., Bohle B. // Clin. Exp. Allergy. 2009. V. 39. № 11. P. 1635–1642.
114.Cromwell O., Häfner D., Nandy A. // J. AllergyClin. Immunol. 2011. V. 127. № 4. P. 865–872.
115.Bonura A., Passantino R., Costa M.A., Montana G., Melis M., Bondì M.L., Butteroni C., Barletta B., Corinti S., Di Felice G., et al. // Clin. Exp. Allergy. 2012. V. 42. № 3. P. 471–480.
116.Gómez-Casado C., Garrido-Arandia M., Gamboa P., Blanca-López N., Canto G., Varela J., Cuesta-Herranz J., Pacios L. F., Díaz-Perales A., Tordesillas L. // Clin. Dev. Immunol. 2013. V. 2013. P. 1–12.

# Monogenec Arrhythmic Syndromes: From Molecular and Genetic Aspects to Bedside

Golukhova E.Z., Gromova O.I., Shomahov R.A., Bulaeva N.I., Bockeria L.A.
Bakoulev Centre for Cardiovascular Surgery, Rublevskoye sh. 135, 121552, Moscow, Russia
*E-mail: gromova3112@gmail.com
Received 17.10.2015


**ABSTRACT** **The abrupt cessation of effective cardiac function that is generally due to heart rhythm disorders can cause sudden and unexpected death at any age and is referred to as a syndrome called "sudden cardiac death" (SCD). Annually, about 400,000 cases of SCD occur in the United States alone. Less than 5% of the resuscitation techniques are effective. The prevalence of SCD in a population rises with age according to the prevalence of coronary artery disease, which is the most common cause of sudden cardiac arrest. However, there is a peak in SCD incidence for the age below 5 years, which is equal to 17 cases per 100,000 of the population. This peak is due to congenital monogenic arrhythmic canalopathies. Despite their relative rarity, these cases are obviously the most tragic. The immediate causes, or mechanisms, of SCD are comprehensive. Generally, it is arrhythmic death due to ventricular tachyarrythmias – sustained ventricular tachycardia (VT) or ventricular fibrillation (VF). Bradyarrhythmias and pulseless electrical activity account for no more than 40% of all registered cardiac arrests, and they are more often the outcome of the abovementioned arrhythmias. Our current understanding of the mechanisms responsible for SCD has emerged from decades of basic science investigation into the normal electrophysiology of the heart, the molecular physiology of cardiac ion channels, the fundamental cellular and tissue events associated with cardiac arrhythmias, and the molecular genetics of monogenic disorders of the heart rhythm (for example, the long QT syndrome). This review presents an overview of the molecular and genetic basis of SCD in the long QT syndrome, Brugada syndrome, short QT syndrome, catecholaminergic polymorphic ventricular tachycardia and idiopathic ventricular fibrillation, and arrhythmogenic right ventricular dysplasia, and sudden cardiac death prevention strategies by modern techniques (including implantable cardioverter-defibrillator).**
**KEYWORDS** **sudden cardiac death, monogenic canalopathy, long QT syndrome, Brugada syndrome, arrhythmic right ventricular dysplasia, implantable cardioverter-defibrillator.**
**ABBREVIATIONS** **ARVD – arrhythmogenic right ventricular dysplasia; SCD – sudden cardiac death; CAD – coronary artery disease; ICD – implantable cardioverter-defibrillator; CPVT – catecholaminergic polymorphic ventricular tachycardia; LV – left ventricle; MRI – magnetic-resonance imaging; VT – ventricular tachycardia; BS – Brugada syndrome; SPR - sarcoplasmic reticulum; LV EF – left ventricular ejection fraction; VF – ventricular fibrillation; CHF – congestive heart failure; ECG – electrocardiography; PEA – pulseless electrical activity; EPS – electrophysiological study; cAMF – cyclic adenosin monophosphate; HCN-cannels - hyperpolarized activated channels; LQTS – long QT syndrome; SQTS – short QT syndrome**

## INTRODUCTION

The term "sudden cardiac death" (SCD) is used to denote death, presumably from cardiac causes, which occurs within 1 h after the onset of acute symptoms [1]. As a rule, the direct cause of such an outcome is cardiac arrhythmias: ventricular tachycardia (VT) and ventricular fibrillation (VF), which disrupt the pumping function of the heart leading to acute circulatory disorders and, in sufficient duration, to irreversible consequences with a fatal outcome. According to U.S. registers, the annual incidence of SCD in the United States is 50–100 per 100,000 of the population [2], or ca. 350–400,000 cases per year [3]. In Russia, 200–250,000 cases of SCD are registered each year [4].

The majority of SCD cases (75–80%) occur in adults and is associated with coronary artery disease (CAD). The period of acute myocardial infarction is the most susceptible to the development of ventricular arrhythmias. According to population studies, the incidence of SCD increases with age proportionally to the increase in CAD prevalence. For example, at the age below 35 years, the incidence of SCD is minimal (up to six cases

per 100,000), and it gradually increases in middle and older age groups and reaches its maximum (346 cases per 100,000) for people aged 75 to 84 years. However, there is an additional peak in SCD incidence in children under the age of 5 (17 per 100,000), which is due to familial arrhythmogenic canalopathies [5].

The second most common cause of SCD is cardiomyopathies: hypertrophic cardiomyopathy and non-ischemic dilated cardiomyopathy, which accounts for about 10–15% of all sudden arrhythmic deaths [6]. Infiltrative, inflammatory, and valvular heart diseases of different etiologies account for the majority of the remaining causes. Children and young adults are also susceptible to SCD usually due to genetic diseases, so-called canalopathies, which represent only a small portion of SCD causes (no more than 1–2%) [6].

Despite the different etiologies of sudden death, the causes behind this event are universal. As has already been mentioned, most commonly cardiac arrest is caused by sustained VT or VF. Primary pulseless electrical activity (PEA) or bradyarrhythmias is less common, accounting for no more than 40% of all SCD cases [5], and more often the two are outcomes of ventricular tachyarrhythmias. VT and/or VF hold the greatest potential for reversibility; only during this short period, until the transition to PEA or asystole, can normal heart rhythm be restored by electrical defibrillation. The need to capitalize on this "therapeutic window" dictates the need for the fastest possible diagnosis and immediate defibrillation.

The widespread use of implantable cardioverter-defibrillators (ICD) for both primary and secondary prevention of SCD has significantly reduced mortality in high-risk patients. Nevertheless, the incidence of SCD remains high. Even now, in an era of high-speed and new methods of information transfer, the survival rate after resuscitation does not exceed 5% in developed countries [6].

This review is dedicated to the rarest congenital causes of sudden death: monogenic arrhythmic disorders, as well as arrhythmogenic right ventricular dysplasia and modern approaches to sudden death risk stratification in these patients.

## CELLULAR BASIS OF ELECTROPHYSIOLOGY

The physiological processes of formation and propagation of electrical impulses in the heart muscle, as well as the "excitation-contraction" process, are remarkably fine-tuned and occur under the influence of harmonious workings of ion channels in accord with a variety of regulatory bioactive substances. Ion channels are proteins that enable selective permeability of the cell membrane for a particular ion. Voltage-gated ion channels open and close under the influence of the membrane potential, and ligand-gated ion channels require binding to an intra- or extracellular molecule to open an ion pore. In addition to ion channels, the intracellular homeostasis of ions is also maintained by ion pumps and exchangers that enable transmembrane transport of only certain ions with (pumps) or without (exchangers) use of ATP energy resources.

The cardiomyocyte's action potential is initiated by a regional change in the membrane potential that activates voltage-gated sodium ($Na^+$) channels and initiate a fast but transient sodium current ($I_{Na}$) that produces the typical ascending slope of the action potential curve known as Phase 0 depolarization (*Fig. 1*). Fast Phase 1 early repolarization is due to several ionic currents: the transient potassium current ($K^+$), $I_{to}1$ (transient outward), and the calcium-activated chloride current ($Cl^-$), $I_{to}2$ [7]. During Phases 0 and 1, $Na^+$-channels are rapidly inactivated, whereas voltage-gated calcium ($Ca2^+$) channels (L-type) are activated and participate in the formation of the sustained plateau of membrane depolarization. The plateau phase (Phase 2) is sustained by a delicate balance between the inward $Ca^{2+}$ current ($I_{Ca}$) through L-type channels, with the small residual Na current ($I_{Na}$) and the emerging outflow $K^+$ current. The activation of $K^+$-channels, together with inactivation of $Ca^{2+}$ channels, shifts this balance towards the outward currents, thereby initiating Phase 3 repolarization.

The outward potassium current (the so-called delayed rectifier current) consists of at least three components: ultra-rapid ($I_{Kur}$), rapid ($I_{Kr}$), and slow ($I_{Ks}$), which differ in the rate of activation and pharmacological sensitivity [7]. These differences define the unequal duration of the action potential in different portions of the myocardium based on the level of channel expression [8]. The expression of genes encoding subunits of rapid $K^+$-channels ($I_{Kr}$ current), *KCNH2*, is subject to pronounced diurnal variation, playing the role of a "molecular clock" of sort. Disruptions of the circadian clock mechanism may be associated with an increased risk of sudden death [9].

Finally, an abnormal inward rectifier current ($I_K1$) completes the process of cardiomyocyte membrane repolarization. This current is called abnormal because its formative $K^+$-channels are activated only in the case of negative charge of the membrane potential and enable, primarily, an inward current.

Pacemaker myocardial cells (*Fig. 2*) possess a special mechanism for the action potential buildup, which can spontaneously generate the action potential. Even the cardiomyocytes of the sino-atrial node that are isolated from all surrounding tissues maintain spontaneous diastolic depolarization. [7]. This ability is enabled through a special ion flow, called "funny" – $I_f$ – due to its unusual properties. The $I_f$ current is a mixed inward

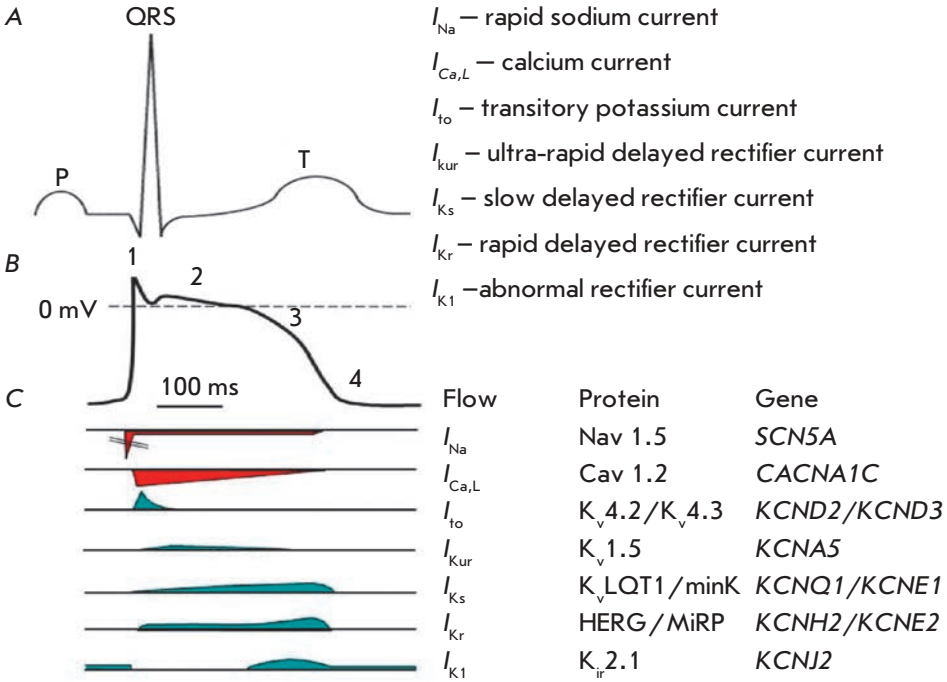


Fig. 1. Approximate temporal relationships between surface ECG (A) and typical ventricular action potential (B) and ionic currents (C) through the membrane of cardiomyocyte. 0 – depolarization phase: 1 – rapid repolarization phase; 2 – plateau; 3 – repolarization; 4 – resting phase

calcium-sodium current which is gradually initiated during the hyperpolarization (after the completion of Phase 4 repolarization) at a transmembrane potential of −40/−50 mV and is fully activated at a potential of about −100 mV, initiating the action potential. The pacemaker current is implemented through a family of ion channels discovered in the 1990s and called HCN channels (hyperpolarization-activated channels). The autonomic modulation of the pacemaker current has undeniable significance for normal physiology of cardiac activity and is implemented through cAMP. There are four isoforms of HCN-channels which differ in the rate of activation and inactivation, as well as in sensitivity to cAMP. Experiments have shown that adrenergic and cholinergic neurotransmitters cause an increase or decrease in the level of intracellular cAMP, respectively. Subsequently, cAMP binds directly to the HCN-channel, strengthening or weakening the $I_f$ current, resulting in acceleration or deceleration of spontaneous depolarization.

Ion exchangers and pumps play a crucial role in the disposal of the excess of ions arising during the formation of each action potential, as well as in the maintenance of exact levels of ions within the cell. The two most studied ion pumps are the membranes $Na^+$-$K^+$-ATP-ase and $Ca^{2+}$-ATP-ase and the two most studied ion exchangers are the membranes $Na^+$-$Ca^{2+}$ and $Na^+$-$H^+$.

$Na^+$-$K^+$-ATP-ase is a magnesium-activated ($Mg^{2+}$) cardiomyocyte membrane enzyme. Under physiological conditions, the pump maintains a normal resting potential, ensuring the transfer of three $Na^+$ ions out

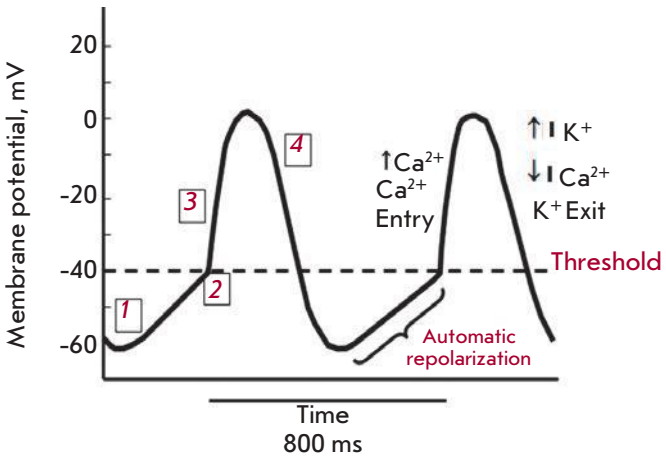


Fig. 2. Action potential of pacemaker cell. 1 – automatic depolarization – $I_f$ channels are open; 2 – membrane potential reaches the threshold level – transient T-type calcium channels are opening; 3 – slow (L-type) calcium channels are opening – depolarization; 4 – L-type calcium channels are closing, potassium channels are opening – hyperpolarization

of the cell in exchange for the influx of two $K^+$ ions into the cell. The function of the $Na^+$-pump is critical in maintaining the level of intracellular $Na^+$, and, consequently, it affects cardiomyocyte contractility and excitability [7].

The membrane $Ca^{2+}$ pump (ATPase), together with the $Na^+$-$Ca^{2+}$ exchanger, removes intracellular $Ca^{2+}$. However, its role in the utilization of $Ca^{2+}$ is presuma-

bly small. $Ca^{2+}$-ATP-ase of the sarcoplasmic reticulum is much more important. The primary role in removing excess intracellular $Ca^{2+}$ belongs to the $Na^+$-$Ca^{2+}$ exchanger. Switching-off of the gene encoding the sarcolemmal protein leads to the death of an embryo on Days 9–10 after conception [7]. The $Na^+$-$Ca^{2+}$ exchanger is a quantitative transfer protein providing transport of $Na^+$ in exchange for $Ca^{2+}$ (3:1). However, the function of the $Na^+$-$Ca^{2+}$ exchanger is coordinated with the ever-changing inward flow of $Ca^{2+}$: the system removes the exact amount of $Ca^{2+}$ that has entered into the cell during the ongoing cardiac cycle. Two systems – the Na+-$Ca^{2+}$ exchanger and the sarcoplasmic reticulum (SPR) – participate in the removal of $Ca^{2+}$ from the cytoplasm during the relaxation of the myocardium. Experiments have proven that each system alone is able to fully enable myocardial relaxation. $Ca^{2+}$-ATP-ase of the sarcoplasmic reticulum can ensure rapid relaxation of the heart muscle, but it is unable to work on its own over several consecutive contractions. In contrast, the $Na^+$-$Ca^{2+}$ exchanger enables repeated outflow of $Ca^{2+}$ from one contraction to another. Depending on the electrochemical gradients, the $Na^+$-$Ca^{2+}$ exchanger is able to provide not only the outflow of $Ca^{2+}$, but also the inward $Ca^{2+}$ current in the cell to maintain or enhance myocardial contractility.

The $Na^+$-$H^+$-exchanger is also a quantitative transfer protein; it replaces one intracellular proton with one extracellular sodium ion and plays an essential role in the maintenance of intracellular pH.

Ion channels function is regulated by a variety of intra- and extracardiac factors, the most significant of which is β-adrenergic stimulation. For example, upon physiological activation of the sympathetic nervous system due to physical exertion or emotional stress, known in English literature as "fight or flight" reaction, the increased heart rate requires immediate shortening of the cardiomyocytes action potential, which is implemented through an increase of $I_{Ks}$ via β-adrenergic stimulation [7]. In addition, the sympathetic stimulation enhances myocardial contractility, mainly through an increase in the inward $Ca^{2+}$ current and increased accumulation of $Ca^{2+}$ in the sarcoplasmic reticulum, for subsequent enhanced release inside the cell.

Intracellular $Ca^{2+}$ homeostasis mainly depends on normal operation of the SPR. Voltage-gated $Ca^{2+}$-channels in the SPR membrane are regulated by the so-called ryanodine receptors, RyR2, whose dysfunction can lead to cell overload with $Ca^{2+}$ and subsequent increase in triggering of myocardial activity.

## MONOGENIC CAUSES OF SUDDEN CARDIAC DEATH

The symphony of ion channel performance is disturbed by genetically predetermined ion canalopathies. Such defects can trigger fatal arrhythmias, which usually occur in childhood or at a young age. Despite a low incidence, these diseases can be identified by molecular diagnostics, which have allowed to elucidate the most frequent causes of these genetic abnormalities over almost two decades. Currently, more than 25 genes are known whose disruption of expression can cause susceptibility to ventricular tachyarrhythmias. Only few isolated nosological forms are identified clinically. The main ones are long QT syndrome (LQTS), short QT syndrome (SQTS), Brugada syndrome (BS), catecholaminergic polymorphic ventricular tachycardia (CPVT), and idiopathic VF. These diseases are based on three pathophysiological mechanisms: impaired repolarization (LQTS, SQTS, Brugada syndrome), delayed ventricular conduction (Brugada syndrome), and disruption of intracellular $Ca^{2+}$ homeostasis (CPVT).

### Congenital long QT syndrome (LQTS)

The most common variant of LQTS occurs in the Romano-Ward syndrome, which is inherited through an autosomal dominant mechanism (incidence of about 1 in 2,500 live births) [10]. A less frequent variant is the Jervell-Lange-Nielsen syndrome, which is autosomal-recessive and combined with deafness. Genetically, LQTS is very heterogeneous; there are at least 8 identified variants. The most common genetic subtype is LQTS1, which is caused by mutations in the *KCNQ1* gene that encodes a subunit of the voltage-gated $K^+$ channel responsible for the slow outward $K^+$ current ($I_{Ks}$). Mutations in the *KCNH2* gene that defines the structure of another version of the $K^+$ channel subunit responsible for a rapid outward $K^+$ current ($I_{Kr}$) result in the development of the second major subtype, LQTS2. Heterozygous mutations in *KCNQ1* and *KCNH2* cause a loss of function by the respective channels, decreasing $I_{Ks}$ or $I_{Kr,}$ respectively, which slows down the repolarization and prolong the ventricular action potential. An increased heart rate during sympathetic activation reveals the inability of the cardiomyocytes in such people to increase $I_{Ks}$. It explains the fact that exercise and emotional stress provoke the onset of life-threatening arrhythmias in patients with LQTS1. At the same time, trigger factors for patients with LQTS2 are sharp acoustic stimuli (cry, alarm clock, etc.) [11]. The genetic specificity of arrhythmogenic triggers has been demonstrated in a sample of 700 patients with a known LQTS genotype. For example, 99% of arrhythmic events during swimming occurred in patients with LQTS1, whereas 80% of the events provoked by sudden sounds occurred in patients with LQTS2 [12].

Ca. 10% of all LQTS are caused by mutations in the *SCN5A* gene (LQTS3), which encodes the α-subunit of the $Na^+$-channel, which enables a rapid inward $Na^+$

current during Phase 0 depolarization. Typically, these are gains of function mutations that disrupt channel inactivation and increase in a constant $I_{Na}$ [13]. A similar phenotype has been observed for the mutations in other genes (including *CAV3*, *SCN4B,* and *SNTA1*) which encode proteins that directly or indirectly affect sodium channels. A constantly elevated $Na^+$ current disrupts the physiological balance between inward and outward ions flows during the plateau phase, causing delayed repolarization, prolongation of the action potential, and predisposition to re-entry arrhythmias. Selective blockade of the constant $Na^+$ current by some antiarrhythmic drugs (such as mexiletine) or the antianginal drug ranolazine may serve as a pathophysiologically based approach to LQTS3 treatment [14, 15]. It should be noted that the *KCNQ1*, *KCNH2,* and *SCN5A* genes, mutations in which cause LQTS 1, 2 and 3, respectively, are so-called "major" LQTS genes, and mutations in them imply a high probability of congenital LQTS and is important for risk stratification (see below).

Acquired LQTS are more common than congenital ones, and they have very similar pathophysiological mechanisms. The most common variant of acquired LQTS is medical prolongation of the QT interval that occurs when cardiac or noncardiac medications are used to block the $K^+$ channels that enable $I_{Kr}$ (HERG-channel), which leads to a slowing-down of ventricular repolarization. There are also variants of genetic predisposition to drug-related prolongation of the QT interval [16]. These conditions are associated with partial loss of function in respect to $I_{Ks}$, which leads to a decrease in the so-called repolarization reserve that can manifest itself in the case of $I_{Kr}$ inhibition with drugs. There are also individual cases of manifestation of latent congenital LQTS in patients receiving drugs that block HERG-channels (e.g., antiarrhythmic drugs such as amiodarone, sotalol, dofetilide, propafenone) [13], or in case of other pathological conditions, such as myocardial infarction [17].

In addition to the Jervell-Lange-Nielsen syndrome, there are two other types of LQTS with extracardiac manifestations. The Andersen syndrome is an autosomal dominant disease characterized by ventricular arrhythmias, periodic paralysis, and bone manifestations [12]. Anderson syndrome is phenotypically heterogeneous, often with one or two clinical signs. Although ventricular arrhythmias can be classified as major manifestations of the disease, they rarely result in sudden death [13]. Andersen syndrome is associated with a mutation in the *KCNJ2* gene that encodes the $K^+$-channel which enables an abnormal inward rectifier current, $I_{K1}$, an important component of Phase 3 repolarization. Disruption of the channel function leads to a lengthening of the action potential and increased tendency towards re-entry.

The Timothy syndrome is associated with a mutation in the *CACNA1C* gene that encodes the subunit of the voltage-gated $Ca^{2+}$ channel. Symptoms of Timothy syndrome include heart rhythm abnormalities, syndactyly, and autism [13]. The mutation causes pronounced disruption of $Ca^{2+}$ channel inactivation and an excessive $Ca^{2+}$ current during the plateau phase.

LQTS is characterized by a particular electrocardiographic pattern immediately prior to the ventricular tachycardia, the so-called short-long-short sequence (SLS) or "cascade" phenomenon, which includes alternation of shortening of RR intervals due to supraventricular premature contraction (short), followed by post-premature contraction pause (long) and repeated ventricular premature contraction (short), with subsequent "torsades de pointes" tachycardia (*Fig. 3*) [12, 18]. In 2011, P. Schwartz presented updated diagnostic criteria for LQTS (*Table 1*). A total score of ≥ 3.5 justifies a LQTS diagnosis (in the absence of secondary causes) [19–21]. Furthermore, a LQTS diagnosis can be established by identifying tcharacteristic genetic mutation, regardless of the duration of the QT interval [21].

Both the genetic status and clinical data are important for a stratification of the risk of arrhythmic events in patients with LQTS. Researchers at the Mayo

**Table 1.** Diagnostic criteria for long QT syndrome. P. Schwartz score (2011) [19]

| Criteria | Points |
|---|---|
| QTc > 480 ms | 3 |
| QTc = 460–470 msc | 2 |
| QTc = 450 ms (men) | 1 |
| QTc 4th minute of recovery from exercise stress test ≥ 480 ms | 1 |
| Torsades-de-Pointes | 2 |
| T-wave alternans | 1 |
| Notched T wave in 3 leads | 1 |
| Low heart rate for age | 0.5 |
| Stress-induced syncope | 2 |
| Stress-free syncope | 1 |
| Congenital deafness | 0.5 |
| Family members with definite LQTS | 1 |
| Unexplained sudden cardiac death younger than age 30 among immediate family members | 0.5 |

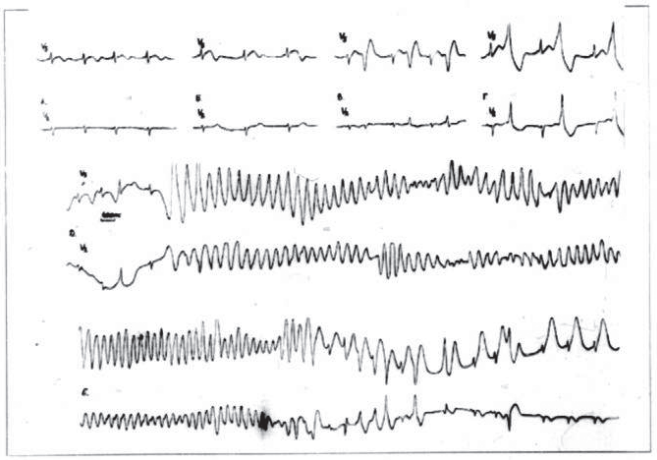

Fig. 3. Fragment of ECG Holter monitoring of a patient, female, 13 y.o., diagnosis congenital long QT syndrome. Paroxysm of torsades de pointes (own data)

Clinic Giudicessi J.R. *et al.* [22] have developed a risk stratification scheme for primary and recurrent cardiac events, including syncope, sudden cardiac arrest or sudden cardiac death before the age of 40 years, based on recent studies that examined adverse events in LQTS patients (*Fig. 4*).

Currently, beta-blockers are the only class of drugs recommended for patients with LQTS - [22, 23]. They are particularly effective in LQTS1 patients whose trigger factors are physical exercise and whose tone of the sympathetic nervous system is significantly elevated. The protective effect of beta-blockers is less pronounced in LQTS2 and LQTS3.

In addition to drug therapy, the frequency of arrhythmic events in LQTS patients can be reduced by extrapleural or thoracoscopic left-sided cardiac sympathectomy, including removal of the lower half of the stellate ganglion (T1) and thoracic ganglia (T2–T4). Schwartz *et al.* have demonstrated a decrease in the frequency of arrhythmic events by more than 90% within 8 years after surgical denervation in a group of 147 high-risk LQTS patients (average QTc 563 ± 65 ms; 99% symptomatic) [24].Modern concepts suggest the use of left-sided cardiac sympathectomy in patients who cannot tolerate β-blockers or for whom they are inefficient [22].

The decision about implantation of a cardioverter-defibrillator (ICD) should be made on an individual basis. According to the observation of 233 LQTS patients within <5 years after ICD implantation, 28% of them underwent efficient electrotherapy. At the same time, at least 31% of them had at least one post-implantation complication [25]. In 2012, Schwartz *et al.* developed a clinical M-FACT scale to identify patients in need of ICD (*Table 2*). According to the authors, implantation of ICD is justified at a score of ≥ 1 point.

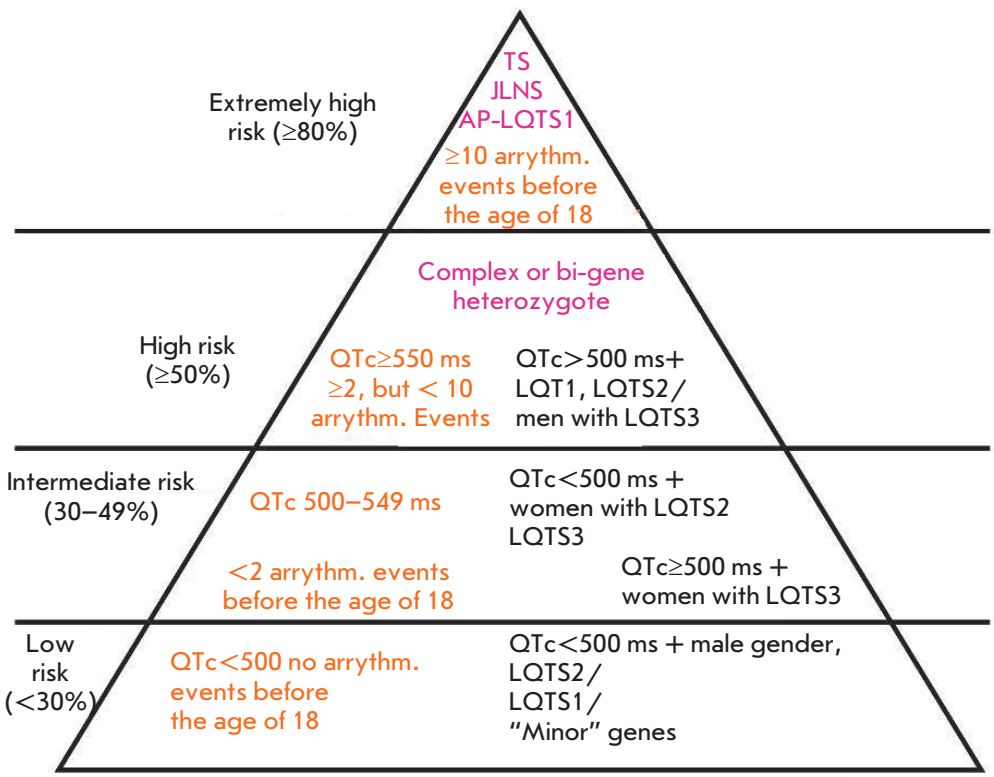


Fig. 4. Genotype- and phenotype-guided risk classification of long QT syndrome patients. Phenotype-guided recommendations are indicated by orange text, Genotype-guided recommendations are indicated by purple text, and a combination of genotype- and phenotype-guided recommendations is indicated by black text within the figure. LQTS, long QT syndrome; Arrythm. events, arrhythmic events; AP-LQTS1, autosomal recessive LQTS; JLNS, Jervell-Lange-Nielsen syndrome; TS, Timothy syndrome.

Table 2. M-FACT risk scale for a decision on implantation of cardioverter-defibrillator in patients with long QT syndrome (Schwartz et al., 2012) [26]

| Criteria | − 1 point | 0 points | 1 point | 2 points |
|---|---|---|---|---|
| Event free on therapy for >10 y | Yes | | | |
| QTc, ms | | ≤ 500 | > 500 ≤ 550 | > 550 |
| Prior ACA | | No | Yes | |
| Events on therapy | | No | Yes | |
| Age at implant, years | | > 20 | ≤ 20 | |

Note. M-FACT is deciphered as M for Minus 1 point for being free of cardiac events, while on therapy for >10 y; F for Five hundred and Five hundred and Fifty millisecond QTc; A for Age ≤20 y at implant; C for Cardiac arrest; T for events on Therapy; ACA, aborted cardiac arrest.

## Short QT interval syndrome (SQTS)

The short QT interval syndrome (SQTS) was first described as late as in 2000. This repolarization disorder is characterized by QT shortened to 320 ms and lower, high T-wave, and relative increase in the interval between the peak and the end of the T-wave [27]. However, according to population studies, shortening of the QT interval does not always imply true congenital SQTS and is not always accompanied by susceptibility to life-threatening arrhythmias [28]. In addition to a consistently shortened QT, patients with congenital SQTS are characterized by shortening of the ST segment up to its complete absence and start of the T-wave directly from the S-wave.

The shortening of the QT interval, as well as its prolongation, is associated with life-threatening arrhythmias and SCD, often in childhood. Mutations in six different genes encoding subunits of the $K^+$ (*KCNQ1*, *KCNH2*, *KCNJ2*) or $Ca2^+$ (*CACNA1C*, *CACNB2*, *CACNA2D1*) channel have been identified as associated with this phenotype. Many of these genes are similar to those implicated in LQTS: however, the functional outcome of the mutations is exactly the opposite. Gain-of-function mutations of $K^+$-channels genes lead to increased repolarization and shortening of the action potential. Mutations in $Ca^{2+}$-channels genes, on the contrary, lead to loss-of-function.

A diagnosis of SQTS can be established at QTc ≤ 340 ms. At QTc ≤ 360 ms, the diagnosis is valid in the presence of characteristic genetic mutations, family history of SQTS, familial cases of sudden death at an age <40 years or VT/VF episodes without cardiac pathology [21].

According to the latest European guidelines, implantation of a cardioverter-defibrillator is advised only as a secondary prevention. Sotalol or quinidine can be used as antiarrhythmic therapy (recommendation grade IIb) [21].

## Brugada syndrome (BS)

Patients with the Brugada syndrome are prone to developing fatal arrhythmias mainly during sleep, in the absence of myocardial ischemia, electrolyte abnormalities, and structural heart diseases [13]. Changes in resting ECG characteristics for BS patients are well-known: ST-segment elevation in the right precordial leads, signs of a right bundle branch blockage combined with normal duration of the QT interval (*Fig. 5*). Prescription of $Na^+$-channels blockers (procainamide, flecainide, ajmaline), as well as fever, may reveal hidden ECG disorders. Cases of unexplained sudden death in the family history are quite typical. The prevalence of the Brugada syndrome in Europe and America is about 1:10,000 of population [13].

A total of 350 different variants of gene mutations associated with BS [29] [30] has been described to date: in 30% of cases, they are mutations in the *SCN5A* gene that encodes the α-subunit of rapid $Na^+$-channels; in 5%, mutations in other genes, including those encoding $Ca^{2+}$- and $K^+$ channels proteins; and in 65% of cases, the genetic substrate is not identified [31, 32]. *SCN5A* gene mutations lead to a decrease in the number of $Na^+$-channels and acceleration of their inactivation in the right ventricular epicardium cells, which locally reduces $I_{Na}$ in the epicardium. The resulting disruption of ventricle wall repolarization leads to a transmural voltage gradient, which manifests itself at ECG as ST-segment elevation and serves as a substrate for re-entry into the ventricular myocardium [33].

According to other researchers, the inhibition of the inward sodium current slows down pulse conduction in the right ventricle, causing delayed activation of the myocardium in the right ventricular exit sites. This leads to asynchronous depolarization and electrical instability in this section of the heart with possible development of ventricular arrhythmias by the re-entry mechanism [13, 34]. It is unclear whether these two hypotheses are mutually exclusive or if all BS variants are subject to a single pathophysiological mechanism.

A genetic analysis to identify mutations in genes typical for BS is useful for verification of the diagnosis, but it has no independent value in the risk stratification. Moreover, the absence of mutations does not preclude the diagnosis.

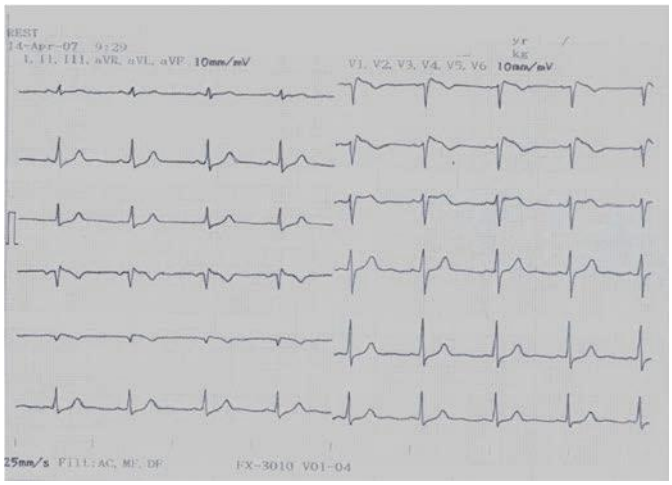

Fig. 5. ECG of a patient with Brugada syndrome (own data)

Risk stratification in asymptomatic patients with Brugada syndrome is the most important and, at the same time, controversial issue. The annual incidence of cardiac arrest or syncopes in BS patients with a history of sustained VT or VF is between 1.9 [35] and 8.8 [36], 7.7 [37] and 13.8% [38], respectively. Implantation of ICD to such patients is the only truly effective treatment [37]. However, most patients (64% according to a large-scale FINGER study) [35] have no clinical manifestations of the disease at the time of verification of the diagnosis. The incidence of arrhythmic events in such patients is significantly lower and ranges from 0 to 0.8% (0.5% according to FINGER data) [37]. On the other hand, the young age of these patients and the absence of structural heart diseases suggest that a low annual risk of cardiac events is only temporary and will increase in the subsequent few decades.

The role of programmed ventricular stimulation in invasive EPS for risk stratification in asymptomatic patients has been actively discussed since BS was described for the first time. Recent studies, including the largest ones, FINGER and PRELUDE, found no independent effect of invasive electrophysiologic studies on arrhythmic events over an average of 32 and 18 months [35, 38]. However, according to a recently published meta-analysis of 14 studies, which included 3,536 patients with an asymptomatic Brugada syndrome phenotype, a typical spontaneous pattern of type 1 ECG (i.e. ST elevation in the right precordial leads of more than 2 mm with a negative T-wave and J-wave) (*Fig. 5*), as well as the induction of ventricular tachyarrhythmias by the programmed ventricular stimulation, increases the risk of future arrhythmic events. The length of the follow-up period was 20 to 77 months [39]. Therefore, at the moment the recommendation of ICD implantation on the basis of EPS data has class of recommendation IIb; i.e., "can be considered" for the induction of VF during the programmed ventricular stimulation with two or three extrastimules in two points (Clinical Recommendations for Diagnosis and Treatment of Ventricular Arrhythmias, European Society of Cardiology, 2015) [21].

In other cases, ICD implantation is indicated for BS patients as secondary prevention (class of recommendation I), and it should be considered in case of a spontaneous manifestation of type I ECG and history of syncope of unknown origin (class of recommendation IIa) [21]. Quinidine and isoproterenol are recommended as preventive antiarrhythmic therapy, including for the treatment of "electrical storm" (class of recommendation IIa). In addition, BS patients are advised to observe a number of rules to minimize the known factors that trigger arrhythmia, such as excluding administration of drugs that can aggravate ST elevation in the right precordial leads, avoiding excessive use of alcohol and heavy meals, and using antipyretics in a fever of any origin as soon as possible [21].

## Catecholaminergic polymorphic ventricular tachycardia (CPVT)

Disruption of intracellular $Ca^{2+}$ homeostasis leads to serious arrhythmogenic effects. Mutations in the *RyR2* gene encoding the ryanodine receptors that are responsible for the release of calcium from the sarcoplasmic reticulum of the cardiomyocyte cause the development of an autosomal dominant variant of catecholaminergic polymorphic ventricular tachycardia. Autosomal recessive types of the disorder are caused by impairments of the *CASQ2* gene function, which encodes the calsequestrin protein that binds $Ca^{2+}$ of the sarcoplasmic reticulum, or mutations in the *TRDN* gene that encodes triadin which binds calsequestrin to RyR2-receptors [13]. These three proteins are located in the terminal SPR cistern, where the intracellular membrane is in close proximity to the region of transverse tubulae (T-tubulae) of the plasma membrane. Normally, electrical pulses are delivered into the T-tubulae system and activate L-type $Ca^{2+}$-channels, causing fluctuations in $Ca^{2+}$ concentration sufficient to cause a $Ca^{2+}$-induced release of $Ca^{2+}$ via ryanodine receptors. Release of $Ca^{2+}$ from the SPR causes contraction of the myocyte, which ends in the removal of $Ca^{2+}$ from the cytosol, mainly via the $Ca^{2+}$-ATP-ase and $Na^{+}/Ca^{2+}$ pumps. Disruption of the function of these receptors leads to cardiomyocyte overload with $Ca^{2+}$, electrical instability of the cells, and the formation of post-depolarization potentials. Catecholamines that enter the blood in time of stress and/

or exercise cause contraction of the heart muscle via phosphorylation of protein kinase of the ryanodine receptor [40–42].

Other genes associated with polymorphic VT have also been identified. It is believed that mutation in the *KNJ2* gene, which is associated with the development of the Andersen syndrome, may be the cause of familial catecholaminergic VT. There are reports on mutations in the ankyrin B gene, which are also present in LQTS4. Recently, it has been suggested that idiopathic ventricular fibrillation can be a form of familial polymorphic ventricular tachycardia [43].

The diagnosis of catecholaminergic polymorphic VT is basically an exclusion diagnosis in which bi-directional VT or VF in response to physical or emotional stress occurs in patients without a structural heart disease and changes in resting ECG.

Drug therapy consists of the prescription of beta-blockers. There are several reports on the effectiveness of calcium channel blockers (verapamil) in familial polymorphic ventricular tachycardia. In general, a lifestyle change is indicated to all patients, including exclusion of physical activities and exercise.

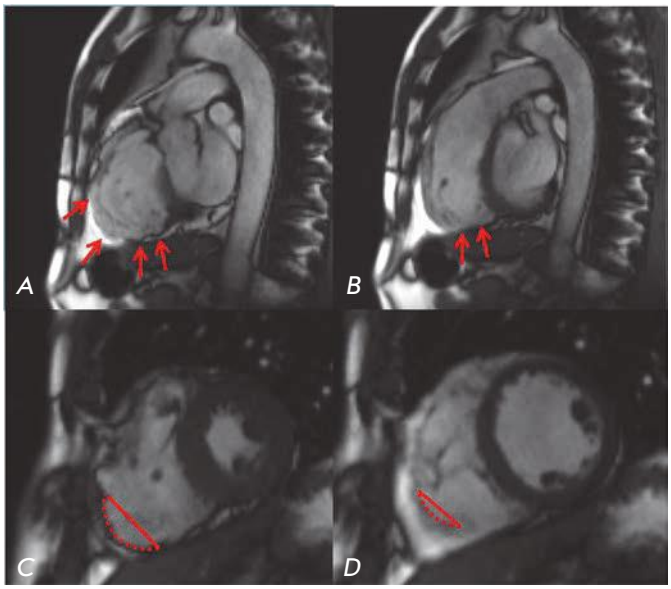


Fig. 6. Cardiac MRI of a patient with ARVD (own data). Bright blood images in the right ventricular outflow tract (RVOT) plane obtained in end diastole (A) and end systole (B) show microaneurysms (arrows) in the right ventricle free wall with persistent bulge in both phases. Short-axis bright blood images obtained in end diastole (C) and end systole (D) demonstrate dyskinesis (bulge in systole, arrows) at the acute angle of the right ventricle

## Idiopathic ventricular fibrillation

Idiopathic ventricular fibrillation is a rare disease of unknown etiology, which manifests itself as syncope and SCD in the absence of data in favor of an organic heart disease or canalopathy. Idiopathic VF is characterized by spontaneous development of fatal arrhythmia unrelated to physical stress, often during sleep. VF is initiated by premature ventricular contraction with a very short coupling interval. It has been demonstrated that Purkinje fibers are involved in the induction and maintenance of arrhythmia with a re-entry mechanism [44].

## Arrhythmogenic right ventricular dysplasia (ARVD)

Arrhythmogenic right ventricular dysplasia (or cardiomyopathy) (ARVD) is a rare inherited disease characterized by ventricular arrhythmias, sudden cardiac death, and dysfunction of the right ventricle. More than 30 years have passed since the first detailed description of ARVD in 1982. Numerous clinical and experimental studies of this disease have been published since. For example, it has been established that the most common genetic causes of ARVD are mutations in desmosome proteins, the basic elements of cell-cell adhesion structures present in the multilayered epithelium and the myocardium; e.g., the results of a recently published study involving 577 patients in the U.S. (Johns Hopkins registry) and Danish ARVD registers showed that 80% of patients had a mutation in the *PKP2* gene encoding plakophilin, one of the desmosomal proteins. The remaining participants in the study had mutations in other desmosomal protein genes: *DSG2* (desmoglein), *PLN* (plakophilin), *DSP* (desmoplakin), *DSC2* (desmocollin), *JUP* (junction plakoglobin), *TMEM43* (transmembrane protein 43) [45].

This myocardium dysplasia can be called "cardiomyopathy of intercellular contacts" [11]. Defective desmosomal proteins disrupt the mechanical connection between adjacent muscle cells, which leads to their separation, especially in the context of myocardial stretching. The accompanying inflammation, fibrosis, and adipocytosis may be a nonspecific response to damage, similar to the one caused by any damage to the myocardium [46]. This pathogenetic model explains the fact that prolonged excessive stress, accompanied by myocardial stretching, significantly increases the risk of early clinical manifestation of the disease and increases the risk of SCD. In addition, it explains why the pathological ARVD process often involves the more stretchable and thin-walled right ventricle, especially in the early stages of the disease. Naturally, the mechanical separation leads to electrical heterogeneity, forming an ideal substrate for the development of ventricular re-entry tachycardia [11].

Task Force Criteria (TFC) for the diagnosis of ARVD were proposed in 1994 and revised in 2010 [47]. The diagnostic criteria for ARVD include characteristic changes in depolarization/repolarization on the electrocardiogram, echocardiography, and magnetic resonance imaging (MRI) data (*Fig. 6*) describing changes in morphology and function of the right ventricle, characteristic changes in myocardial tissue observed in endomyocardial biopsy, as well as the presence of ventricular arrhythmias, details of family history and genetic testing (*Table 3*). To justify an ARVD diagnosis, a patient must score four points, with one major criterion being worth two points, and one minor criterion being worth one point. ARVD is considered to be "probable" at three points, whereas a score between one and two should be considered as an absence of ARVD [47].

Proper treatment of ARVD patients largely depends on an adequate diagnosis. Treatment is defined by the following strategies: SCD risk stratification and addressing the issue of implanting a cardioverter-defibrillator (ICD), minimizing the frequency of ICD discharges, and prevention of the progression of the disease. According to the general recommendations for SCD prevention, ICD implantation in ARVD is indicated in patients who have had ventricular fibrillation, or sustained ventricular tachycardia or syncope. The study by Bhonsale A. *et al.* included 84 patients with ARVD who were followed for 4.7 ± 3.4 years after ICD implantation as primary prevention. The predictors of effective electrotherapy were the symptoms (i.e. the status of the subject and not that of a family member), induction of VT at electrophysiological study, presence of unstable ventricular tachycardia, and more than 1,000 premature ventricular contractions (PVC) per day. The induction of ventricular tachyarrhythmias at EPS was an independent risk factor for the effective discharge of ICD [48].

Therefore, currently ICD implantation is indicated for patients who meet TFC criteria, especially if they have a history of SCD, sustained VT or arrhythmogenic syncope, a high number of PVCs, and/or unstable VT [46]. Clinicians should be especially attentive to SCD risk stratification in patients for whom ARVD was identified during a family screening. Typically, such patients are at earlier stages of the disease. Limitation on physical activity and the use of β-blockers can reduce the risk of SCD in such individuals. However, careful monitoring of the patient's condition is recommended for all patients with a decision not to implant ICD.

β-blockers are indicated for all patients with ARVD. Amiodarone, or sotalol is recommended as additional antiarrhythmic therapy. In rare cases, other antiarrhythmic agents are used. If antiarrhythmics and repetitive ICD discharges are ineffective, it is recommended to perform radiofrequency ablation of arrhythmogenic foci. It should be noted that the role of catheter ablation in patients with ARVD is limited to a possible reduction in the number of defibrillator discharges and improved quality of life. According to several studies on the effectiveness of catheter ablation in patients with ARVD, only 25 to 47% were VT-free during the first year of observation, and 5 and 10 years after surgery the numbers were 21 and 15% [46]. Efficacy of epicardial ablation is slightly higher and amounts to 64% during the first year and 45% after 5 years [46]. According to Philips B. *et al.*, in 30 patients with ARVD there were no effective ICD discharges after epicardial radiofrequency ablation in 83, 76, and 70% of cases for 6, 12, and 24 months, respectively [49].

The only currently available effective way to slow the progression of the disease is limitation on physical activity.

## CONCLUSION

In conclusion, we would like to present the survey data published in 2014 by the European Heart Rhythm Association, which included cardiologists from 50 clinics in 23 countries [50]. The survey focused on the diagnosis and treatment of patients with congenital arrhythmic syndromes. According to the study, most patients with canalopathies undergo genetic testing: from 70% among LQTS to 36% among patients with idiopathic VF. Although only a third of clinicians discuss the test results with patients and specialists in genetics, pharmacological tests are relatively frequently used for the diagnosis of congenital canalopathies. For example, 89% of the respondents used sodium channel blockers for the diagnosis of the Brugada syndrome, and 36% used isoproterenol to confirm catecholaminergic ventricular tachycardia. 80–92% of the doctors do not use pharmacological provocation for the diagnosis of the remaining canalopathies. Most clinics (82–98%) do not resort to intracardiac EPS to induce ventricular arrhythmias, with the exception of BS cases (39% of clinics use EFI). From 27 to 54% of the study participants included MRI in the diagnostic protocol for patients with BS and idiopathic ventricular arrhythmias, but only rarely for patients with LQTS and SQTS (11–17% of participants). Coronary angiography is performed in 62% of cases of idiopathic VF/VT. Endomyocardial biopsy is included in the study protocol of 8% of the patients with idiopathic VF. In most clinical centers, ICD implantation for primary prevention is performed only in 0–5% of patients with congenital canalopathies, whereas ICD usage for secondary prevention increases to 90–100%. Recurrent ventricular arrhythmias, leading to multiple ICD discharges, are treated with intensification of therapy, the

Table 3. Diagnostic criteria for arrhythmogenic right ventricular dysplasia (ARVD) (F. Marcus *et al.*, 2010) [47]

| Group | Major criterion | Minor criterion |
|---|---|---|
| Global or regional dysfunction and structural alterations | **By 2D echo:**<br>Regional RV akinesia, dyskinesia, or aneurysm<br>*AND* 1 of the following (end diastole):<br>PLAX RVOT 32 mm<br>PSAX RVOT 36 mm *OR*<br>fractional area change 33%;<br>**By MRI:**<br>Regional RV akinesia or dyskinesia or dyssynchronous RV contraction<br>*AND* 1 of the following:<br>Ratio of RV end-diastolic volume to BSA 110 mL/m$^2$ (male) or 100 mL/m$^2$ (female)<br>RVEF ≤ 40%<br><br>**By RV angiography:**<br>Regional RV akinesia, dyskinesia, or aneurysm | **By 2D echo:**<br>Regional RV akinesia or dyskinesia or dyssynchronous RV contraction<br>*AND* 1 of the following (end diastole):<br>PLAX RVOT 29 to 32 mm;<br>PSAX RVOT 32 to 36 mm *OR*<br>fractional area change 33% to 40%;<br>**By MRI:**<br>Regional RV akinesia or dyskinesia or dyssynchronous RV contraction<br>*AND* 1 of the following:<br>Ratio of RV end-diastolic volume to BSA 100 to 110 mL/m$^2$ (male) or 90 to 100 mL/m$^2$ (female);<br>RVEF> 40 ≤45% |
| Tissue characterization of wall | Residual myocytes 60% by morphometric analysis (or 50% if estimated), with fibrous replacement of the RV free wall myocardium in 1 sample, with or without fatty replacement of tissue on endomyocardial biopsy | Residual myocytes 60% to 75% by morphometric analysis (or 50% to 65% if estimated), with fibrous replacement of the RV free wall myocardium in 1 sample, with or without fatty replacement of tissue on endomyocardial biopsy |
| Repolarization abnormalities | Inverted T waves in right precordial leads ($V_1$, $V_2$, and $V_3$) or beyond in individuals 14 years of age (in the absence of complete right bundle-branch block) | Inverted T waves in leads $V_1$ and $V_2$ in individuals 14 years of age (in the absence of complete right bundle-branch block) or in $V_4$, $V_5$, or $V_6$<br>Inverted T waves in leads $V_1$, $V_2$, $V_3$, and $V_4$ in individuals 14 years of age in the presence of complete right bundle-branch block |
| Depolarization/conduction abnormalities | Epsilon wave (reproducible low-amplitude signals between end of QRS complex to onset of the T wave) in the right precordial leads ($V_1$ to $V_3$) | Late potentials by SAECG in 1 of 3 parameters in the absence of a QRS duration of 110 ms on the standard ECG:<br>fQRS ≥ 114 ms<br>Duration of terminal QRS 40 μV (low-amplitude signal duration) 38 ms<br>Root-mean-square voltage of terminal 40 ms QRS ≤ 20 ms<br>Terminal activation duration of QRS 55 ms measured from the nadir of the S wave to the end of the QRS, including R', in $V_1$, $V_2$, or $V_3$, in the absence of complete right bundle-branch block |
| Arrhythmias | Nonsustained or sustained ventricular tachycardia of left bundle-branch morphology with superior axis (negative or indeterminate QRS in leads II, III, and aVF and positive in lead aVL) | Nonsustained or sustained ventricular tachycardia of RV outflow configuration, left bundle-branch block morphology with inferior axis (positive QRS in leads II, III, and aVF and negative in lead aVL) or of unknown axis<br>500 ventricular extrasystoles per 24 hours (Holter) |
| Family history | ARVC/D confirmed in a first-degree relative who meets current Task Force criteria<br>ARVC/D confirmed pathologically at autopsy or surgery in a first-degree relative<br>Identification of a pathogenic mutation† categorized as associated or probably associated with ARVC/D in the patient under evaluation | History of ARVC/D in a first-degree relative in whom it is not possible or practical to determine whether the family member meets current Task Force criteria<br>Premature sudden death (35 years of age) due to suspected ARVC/D in a first-degree relative<br>ARVC/D confirmed pathologically or by current Task Force Criteria in second-degree relative |

BSA, body surface area; RVOT, RV outflow tract; PVC, premature ventricular contraction; EDV RV, end-diastolic volume of the right ventricle; LBBB - left bundle branch block; RV – right ventricle; PLAX parasternal long-axis view; PSAX, parasternal short-axis view; RVEF, right ventricle ejection fraction; CM – Holter ECG monitoring; Echo, echocardiography; EMB – endomyocardial biopsy.

use of β-blockers, and various antiarrhythmic drugs (isoproterenol infusion, quinidine at SQTS), and cardiac sympathetic denervation. Radiofrequency ablation (RFA) is considered to be the preferred method in idiopathic ventricular fibrillation (20%), whereas for the remaining canalopathies the frequency of RFA use does not exceed 8%.

The authors of the survey conclude that the study participants share a commitment to the present recommendations; however, they point out that more than 50% of all centers participating in the survey do not participate in any of the registers (local, national or international), which, of course, complicates the task of studying the course of the disease, effectiveness of therapy, risk stratification, and prognosis in patients with primary arrhythmogenic syndromes.

*This work was supported by a grant from the Government of the Russian Federation for state support of scientific research conducted under the supervision of leading scientists at Russian scientific institutions and public research centers of the Russian Federation "Molecular mechanisms of atrial fibrillation" (№ 14.Z50.31.0026).*

REFERENCES

1. Zipes D.P., Rubart M. // Heart Rhythm. 2006. V. 3. P. 108–113.
2. Fishman G.I., Chugh S.S., Dimarco J.P., Albert C.M., Anderson M.E., Bonow R.O., Buxton A.E., Chen P.S., Estes M., Jouven X., et al. // Circulation. 2010. V. 122. P. 2335–2348.
3. Revishvili A.Sh., Ardashev AV, Bojcov SA, Bockeria LA, Golukhova EZ, Davtyan KV, Zenin SA, Kuznetcov VA, Kupcov VV, Lebedev DS et al. Clinical guidelines for electrophysiological studies, catheter ablation and implantable antiarrythmic devices usage. M.: MAKS Press; 2013: P.596 (in Russian)..
4. Bockeria LA, Revishvili A.Sh. Neminshchii I.M. Sudden cardiac death. M.: GEOTAR-Media; 2011. P. 272. (in Russian)..
5. Chugh S.S., Reinier K., Teodorescu C., Evanado A., Kehr E., Al Samara M., Mariani R., Gunson K., Jui J. // Prog. Cardiovasc Dis. 2008. V. 51(3). P. 213–228. doi: 10.1016/j.pcad.2008.06.003.
6. Nichol G., Thomas E., Callaway C.W., Hedges J., Powell J.L., Aufderheide T.P., Rea T., Lowe R., Brown T., Dreyer J., et al. // JAMA. 2008. V. 300. P. 1423–1431.
7. Zipes D.P., Jalife J. Cardiac electrophysiology: from cell to bedside. 4-th ed. Philadelphia. WB Saunders, 2004. 1155 p.
8. Bockeria O.L., Akhobekov A.A. // Annaly aritmologii. 2014. № 3. P. 176-184. DOI: 10.15275/annaritmol.2014.3.6 (In Russian).
9. Schroder E.A., Burgess D.E., Zhang X., Lefta M., Smith J.L., Patwardhan A., Bartos D.C., Elayi C.S., Esser K.A., Delisle B.P. // Heart Rhythm. 2015. pii: S1547–5271(15)00198-8. doi: 10.1016/j.hrthm.2015.02.019.
10. Schwartz P.J., Stramba-Badiale M., Crotti L., Pedrazzini M., Besana A., Bosi G., Gabbarini F., Goulene K., Insolia R., Mannarino S., et al. // Circulation. 2009. V. 120. № 18. P. 1761–1767.
11. Bockeria AL, Golukhova EZ. Ventricular arrhythmias and sudden cardiac death. Clinical cardiology: diagnostic and treatment. – M.: Bakoulev Centre for cardiovasc surgery. 2011: P. 598. (in Russian)
12. Schwartz P.J., Ackerman M.J., George Jr. A.L., Wilde A. // J. Am. Coll. Cardiol. 2013. V. 62. № 3. P. 169–180. doi: 10.1016/j.jacc.2013.04.044.
13. Alfred L. George Jr. // J. Clin. Invest. 2013. V. 123. № 1. P. 75–83. doi: 10.1172/JCI62928.
14. Moss A.J., Zareba W., Schwarz K.Q., Rosero S., McNitt S., Robinson J.L. // J. Cardiovasc. Electrophysiol. 2008. V. 19. № 12. P. 1289–1293.
15. Kannankeril P., Roden D.M., Darbar D. // Pharmacol. Rev. 2010. V. 62. № 4. P. 760–781.
16. Roden D.M. // J. Intern. Med. 2006. V. 259. № 1. P. 59–69.
17. Crotti L., Hu D., Barajas-Martinez H., De Ferrari G.M., Oliva A., Insolia R., Pollevick G.D., Dagradi F., Guerchicoff A., Greco F., et al. // Heart Rhythm. 2012. V. 9. № 7. P. 1104–1112.
18. Bockeria L. A., Revishvili A. Sh., Pronicheva I. V. // Annaly aritmologii. 2005. № 4. P. 7-12 (in Russian).
19. Schwartz P.J., Crotti L. // Circulation. 2011. V. 124. P. 2181–2184.
20. Mizusawa Y., Horie M., Wilde A. // Circulation J. 2014. V. 78. P. 2827–2833.
21. Priori S., Blomstrom-Lunqvist C., Mazzanti A., Blom N., Borggrefe M., Camm J., Elliott P.M., Fitzsimons D., Hatala R., Hindricks G., et al. // Eur. Heart J. 2015. V. 36. № 41. P. 2793–2867. doi: 10.1093/eurheartj/ehv316.
22. Giudicessi J.R., Ackerman M.J. // Curr. Probl. Cardiol. 2013. V. 38. № 10. P. 417–455. doi: 10.1016/j.cpcardiol.2013.08.001.
23. Priori S.G., Wilde A.A., Horie M., Cho Y., Behr E.R., Berul C., Blom N., Brugada J., Chiang C.E., Huikuri H., Kannankeril P., Krahn A., Leenhardt A., et al. // Europace. 2013. V. 15. P. 1389–1406.
24. Schwartz P.J., Priori S.G., Cerrone M., Spazzolini C., Odero A., Napolitano C., Bloise R., De Ferrari G.M., Klersy C., Moss A.J., et al. // Circulation. 2004. V. 109. P. 1826–1833.
25. Schwartz P.J., Spazzolini C., Priori S.G., Crotti L., Vicentini A., Landolina M., Gasparini M., Wilde A.A., Knops R.E., Denjoy I., et al. // Circulation. 2010. V. 122. P. 1272–1282.
26. Schwartz P.J., Crotti L., Insolia R. // Circ. Arrhythm. Electrophysiol. 2012. V. 5. P. 868–877.
27. Adeniran I., Hancox J.C., Zhang H. // Front. Physiol. 2013. V. 4. Art. 166. P. 1–16. doi: 10.3389/fphys.2013.00166.
28. Crotti L., Taravelli E., Girardengo G., Schwartz P. // Indian Pacing Electrophysiol. J. 2010. V. 10. № 2. P. 86–95.
29. Nielsen M.W., Holst A.G., Olesen S.P., Olesen M.S. // Front. Physiol. 2013. V. 15. № 4. Art. 179. P. 1—11.
30. Brugada R., Campuzano O., Sarquella-Brugada G., Brugada J., Brugada P. // Methodist Debakey Cardiovasc. J. 2014. V. 10. № 1. P. 25–28.
31. Kapplinger J.D., Tester D.J., Alders M., Benito B., Berthet M., Brugada J., Brugada P., Fressart V., Guerchicoff A., Harris-Kerr C., et al. // Heart Rhythm. 2010. V. 7. № 1. P. 33–46.
32. Baroudi G., Pouliot V., Denjoy I., Guicheney P., Shrier A., Chahine M. // Circ. Res. 2001. V. 88. P. E78–E83.

33. Bockeria L. A., Bockeria O. L., Kirtbaya L. N. // Annaly aritmologii. 2010. V. 3. P. 16-30 (in Russian).
34. Laitinen P.J., Brown K.M., Piippo K., Swan H., Devaney J.M., Brahmbhatt B., Donarum E.A., Marino M., Tiso N., et al. // Circulation. 2001. V. 103. P. 485–490.
35. Probst V., Veltmann C., Eckardt L., Meregalli P.G., Gaita F., Tan H.L., Babuty D., Sacher F., Giustetto C., Schulze-Bahr E., et al. // Circulation. 2010. V. 121. № 5. P. 635–643.
36. Brugada J., Brugada R., Antzelevitch C., Towbin J., Nademanee K., Brugada P. // Circulation. 2002. V. 105. № 1. P. 73–78.
37. Naseef A., Behr E.R., Batchvarov V.N. // J. Saudi Heart Assoc. 2015. V. 27. P. 96–108.
38. Priori S.G., Gasparini M., Napolitano C., Della Bella P., Ottonelli A.G., Sassone B., Giordano U., Pappone C., Mascioli G., Rossetti G., et al. // J. Am. Coll. Cardiol. 2012. V. 59. № 1. P. 37–45.
39. Letsas K.P., Liu T., Shao Q., Korantzopoulos P., Giannopoulos G., Vlachos K., Georgopoulos S., Trikas A., Efremidis M., Deftereos S., et al. // Am. J. Cardiol. 2015. V. 116. № 1. P. 98–103. doi: 10.1016/j.amjcard.2015.03.044.
40. Priori S.G., Napolitano C., Memmi M. // Circulation. 2002. V. 106. P. 69–74.
41. Liu N., Colombi B., Memmi M., Zissimopoulos S., Rizzi N., Negri S., Imbriani M., Napolitano C., Lai F.A., Priori S.G. // Circ. Res. 2006. V. 99. № 3. P. 292–298.
42. Bockeria E. L. // Annaly aritmologii. 2005. № 4. P. 30-35 (in Russian)..
43. Bockeria L. A., Bockeria O. L., Zavarina A. Yu., Kudzoeva Z. // Annaly aritmologii. 2010. № 4. P. 5-16 (in Russian).
44. Bockeria L. A., Bockeria O. L., Kirtbaya L. N. // Annaly aritmologii. 2009. № 4. P. 7-20 (in Russian)
45. Bhonsale A., Groeneweg J.A., James C.A., Dooijes D., Tichnell C., Jongbloed J.D., Murray B., te Riele A.S., van den Berg M.P., Bikker H., et al. // Eur. Heart J. 2015. V. 36. № 14. P. 847–855. doi: 10.1093/eurheartj/ ehu509.
46. Calkins H. // Circ. J. 2015. V. 79. № 5. P. 901–913. doi: 10.1253/circj.CJ-15-0288.
47. Marcus F.I., McKenna W.J., Sherrill D., Basso C., Bauce B., Bluemke D.A., Calkins H., Corrado D., Cox M.G., Daubert J.P., et al. // Circulation. 2010. V. 31. P. 1533–1541.
48. Bhonsale A., James C.A., Tichnell C., Murray B., Gagarin D., Philips B., et al. // J. Am. Coll. Cardiol. 2011. V. 58. P. 1485–1496.
49. Philips B., Te Riele A.S., Sawant A., Kareddy V., James C.A., Murray B., et al. // Heart Rhythm. 2015. V. 12. P. 716–725.
50. Hocini M., Pison L., Proclemer A., Larsen T.B., Madrid A. // Europace. 2014. V. 16. P. 600–603. doi: 10.1093/europace/ euu074.

# Heat Stress-Induced DNA Damage

O.L. Kantidze[1*], A.K. Velichko[1], A.V. Luzhin[1], S.V. Razin[1,2*]
[1]Institute of Gene Biology, Russian Academy of Sciences, Vavilova str. 34/5, 119334, Moscow, Russia
[2]Lomonosov Moscow State University, Faculty of Biology, Leninskie Gory 1, bldg. 12, 119991, Moscow, Russia
*E-mail: kantidze@gmail.com; sergey.v.razin@usa.net
Received:17.12.2015


**ABSTRACT** **Although the heat-stress response has been extensively studied for decades, very little is known about its effects on nucleic acids and nucleic acid-associated processes. This is due to the fact that the research has focused on the study of heat shock proteins and factors (HSPs and HSFs), their involvement in the regulation of transcription, protein homeostasis, etc. Recently, there has been some progress in the study of heat stress effects on DNA integrity. In this review, we summarize and discuss well-known and potential mechanisms of formation of various heat stress-induced DNA damage.**
**KEYWORDS** **heat shock, DNA repair, DNA damage, DNA replication, topoisomerase**
**ABBREVIATIONS AND TERMS SSB – single-stranded DNA break; DSB –double-stranded DNA break; top1 – DNA topoisomerase I; top2 – DNA topoisomerase II.**

## INTRODUCTION

Heat stress (heat shock, hyperthermia) is one of the most well-studied complex stress factors. Cell response to heat stress involves most sub-cellular compartments and metabolic processes [1—3]. It has long been known that cells exposed to heat stress display an increased sensitivity to agents inducing double-stranded DNA breaks (DSBs), in particular to ionizing radiation [4, 5]. This phenomenon is called "heat radiosensitization." It was assumed that this effect is caused by the fact that heat stress can inhibit the DNA repair system [5]. Indeed, several decades-long studies have shown that heat stress can inhibit the key components of virtually all repair systems *(Figure)*. Heat stress inhibits the activity of the base excision repair (BER) system [6–9] and nucleotide excision repair (NER) system [10, 11]. The effect of heat stress on base excision repair has been the most extensively studied: heat stress can directly inactivate DNA polymerase β and certain DNA glycosylases [6, 9]. Recently, it has been shown that heat stress may also inhibit the mismatch repair system [12]. Inhibition of DSB repair systems resulting from heat stress makes the largest contribution to heat-induced radiosensitization. It is known that heat stress inhibits the functioning of both the non-homologous DNA end joining (NHEJ) system and the homologous recombination (HR) system. In the case of NHEJ, the effect of heat stress is limited by the complex of DNA-dependent protein kinase (DNA-PK): it was shown that hyperthermia can lead to aggregation of the Ku70/80 heterodimer (and therefore reduction in its DNA-binding activity), inhibition of Ku80 expression and/or inhibition of the DNA-PK catalytic subunit [13–15]. The situation is different with HR: heat stress may inhibit this repair system at several key stages [16]. The impact of hyperthermia on DNA repair systems in higher eukaryotes is discussed in the recently published review by P.M. Krawczyk *et al.* [17]; so we suggest that our readers consult this review, while our mini-review will mainly focus on direct heat stress-induced DNA damage *(Figure)*.

### Single-stranded DNA breaks induced by heat stress.

Heat stress not only inhibits DNA repair systems, but can also act as a DNA damaging agent. It is known that heat stress can lead to the accumulation of 8-oxoguanine, deaminated cytosine, and apurinic DNA sites (AP-sites) in a cell [18–20]. It can be suggested that such DNA damage, as well as single-stranded DNA breaks (SSBs), is passively accumulated in the cell due to heat stress-induced inhibition of excision repair systems. A more interesting and controversial question is related to the nature of heat stress-induced DSBs, as well as the possibility of active heat stress induction of SSBs. For a long time, it was believed that heat stress does not induce DSBs, but rather leads to the generation of SSBs, which are formed as a result of inhibition of DNA replication due to hyperthermia [21–23]. We used several complementary approaches (comet assay, fluorescent *in situ* labeling of DNA breaks using DNA

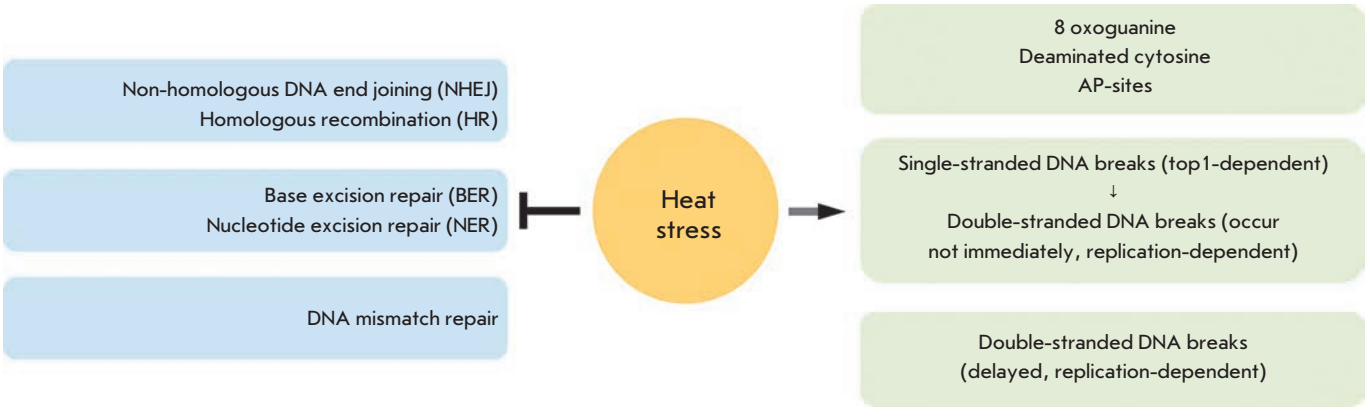


Fig. 1. The effect of heat stress on the integrity of DNA and the repair system (see text for details)

polymerase I) to demonstrate that heat stress, indeed, induces SSBs in cells during the S-phase of the cell cycle [24]. In the same paper, it was shown that hyperthermia can inhibit DNA replication: heat stress leads to either a slowing-down or arrest of replication forks, depending on the temperature and cell line [24]. However, it should be noted that the occurrence of SSBs in S-phase cells is not associated with heat stress-induced inhibition of DNA replication [25]. Recently, we have identified the mechanism of heat stress-induced SSBs. It was found that heat stress induces SSBs by inhibition of DNA topoisomerase I (top1), an enzyme that relaxes DNA supercoils by introducing temporary SSB into DNA [25]. The catalytic cycle of top1 includes cleavage of one DNA strand, accompanied by formation of an intermediate complex consisting of the enzyme covalently bound to the DNA. Stabilization of this complex is the main mechanism of genotoxic action of top1 poisons (e.g., camptothecin and its derivatives) [26, 27]. Heat stress (45°C) can not only inhibit the catalytic activity of the enzyme, but also lead to the accumulation of covalently bound top1-DNA complexes in the cell. It can be concluded that the effect of hyperthermia on top1 is similar to the action of poisons. The only difference is that heat stress is likely to suppress top1 activity at all stages of the catalytic cycle. Although it is known that top1 can bind to preexisting SSBs in the cell [28, 29], in the case of heat stress it is top1 that causes their emergence. The most convincing evidence of this was obtained in experiments with inhibition of enzyme expression through RNA interference [25]. It has been shown that, in the case of decreased expression of top1, the cellular senescence program, which depends on SSBs induction and their conversion into persistent DSBs, is not activated [25]. This is indicative of the fact that no heat stress-induced formation of SSBs occurs in cells not expressing top1. Therefore, the role of top1 in the formation of heat stress-induced SSBs seems to be quite obvious. It is also interesting that, in HeLa cells, covalently bound complexes between top1 and DNA are effectively formed only at temperatures above 44°C. Therefore, SSBs should not form at the clinically relevant temperatures of 41–43°C. Heat stress-induced formation of SSBs is mainly observed in the S-phase of the cell cycle, because the main function of top1 is to resolve topological problems that occur during DNA replication. We can state that the sensitivity of non-proliferating cells (terminally differentiated, arrested in G0 phase, etc.) should be significantly reduced in terms of the formation of SSBs. It cannot be completely absent, as the function of top1 in the cell is not limited to the DNA replication process. In this regard, it is worth noting that heat stress induction of SSBs is likely to occur not only in the S-phase of the cell cycle. SSBs also form in the G1 and G2 phases, but with very low frequency. According to our unpublished data, the number of SSBs formed due to heat stress in various cell lines directly correlates with the level of top1 expression. Summarizing these findings, we can conclude that heat stress inhibits the *in vivo* activity of top1 and leads to the formation of covalently bound complexes between the enzyme and the DNA and, as a consequence, formation of SSBs.

**Double-stranded DNA breaks induced by heat stress.** Heat stress-induced SSB is a source of DSB formation. These DSBs have several interesting features: they are specific to the S-phase of the cell cycle and occur in the cell not immediately after the heat stress, but rather 3–6 hours later [25]. These delayed DSBs occur due to the collision of replication forks which were re-started after heat stress-induced arrest, with SSBs, resulting from top1 inhibition [25]. Slow kinetics of the formation of these DSBs is associated with heat stress-induced inhibition of DNA replication, on the one hand, and inhibition of the transcription process, on the other hand

[25]. Active transcription process is required for the detection and subsequent removal of the top1 complex covalently bound to DNA, resulting in SSB unmasking and the possibility of their collision with replication forks [30, 31]. Apparently, delayed DSBs are effectively recognized by cellular systems, as evidenced by ATM/ATR-dependent phosphorylation of H2AX (DSB marker), followed by the involvement of other repair factors to the break site (53BP1, Rad51, etc.). However, repair of these breaks does not occur, which leads to the occurrence of a persistent DNA damage signal in the cell and, consequently, to initiation of a premature cellular senescence program [25, 32].

As can be seen from the abovementioned, we were the first to established the mechanism of delayed DSB formation under heat stress conditions. However, the question of whether heat stress can immediately induce DSB has long remained a controversial one. In recent years, it has been shown in different laboratories that heat stress can induce phosphorylation of H2AX histone [33-37], which is one of the first events in the processes of DSB recognition and repair [38, 39]. However, interpretation of these results is quite contradictory: some researchers have stated that γH2AX foci mask heat-induced DSBs [34, 37]; others believe that heat shock itself does not lead to DNA damage and, in this case, γH2AX is a byproduct of the cellular response to stress [33, 35, 36]. Recently, we have proved that hyperthermia can provoke the formation of DSBs [24, 40]. This was confirmed using two independent approaches: comet assay and labeling of DNA ends with terminal deoxynucleotidyl transferase. However, heat stress induces DSBs only in G1- and G2-phase cells. These DSBs are marked by ATM-dependent phosphorylation of H2AX [24]. Interestingly, other repair factors, such as the 53BP1 protein, are not attracted to γH2AX foci immediately after exposure to hyperthermia [24, 41]. At the same time, these DSBs are effectively repaired within the first 3—6 hours after heat stress. This probably means that active repair of heat stress-induced DSBs does not begin immediately after exposure, but rather some time after – when heat stress-inhibited repair systems have recovered. However, the mechanism (trigger) of immediate formation of DSBs under heat stress conditions is still not understood. The following processes can be considered as possible candidates for this role: activation of retroelements [42, 43], generation of reactive oxygen species [18], and transcription arrest [44, 45]. It is well-known that the aforementioned processes can lead to the formation of DSBs and, under certain conditions, occur during heat stress. However, none of these hypotheses can provide a convincing explanation of heat stress induction of DSBs in non-S-phase cells only. In our opinion, the most probable mechanism of heat stress-induced formation of DSBs is to inhibit the activity of DNA topoisomerase II (top2), an enzyme that changes DNA topology by introducing temporary DSBs [46]. Such discontinuities are accompanied by the formation of a covalent bond between the protein molecule and one end of the DNA chain. Inhibition of top2 at the stage of covalently bound complex leads to the formation of DSBs [46]. The results showing that heat stress can inhibit the activity of top2 *in vitro* were obtained long ago [47]. The fact that heat stress can reduce the genotoxic potential of top2 poisons is also indicative of the influence of hyperthermia on this enzyme [48]. There are two isoforms of top2, and expression of one of them depends on the stage of the cell cycle [49, 50]. This dynamics of expression could easily explain the dependence of DSB induction on the cell cycle phase.

## CONCLUSION

In summary, we can state that, in addition to complex suppression of almost all the repair systems in the cells of higher eukaryotes, heat stress directly results in the formation of various DNA damage. Interestingly, the type and the fate of the heat stress-induced damage depends on the stage of the cell cycle when the cell is exposed to high temperatures. For example, in the S phase of the cell cycle, hyperthermia leads to a top1-dependent formation of SSBs, some of which can be converted into difficult-to-repair DSBs several hours later. At the same time, heat stress immediately induces DSB formation in cells that are at the G1 or G2 stage of the cell cycle. Although this scheme of heat stress action is characteristic of all cell lines analyzed in our study, it should be kept in mind that the number of breaks and the degree of repair response of the cell can considerably vary depending on the strength of the heat stress and the cell type (line).

*This work was supported by the Russian Science Foundation (grant № 14-24-00022).*

REFERENCES

1. Richter K., Haslbeck M., Buchner J. // Mol. Cell. 2010. V. 40. P. 253–266.
2. Velichko A.K., Markova E.N., Petrova N.V., Razin S.V., Kantidze O.L. // Cell Mol. Life Sci. 2013. V. 70. P. 4229–4241.
3. Kantidze O.L., Velichko A.K., Razin S.V. // Biochemistry (Mosc). 2015. V. 80. P. 990–993.
4. Dewey W.C., Sapareto S.A., Betten D.A. // Radiat. Res. 1978. V. 76. P. 48–59.
5. Iliakis G., Wu W., Wang M. // Int. J. Hyperthermia. 2008. V. 24. P. 17–29.
6. Dikomey E., Becker W., Wielckens K. // Int. J. Radiat. Biol.

Relat. Stud. Phys. Chem. Med. 1987. V. 52. P. 775–785.
7. Raaphorst G.P., Feeley M.M., Chu G.L., Dewey W.C. // Radiat. Res. 1993. V. 134. P. 331–336.
8. Batuello C.N., Kelley M.R., Dynlacht J.R. // Anticancer Res. 2009. V. 29. P. 1319–1325.
9. Fantini D., Moritz E., Auvre F., Amouroux R., Campalans A., Epe B., Bravard A., Radicella J.P. // DNA Repair (Amst.). 2013. V. 12. P. 227–237.
10. Hettinga J.V., Konings A.W., Kampinga H.H. // Int. J. Hyperthermia. 1997. V. 13. P. 439–457.
11. Muenyi C.S., States V.A., Masters J.H., Fan T.W., Helm C.W., States J.C. // J. Ovarian Res. 2011. V. 4. P. 9.
12. Nadin S.B., Cuello-Carrion F.D., Sottile M.L., Ciocca D.R., Vargas-Roig L.M. // Int. J. Hyperthermia. 2012. V. 28. P. 191–201.
13. Burgman P., Ouyang H., Peterson S., Chen D.J., Li G.C. // Cancer Res. 1997. V. 57. P. 2847–2850.
14. Qi D., Hu Y., Li J., Peng T., Su J., He Y., Ji W. // PLoS One. 2015. V. 10. P. e0122977.
15. Ihara M., Takeshita S., Okaichi K., Okumura Y., Ohnishi T. // Int. J. Hyperthermia. 2014. V. 30. P. 102–109.
16. Eppink B., Krawczyk P.M., Stap J., Kanaar R. // Int. J. Hyperthermia. 2012. V. 28. P. 509–517.
17. Oei A.L., Vriend L.E., Crezee J., Franken N.A., Krawczyk P.M. // Radiat. Oncol. 2015. V. 10. P. 165.
18. Bruskov V.I., Malakhova L.V., Masalimov Z.K., Chernikov A.V. // Nucleic Acids Res. 2002. V. 30. P. 1354–1363.
19. Lindahl T., Nyberg B. // Biochemistry. 1974. V. 13. P. 3405–3410.
20. Warters R.L., Brizgys L.M. // J. Cell Physiol. 1987. V. 133. P. 144–150.
21. Corry P.M., Robinson S., Getz S. // Radiology. 1977. V. 123. P. 475–482.
22. Jorritsma J.B., Konings A.W. // Radiat. Res. 1984. V. 98. P. 198–208.
23. Warters R.L., Brizgys L.M., Axtell-Bartlett J. // J. Cell Physiol. 1985. V. 124. P. 481–486.
24. Velichko A.K., Petrova N.V., Kantidze O.L., Razin S.V. // Mol. Biol. Cell. 2012. V. 23. P. 3450–3460.
25. Velichko A.K., Petrova N.V., Razin S.V., Kantidze O.L. // Nucleic Acids Res. 2015. V. 43. P. 6309–6320.
26. Pommier Y. // Nat. Rev. Cancer. 2006. V. 6. P. 789–802.
27. Ashour M.E., Atteya R., El-Khamisy S.F. // Nat. Rev. Cancer. 2015. V. 15. P. 137–151.
28. Lebedeva N., Rechkunova N., Boiteux S., Lavrik O. // IUBMB Life. 2008. V. 60. P. 130–134.
29. Lebedeva N., Auffret Vander Kemp P., Bjornsti M.A., Lavrik O., Boiteux S. // DNA Repair (Amst.). 2006. V. 5. P. 799–809.
30. Lin C.P., Ban Y., Lyu Y.L., Desai S.D., Liu L.F. // J. Biol. Chem. 2008. V. 283. P. 21074–21083.
31. Lin C.P., Ban Y., Lyu Y.L., Liu L.F. // J. Biol. Chem. 2009. V. 284. P. 28084–28092.
32. Petrova N.V., Velichko A.K., Razin S.V., Kantidze O.L. // Cell Cycle. 2016. V. 15. P. 337–344.
33. Hunt C.R., Pandita R.K., Laszlo A., Higashikubo R., Agarwal M., Kitamura T., Gupta A., Rief N., Horikoshi N., Baskaran R., et al. // Cancer Res. 2007. V. 67. P. 3010–3017.
34. Kaneko H., Igarashi K., Kataoka K., Miura M. // Biochem. Biophys. Res. Commun. 2005. V. 328. P. 1101–1106.
35. Laszlo A., Fleischer I. // Int. J. Hyperthermia. 2009. V. 25. P. 199–209.
36. Laszlo A., Fleischer I. // Cancer Res. 2009. V. 69. P. 2042–2049.
37. Takahashi A., Mori E., Somakos G.I., Ohnishi K., Ohnishi T. // Mutat. Res. 2008. V. 656. P. 88–92.
38. Rogakou E.P., Boon C., Redon C., Bonner W.M. // J. Cell. Biol. 1999. V. 146. P. 905–916.
39. Rogakou E.P., Pilch D.R., Orr A.H., Ivanova V.S., Bonner W.M. // J. Biol. Chem. 1998. V. 273. P. 5858–5868.
40. VelichkoA.K., RazinS.V. KantidzeO.L. // Dokl. Acad. Nauk. 2013. V. 450. P. 224–227.
41. Petrova N.V., Velichko A.K., Kantidze O.L., Razin S.V. // Cell Biol. Int. 2014. V. 38. P. 675–681.
42. Belgnaoui S.M., Gosden R.G., Semmes O.J., Haoudi A. // Cancer Cell Int. 2006. V. 6. P. 13.
43. Gasior S.L., Wakeman T.P., Xu B., Deininger P.L. // J. Mol. Biol. 2006. V. 357. P. 1383–1393.
44. Sordet O., Nakamura A.J., Redon C.E., Pommier Y. // Cell Cycle. 2010. V. 9. P. 274–278.
45. Sordet O., Redon C.E., Guirouilh-Barbat J., Smith S., Solier S., Douarre C., Conti C., Nakamura A.J., Das B.B., Nicolas E., et al. // EMBO Rep. 2009. V. 10. P. 887–893.
46. Nitiss J.L. // Nat. Rev. Cancer. 2009. V. 9. P. 338–350.
47. Osheroff N., Shelton E.R., Brutlag D.L. // J. Biol. Chem. 1983. V. 258. P. 9536–9543.
48. Kampinga H.H. // Br. J. Cancer. 1995. V. 72. P. 333–338.
49. Goswami P.C., Roti Roti J.L., Hunt C.R. // Mol. Cell. Biol. 1996. V. 16. P. 1500–1508.
50. Kimura K., Saijo M., Ui M., Enomoto T. // J. Biol. Chem. 1994. V. 269. P. 1173–1176.

# Role of Transcriptional Read-Through in PRE Activity in *Drosophila melanogaster*

P. V. Elizar'ev, D. V. Lomaev, D. A. Chetverina, P. G. Georgiev, M. M. Erokhin*
Institute of Gene Biology, Russian Academy of Sciences, Vavilov str. 34/5, 119334, Moscow, Russia
*E-mail: yermaxbio@yandex.ru
Received 16.02.2016


**ABSTRACT** **Maintenance of the individual patterns of gene expression in different cell types is required for the differentiation and development of multicellular organisms. Expression of many genes is controlled by Polycomb (PcG) and Trithorax (TrxG) group proteins that act through association with chromatin. PcG/TrxG are assembled on the DNA sequences termed PREs (Polycomb Response Elements), the activity of which can be modulated and switched from repression to activation. In this study, we analyzed the influence of transcriptional read-through on PRE activity switch mediated by the yeast activator GAL4. We show that a transcription terminator inserted between the promoter and PRE doesn't prevent switching of PRE activity from repression to activation. We demonstrate that, independently of PRE orientation, high levels of transcription fail to dislodge PcG/TrxG proteins from PRE in the absence of a terminator. Thus, transcription is not the main factor required for PRE activity switch.**
**KEYWORDS** **Polycomb, Trithorax, PRE,** *Drosophila.*
**ABBREVIATIONS** **PcG –Polycomb group proteins; TrxG –Trithorax group proteins;** *bxd* **–** *bithoraxoid.*

## INTRODUCTION

During the early stages of development of multicellular organisms, an individual pattern of gene expression is established in different cell types and then maintained over many cell divisions. Polycomb (PcG) and Trithorax (TrxG) group proteins are responsible for a stable inheritance of the proper pattern. PcG proteins cause repression, while TrxG proteins provide activation of transcription [1–4]. In *Drosophila*, these factors bind to DNA elements called PREs (Polycomb Response Elements). PRE elements contain sites for various DNA-binding factors, the recruitment of which results in association of PcG/TrxG complexes with PRE [5, 6]. Polycomb group proteins are assembled into three main complexes: PRC1, PRC2, and PhoRC [2, 3]. The core subunits of the PRC1 complex are represented by the PC, PH, dRing, and Psc factors [7–9]. The PRC2 complex contains the E(z), Esc, Su(z)12, and Caf1 core components [10–13]. The PhoRC complex includes the dSfmbt and DNA-binding factor Pho [14]. PRC2 complex trimethylates lysine 27 of histone H3 (H3K27me3) through the SET domain of the E(z) catalytic subunit [10–13]. H3K27me3 modification specifically marks the chromatin regions repressed by PcG [15, 16]. TrxG proteins represent a heterogeneous group which in particular includes the Trx, Trr, dCBP, Ash1, and UTX factors and DNA-binding factor GAF, also known as Trl (Trithorax-like) [17].

The activity of PREs can be modulated. For example, the repressor activity of PREs in transgenic systems can be turned off either by enhancers or the yeast exogenous activator GAL4 [18–24]. It has been previously suggested that inactivation of repression is provided by the induction of transcription through PRE by the GAL4 activator, which, in turn, leads to the removal of PRE-associated repressor factors from DNA due to the passage of RNA polymerase II and transcription factors [24].

However, we have recently demonstrated that even a high level of transcription through the 660 bp *bxd*PRE does not lead to complete elimination of proteins from *bxd*PRE in *Drosophila* transgenic constructs [21]. Transcription was initiated from the UAS-promoter: the minimal promoter of the *hsp70* gene under the control of five binding sites for the GAL4 protein. We showed that inactivation of PRE-mediated repression was independent of whether GAL4-induced transcription was directed towards or in opposite direction from *bxd*PRE.

In the present study, we show that prevention of transcription through *bxd*PRE by a SV40 terminator does not abrogate inactivation of PRE-mediated repression. The importance of *bxd*PRE orientation in

transcriptional read-through has been also tested. It has been established that, in case of reverse orientation of *bxd*PRE, transcriptional read-through also does not lead to the elimination of PcG/TrxG factors.

## EXPERIMENTAL

### Plasmid constructs design

All constructs were made on the basis of the CaSpeR vector containing *white* gene with partial deletion of the first intron (encodes complete product of *white* gene) [25]. The enhancer of *white* gene (Ee) located in the genome at position −1180...−1849 bp relative to the transcription start site of *white* gene [26] was excised from the Ee-pBluescript SK+ plasmid [27] and inserted in forward orientation into a CaSpeR4 vector cleaved by NotI [En-*white*].

A fragment SmaI-SalI of 4324 bp in length from the plasmid vector CaSpeR-hs43-lacZ carrying the *lacZ* gene with the *adh* leader sequence and SV40 transcription terminator at 3'-terminus (GenBank: X81643.1) was inserted into a pBluescript SK+ vector cleaved by SmaI and SalI [LacZ-SV40-pSK].

The promoter of the *hsp26* gene, 472 bp, was amplified by PCR (primers 5'-ctagaaacttcggctctctca-3' and 5'-gttgaatgaacttgtttgacttgt-3') and inserted into a pBluescript SK+ vector cleaved by EcoRV [hsp26-pSK]. A HindIII−PstI fragment of the hsp26-pSK vector was inserted into the LacZ-SV40-pSK vector at the SmaI site [hsp26-LacZ-SV40-pSK]. A fragment NotI-SalI of the hsp26-LacZ-SV40-pSK vector was incorporated into the En-*white* vector at the BamHI site [hsp26-LacZ-SV40-En-*white*].

A fragment HindIII−EcoRI containing a minimal promoter of the *hsp70* gene and five GAL4 sites at 5' terminus was excised from the pUAST vector [28] and inserted into a pBluescript SK+-sce2 vector at the EcoRV site [sce(UAS)]. The coding region of a *eGFP* gene of 717 bp was amplified by PCR (primers 5'-atg-gtgagcaagggcgaggagct-3' and 5'-cttgtacagctcgtccatgc-cga-3') and cloned into the vector pBluescript SK+ at the EcoRV site [eGFP-pSK].

A HindIII−EcoRI fragment of the eGFP-pSK vector was inserted in forward orientation into the sce(UAS) vector at the HincII site [(UAS)sce-eGFP].

A XbaI−BamHI fragment of 702 bp in length of the pUAST vector containing a transcription terminator was inserted into a pBluescript SK+-lox2 vector cleaved by EcoRV [lox(SV40)]. A XbaI−XbaI fragment of the lox(SV40) vector was incorporated into the (UAS)sce-eGFP vector at the XhoI site [(UAS) sce-eGFP-lox(SV40)].

A HincII−HincII fragment, 1828 bp, of the LacZ-SV40-pSK vector was incorporated into a pBluescript SK+ vector cleaved by EcoRV [*linker*1828bp-pSK]. A fragment XbaI−BamHI of 222 bp of the pGL3basic vector containing the SV40 transcription terminator was inserted into the *linker*1828bp-pSK vector at the SmaI site [*linker1828*-SV40s-pSK].

A fragment NotI−BamHI of the (UAS) sce-eGFP-lox(SV40) vector was inserted into the vector *linker1828*-SV40s-pSK at the EcoRV site [(UAS) sce-eGFP-lox(SV40)-*linker1828*-SV40s-pSK].

A fragment HincII−XbaI containing *bxd*PRE of 656 bp (3R:16764122..16764777) was excised from the frt(PRE) vector [29] and incorporated into the vector (UAS)sce-eGFP-lox(SV40)-*linker1828*-SV40s-pSK at the AorI site in forward [(UAS)sce-eGFP-lox-(SV40)-*linker785*frt(PREdir)*linker1043*-SV40s-pSK] or reverse [(UAS)sce-eGFP-lox(SV40)-*linker785*frt(PRE-rev)*linker1043*-SV40s-pSK] orientation.

*UDTPD construct.* A XbaI−XbaI fragment of the (UAS)sce-eGFP-lox(SV40)-*linker785*frt(PREdir)*link-er1043*-SV40s-pSK vector was incorporated into the vector hsp26-LacZ-SV40-En-*white* at the BamHI site.

*UDTPR construct.* A XbaI−XbaI fragment of the (UAS) sce-eGFP-lox(SV40)-*linker785*frt(PRErev)*linker1043*-SV40s-pSK vector was inserted into the hsp26-LacZ-SV40-En-*white* vector at the BamHI site.

All details of the constructs design are available upon request.

### Transformation of *Drosophila melanogaster* embryos and phenotypic analysis of *yellow* and *white* expression in transgenic lines

DNA constructs and a P element with defective inverted repeats *P25.7wc*, which served as a source of transposase [30], were injected into a $y^1w^{1118}$ line at the stage of preblastodermal embryo according to [31, 32]. The survived flies were crossed with the $y^1w^{1118}$ line. Transgenic flies were selected based on phenotypic manifestation of *white* expression. The number of copies was determined by Southern blot hybridization with a *white* gene fragment. Lines containing a single copy of the construct per genome were selected.

For *in vivo* deletion of the DNA fragment, flies carrying the construct were crossed with transgenic flies expressing Flp ($w^{1118}$; *S2CyO, hsFLP, ISA/Sco;* +) or Cre ($y^1w^1$; *Cyo, P[w+,cre]/Sco;* +) recombinase [33, 34]. Accuracy of fragment removal was confirmed by PCR.

Line $yw^{1118}$; *P[w*$^-$*, tubGAL4]117/TM3,Sb,* a derivative of the Bloomington Stock Center #5138 line with deletion of the *mini-white* marker gene [35], was used for expression of *GAL4* under the control of a tubulin promoter.

The expression of *white* gene was determined by visual evaluation of eye pigmentation using the standard scale: red color is the pigmentation of eyes in wild-type flies (*white* expression in case of complete stimulation by a tissue-specific enhancer), white the color of the eyes is observed in the absence of pigmentation (complete inactivation of *white* gene). Various degrees of mosaic phenotype are observed in case of repression.

In order to analyze the phenotype of transgenic flies, 3- to 5-day-old males developed at 25°C were used. The details of all crosses conducted for the genetic analysis and excision of functional elements can be provided upon request.

### Chromatin immunoprecipitation (X-ChIP)

A total of 150–200 mg of adult flies was collected for each experiment. Chromatin immunoprecipitation was performed according to the technique described previously [21].

### Antibodies

Antibodies to the PH protein [to fragment 86–520 aa, ph-p-PA]; dSfmbt [to fragment 1–348 aa, Sfmbt-PB] [27]; PC [to fragment 191–354 aa, Pc-PA]; TRX-N [to fragment 8–351 aa, trx-PA]; and GAF [1–519 aa, Trl-PB] [21] were obtained in rabbits. Antibodies to H3K27me3: Abcam (ab6002, ChIP Grade).

### Real-time PCR with Hot-Start Taq DNA polymerase

Real-time PCR was conducted using C1000$^{tm}$ ThermalCycler (Bio-Rad) in a 25 μl volume according to the following protocol (per one reaction): 2.5 μl of 10× buffer (0.5 M Tris-HCl, pH 8.8, 0.5 M KCl, 15 mM $MgCl_2$, 1% Tween 20), 2 μl of 25 mM $MgCl_2$, 0.5 μl of 10 mM dNTPs, 1.5 μl of each primer (at a concentration of 5 pmol/ μl), 0.25 μl of SYBR Green100× (Sigma), 0.3 μl of Hot-Start Taq DNA polymerase (SibEnzyme), 11.45 μl of mQ, 5 μl of sample. Data were assessed using the Bio-Rad CFX Manager software and Microsoft Excel. Decimal dilutions of *Drosophila* genomic DNA at a concentration of 0.1 to 100 ng were used as reference standards. The primers used for real-time PCR analysis of the material obtained using chromatin immunoprecipitation are presented in *Table*.

Primers for real-time PCR analysis of the material obtained by chromatin immunoprecipitation

| | |
|---|---|
| 1-ChIP forward | 5'-gagaactctgaatagggaattgg-3' |
| 1-ChIP reverse | 5'-agctcctcgcccttgctcaccat-3' |
| 2-ChIP forward | 5'-ccgaccactaccagcagaac-3' |
| 2-ChIP reverse | 5'-gtccatgccgagagtgatcc-3' |
| 3-ChIP forward | 5'-tcctcgacggtatcgataagcttg-3' |
| 3-ChIP reverse | 5'-ccataatggctgcgccgtaaag-3' |
| 4-ChIP forward | 5'-ggtgaaattatcgatgagcgtgg-3' |
| 4-ChIP reverse | 5'-cagttcaaccaccgcacgataga-3' |
| 5-ChIP forward | 5'-aaaactttctacgcctcagttc-3' |
| 5-ChIP reverse | 5'-gcttattagccctgcaattga-3' |
| 6-ChIP forward | 5'-gcactggatatcattgaacttatctg-3' |
| 6-ChIP reverse | 5'-tggacagagaaggaggcaaaca-3' |
| *Ras64B* forward | 5'-gagggattcctgctcgtcttcg-3' |
| *Ras64B* reverse | 5'-gtcgcacttgttacccaccatc-3' |
| *bxd*PRE adjacent forward (site adjacent to *bxd*PRE in genome) | 5'-aagagcaaggcgaaagagagc-3' |
| *bxd*PRE adjacent reverse (site adjacent to *bxd*PRE in genome) | 5'-cgttttaagtgcgactgagatgg-3' |

## RESULTS

### Model system for studying the impact of transcription on the recruitment of Polycomb and Trithorax group proteins to PRE

The influence of transcriptional read-through on PRE activity was studied using transgenic constructs integrated into the *D. melanogaster* genome by microinjection of embryos with plasmid DNA due to the 5' and 3' termini of the P element flanking the transgene. The 660 bp *bxd*PRE element from the regulatory region of the *Ubx* gene was used [36, 37]. This PRE element is well studied and has binding sites for various PcG and TrxG proteins [15, 21, 36, 37].

Two constructs were created containing *bxd*PRE inserted between the UAS promoter and the reporter genes: *lacZ* under the control of the *hsp26* gene promoter and *white* gene. The marker *white* gene is responsible for eye pigmentation. Increased level of *white* gene expression in the eyes of flies was obtained by insertion of a tissue-specific enhancer directly upstream of the *white* promoter. The UAS promoter used for induction of transcription through *bxd*PRE is the minimal promoter of the *hsp70* gene with five upstream binding sites for yeast GAL4 activator. A high level of transcription is achieved upon induction of the UAS promoter (by crossing transgenic lines with a line carrying the *GAL4* gene under the control of the tubulin promoter). In both constructs, the UAS promoter is di-

*A*

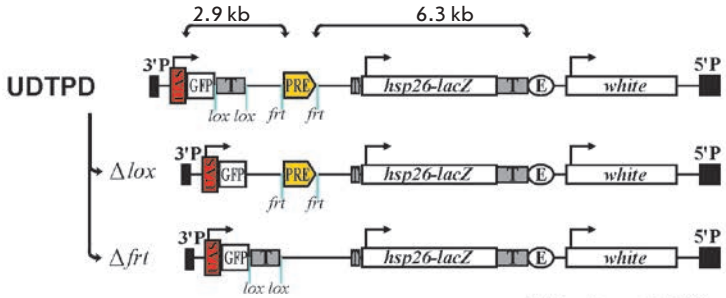


| | P/P | P/+ | P/+; tubGAL4 | PΔlox/ PΔlox | PΔlox/+ | PΔlox/+; tubGAL4 | PΔfrt/ PΔfrt | PΔfrt/+ | PΔfrt/+; tubGAL4 |
|---|---|---|---|---|---|---|---|---|---|
| 1 | Mosaic: 90%w/ 10%pY | Mosaic: 50%pY/ 50%dY | R | Mosaic: 90%w/ 10%pY | Mosaic: 50%pY/ 50%dY | R | R | R | R |
| 2 | Mosaic: 95%w/ 5%ppY | Mosaic: 50%pY/ 50%dY | R | Mosaic: 95%w/ 5%ppY | Mosaic: 50%pY/ 50%dY | R | R | R | R |
| 3 | Mosaic: 90%w/ 10%ppY | dOr | R | Mosaic: 90%w/ 10%ppY | dOr | R | R+ | R | R |
| 4 | Mosaic: 80%w/ 20%R | R | R | Mosaic: 80%w/ 20%R | R | R | R | R | R |

*B*

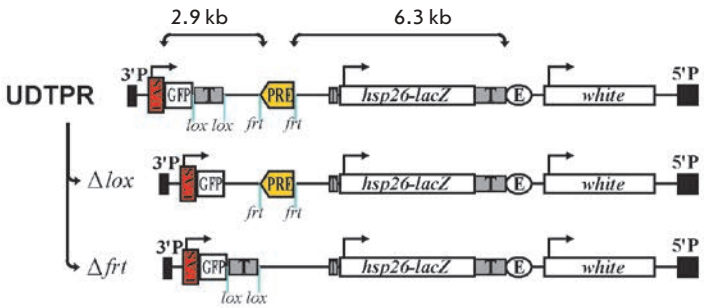


| | P/P | P/+ | P/+; tubGAL4 | PΔlox/ PΔlox | PΔlox/+ | PΔlox/+; tubGAL4 | PΔfrt/ PΔfrt | PΔfrt/+ | PΔfrt/+; tubGAL4 |
|---|---|---|---|---|---|---|---|---|---|
| 1 | Mosaic: 95%R/ 5%pY | R | R | Mosaic: 95%R/ 5%pY | R | R | R+ | R | R |
| 2 | Mosaic: 50%dY/ 50%pY | dOr | R | Mosaic: 50%dY/ 50%pY | dOr | R | R+ | R | R |
| 3 | not viable | Mosaic: 60%dY/ 40%pY | R | not viable | Mosaic: 60%dY/ 40%pY | R | R | R | R |

Fig. 1. Schematic representation of transgenic constructs and phenotype analysis of flies. *A* – UDTPD transgene. Minimal promoter of *hsp70* gene under the control of binding sites for activator protein GAL4 (UAS) triggers transcription through *eGFP* and *bxd*PRE "T" – transcription terminator; *hsp26-lacZ* and *white* – reporter genes; "E" – *white* gene enhancer. Phenotypes of the obtained lines are shown below. P/P – homozygous line; P/+ – heterozygous line; P/+ tubGAL4 – heterozygous line expressing GAL4; PΔlox/PΔlox – homozygous line carrying a deletion of the transcription terminator; PΔlox/+ – heterozygous line with deletion of the transcription terminator; PΔlox/+ tubGAL4 – heterozygous line expressing the GAL4 protein with deletion of the terminator; PΔfrt/PΔfrt – homozygous line with deletion of *bxd*PRE; PΔfrt/+ – heterozygous line with deletion of PRE; PΔfrt/+ tubGAL4 – heterozygous line expressing GAL4 with deletion of *bxd*PRE. Scale of eye pigmentation depending on the level of *white* expression: R+ – dark red (wild-type); R – red; BrR – brownish-red; Br – brown; dOr – dark orange; Or – orange; dY – dark yellow; pY – pale yellow; ppY – very light yellow; w – white. Mosaic pigmentation of eyes is indicated as *mosaic*. *B* – UDTPR transgene

rected towards *bxd*PRE. However, the first construct (UDTPD) carries *bxd*PRE in forward orientation, while in the second construct (UDTPR) *bxd*PRE is located in reverse orientation relative to the UAS promoter (*Fig. 1*). In order to suppress internal transcripts of the transgene, two SV40 terminators were used: upstream of the *hsp26-lacZ* gene and upstream of the *white* gene enhancer. An additional transcription terminator, SV40, was inserted at the 5' side of *bxd*PRE in order to block transcription from the UAS promoter.

Key elements, *bxd*PRE and the SV40 terminator at the 5' side of *bxd*PRE in both constructs, were flanked by the LOX or FRT site for site-specific recombinases Cre or Flp, respectively. This approach allows one to excise *in vivo* the selected DNA fragments and to compare the expression of the marker gene and functional changes in the system in the presence or absence of key elements at the same genome position (sites of transgene integration).

As a result of construct transformation, four independent transgenic lines for UDTPD (*Fig. 1A*) and three lines for UDTPR (*Fig. 1B*) were obtained with *bxd*PRE in repressed state. Repression of the *white* gene was enhanced in homozygous flies. This effect is characteristic of PRE elements and called PSS (Pairing Sensitive Silencing) [38]. The phenotypes of the UDTPD and UDTPR transgenes were similar; i.e., the effects were independent of *bxd*PRE orientation. Deletion of the transcription terminator located between the UAS promoter and PRE did not result in any phenotypic changes. However, the induction of the UAS promoter by GAL4 led to derepression of the *white* gene both in the case of terminator deletion and in intact lines. Thus, GAL4 inactivates *bxd*PRE in the studied system regardless of orientation and presence of a terminator between the UAS promoter and *bxd*PRE.

### Transcription through *bxd*PRE does not lead to elimination of Polycomb and Trithorax group factors from *bxd*PRE

We have previously shown that even robust transcription does not lead to complete elimination of PcG/TrxG complexes from *bxd*PRE if it is oriented forward in the transgene. We tested the influence of transcriptional read-through in the case of reverse orientation of *bxd*PRE. For this purpose, we conducted immunoprecipitation of chromatin isolated from adult homozygous flies in the presence or absence of GAL4 (*Fig. 2*). Immunoprecipitation was carried out using samples obtained from the transgenic line UDTPR (№ 2) with a deleted SV40 transcription terminator. Six areas of the construct were used for PCR analysis: 1 – UAS promoter, 2 – *eGFP* gene coding region, 3 – *bxd*PRE, 4 – *LacZ* gene coding region, 5 – *white* gene enhancer, and 6 – *white* gene promoter. As a positive control, we used the genomic region of *bxd*PRE adjacent to the element utilized in transgenic constructs, while the coding region of the *Ras64B* gene was used as a negative control (*Fig. 2*).

It has been shown that the peak of the PH (PRC1 complex, *Fig. 2A*) and dSfmbt (PhoRC complex, *Fig. 2B*) factors recruitment corresponds to *bxd*PRE in the transgene. Localization of these factors is consistent with the data according to which PH and dSfmbt are found predominantly in PRE elements but not in other regions of the repressed domain [14, 15, 21, 39, 40].

The level of recruitment of these factors decreases upon induction of transcription through *bxd*PRE, but they are not eliminated completely. A similar result was obtained when analyzing the impact of transcription on the recruitment of the PH and dSfmbt factors to *bxd*PRE located in transgene in forward orientation relative to the UAS promoter [21].

Factor PC of the PRC1 complex specifically interacts with histone 3 trimethylated at lysine 27 (H3K27me3) [41, 42], a modification characteristic of PcG-repressed chromatin [16, 40]. Recruitment of the PC factor, as well as H3K27me3, contrary to other core components of PcG complexes, is not limited to PRE and covers a wider area subjected to repression [16, 21, 40, 43]. In agreement with this, a wider profile of distribution of the PC factor (*Fig. 2C*) and H3K27me3 modification (*Fig. 2D*) has been found in the derivative of the UDTPR transgene. Introduction of a GAL4 activator did not lead to complete elimination of PC and H3K27me3, but there was a significant decrease in the level of their recruitment to *bxd*PRE and the surrounding areas of the transgene.

We also analyzed the recruitment of the TrxG factors Trx (*Fig. 2E*) and GAF (*Fig. 2F*). It was established that the induction of transcription through *bxd*PRE leads to a 2-fold increase in the recruitment of both factors to *bxd*PRE.

Thus, transcription through PRE leads to a change in the level of PcG/TrxG factors recruitment but not to complete displacement of these proteins from DNA.

## CONCLUSION

The repression/activation of various *Drosophila* genes requires PcG/TrxG proteins [1–4] that bind to the DNA elements termed PREs [5, 6]. A series of studies has shown that a lack of PRE-mediated repression correlates with the presence of non-coding transcripts [24, 44]. On this basis, a model was proposed according to which transcriptional read-through physically dislodges PRE-associated factors and replaces repressive histone modifications with active ones [24]. Despite its apparent clarity, this hypothesis has not been tested directly.

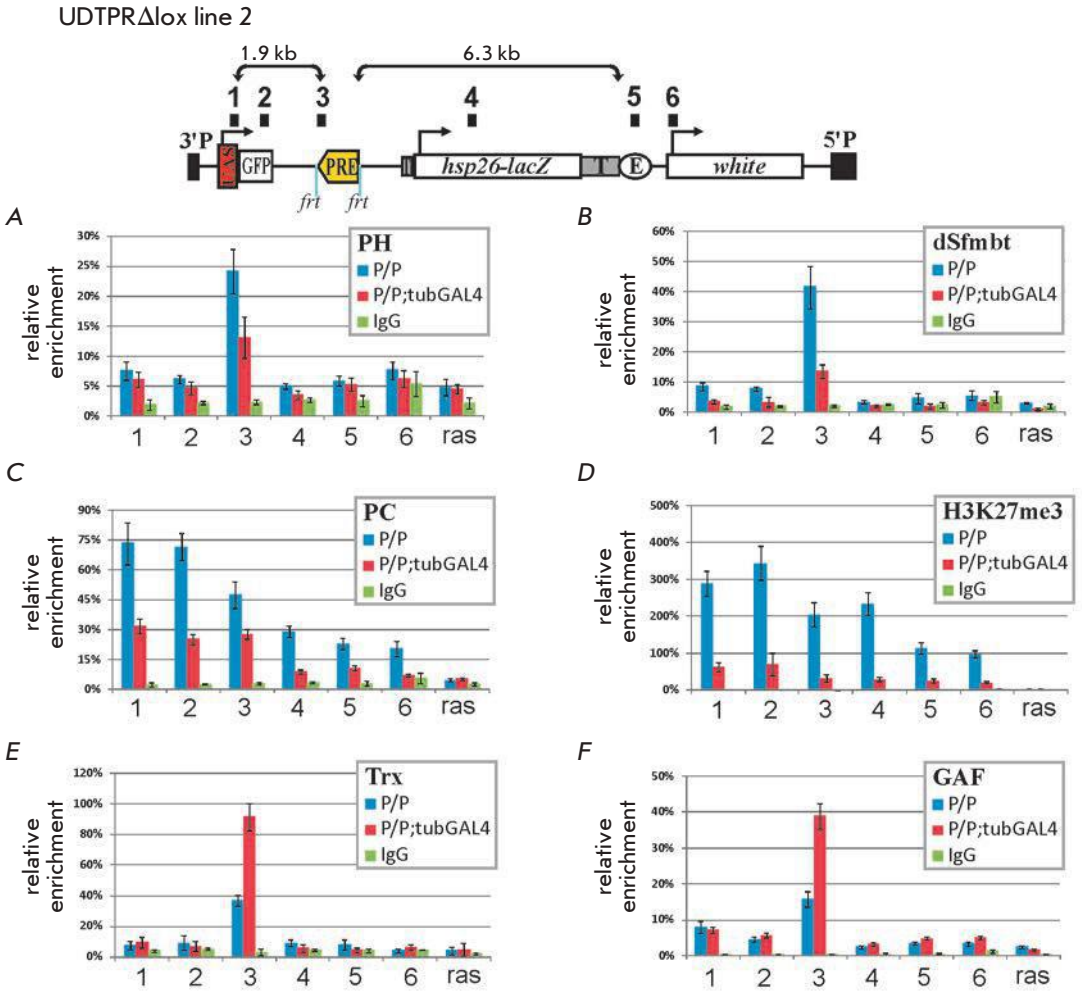


Fig. 2. Analysis of PcG/TrxG recruitment during transcriptional read-through. X-ChIP experiment with chromatin isolated from adult flies was performed. Numbers on top of the constructs (1, 2, 3, 4, 5 and 6) indicate the primer pairs used for qPCR. X-ChIP results are presented as a percentage of Iput sample normalized to the endogenous positive control, region adjacent to 660 bp *bxd*PRE in the genome. The coding part of the *Ras64B* gene was used as a negative control (ras). Blue bars on the diagrams indicate relative X-ChIP signal levels in homozygote lines (P/P), red bars indicate relative X-ChIP signal levels in homozygote lines expressing GAL4 (P/P; tubGAL4), and green bars indicate signal levels obtained using nonspecific antibodies. Vertical lines indicate SDs. X-ChIP experiments were performed with antibodies against PH (*A*), dSfmbt (*B*), PC (*C*), H3K27me3 (*D*), Trx (*E*), and GAF (*F*)

On the other hand, according to other data, non-coding RNAs from *Ubx* locus (lncRNA-*bxd* and lncRNA iab-8) are associated with the domain subjected to repression [45, 46]. Moreover, in spite of scrupulous studies, non-coding RNAs have not been detected in the regions of PRE elements of several loci (*invected, engrailed*), which indicates the absence of a key role for transcription, at least in the functioning of several PRE elements [47].

Previously, we tested the effect of transcription on GAL4-mediated activity switch of PRE [21]. As a result, we found that even robust transcription through *bxd*PRE does not lead to complete elimination of PcG/TrxG factors but changes the ratio in the binding of these proteins: recruitment of PcG decreases, while the recruitment of TrxG increases. The transcriptional effect was analyzed in detail for *bxd*PRE incorporated into transgene in direct orientation [21]. At the same time, active and inactive states of PRE in *vg* locus correlate with transcriptional read-through from different DNA strands [48]. Therefore, the direction of transcription through PRE can potentially be crucial for the activity of PRE. We have tested this possibility and found that alteration of *bxd*PRE orientation does not lead to a

change in the transcriptional read-through effect. Recruitment of PcG/TrxG factors is not abolished upon transcription. However, the recruitment of the TrxG proteins Trx and GAF increases, while the recruitment of PcG proteins (PH, dSfmbt, PC) decreases.

The presence of the strong terminator SV40 between the UAS promoter and *bxd*PRE also does not prevent abolition of repression. Apparently, the GAL4-binding sites themselves are capable of neutralizing PRE-mediated repression and transcription though PRE does not play a crucial role in this process.

PRE elements regulate genes the expression of which is changed during differentiation and development. Thus, a particular gene must be expressed in certain cells at a certain stage of development, and then its expression should be suppressed. Apparently, the recruitment of repressor factors to PRE in activating state could be required for the quick PRE activity switch to the repressing state and to abort the expression of the target gene at a certain moment in time. A logically similar mechanism has been described for many eukaryotic promoters: pausing of RNA polymerase II. In this case, RNA polymerase II binds to a transcriptionally inactive promoter and, if necessary, quickly triggers transcription.

The mechanism that allows the recruitment of proteins to PRE during transcriptional read-through is unclear. A series of DNA-binding factors with zinc finger motifs are known to be associated with PREs. It is possible that transcription does not interfere with direct DNA-protein contacts. On the other hand, there is a possibility that retention of complexes at PRE during transcriptional read-through is mediated by the contacts between the PcG/TrxG factors and histone proteins. In accordance, PcG proteins contain domains capable of interacting directly with nucleosomes (for example, the MBT domains of dSfmbt and Scm) [14, 49, 50] and transcription does not result in complete dissociation of nucleosomes [51]. However, the details of these processes are currently unclear and require further investigation.

*This work was performed using equipment from the Center of Collective Use at the Institute of Gene Biology RAS. This work was supported by Russian Science Foundation (project № 14-24-00166).*

REFERENCES

1. Beisel C., Paro R. // Nat. Rev. Genet. 2011. V. 12. № 2. P. 123–135.
2. Muller J., Verrijzer P. // Curr. Opin. Genet. Dev. 2009. V. 19. № 2. P. 150–158.
3. Schwartz Y.B., Pirrotta V. // Nat. Rev. Genet. 2013. V. 14. № 12. P. 853–864.
4. Steffen P.A., Ringrose L. // Nat. Rev. Mol. Cell Biol. 2014. V. 15. № 5. P. 340–356.
5. Kassis J.A., Brown J.L. // Adv. Genet. 2013. V. 81. P. 83–118.
6. McElroy K.A., Kang H., Kuroda M.I. // Open. Biol. 2014. V. 4. P. 140006.
7. Francis N.J., Saurin A.J., Shao Z., Kingston R.E. // Mol. Cell. 2001. V. 8. № 3. P. 545–556.
8. Saurin A.J., Shao Z., Erdjument-Bromage H., Tempst P., Kingston R.E. // Nature. 2001. V. 412. № 6847. P. 655–660.
9. Shao Z., Raible F., Mollaaghababa R., Guyon J.R., Wu C.T., Bender W., Kingston R.E. // Cell. 1999. V. 98. № 1. P. 37–46.
10. Cao R., Wang L., Wang H., Xia L., Erdjument-Bromage H., Tempst P., Jones R.S., Zhang Y. // Science. 2002. V. 298. № 5595. P. 1039–1043.
11. Czermin B., Melfi R., McCabe D., Seitz V., Imhof A., Pirrotta V. // Cell. 2002. V. 111. № 2. P. 185–196.
12. Kuzmichev A., Nishioka K., Erdjument-Bromage H., Tempst P., Reinberg D. // Genes Dev. 2002. V. 16. № 22. P. 2893–2905.
13. Muller J., Hart C.M., Francis N.J., Vargas M.L., Sengupta A., Wild B., Miller E.L., O'Connor M.B., Kingston R.E., Simon J.A. // Cell. 2002. V. 111. № 2. P. 197–208.
14. Klymenko T., Papp B., Fischle W., Kocher T., Schelder M., Fritsch C., Wild B., Wilm M., Muller J. // Genes Dev. 2006. V. 20. № 9. P. 1110–1122.
15. Papp B., Muller J. // Genes Dev. 2006. V. 20. № 15. P. 2041–2054.
16. Schwartz Y.B., Kahn T.G., Nix D.A., Li X.Y., Bourgon R., Biggin M., Pirrotta V. // Nature Genetics. 2006. V. 38. № 6. P. 700–705.
17. Schuettengruber B., Martinez A.M., Iovino N., Cavalli G. // Nat. Rev. Mol. Cell Biol. 2011. V. 12. № 12. P. 799–814.
18. Cavalli G., Paro R. // Cell. 1998. V. 93. № 4. P. 505–518.
19. Cavalli G., Paro R. // Science. 1999. V. 286. № 5441. P. 955–958.
20. Dejardin J., Cavalli G. // EMBO J. 2004. V. 23. № 4. P. 857–868.
21. Erokhin M., Elizar'ev P., Parshikov A., Schedl P., Georgiev P., Chetverina D. // Proc. Natl. Acad. Sci. USA. 2015. V. 112. № 48. P. 14930–14935.
22. Maurange C., Paro R. // Genes Dev. 2002. V. 16. № 20. P. 2672–2683.
23. Perez L., Barrio L., Cano D., Fiuza U.M., Muzzopappa M., Milan M. // Development. 2011. V. 138. № 15. P. 3125–3134.
24. Rank G., Prestel M., Paro R. // Mol. Cell. Biol. 2002. V. 22. № 22. P. 8026–8034.
25. Pirrotta V. // Biotechnology. 1988. V. 10. P. 437–456.
26. Qian S., Varjavand B., Pirrotta V. // Genetics. 1992. V. 131. № 1. P. 79–90.
27. Erokhin M., Davydova A., Parshikov A., Studitsky V.M., Georgiev P., Chetverina D. // Epigenet. Chromatin. 2013. V. 6. № 1. P. 31.
28. Brand A.H., Perrimon N. // Development. 1993. V. 118. № 2. P. 401–415.
29. Erokhin M., Parshikov A., Georgiev P., Chetverina D. // Chromosoma. 2010. V. 119. № 3. P. 243–253.
30. Karess R.E., Rubin G.M. // Cell. 1984. V. 38. № 1. P. 135–146.
31. Rubin G.M., Spradling A.C. // Science. 1982. V. 218. № 4570. P. 348–353.
32. Spradling A.C., Rubin G.M. // Science. 1982. V. 218. № 4570. P. 341–347.
33. Golic K.G., Lindquist S. // Cell. 1989. V. 59. № 3. P. 499–509.

34. Siegal M.L., Hartl D.L. // Meth. Mol. Biol. 2000. V. 136. P. 487–495.
35. Kyrchanova O., Toshchakov S., Parshikov A., Georgiev P. // Mol. Cell. Biol. 2007. V. 27. № 8. P. 3035–3043.
36. Comet I., Savitskaya E., Schuettengruber B., Negre N., Lavrov S., Parshikov A., Juge F., Gracheva E., Georgiev P., Cavalli G. // Dev. Cell. 2006. V. 11. № 1. P. 117–124.
37. Orlando V., Jane E.P., Chinwalla V., Harte P.J., Paro R. // EMBO J. 1998. V. 17. № 17. P. 5141–5150.
38. Kassis J.A. // Genetics. 1994. V. 136. № 3. P. 1025–1038.
39. Beisel C., Buness A., Roustan-Espinosa I.M., Koch B., Schmitt S., Haas S.A., Hild M., Katsuyama T., Paro R. // Proc. Natl. Acad. Sci. USA. 2007. V. 104. № 42. P. 16615–16620.
40. Schuettengruber B., Ganapathi M., Leblanc B., Portoso M., Jaschek R., Tolhuis B., van Lohuizen M., Tanay A., Cavalli G. // PLoS Biol. 2009. V. 7. № 1. P. e13.
41. Fischle W., Wang Y., Jacobs S.A., Kim Y., Allis C.D., Khorasanizadeh S. // Genes Dev. 2003. V. 17. № 15. P. 1870–1881.
42. Min J., Zhang Y., Xu R.M. // Genes Dev. 2003. V. 17. № 15. P. 1823–1828.
43. Bowman S.K., Deaton A.M., Domingues H., Wang P.I., Sadreyev R.I., Kingston R.E., Bender W. // Elife. 2014. V. 3. P. e02833.
44. Bae E., Calhoun V.C., Levine M., Lewis E.B., Drewell R.A. // Proc. Natl. Acad. Sci. USA. 2002. V. 99. № 26. P. 16847–16852.
45. Petruk S., Sedkov Y., Riley K.M., Hodgson J., Schweisguth F., Hirose S., Jaynes J.B., Brock H.W., Mazo A. // Cell. 2006. V. 127. № 6. P. 1209-1221.
46. Gummalla M., Maeda R.K., Castro Alvarez J.J., Gyurkovics H., Singari S., Edwards K.A., Karch F., Bender W. // PLoS Genetics. 2012. V. 8. № 5. P. e1002720.
47. Langlais K.K., Brown J.L., Kassis J.A. // PloS One. 2012. V. 7. № 11. P. e48765.
48. Herzog V.A., Lempradl A., Trupke J., Okulski H., Altmutter C., Ruge F., Boidol B., Kubicek S., Schmauss G., Aumayr K., et al. // Nat. Genet. 2014. V. 46. № 9. P. 973–981.
49. Grimm C., de Ayala Alonso A.G., Rybin V., Steuerwald U., Ly-Hartig N., Fischle W., Muller J., Muller C.W. // EMBO Repts. 2007. V. 8. № 11. P. 1031–1037.
50. Grimm C., Matos R., Ly-Hartig N., Steuerwald U., Lindner D., Rybin V., Muller J., Muller C.W. // EMBO J. 2009. V. 28. № 13. P. 1965–1977.
51. Kulaeva O.I., Hsieh F.K., Chang H.W., Luse D.S., Studitsky V.M. // Biochim. Biophys. Acta. 2013. V. 1829. № 1. P. 76–83.

# A New Approach To the Diagnosis of Point Mutations in Native DNA Using Graphene Oxide

A.A. Kuznetsov*, N.R. Maksimova, V.S. Kaimonov, G.N. Alexandrov, S.A. Smagulova
M. K. Ammosov North-Eastern Federal University, Belinskogo str. 58, 677000, Yakutsk, Russia
*E-mail: kuznecov.artem@mail.ru
Received: 19.11.2015


**ABSTRACT** **Development of new methods for the diagnosis of point mutations is a pressing issue. We have developed a new approach to the design of graphene oxide-based test systems for the diagnosis of point mutations in native DNA. This new approach is based on the use of graphene oxide for the adsorption and quenching of fluorescently labeled primers in a post-amplification PCR mixture followed by detection of fluorescently labeled PCR products. It is possible to detect fluorescently labelled amplicons in the presence of an excess of primers in a PCR product solution due to the different affinities of single-stranded and double-stranded DNA molecules to graphene oxide, as well as the ability of graphene oxide to act as a quencher of the fluorophores adsorbed on its surface. The new approach was tested by designing a graphene oxide-based test system for the DNA diagnosis of the point mutation associated with the development of the 3M syndrome in Yakuts. The developed approach enables one to design graphene oxide-based test systems suitable for the diagnosis of any point mutations in native DNA.**

**KEYWORDS** **point mutations, test system, graphene oxide, diagnosis**

**ABBREVIATIONS** **PM – point mutation, PCR – polymerase chain reaction, RFLP analysis – analysis of restriction fragment length polymorphisms; FAM – 6-carboxyfluorescein, ROX – carboxy-X-rhodamine.**

## INTRODUCTION

The diagnosis of point mutations (substitutions, insertions, deletions, hereinafter abbreviated as PMs) is extremely important in modern medicine, since it enables the evaluation of predisposition to various diseases, adequate selection of drugs, and opens the way to the study of genes' functions. Modern medical genetics uses several basic methods to diagnose PMs in native DNA [1]: PCR-RFLP analysis, fluorescent methods (real-time PCR,end-point PCR), biochip techniques, and sequencing. However, all these methods have certain limitations, and, therefore, discovery of novel approaches to PM diagnosis in native DNA which are faster, more cost-efficient, and effective is a pressing issue [2].

Graphene oxide has two unique properties: quenching of the fluorescence of nearby fluorophores [3] and different affinities to single-stranded and double-stranded DNA molecules [4]. In addition, it is a low-cost and easy-to-synthesize material. For these reasons, it is extensively used in searching for new approaches to PM diagnosis. The use of these properties over the last 5 years has resulted in the development of numerous approaches to PM diagnosis using graphene oxide; for example, [5–9]. However, these approaches are effective in the case of PM diagnosis in short, single-stranded oligonucleotides, and none of them enables PM diagnosis in native DNA [10]. This study was aimed at developing a new approach to PM diagnosis in native DNA using graphene oxide.

## EXPERIMENTAL

### Materials

Graphene oxide was synthesized from natural graphite powder according to the modified Hummers *et al.* method [11]. We synthesized graphene oxide using reagents supplied by Vostokreaktiv company (Russia), MFPI MF-1230-45 Rusbiolink dialysis bags (Russia), and PCR reagents (PCR buffer, $MgCl_2$, dNTP, DNA polymerase) purchased from Evrogen (Russia). We used allele-specific SNPdetect DNA polymerase (Evrogen). The structure of PCR primers is shown in Table.

PCR products were incubated with graphene oxide using sodium phosphate buffer diluted with deionized water (10 ×, Gibco, USA). Deionized water (18.2 MΩ × cm) was obtained using the Advantage A10 Milli-Q purification system (Merck Millipore, Germany).

The structures of the used primers

| Designation | Primer type | Nucleotide sequence, 5'–3' |
|---|---|---|
| R | Reverse | GATGAGGCAGTTCAGAAGATTCC |
| F-FAM | FAM-labeled forward | FAM-CAGGGGTCCTCAAGATTTCG |
| F-ROX | ROX-labeled forward | ROX-CAGGGGTCCTCAAGATTCG |

The characteristics of the test system were measured in three groups of DNA samples (16 samples in each group, including patients with the 3M syndrome with a confirmed homozygous 4582insT mutation, heterozygous carriers of the 4582insT mutation, and healthy individuals), isolated from the peripheral blood of patients who gave their informed consent. Additionally, 16 negative controls were used. All DNA samples were genotyped using the TestGen test system based on the real-time PCR method *(Fig.1)*.The study was approved by the local ethics committee.

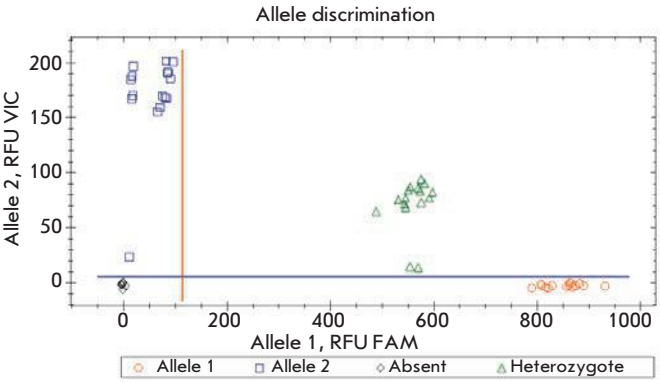


Fig. 1. The results of DNA samples genotyping using a real-time PCR test system (FAM channel – 4582InsT mutation, VIC channel – wild type).

## Equipment

We used the Intelli-Stirrer MSH-300i magnetic stirrer (Biosan, Latvia), as well as a IL100-6/3 (INLAB, Russia) ultrasonic disperser and MiniSpin Plus centrifuge (Eppendorf, Germany) to synthesize graphene oxide. PCR was performed using a C1000 thermal cycler (Bio-Rad, USA); fluorescence intensity was measured using a Jean-4 fluorometer (DNA-Technology, Russia).

## Graphene oxide synthesis

Graphite powder (0.1 g, Sigma Aldrich, USA) and sodium nitrate (0.05 g, reagent grade) were added to 14 ml of concentrated sulfuric acid (extra-pure grade). Then, 0.4 g of potassium permanganate (analytical grade) was gradually added in small portions. The resulting reaction mixture was stirred for 3 weeks in a beaker on a magnetic stirrer at 75°C. After stirring, the mixture was diluted to a double volume with deionized water. Further, a 5% hydrogen peroxide solution (7 mL) was added to the mixture until a brilliant-yellow color developed. The brilliant-yellow mixture was filtered using a 70 mm Buchner funnel and ashless filter (yellow band) and washed with 300 ml of deionized water until a neutral pH of the filtrate. This yielded a brown gel-like mass, which was transferred from the filter to a beaker and diluted with 50 ml of water, followed by sonication on the IL100-6/3 disperser with a power of 750 W for 5 minutes. After dispersing, the suspension was centrifuged at 14,500 rpm (14.1 g) for 5 min and particles of graphite oxide that were not delaminated by ultrasonic treatment were removed by decantation of the graphene oxide solution above the precipitate. At the last step, the solution was dialyzed in dialysis bags (MWCO: 12000–14000) for 3 days with triple change of deionized water in a 1 liter beaker with the dialysis bag. As a result, 50 mL of a uniform dark brown suspension of graphene oxide was obtained. The atomic proportion of carbon and oxygen was assessed in the dried suspension of graphene oxide by energy-dispersive x-ray spectroscopy and amounted to ~58 and ~42%, respectively. The concentration of graphene oxide in the suspension was determined gravimetrically by weighing a dry residue of 1 ml of the suspension dried at 170°C during 5 min.

## Allele-specific PCR

For each DNA sample, we prepared 25 μl of the mixture containing 1 × PCR buffer, 3 mM $MgCl_2$, 0.28 mM dNTP, 0.2 μM primer R, 0.6 μM primer F-FAM, 66.4 nM primer F-ROX, 2.5 activity units of SNP detect DNA polymerase, and 1.2 ng/μl DNA. The PCR temperature profile consisted of denaturation at 95°C for 3 min, 38 amplification cycles (30 sec denaturation at 95°C, 30 sec annealing at 60°C, 1 min elongation at 72°C), and final elongation at 72°C for 5 min. Amplification was verified by gel electrophoresis of PCR products in 3% agarose gel without ethidium bromide. The length of the amplified product was 149 bps (150 bps in the case of mutant allele amplification); GC-composition was 55.7%.

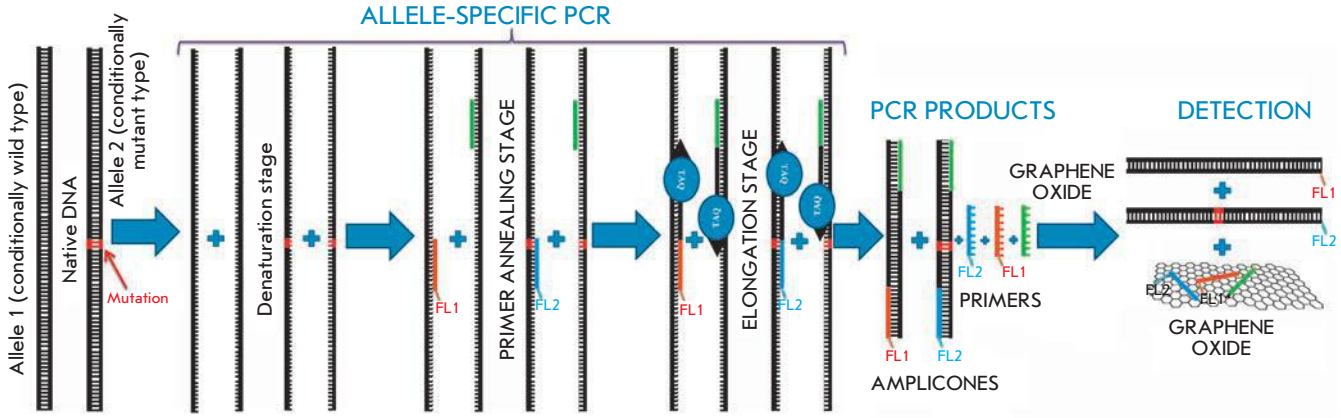


Fig. 2. Schematic representation of point mutation diagnosis in native DNA using the developed approach

### Addition of graphene oxide to PCR products and fluorescence measurements.

We sampled 15 μl of the post-amplification PCR mixture from each tube and placed it into a 0.6 ml transparent microcentrifuge tube. Further, 3.6 μl of 5 × sodium phosphate buffer (Gibco, USA) and a 4 μl of graphene oxide suspension (0.5 mg/ml) in 1 × sodium phosphate buffer (Gibco, USA) were added and incubated at room temperature on an orbital shaker for 20 min (450 rpm). The fluorescence intensity was measured for FAM- and the ROX-channels in each tube using a Jean-4 fluorometer (DNA-Technology, Russia).

## RESULTS AND DISCUSSION

### Description of the developed approach

*Figure 2* shows a schematic diagram of the developed approach.

At the first stage of the diagnosis, we carried out allele-specific PCR, which uses allele-specific DNA polymerase and three primers as opposed to conventional PCR. One of the primers (reverse, highlighted in green in *Fig. 2*) can be complementarily annealed to the DNA of both allele types (wild-type and mutant). Two other primers (forward, highlighted in blue and orange in *Fig.* 2) contain different fluorophores – FL1 and FL2 – with non-overlapping excitation/emission spectra at their 5'-termini. Each of the forward primers can bind to only one type of allele, since they are complementary to the DNA of different alleles at the mutation site.

Depending on the genotype of tDNA donor, three types of the post-amplification mixture can form: with FL1-labeled amplicons (homozygous wild type); FL2-labeled (homozygous mutant type), and with amplicons labeled with both fluorophores (heterozygous type). In either case, the PCR products will contain an excess of fluorescently labeled primers.

When adding the aqueous suspension of graphene oxide to the post-amplification PCR mixture, adsorption of single-stranded DNA molecules, fluorescently labeled primers, will occur on a surface of graphene oxide nanosheets, resulting in quenching of their fluorescence. Double-stranded DNA molecules (amplicons) will remain in solution because of their low affinity to graphene oxide and can generate a fluorescent signal.

The genotype of the DNA donor can be determined by adding an excess of graphene oxide and comparing the fluorescence intensity of each fluorophore in the final solution (for the test DNA sample) and fluorescence intensity in the negative control.

### Testing of the developed approach

We have developed a test system based on this approach suitable for the DNA diagnosis of the mutation associated with development of the 3M syndrome in Yakuts. The 3M syndrome is a wide-spread autosomal recessive hereditary disease caused by a 4582insT mutation in exon 25 of the *CUL7* gene (KIAA0076, Cullin-7) [12]. The 3M syndrome was chosen to develop the graphene oxide-based test system due to the high incidence of heterozygous carriership of the mutation associated with this disease in Yakuts (about 30 individuals per 1,000).

We used the Primer Blast service (http://www.ncbi.nlm.nih.gov) to select ROX- and FAM-labeled primers for different alleles which were complementary to the DNA sequence at the mutation region by 3'-end *(table)*.

We used the graphene oxide solution (0.5 mg/ml) in 1 × sodium phosphate buffer to add graphene oxide to the PCR products and the buffer alone to neutralize the effect of pH on the fluorescence intensity. The fluorescence intensity of each sample (including negative controls) was then measured for the FAM- and ROX-channels, followed by calculation of the average

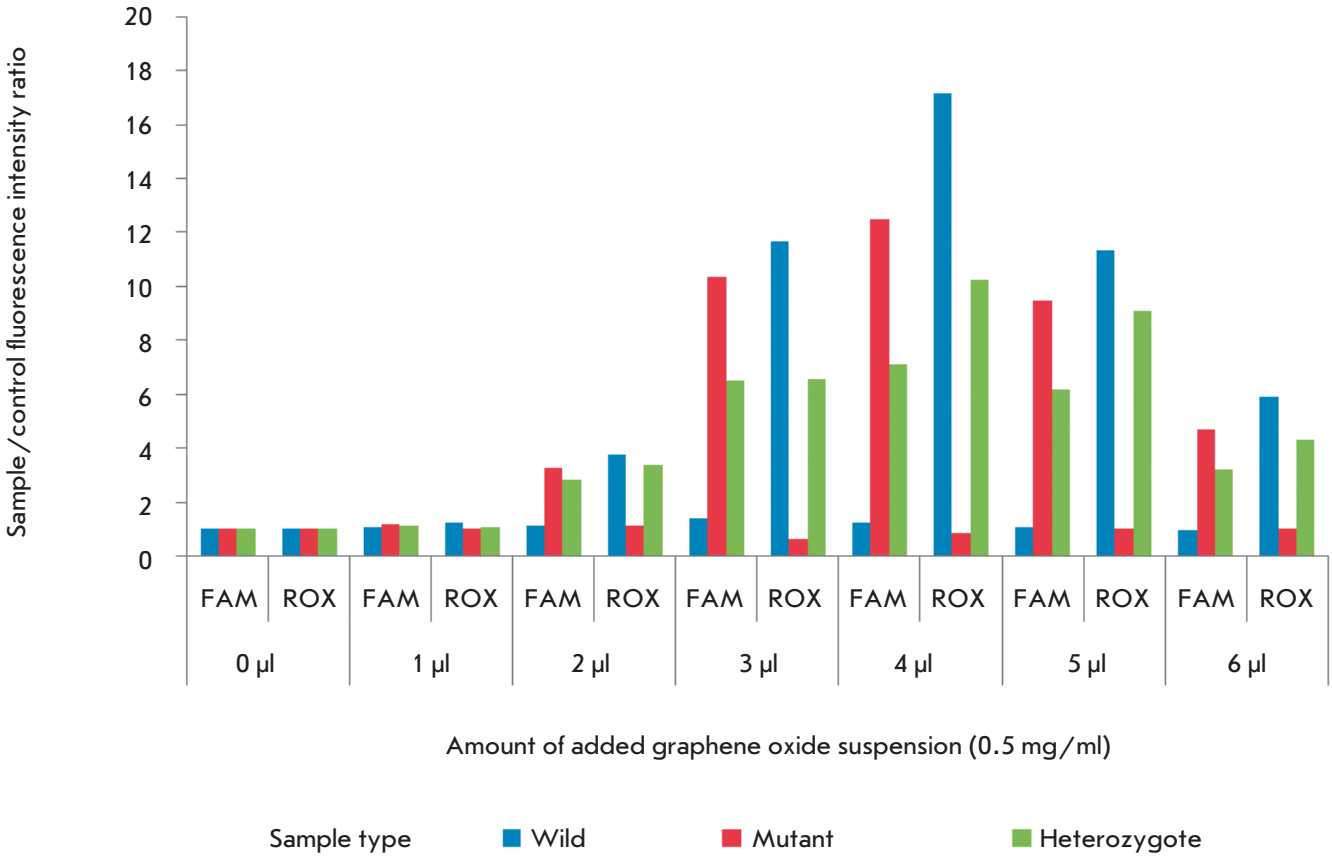


Fig. 3. Sample/control fluorescence intensity ratios **N** for each group of clinical samples for the FAM- and ROX-channels with different amounts of the added graphene oxide suspension.

fluorescence intensity and sample/control intensity ratio in each group of clinical samples for each fluorescence channel individually. Conditions of allele-specific PCR, composition of the PCR mixture, amplified portion length, and amount of graphene oxide were varied to maximize the sample/control intensity ratio for each fluorescence channel.

We optimized the test system using a population consisting of six DNA samples from carriers of the 4582insT mutation and healthy donors (two samples of each type) and two negative controls in seven equivalent experiments with different amounts of the added graphene oxide suspension. In this way, we determined the amount of graphene oxide ensuring the most effective interpretation of the results of the DNA diagnosis, which amounted to 4µl with a concentration of 0.5 mg/ml in 1 × sodium phosphate buffer *(Fig. 3)*.

Testing of the developed test system for genotyping of the control population consisting of 48 DNA samples from carriers of the 4582insT mutation and healthy individuals (16 samples of each type) yielded good results *(Fig.*4).

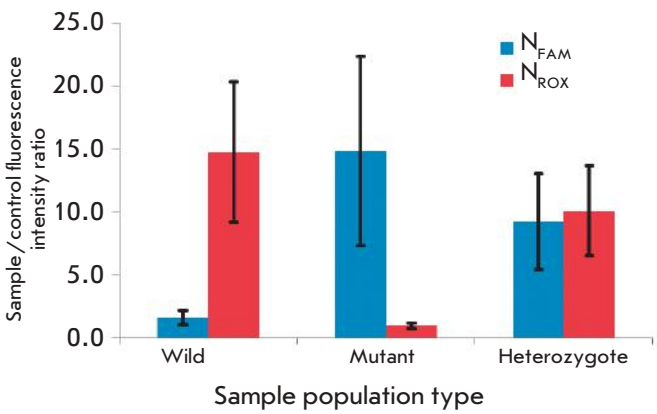


Fig. 4. Sample/control fluorescence intensity ratios **N** for each group of clinical samples for the FAM- and ROX-channels.

The confidence intervals in *Fig. 4* were constructed using standard deviations calculated as the sum of relative standard deviations of the fluorescence intensities of the controls and known samples for each channel.

According to the results shown in *Fig. 4*, the developed test system can reliably diagnose all three combinations of allelic variants in the *CUL7* gene.The use of graphene oxide as a nanostructured fluorescence quencher for fluorescently labeled primers in a post-amplification PCR mixture provided an almost complete fluorescence quenching. At the same time, the fluorescence of the labeled PCR product was largely preserved, which enabled a statistically significant analysis of the post-amplification mixture in terms of its fluorescent properties. The specificity of the test system was 100% in the tested population of clinical samples (since all the samples can be unambiguously attributed to clinical groups), while the sensitivity was no less than 1.2 ng of DNA, which is indicative of the suitability of this approach for the genotyping of point mutations in a conventional genetic laboratory. The apparent advantages of this method are its simplicity (three stages) and rapidity (2 hours). Moreover, in theory, the developed approach is not limited to a specific type of detected point mutations (insertions, deletions, substitutions), since it is based on the use of allele-specific PCR, which enables adaptation of the method to the diagnosis of any point mutation provided that an optimal structure of the primers and optimal diagnostic conditions are selected. Given the simplicity of the method, the low cost of commercial graphene oxide, and availability of the equipment used for DNA diagnostics, the method may be of interest to genetic laboratories involved in pharmacogenetic studies, as well as the diagnosis of genetic diseases caused by DNA point mutations.

## CONCLUSIONS

We have developed an approach that involves the use of graphene oxide as a nanostructured fluorescence quencher for the diagnosis of PMs using allele-specific PCR. The method may be of interest to diagnostic laboratories using inexpensive equipment, such as PCR fluorometers, for the diagnosis of point mutations (substitutions, insertions, deletions) in native DNA. The reliability, specificity, and good sensitivity of this approach were confirmed by the development of a test system for the DNA diagnosis of carriership of the mutation associated with the 3M syndrome in Yakuts. This approach enables one to produce test systems suitable for the diagnosis of any point mutations.

*This work was supported by the Ministry of Education and Science of the Russian Federation as a part of the federal special-purpose program "Research and development on the priority directions of scientific and technological complex of the Russian Federation for 2014–2020" (unique identifier of the project: RFMEFI57514X0015).*

REFERENCES

1. Mamotte C.D.S. // Clin. Biochem. Rev. 2006. V. 27. № 1. P. 63–75.
2. Ye S., Dhillon S., Ke X., et al. // Nucl. Acids Res. 2001. V. 29. № 17. P. e88.
3. Li F., Pei H., Wang L., Lu J., Gao J., Jiang B., Zhao X., Fan C. // Adv. Funct. Mater. 2013. V. 23. № 33. P. 4140–4148.
4. Huang P.-J., Liu J. // Nanomaterials. 2013. V. 3. № 2. P. 221–228.
5. Lu C.H., Yang H.H., Zhu C.L., Chen X., Chen G.N. // Angew. Chemie. Int. Ed. 2009. V. 48. № 26. P. 4785–4787.
6. He S., Song B., Li D., Zhu C., Qi W., Wen Y., Wang L., Song S., Fang H., Fan C. // Adv. Funct. Mater. 2010. V. 20. № 3. P. 453–459.
7. Li J., Huang Y., Wang D., Song B., Li Z., Song S., Wang L., Jiang B., Zhao X., Yan J., et al. // Chem. Commun. (Camb.). 2013. V. 49. № 30. P. 3125–3127.
8. Li Z., Zhu W., Zhang J., Jiang J., Shen G., Yu R. // Analyst. 2013. V. 138. № 13. P. 3616–3620.
9. Xiang D., Zheng A.H., Luo M., Ji X.H., He Z.K. // Sci. China Chem. 2013. V. 56. № 3. P. 380–386.
10. Kuznetsov A.A., Maksimova N.R., Alexandrov G.N., Smagulova S.A. // Yakut Med. J. 2014. V. 4. № 48. P. 142–149.
11. Hummers W.S., Offeman R.E. // J. Am. Chem. Soc. 1958. V. 80. № 6. P. 1339–1339.
12. Maksimova N., Hara K., Miyashia A., Nikolaeva I., Shiga A., Nogovicina A., Sukhomyasova A., Argunov V., Shvedova A., Ikeuchi T., et al. // J. Med. Genet. 2007. V. 44. № 12. P. 772–778.

# Testing Transgenic Aspen Plants with *bar* Gene for Herbicide Resistance under Semi-natural Conditions

V. G. Lebedev[1*], V. N. Faskhiev[1], N. P. Kovalenko[1], K. A. Shestibratov[1], A. I. Miroshnikov[1,2]
[1]Branch of Shemyakin and Ovchinnikov Institute of Bioorganic Chemistry, Russian Academy of Sciences, Science av., 6, 142290, Pushchino, Russia
[2]Lomonosov Moscow State University, Leninskie Gory, 1/51, 119991, Moscow, Russia
*E-mail: vglebedev@mail.ru
Received 21.10.2015


**ABSTRACT** **Obtaining herbicide resistant plants is an important task in the genetic engineering of forest trees. Transgenic European aspen plants (*Populus tremula* L.) expressing the *bar* gene for phosphinothricin resistance have been produced using *Agrobacterium tumefaciens*-mediated transformation. Successful genetic transformation was confirmed by PCR analysis for thirteen lines derived from two elite genotypes. In 2014–2015, six lines were evaluated for resistance to herbicide treatment under semi-natural conditions. All selected transgenic lines were resistant to the herbicide Basta at doses equivalent to 10 l/ha (twofold normal field dosage) whereas the control plants died at 2.5 l/ha. Foliar NH4-N concentrations in transgenic plants did not change after treatment. Extremely low temperatures in the third ten-day period of October 2014 revealed differences in freeze tolerance between the lines obtained from Pt of f2 aspen genotypes. Stable expression of the *bar* gene after overwintering outdoors was confirmed by RT-PCR. On the basis of the tests, four transgenic aspen lines were selected. The *bar* gene could be used for retransformation of transgenic forest trees expressing valuable traits, such as increased productivity.**
**KEYWORDS** **aspen, transgenic plants, *bar* gene, phosphinothricin, herbicide resistance.**

## INTRODUCTION

In the early stages of their growth, many trees (such as willow and poplar) cannot compete with weeds, making weed control essential [1]. This problem is particularly acute in nurseries, where the low competitiveness of young plants reduces their survival rate and weakens their growth. Therefore, nurseries spend 50–70% of the funds allocated to the cultivation of standard planting material on weed control [2]. Mechanical methods are labor-intensive and have low efficiency. Easy-to-use, efficient, and economical herbicides are more promising.

In the temperate zone, forest nurseries grow various types of *Populus*; however, the use of selective herbicides is almost impossible, since poplars are very sensitive to most herbicides [3]. It seems preferable to grow plants that are resistant to highly efficient non-selective herbicides that are relatively safe for the environment.

To this end, various genes conferring resistance to herbicides were inserted into woody plants. The first such gene was *aroA* that confers resistance to glyphosate [4]. There were also reports on a transfer of the *crsl-1* gene to acquire resistance to sulfonylurea [5], the *CP4* and *GOX* genes for glyphosate resistance [6]. However, the most frequently used gene is the *bar* gene from soil bacterium *Streptomyces hygroscopicus*, which confers resistance to broad-spectrum herbicides (Liberty, Basta, Finale, etc.) that are based on phosphinothricin (PPT, ammonium glufosinate). PPT is an analogue of *L*-glutamic acid and a potent inhibitor of glutamine synthetase (GS), which plays the central role in ammonium assimilation and regulation of nitrogen metabolism in plants [7]. Inhibition of GS results in rapid accumulation of ammonium in a plant cell and its subsequent death [8]. The *bar* gene encodes the PPT acetyltransferase enzyme which acetylates a free amino group in PPT and thereby inactivates it [9]. The *bar* gene was inserted into different species and hybrids of *Populus* [3, 10] and *Eucalyptus* [11, 12], as well as oak [13] and various coniferous [14, 15]; however, aspen plants have not been transformed. The aim of our work was to create herbicide-resistant aspen plants by transforming Russian highly productive aspen genotypes with the *bar* gene and to use testing under semi-natural conditions to select lines that look promising for plantation forestry.

## MATERIAL AND METHODS

We used aspen plants (*P. tremula* L.) of two genotypes: Pt and f2. Plants of the Pt genotype were discovered in the Leningrad region, and it is characterized by rapid growth and resistance to trunk rot (SPbNIILH, A.V. Zhigunov, personal communication), whereas plants of the f2 genotype represent *in vitro* culture of clone 34, which was discovered by S.N. Bagaev in the Kostroma region [16]. The plants were grown *in vitro* at 22–24 ˚C on the WPM medium [17] with 0.5 mg/l gibberellin and a photoperiod of 16 hours.

The transformation was performed by the *Agrobacterium tumefaciens* CBE21 strain with a binary pBIBar vector [18] containing the nos-*nptII* and 35S-*bar* genes according to [19]. Kanamycin-resistant transformants were analyzed by PCR. Plant DNA was isolated according to [20]. Potential agrobacterial contamination of DNA preparations was checked by amplification of the *virB* gene sequence. The following primer pairs were used:

Vir-B1 – 5'-GGCTACATCGAAGATCGTATGAATG-3';
Vir-B2 – 5'-GACTATAGCGATGGTTACGATGTTGAC-3';
Nos – 5'-CGCGGGTTTCTGGAGTTTAATGAGCTAAG-3';
NptII – 5'-GCATGCGCGCCTTGAGCCTGG-3';
Bar-1 – 5'-TGCACCATCGTCAACCACTA-3';
Bar-2 – 5'-ACAGCGACCACGCTCTTGAA-3'.

The reaction mixture contained 16 mM $(NH_4)_2SO_4$, 0.01% bovine serum albumin, 200 μM of each dNTP, 0.4 μM of each oligonucleotide, 0.05 activity units/l Taq-polymerase, and 1–5 ng/μl genomic DNA. The PCR conditions: denaturation at 96 ˚C (3 min); 30 cycles at 94 ˚C (1 min), 60 ˚C (*nptII*, *bar*) or 58 ˚C (*virB*) for 1 min, 72 ˚C (1 min); elongation at 72 ˚C (5 min). The reaction was carried out in a MJ Mini™ Gradient Thermal Cycler (Bio-Rad, USA).

The resistance of transgenic lines was assessed *in vitro* by rooting plants in the WPM medium with 0, 0.5 or 5 mg/l PPT. Rate of rooting, number of roots, and their length were assessed two weeks after planting. To evaluate the resistance to herbicide treatment, the transgenic and control plants were micropropagated, acclimatized to greenhouse conditions and following the transplantation into 1L plastic pots with peat:perlite substrate (3:1) were transferred outdoors at the Branch of the Shemyakin and Ovchinnikov Institute of Bioorganic Chemistry RAS in Pushchino in the beginning of June 2014. In mid-July, the plants were treated with water (control) or 0.5, 1 and 2% aqueous solution of herbicide Basta (Bayer CropScience, 150 g/l PPT) in doses equivalent to 2.5, 5, and 10 l/ha (four plants of each line for each treatment). Visual assessment of the damage was performed 3, 7, 14, and 28 days after the treatment using the following scale: 0 points, no damage; 1, 0–25% necrosis of leaf surface; 2, 25–50% necrosis; 3, 50–75% necrosis; 4, 75–100% necrosis; 5, complete necrosis of leaves. On the day of treatment and 3 days after the treatment, the leaves were collected to assess the content of ammonium nitrogen and water. The plant material was extracted according to [21]. Ammonium nitrogen was determined according to [22]. Water content was determined by drying at 105 ˚C for 24 h. During the 2014 growing season, plant height and number of leaves were measured every four weeks and basal diameter was measured every 8 weeks.

In May 2015, the plants were transplanted into 3L pots after overwintering outdoors. The degree of frost damage to plants was determined by the ratio of the living part to the total stem length. Meteorological data were obtained from the automatic weather station UGT in Puschino (ca. 600 m away from the test area). The expression of the *bar* gene was evaluated in June 2015 by RT-PCR (actin gene was used as the internal control). RNA was isolated by a modified method [23]. cDNA was synthesized in two steps. At the first stage, the reaction mixture (0.1–5 μg RNA, 0.5 μg oligo-dT-primer, 10 activity units of the RNase inhibitor) was heated for 5 min at 70 ˚C and transferred into ice. At the second stage, 0.4 mM dNTP, reverse transcriptase buffer, and 4 activity units/μl of M-MuLV reverse transcriptase were added to the mixture and it was incubated for 1.5 h at 37˚C and then heated (15 min at 70˚C). PCR was performed using the following primers for the *bar* gene and actin:

Actin 1 up – 5'-TATGCCCTCCCACATGCCAT-3';
Actin 1 low – 5'-CATCTGCTGGAAGGTGCTGA-3'.

The reaction mixture contained ScreenMix-HS ("Evrogen"), 0.8 mM primers, 0.1–5 μg RNA or cDNA. PCR conditions were the following: denaturation at 95˚C (5 min); 31 cycles at 95˚C (45 s), 59˚C (30 s), 72˚C (1 min); and elongation at 72˚C (10 min). In July 2015, the plants were treated with herbicide according to the procedure described above.

Statistical processing was performed using the Statistica 6.1 (StatSoft, USA) software.

## RESULTS

Genetic transformation with the pBIBar vector produced eighteen kanamycin-resistant aspen lines: ten lines of the Pt genotype and eight lines of the f2 genotype. DNA for PCR analysis was isolated from the 14 best *in vitro* growing lines (seven of each genotype). PCR analysis of the *virB* gene revealed no agrobacterial contamination of DNA samples. The presence of a *nptII* selective gene sequence was confirmed in all lines (data not shown). Insertion of the target *bar* gene

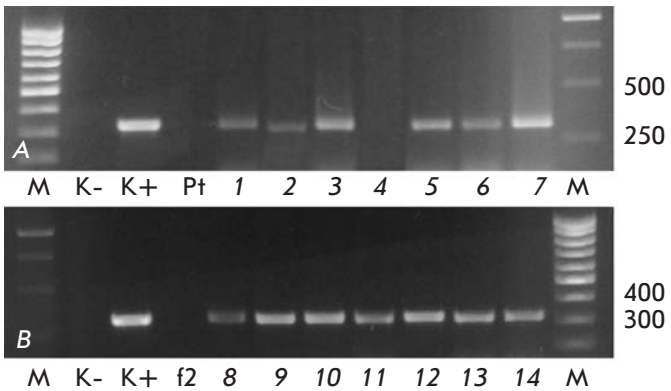


Fig. 1. PCR analysis of transgenic aspen plants for integration of the *bar* gene (A – genotype Pt, B – genotype f2). M – marker; K- – water; K+ – pBIBar; Pt, f2 – non-transgenic control; 1 – PtXIBar4a; 2 – PtXIBar9a; 3 – PtXIBar14a; 4 – PtXIBar23a; 5 – PtXIBar29a; 6 – PtXIBar30a; 7 – PtXIBar31a; 8 – f2XIBar1a; 9 – f2XIBar2a; 10 – f2XIBar3a; 11 – f2XIBar4a; 12 – f2XIBar5a; 13 – f2XIBar6a; 14 – f2XIBar8a

into the aspen genome was detected in six out of seven Pt lines (except for PtXIBar23a); all f2 lines contained amplification of the DNA fragment of the expected size (310 bp, *Fig. 1*).

*In vitro* resistance of aspen plants (13 lines and two source genotypes) was determined by rooting in a medium containing 0 (control), 0.5 mg/l (sublethal concentration), or 5 mg/l (lethal concentration) of PPT. Two weeks after planting, the non-transgenic plants in the medium with 0.5 mg/l PPT displayed a dramatically decreased rate of rooting, number and length of roots, whereas all non-transgenic plants in the medium with 5 mg/l PPT had died. PPT treatment did not affect the rate of rooting of the transgenic plants, although some lines had a lower number and shorter length of roots. Three transgenic lines of each genotype were selected based on the results of the *in vitro* experiment: PtXIBar9a, PtXIBar14a, PtXIBar29a, f2XIBar2a, f2XIBar3a, and f2XIBar5a, all of which displayed no decrease in rooting parameters in the medium with PPT. These lines were evaluated for resistance to Basta herbicide outdoors. The one-year-old non-transgenic aspen plants displayed low resistance: within 3 days all leaves on plants of both genotypes were completely necrotic, regardless of the herbicide doses used (*Tables 1* and *2*). All transgenic lines were resistant to treatment with 2.5 l/ha of the herbicide, and two lines of the f2 genotype were also resistant to a dose of 5 l/ha. In the remaining cases, some leaves had small spots of necrosis, up to 5–10% of leaf area. Within 7 days after treatment with Basta at the maximum dose, the degree of

Table 1. Resistance of aspen plants of the Pt genotype to Basta herbicide treatment

| Line | Herbicide dose, l/ha | Degree of necrosis, points | |
|---|---|---|---|
| | | After 3 days | After 7 and 14 days |
| Pt | 2.5 | 5 | 5 |
| | 5 | 5 | 5 |
| | 10 | 5 | 5 |
| PtXIBar9a | 2.5 | 0 | 0 |
| | 5 | < 1* | < 1 |
| | 10 | < 1 | 1** |
| PtXIBar14a | 2.5 | 0 | 0 |
| | 5 | < 1 | < 1 |
| | 10 | 1 | 1 |
| PtXIBar29a | 2.5 | 0 | 0 |
| | 5 | < 1 | < 1 |
| | 10 | < 1 | 1 |

*Up to 1/3 of all leaves were affected (necrosis up to 5–10% of the total area).
**Up to 1/2–2/3 of all leaves were affected (necrosis up to 25% of the total area).

Table 2. Resistance of aspen plants of the f2 genotype to Basta herbicide treatment

| Line | Herbicide dose, l/ha | Degree of necrosis, points | |
|---|---|---|---|
| | | After 3 days | After 7 and 14 days |
| f2 | 2.5 | 5 | 5 |
| | 5 | 5 | 5 |
| | 10 | 5 | 5 |
| f2XIBar2a | 2.5 | 0 | 0 |
| | 5 | 0 | 0 |
| | 10 | < 1 | 1 |
| f2XIBar3a | 2.5 | 0 | 0 |
| | 5 | 0 | < 1 |
| | 10 | < 1 | 1 |
| f2XIBar5a | 2.5 | 0 | 0 |
| | 5 | < 1 | < 1 |
| | 10 | < 1 | < 1 |

damage had increased in some transgenic lines: a higher number of affected leaves and larger necrosis area (up to 25% of the leaf area). 14 and 28 days after the treatment there was no further progression of damage in the transgenic plants, while all leaves fell from the control plants that died. The appearance of the plants 7 days after the treatment is shown in *Fig. 2*.

Foliar NH4-N concentrations were similar in all one-year-old transgenic aspen plant lines, while the am-

Fig. 2. One-year control and transgenic aspen plants (genotype Pt) 7 days after treatment with water or the Basta herbicide at doses of 2.5, 5, 10 l/ha in 2014. Left – untransformed control plant, right – transgenic line PtXIBar14a

Table 3. Water content in aspen leaves before and after Basta herbicide treatment

| Genotype | Line | Treatment | Water content, % | |
|---|---|---|---|---|
| | | | Prior to treatment | After treatment |
| Pt | Pt | Water | 64.0 | 61.6 |
| | | Herbicide | 61.3–64.1 | 20.3–24.0 |
| | PtXIBar9a | Water | 59.5 | 55.7 |
| | | Herbicide | 56.0–60.4 | 53.9–57.2 |
| | PtXIBar14a | Water | 59.8 | 56.7 |
| | | Herbicide | 60.5–62.1 | 59.5–60.8 |
| | PtXIBar29a | Water | 59.7 | 59.2 |
| | | Herbicide | 57.4–61.7 | 56.9–61.0 |
| f2 | f2 | Water | 55.9 | 52.6 |
| | | Herbicide | 59.1–61.5 | 22.7–25.3 |
| | f2XIBar2a | Water | 60.6 | 59.5 |
| | | Herbicide | 60.9–61.6 | 58.7–61.3 |
| | f2XIBar3a | Water | 60.8 | 61.1 |
| | | Herbicide | 60.6–62.9 | 60.7–63.3 |
| | f2XIBar5a | Water | 59.9 | 59.0 |
| | | Herbicide | 62.4–63.2 | 60.4–61.6 |

monium content in the control plants was significantly higher: 17.5–19.6 and 24.2 μg $NH4^+$/g of fresh weight for the Pt genotype ($p$ <0.001) and 18.9–20.6 and 24.1 μg $NH4^+$/g of fresh weight for the f2 genotype ($p$ <0.05), respectively. Three days after the treatment, the ammonium concentration in the control plants had increased in a dose-dependent manner: 2.7–4.6-fold for the Pt genotype (*Fig. 3*) and 2.2–3.7-fold for the f2 genotype (*Fig. 4*). In most transgenic lines, the ammonium concentration had decreased (up to −36% from the baseline); however, for all versions of the PtXIBar9a line its concentration had increased by 14–60% (with no significant difference compared to water treatment in absolute terms).

Prior to the treatment, aspen leaves contained, depending on the line, 55.9–64.1% of water (*Table 3*). Herbicide treatment caused sharp dehydration in the control plants: water content dropped to 20.3–24.0% for plants with the Pt genotype and to 22.7–25.3% for plants with the f2 genotype. There was almost no change in this parameter in the transgenic plants, with post-treatment values of 53.9–63.3% (95–102% of the baseline). There were no significant differences between various herbicide treatment options.

Measurements of biometric parameters of the aspen plants in the 2014 season did not reveal any negative impact of the herbicide treatment on the growth of the transgenic lines. There were no statistically significant differences between various treatments in plant height as measured at the end of the growing season (*Fig. 5*). The transgenic lines also did not differ in height from each other or from the control plants. There were no significant differences in foliage (data not shown), but the basal diameter of the f2XIBar5a plant line treated with 2.5 or 5 l/ha was significantly higher than in the same line treated with water: 6.9, 7.0, and 6.3 mm, respectively ($p$ <0.05).

To assess the impact of abiotic factors on the stability of the transferred gene expression, the plants were subjected to overwintering outdoors. In late October 2014, anomalously low temperatures were observed throughout the European part of Russia. In Pushchino, the temperature dropped to -12.6 ˚C, which is ca. 10 ˚C lower than average long-term values (*Fig. 6*).

In spring, after breaking of buds it was discovered that this frost caused partial freezing of one-year-old shoots and even plant death (*Fig. 7*). The f2 genotype displayed significantly lower freeze tolerance than the Pt genotype. All plants of the f2XIBar5a line had died; all shoots of the f2XIBar3a line were partially frost-damaged (on average 22.9% of their length were affected) and only in line f2XIBar2a and in the controls did roughly one half of the plants sustain no damage. None of the Pt genotype plants had died, and the share of those was 41.2–70.6% with a lower degree of shoot frost damage.

RT-PCR analysis of total RNA of the five surviving aspen transgenic lines revealed a positive signal of the expected size for all lines, confirming the transcription of the *bar* gene (*Fig. 8*). There was no transcription of the *bar* gene in non-transgenic plants of both genotypes.

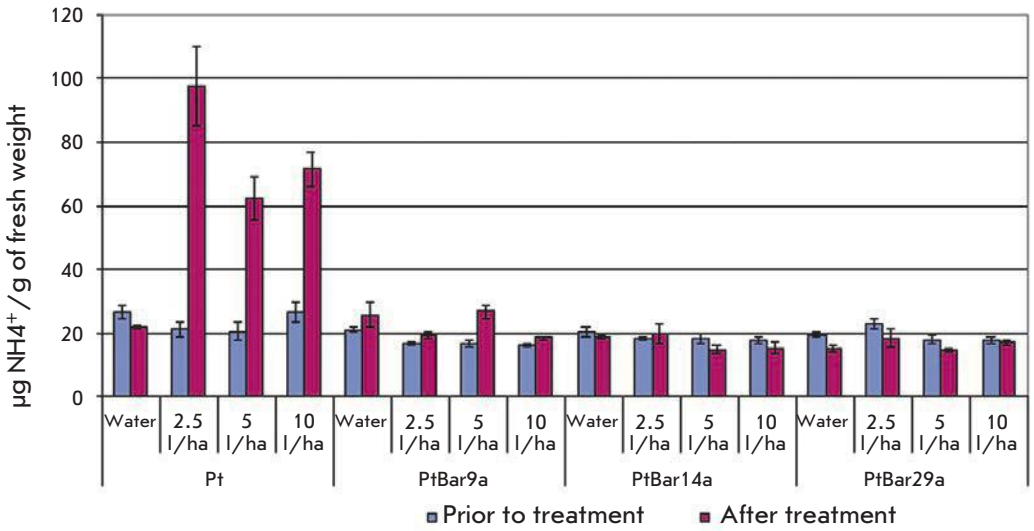


Fig. 3. Foliar ammonia concentrations in leaves of aspen plants (genotype Pt) before and 3 days after Basta herbicide treatment

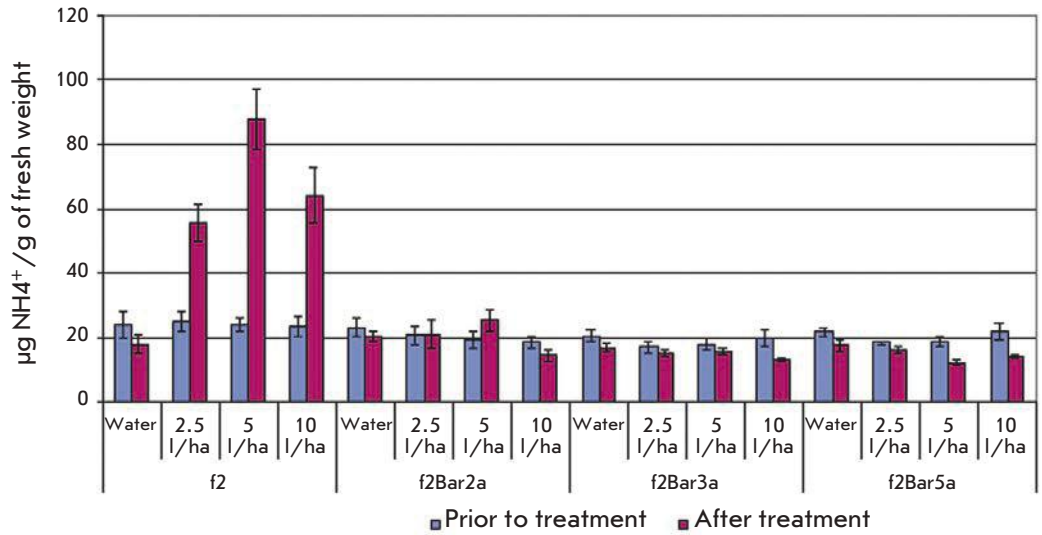


Fig. 4. Foliar ammonia concentrations in leaves of aspen plants (genotype f2) before and 3 days after Basta herbicide treatment

In 2015, the surviving plants of the five transgenic aspen lines and the initial genotypes were re-treated with Basta herbicide (the lost control plants had been replaced with the reserve). The onset of damage signs in two-year-old non-transgenic plants had slightly slowed down compared to the one-year-old ones back in 2014: three days after the treatment at doses equivalent to 2.5 and 5 l/ha, the leaves still had living tissue sections (four-point damage). However, 7 days after the treatment all the leaves of non-transgenic plants were completely necrotic (*Fig. 9*). There were no significant differences in resistance among the transgenic lines. All plants were fully resistant to the 2.5 l/ha dose. Treatment with 5 l/ha did not cause any damage within 3 days: within 7 days, small necrosis spots (up to 1 mm) had appeared on some leaves, and within 14 days approximately 25% of all of the leaves displayed signs of damage in the form of necrotic spots or strips along the edges of a leaf no more than 1 mm in width. The effect of treatment with a twofold normal field dosage (10 l/ha) was more pronounced: small spots of necrosis on single leaves were detected already on Day 3 after the treatment, and within 7 days up to a third of all leaves were affected, with the number of affected leaves increasing to nearly half after 14 days. For this treatment, small spots of necrosis (1–2 mm in diameter) were observed primarily on the edges of the leaves, and only in some leaves at the top of the shoots (2–3 leaves per plant) had the necrosis affected 10–15% of the area. 14 days after the treatment, there was no further progression of the damage.

Four transgenic lines PtXIBar9a, PtXIBar14a, PtXIBar29a, and f2XIBar2a were selected based on the re-

Fig. 5. Effect of Basta herbicide treatment on the growth of control and transgenic aspen plants in 2014

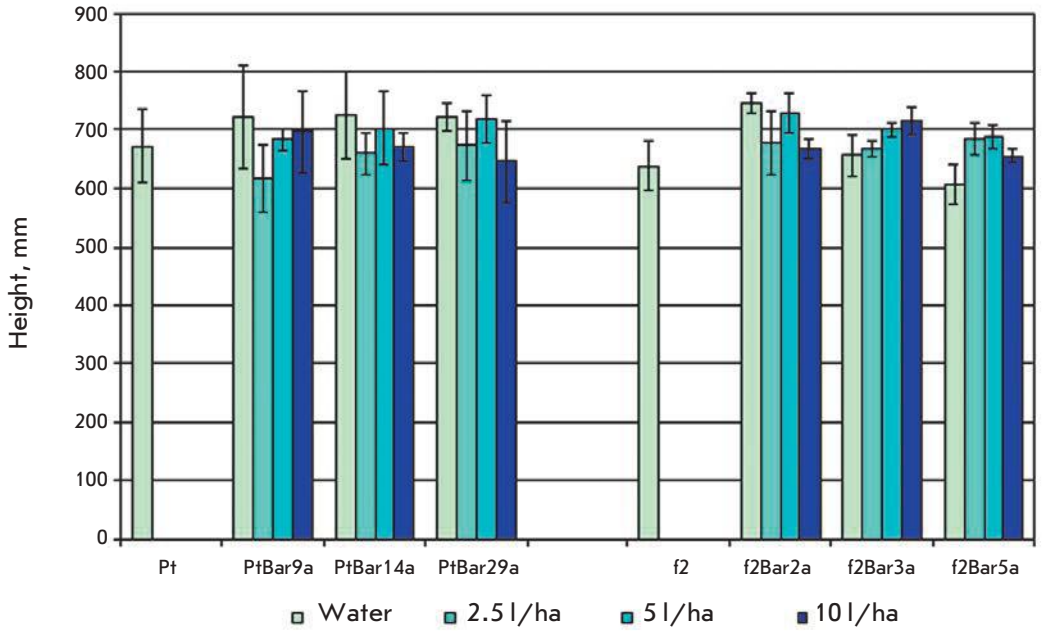


Fig. 6. Minimum temperature in 21-31 October for 2004-2015 in Pushchino

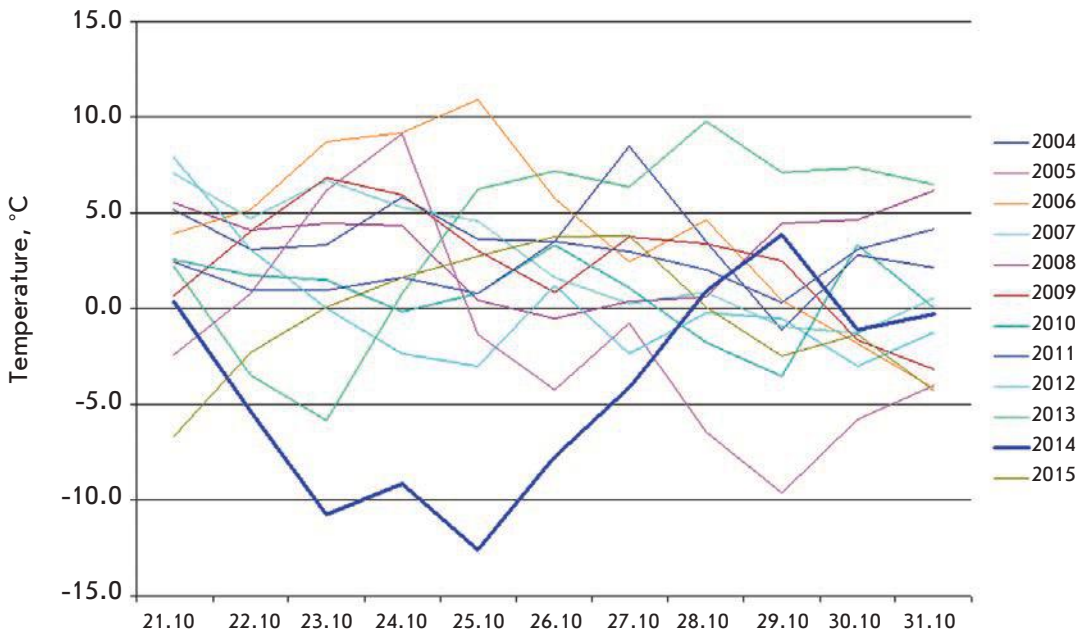


sults of the study as highly resistant to PPT herbicide with a maximum level of freeze tolerance.

## DISCUSSION

Modern forest plantations are intensively managed artificial forests for wood production with a level of efficiency much higher than the productivity of natural forests. There are several ways to achieve this: e.g. the use of elite genotypes, including transgenic ones. For example, in April 2015 Brazil approved commercial use of transgenic eucalyptus with accelerated growth [24]. An equally important issue is the quality of management and the use of high-quality planting material, whose cultivation in nurseries is impossible without weed control. A chemical method of weed control can increase the yield of planting material and improve its quality, while simultaneously significantly reducing both labor and financial costs. Imparting re-

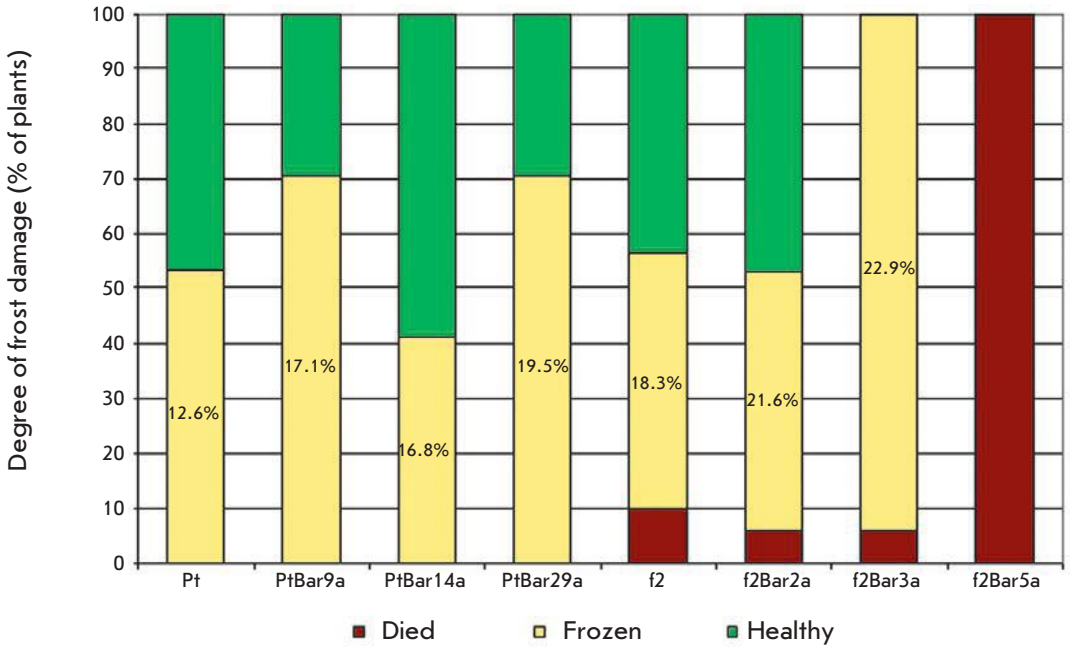


Fig. 7. Damage of aspen plants after overwintering

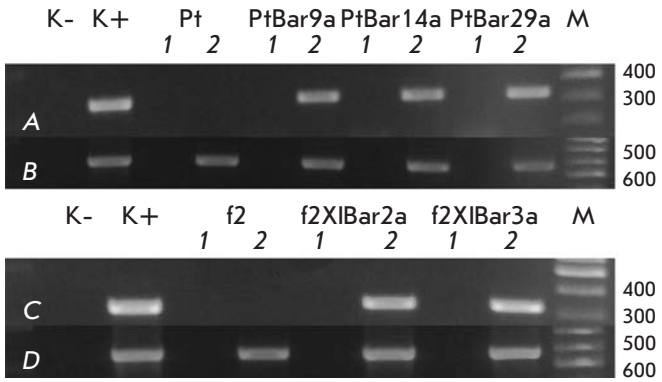


Fig. 8. RT-PCR analysis of the expression of the *bar* gene (A, C) in transgenic aspen plants (A, B – genotype Pt, C, D – genotype f2). Actin was used as an internal control (B, D). K- – water; K+ – DNA non-transgenic plants (actin) or pBIBar (*bar*); 1 – RNA from transgenic lines; 2 – cDNA from transgenic lines; M – marker

Fig. 9. Two-year control and transgenic aspen plants (genotype f2) 7 days after treatment with water or the Basta herbicide at doses of 2.5, 5, 10 l/ha in 2015. Left – untransformed control plant, right – transgenic line f2XIBar2a

sistance to herbicides by genetic engineering methods simplifies the implementation of a chemical method of weed control without damaging the cultivated plants. For this purpose, the *bar* gene from soil bacterium *S. hygroscopicus* [9] was inserted into aspen plants. In addition to conferring resistance to PPT-based herbicides, this gene is also one of the most widely used selective genes in genetic engineering [25]. Moreover, unlike most other herbicide-resistance genes, the *bar* gene ensures inactivation of the active ingredient of a herbicide.

Elite aspen genotypes of Russian origin, characterized by rapid growth and resistance to trunk rot, were used for the transformation. For example, the plantings of clone 34 (the source material for the *in vitro* culture of the f2 genotype) at the age of 47 years exceeded plantings of common aspen in the sum of basal area by 51%, in stock by 43%, while the share of trees

with trunk rot in this clone was 4.7 times lower [26]. PCR confirmed *bar* gene insertion in 13 transformants. An *in vitro* experiment demonstrated the resistance of all transgenic lines to PPT concentration in the medium, which is lethal for non-transgenic plants, confirming expression of the inserted gene. Further tests of aspen plants resistance to herbicides were carried out under semi-natural conditions: the growth of the root system was limited by the volume of the planting container, but the plants were kept outdoors and were exposed to all effects of the environment. Currently, it is the closest possible approximation of natural conditions for transgenic plants available in Russia, since field tests have not been performed for approximately 10 years. The plants were treated with water or Basta herbicide at doses equivalent to 2.5, 5, and 10 l/ha. This herbicide is used as a desiccant at a dose of 1.5–2.5 l/ha and as an herbicide at a dose of 4–5 l/ha. Therefore, the maximum concentration was equivalent to twofold normal field dosage. To assess the consistency of the transferred trait, the treatment was performed in 2014 and 2015, after overwintering outdoors.

Treatment of one-year-old plants demonstrated that aspen is very sensitive to PPT: 3 days after the treatment, all leaves of the untransformed controls were completely necrotic. The high sensitivity of plants of the genus *Populus* to PPT has been reported previously: complete necrosis of *P. alba* leaves was observed as early as 2 days after treatment with a standard field dosage of the herbicide [3]. In contrast to the controls, transgenic aspen plants carrying the *bar* gene demonstrated a high degree of resistance: treatment with 5 and 10 l/ha doses resulted in only small spots of necrosis. The herbicide did not cause retardation of growth in any of the six aspen lines, whereas Meilan *et al.* [6] observed a decrease in the growth of 25% of *Populus* hybrid lines treated with a single dose of the herbicide and in 17–61% of plants treated with a double dose. Other trees with the *bar* gene also exhibited a high degree of resistance: eucalyptus [11] and *P. alba* [3] plants proved resistant to a double dose of PPT herbicides. We have observed differences between the genotypes in their response to herbicide treatment: signs of damage were more pronounced in transgenic lines of the Pt genotype than in those of the f2 genotype. Our *P. tremula* plants that died after treatment with 375 g/ha PPT proved to be more sensitive to PPT than the *P. alba* × *P. tremula* hybrid, which survived after being treated with 400 g/ha PPT [10].

In plant cells, the ammonium, released after nitrate reduction, amino acid degradation and photorespiration, can only be effectively detoxified by glutamine synthetase [7]; therefore, plants are highly sensitive to inhibitors of this enzyme, including PPT. The accumulation of ammonium in PPT-treated plants is widely used as a biochemical marker of glutamine synthetase inhibition [27]. Three days after treatment, the ammonium concentration in one-year-old non-transgenic aspen plants increased 2.2–4.6-fold depending on both the dose and the genotype. Apparently, the Pt genotype is more sensitive to the action of the herbicide (2.7–4.6-fold increase) than f2 (2.2–3.7-fold increase). The observed increase in ammonium concentration in aspen was far less pronounced than in the *P. alba* × *P. tremula* hybrid, for which within 24 hours after the treatment there was nearly a 100-fold increase in ammonium content: from 9 to 800–900 μg/g of fresh weight [10]. This can be attributed to the differences in genotype, time after treatment (72 and 24 hours), dose of PPT (0.375–1.5 and 4 kg/ha), and metabolic rate associated with the age of the plant, as well as to being in a greenhouse or outdoors. In all six lines of transgenic aspen, treatment with the herbicide did not cause any significant increase in ammonium concentration, which was quite similar in all cases (12.4–27.0 μg/g of fresh weight). In this respect, our results differ from the data by Asano et al. [28], who observed an approximately 10-fold variation in the ammonium concentration in six transgenic *Agrostis* lines carrying the *bar* gene, which almost reached the level of non-transgenic plants 3 days after treatment. In contrast, we observed a decrease in ammonium concentration in most lines and in three cases this decrease reached 34–36%, which was statistically significant (f2XIBar3a after 10 l/ha treatment, f2XIBar5a and after 5 and 10 l/h treatment). This may be associated with some processes occurring within this 3-day period, such as incorporation of ammonium into nitrogen metabolism. High doses of the herbicide that caused necrosis of leaves in the transgenic plants did not affect the ammonium content.

The toxicity of the accumulated ammonium is considered to be the major factor of PPT herbicidal activity [8, 29]. On the other hand, it has been demonstrated that the action of the herbicide is primarily due not to the accumulation of ammonia, but to the lack of glutamine, which makes it impossible to synthesize important nitrogen-containing compounds that are normally produced from glutamine amide and amine nitrogen [30]. Complete necrosis of the non-transgenic aspen plants leaves that occurs only at a 2.2-fold increase in ammonium levels, the lack of correlation between leaves damage and levels of ammonium in the transgenic plants, as well as the plants ability to survive despite a manifold increase in ammonium levels [31] taken together suggest that ammonium phytotoxicity is not the primary cause of aspen plants death after PPT treatment.

To assess PPT sensitivity, we used such an indicator as the decrease in fresh [8] or dry [32] weight. Since Basta herbicide is used also as a desiccant, we decided to use the rate of dehydration of leaf tissue. The herbicide caused sharp dehydration in non-transgenic plants: there was an almost 3-fold drop in water content, regardless of the dose. Apparently, already a dose of 2.5 l/ha (the standard dose for desiccation) is enough for a plant to reach a certain physiological limit of dehydration. The appearance of necrotic spots on the leaves of transgenic plants after treatment with doses of 5 and 10 l/ha of the herbicide had no effect on their water content, which was within 95–102% of the baseline values for all plants, including those treated with water. It should be noted that there was a smaller decrease in the water content of control plants of the f2 genotype (2.4–2.7-fold) than in Pt plants (2.6–3-fold).

In mid- to late October 2014, there was a sharp drop in temperature throughout the European part of Russia, which was observed for the first time since 1982 [33]. Negative anomalies during this period reached 8–11°C, and the temperature corresponded to a mid-December one. These unplanned tests for freeze tolerance resulted in the death of all plants of the f2XIBar5a line and freezing of all plants of the f2XIBar3a line. This suggests that these lines have changes that significantly reduce their resistance to low temperatures in autumn. Interestingly, of the three transgenic lines of the f2 genotype, the two most affected ones also exhibited a significant decrease in ammonium levels after treatment with the herbicide. Freeze tolerance of the other four transgenic aspen lines was considerably higher and remained at the level of non-transgenic plants of both genotypes. This case once again confirms the need to conduct field trials of perennial plants for long periods of time and in different climatic zones.

In addition to the level of expression of the inserted genes, it is also important to test trees for the stability of its expression as trees keep growing for many years, and each year they are subjected to periods of dormancy and growth, as well as to various abiotic and biotic stresses. Unstable expression of the transferred genes and, as a consequence, unstable manifestation of new traits undermines the commercial value of such plants. Stable expression of the *bar* gene in hybrid *Populus* plants without silencing was demonstrated in a field over the course of three [34] or eight years [35]. A high level of resistance to the Basta herbicide was also observed in pears rootstock with the *bar* gene during the 5th year of cultivation in a field [36]. However, field testing of poplar with glyphosate resistance genes over the course of two years revealed a strong increase in damage in the second year in two lines out of 80 that were treated with herbicides, and some lines exhibited morphological changes [6]. In our work, strong abiotic stress did not cause a decrease in the *bar* gene expression in the surviving aspen plants, which was confirmed by RT-PCR analysis. Two-year-old transgenic plants retained a high level of resistance in the second year; however, development of signs of damage had been slowed down in all plants, including the non-transgenic controls. This can be attributed to a significant increase in leaf surface or to lower susceptibility to the herbicide due to a more developed cuticle. A less developed cuticle was used as an explanation for the decreased resistance of *Populus* hybrids with the *bar* gene, which had been treated soon after field-planting: however, 8 years later these plants displayed high resistance [35]. This version is supported by the fact that, in contrast to the first year when necrotic spots were relatively evenly distributed over the surface of the leaves, in the second year the signs of damage were concentrated on leaf edges, which could have had a thinner cuticle. It is also possible that the applied herbicide trickled to leaf edges.

Since herbicide resistance is important primarily in the first few years of tree growth, it is expedient to insert these genes into already transgenic plants. For example, the first re-transformation of woody plants was performed by insertion of the *bar* gene into transgenic pear plants already carrying the *gus* gene [37]. The potential of this approach in forest biotechnology is confirmed by research by ArborGen company (USA) in which herbicide resistance genes were transferred into a transgenic eucalyptus line AGEH427 [38] which already contained genes for freeze tolerance and sterility [39].

## CONCLUSION

Several transgenic aspen lines carrying the *bar* gene conferring resistance to herbicides containing phosphinothricin were produced from elite aspen genotypes. Two years of testing under semi-natural conditions have demonstrated resistance of the transgenic lines to a two-fold normal field dosage of the Basta herbicide. Based on the results of these tests, four lines which displayed both freeze tolerance under extremely low temperatures and high resistance to herbicides (PtXIBar9a, PtXIBar14a, PtXIBar29a, f2XIBar2a) were selected. These plants are promising for further studies, in particular to field testing. In addition, the *bar* gene could be used for retransformation of the transgenic woody plants that have been obtained in our laboratory and have already demonstrated valuable traits, such as increased productivity and modification of the composition of wood [40].

*This work was supported by the Ministry of Education of the Russian Federation (State contract number 14.M 04.12.0009 from June 27, 2014).*

REFERENCES

1. Baum S., Weih M., Busch G., Kroiher F., Bolte A. // Landbauforschung. 2009. V. 59. P. 163–170.
2. Bubnov A.A. // Proceedings of the Saint Petersburg Forestry Research Institute. 2014. № 3. P. 36–42 (in Russian).
3. Confalonieri M., Belenghi B., Balestrazzi A., Negri S., Facciotto G., Schenone G., Delledonne M. // Plant Cell Rep. 2000. V. 19. P. 978–982.
4. Fillatti J.J., Sellmer J., McCown B., Haissig B., Comai L. // Mol. Gen. Genet. 1987. V. 206. P. 192–199.
5. Brasileiro A.C.M., Tourneur C., Leple J.C., Combes V., Jouanin L. // Transgenic Res. 1992. V. 1. P. 133–141.
6. Meilan R., Han K.-H., Ma C., DiFazio S.P., Eaton J.A., Hoien E.A., Stanton B.J, Crockett R.P., Taylor M.L., James R.R., et al. // Can. J. For. Res. 2002. V. 32. P. 967–976.
7. Miflin B.J., Lea P.J. // Annu. Rev. Plant Physiol. 1977. V. 28. P. 299–329.
8. Tachibana K., Watanabe T., Sekizawa Y., Takematsu T. // J. Pestic. Sci. 1986. V. 11. P. 33–37.
9. De Block M., Botterman J., Vandewiele M., Dockx J., Thoen C., Gossel V., Movva N.R., Thompson C., van Montagu M., Leemans J. // EMBO J. 1987. V. 6. P. 2513–2518.
10. De Block M. // Plant Physiol. 1990. V. 93. P. 1110–1116.
11. Harcourt R.L., Kyozuka J., Floyd R.B., Bateman K.S., Tanaka H., Decroocq V., Llewellyn D.J, Zhu X., Peacock W.J., Dennis E.S. // Mol. Breed. 2000. V. 6. P. 307–315.
12. González E., Gugliermoni C., Galvão M., Fagundes M., Ferreira M., Almeida G., Alves H., Gonsalves J., Silva F., Bentivenha S., et al. // BMC Proc. 2011. V. 5 (Suppl. 7). P. 135.
13. Alvarez R., Alvarez J.M., Humara J.M., Revilla A., Ordas R.J. // Biotechnol. Lett. 2009. V. 31. P. 1477–1483.
14. Bishop-Hurley S.L., Zabkiewicz R.J., Grace L., Gardner R.C., Wagner A., Walter C. // Plant Cell Rep. 2001. V. 20. P. 235–243.
15. Parasharami V.A., Naik V.B., von Arnold S., Nadgauda R.S., Clapham D.H. // Plant Cell Rep. 2006. V. 24. P. 708–714.
16. Zhigunov A.V., Shabunin D.A., Butenko O.Yu. // Vestnik of Volga State University of Technology. Series "Forest. Ecology. Nature Management.". 2014. № 4. P. 21-30. (in Russian).
17. Lloyd G., McCown B. // Proc. Int. Plant Prop. Soc. 1981. V. 30. P. 421–427.
18. Padegimas L., Shulga O.A., Skryabin K.G. // Molecular Biology. 2004. V. 28. P. 294–297 (in Russian).
19. . Lebedev V.G., Schestibratov K.A., Shadrina T.E., Bulatova I.V., Abramochkin D.G., Miroshnikov A.I. // Russian Journal of Genetics. 2010. V. 46. P. 1282–1289. (in Russian).
20. Rogers S.O., Bendich A.J. Plant Mol. Biol. Manual. Kluwer Acad. Publ., 1994. P. 1–8.
21. De Block M., De Brouwer D., Tenning P. // Plant Physiol. 1989. V. 91. P. 694–701.
22. Weatherburn M. // Anal. Chem. 1967. V. 39. P. 971–974.
23. Chang S., Puryear J., Cairney J.A. // Plant Mol. Biol. Rep. 1993. V. 11. P. 113–116.
24. Nat. Biotechnol. 2015. V. 33. P. 577. doi: 10.1038/nbt0615-577c.
25. Green J.M., Micheal D.K. // J. Agric. Food Chem. 2011. V. 59. P. 5819–5829.
26. Bagaev S.N., Bagaev E.S. // Forestry. 1990. № 4. P. 45–48. (in Russian).
27. Avila-Garcia W.V., Carol Mallory-Smith C. // Weed Sci. 2011. V. 59. P. 305–309.
28. Asano Y., Ito Y., Fukami M., Sugiura K., Fujiie A. // Plant Cell Rep. 1998. V. 17. P. 963–967.
29. Pornprom T., Chompoo J., Grace B. // Weed Biol. Management. 2003. V. 3. P. 41–45.
30. Evstigneeva Z.G., Solov'eva N.A., Sidel'nikova L.I. // Applied Biochemistry and Microbiology. 2003. V. 39. P. 539–543 (in Russian).
31. Petrović A., Yoshida Y., Ohmori T. // J. Hort. Sci. Biotech. 2009. V. 84. P. 181–186.
32. Nolte S.A., Young B.G., Mungur R., Lightfoot D.A. // Weed Res. 2004. V. 44. P. 335–339.
33. Hydrometeorological Centre of Russia, 03.11.2014, http://meteoinfo.ru/news/1-2009-10-01-09-03-06/10052-03112014-2014-
34. Li J., Brunner A.M., Meilan R., Strauss S.H. // Tree Physiol. 2009. V. 29. P. 299–312.
35. Li J., Meilan R., Ma C., Barish M., Strauss S.H. // West J. Appl. For. 2008. V. 23. P. 89–93.
36. Lebedev V.G., Dolgov S.V. // Acta Hort. 2008. V. 800. P. 373–382.
37. Lebedev V.G., Skryabin K.G., Dolgov S.V. // Acta Hort. 2002. V. 596. P. 193–197.
38. Gulledge E., Judy C., Cunningham M. // AAIC 25th Anniversary Meeting, October 12–16, 2013, Washington, USA. http://www.se-ibss.org/publications-and-patents/presentations/building-herbicide-resistance-for-short-rotation-hardwood-crops
39. Zhang C., Norris-Caneda K.H., Rottmann W.H., Gulledge J.E., Chang S., Kwan B.Y., Thomas A.M., Mandel L.C., Kothera R.T., Victor A.D., et al. // Plant Physiol. 2012. V. 159. P. 1319–1334.
40. Shestibratov K., Lebedev V., Podrezov A., Salmova M. // BMC Proc. 2011. V. 5 (Suppl. 7). P. 124.

# Cytomegalovirus in Plasma of Acute Coronary Syndrome Patients

E. A. Nikitskaya[1], J.-C. Grivel[2+], E. V. Maryukhnich[1], A. M. Lebedeva[1], O. I. Ivanova[1], P. P. Savvinova[1], A. V. Shpektor[1], L. B. Margolis[2], E. Yu. Vasilieva[1*]

[1]Laboratory of Atherothrombosis, Cardiology Department, Evdokimov Moscow State University of Medicine and Dentistry, Delegatskaya str. 20/1, 127473, Moscow, Russia;

[2]Section on Intercellular Interactions, Eunice Kennedy Shriver National Institute of Child Health and Human Development, National Institutes of Health, Bethesda, MD, USA

[+]Current affiliation: Sidra Medical and Research Center, P.O. Box 26999, Doha, Qatar

[*]E-mail: vasilievahelena@gmail.com

Received 02.09.2015



**ABSTRACT** **The relationship between acute coronary syndrome (ACS) and local and systemic inflammation, including accumulation of macrophages in atherosclerotic plaques and upregulation of blood cytokines (e.g., C-reactive protein (CRP)), has been known for more than 100 years. The atherosclerosis-associated inflammatory response has been traditionally considered as an immune system reaction to low-density lipoproteins. At the same time, some data have indicated a potential involvement of cytomegalovirus (CMV) in the activation and progression of atherosclerosis-associated inflammation, leading to ACS. However, these data have been tangential and mainly concerned the relationship between a coronary artery disease (CAD) prognosis and the anti-CMV antibody titer. We assumed that ACS might be associated with CMV reactivation and virus release into the bloodstream. The study's aim was to test this assumption through a comparison of the plasma CMV DNA level in patients with various CAD forms and in healthy subjects. To our knowledge, no similar research has been undertaken yet. A total of 150 subjects (97 CAD patients and 53 healthy subjects) were examined. Real-time polymerase chain reaction (RT-PCR) was used to determine the number of plasma CMV DNA copies. We demonstrated that the number of plasma CMV genome copies in ACS patients was significantly higher than that in healthy subjects ($p = 0.01$). The CMV genome copy number was correlated with the plasma CRP level ($p = 0.002$). These findings indicate a potential relationship between CMV activation and atherosclerosis exacerbation that, in turn, leads to the development of unstable angina and acute myocardial infarction. Monitoring of the CMV plasma level in CAD patients may be helpful in the development of new therapeutic approaches to coronary atherosclerosis treatment.**

**KEYWORDS** **coronary artery disease, acute coronary syndrome, human herpes viruses, cytomegalovirus, polymerase chain reaction.**

**ABBREVIATIONS** **HHV – human herpes virus; hs-CRP – high-sensitivity C-reactive protein; CAD – coronary artery disease; AMI – acute myocardial infarction; SCAD – stable coronary artery disease; ACS – acute coronary syndrome; RT-PCR – real time polymerase chain reaction; CMV – cytomegalovirus.**

## INTRODUCTION

Atherosclerotic coronary artery lesions often lead to the development of a coronary artery disease (CAD) that manifests itself as angina or painless myocardial ischemia. This disease can last for years as stable coronary artery disease (SCAD) forms, with occasional exacerbations presenting themselves clinically as unstable angina or acute myocardial infarction (AMI). These clinical manifestations are grouped under the name of acute coronary syndrome (ACS). The morphological substrate of this exacerbation is supposed to be acute inflammation followed by atherosclerotic plaque rupture and thrombosis formation [1–3]. Despite the fact that the role of inflammation in the development and progression of atherosclerosis has been under discussion for the second century running since the time of Virchow [4], the causes of this inflammation are not completely clear. The very fact of an inflammation is confirmed by the presence of macrophages and lymphocytes in the plaques, an elevated level of inflammatory cytokines in atherosclerosis patients, etc. [5–10]. According to the most accepted theory, the primary trigger of an inflammatory reaction in the vascular wall is the subendothelial accumulation of oxidized low-density lipoproteins [11–13]. At the same time, there are data indicating that atherosclerotic plaques

contain various bacteria and viruses [14–19] that can also induce an inflammatory response. Herpesviruses, in particular the cytomegalovirus (CMV), are of huge interest. Many epidemiological studies have revealed a relationship among the incidence of coronary atherosclerosis, the incidence of acute myocardial infarction, and the blood level of anti-CMV antibodies [20, 21]. However, this is insufficient to assess the viral infection activity during atherosclerosis exacerbation. An exception is a study by S. Gredmark *et al.* [22], demonstrating that CMV RNA in the monocytes of ACS patients occurs more often than in those of healthy donors and patients with chronic forms of CAD, which may indicate activation of the virus during ACS. At the same time, no direct analysis of the plasma CMV level in patients with atherosclerotic coronary artery disease has been previously performed. The presence of the virus in plasma may indicate its activation [23–25]. In this work, we present a comparative study of CMV in plasma of patients with various forms of CAD and healthy volunteers.

## MATERIAL AND METHODS

### Characterization of groups of patients and healthy volunteers

The study involved 150 participants, including 97 CAD patients and 53 healthy volunteers. Seventy-one patients were admitted to the Cardiac Critical Care Department of the Davydovskiy Municipal Clinical Hospital with a diagnosis of acute coronary syndrome. Of these, 47 patients were diagnosed with AMI with or without ST-segment elevation in accordance with the universal definition of the European Society of Cardiology [26]; unstable angina was diagnosed in 24 cases. Twenty-six patients were admitted electively. CAD was diagnosed based on the clinical picture and positive stress test results, which was later confirmed by coronary angiography [27]. In all patients, the clinical prognosis was evaluated; there were no cases of death, hemodynamically significant bleeding, stroke, or stent thrombosis. At admission, two ACS patients were diagnosed with cardiogenic shock; two patients had acute heart failure; 12 patients had acute left ventricular aneurysm; seven patients with a severe coronary artery disease had repeated angina attacks.

An examination of healthy volunteers included a survey, blood chemistry, ultrasound of the heart and carotid arteries, and a stress test. According to the examination data, no subjects with signs of atherosclerosis were identified in the control group.

Patient groups did not differ in age or gender, but they differed in the presence of risk factors, such as obesity, arterial hypertension, and diabetes (*Table 1*).

All participants provided a written informed consent to participate in this study. The study was approved by the local ethics committee of the Evdokimov Moscow State University of Medicine and Dentistry.

### Isolation of viral DNA from plasma

In all patients, a 5-mL blood sample was collected into a test tube with sodium citrate within 24 h after admission. Blood samples were centrifuged at 2,500 rpm for 10 min, after which the plasma was collected, frozen in sterile test tubes, and stored at −80°C until further use.

The samples were thawed, and DNA was isolated from the plasma using QIAamp DNA Blood mini kit columns (Qiagen, Germany) according to a standard protocol. Elution was performed using 60 μL of a special buffer from the same kit. Before conducting the real-time polymerase chain reaction (RT-PCR), DNA samples were stored at −20°C.

Table 1. Clinical characteristics of CAD patients and healthy volunteers

| Indicator | ACS patients | SCAD **patients** | Healthy volunteers | p |
|---|---|---|---|---|
| Number of patients | 71 | 26 | 53 | |
| Mean age | 64.4 ± 9.7 | 66.3 ± 10.6 | 61.3 ± 12.3 | 0.116 |
| Males | 63.4% | 65.4% | 50.9% | 0.298 |
| Smoking | 28.2% | 11.5% | 20.8% | 0.205 |
| Hyperlipidemia | 35.2% | 15.4% | 34.0% | 0.135 |
| Obesity | 45.1% | 23.1% | 15.1% | 0.001* |
| Hypertension | 90.1% | 92.3% | 47.2% | 0.000* |
| Diabetes mellitus | 31.0% | 19.2% | 1.9% | 0.0002* |

The clinical characteristics of all three groups of patients are presented.
*Differences are statistically significant at $p < 0.05$.

Table 2. CMV primers and probes

| Probe/Primer | Nucleotide sequence | 5'-modification | 3'-modification |
|---|---|---|---|
| Probe | tacctggagtccttctgcgagga | CAL Fluor Red 610* | BHQ-2** |
| Forward primer | aaccaagatgcaggtgatagg | | |
| Reverse primer | agcgtgacgtgcataaaga | | |

*CAL Fluor Red 610 is a fluorescent label on the probe.
**BHQ-2 is a fluorescence quencher.

### Quantitative RT-PCR

CMV was detected by RT-PCR (CFX 96 C1000 Touch Thermal Cycler, Bio-Rad, USA) using highly sensitive primers and a 5'-3'-hydrolyzable probe to the CMV tegument protein pp65 gene (*Table 2*). Amplification was evaluated from the standard curve using standard dilution series (Bioresearch Technologies, USA) and ToughMix PCR mixtures (Quanta, USA, Cat # 95147-250).

RT-PCR was performed according to the standard three-step protocol: step 1 – denaturation at 95°C for 5 min, step 2 – 95°C for 30 s, and step 3 – 60°C for 60 s.

Next, the fluorescence signal was detected.

The second and third steps were again repeated for 45 cycles. Fluorescence detectable up to the 37th cycle was considered specific. The results were presented as the CMV DNA copy number in 1 μL of the patient blood plasma.

### Measurement of the high-sensitivity C-reactive protein (hs-CRP)

At admission, all patients underwent an analysis of hs-CRP, whose level is correlated with the risk of cardiovascular events [28]. The protein plasma level was determined on an automatic analyzer (Siemens Dimention Xpand Plus, Germany) using a C-Reactive Protein Flex Reagent kit (Siemens # DF37, Germany).

### Statistical data processing

The statistical analysis was performed using the Statistica 9.0 software. All obtained data had no signs of a normal distribution based on the Shapiro-Wilk test and, therefore, were represented as median and interquartile ranges. Because of the non-parametric distribution, the Mann-Whitney test was used for comparison between two groups. Non-parametric statistics with the Kruskal-Wallis test and multiple comparison rank test were used to compare more than two groups. The Spearman correlation coefficient was also used. Differences between groups were considered statistically significant at the level of $p < 0.05$.

## RESULTS AND DISCUSSION

Small CMV DNA concentrations (over 100 copies in 1 μL of blood plasma) were quite frequently found both in patients and in healthy volunteers. The rate of virus detection in the three groups differed statistically significantly and was highest in ACS patients (*Table 3*).

Comparison of the number of CMV DNA copies in three groups revealed significant differences between ACS patients and healthy volunteers (213.15 [101.21–436.67] versus 82.10 [18.58–188.67], respectively, $p = 0.012$). However, no statistically significant differences between the group of chronic CAD patients and the group of healthy volunteers were found. The results are shown in *Fig. 1*. In addition, a statistically significant ($p = 0.002$) positive correlation between the number of CMV copies and the hs-CRP level was found in this cohort (*Fig. 2*).

Therefore, we had demonstrated that the occurrence and number of CMV copies in the blood plasma of patients with acute CAD forms were significantly higher than those in healthy controls. No differences between the chronic CAD group and the control group were found.

These findings demonstrate that a small amount of the virus is quite often present in the plasma of healthy individuals (*Table 3*). This is consistent with epidemiological study data on a CMV-seropositive adult population in various countries [24, 29–30]. Our data indicate that the number of CMV DNA copies can substantially increase in pathology: in the case of ACS, the number was more than 2 times higher than that in healthy volunteers. Our findings are generally consistent with

Table 3. The CMV occurrence rate in different groups

| | Healthy volunteers | ACS patients | SCAD patients | p |
|---|---|---|---|---|
| Number of virus-positive patients | 46.15% (18/39) | 77.08% (37/48) | 55.56% (10/18) | 0.013 |

epidemiological data on the correlation between the presence of CMV and atherosclerosis progression, with allowance for the anti-CMV antibody titer [31]. For example, one of the epidemiological studies had revealed a correlation between cardiovascular disease mortality and the anti-CMV antibody titer level [17]. An ARIC study also showed that cardiovascular disease mortality was proportional to an increase in the carotid artery intima-media thickness [32]. However, results of seroepidemiological studies are contradictory. For example, a prospective, controlled study by P.M. Ridker *et al.* revealed no relationship between the presence of anti-CMV antibodies and the risk of atherothrombotic events. In this case, the antibody titer height was not evaluated separately [33].

Previously, the herpesvirus DNA was identified in plaques and blood monocytes by PCR [34]. Melnick *et al.* [35] demonstrated for the first time that CMV DNA was present in the artery walls of atherosclerosis patients. The viral DNA concentration was higher in the arterial wall of patients who underwent reconstructive vascular surgery (coronary artery bypass grafting) compared to patients with early atherosclerosis [36]. Later, CMV was found in the atherosclerotic plaques [37]. We also studied samples obtained from patients who had died of acute myocardial infarction or its complications, but we did not find significant differences in the number of CMV DNA copies in the atherosclerotic plaques and coronary arteries without macroscopic signs of atherosclerosis [38].

The inconsistency of these data may be associated with the fact that both CMV seropositivity and the presence of CMV DNA in tissues and blood cells are not sufficient to conclude on virus replication. In the present work, the number of CMV DNA copies was determined in the plasma of patients with various CAD forms. The presence of the virus in plasma indicates productive infection [23, 24, 29–30]. Another indicator of productive infection may be the presence of CMV RNA, which was detected in peripheral blood mononuclear cells [22]. The amount of CMV RNA in blood monocytes of ACS patients was significantly higher than that in stable angina patients and healthy subjects ($p < 0.001$). In this case, the occurrence of CMV RNA in monocytes was relatively small and amounted to 2% in healthy volunteers, 10% in SCAD patients, and 15% in ACS patients [22]. In general, these data are consistent with the results of our work. However, the occurrence rate of the virus in our groups was higher, possibly due to the fact that blood monocytes are not the only body cells secreting CMV into the plasma.

The morphological basis of ACS is an atherosclerotic plaque rupture, probably due to inflammation in the plaque. A number of studies using histochemical tech-

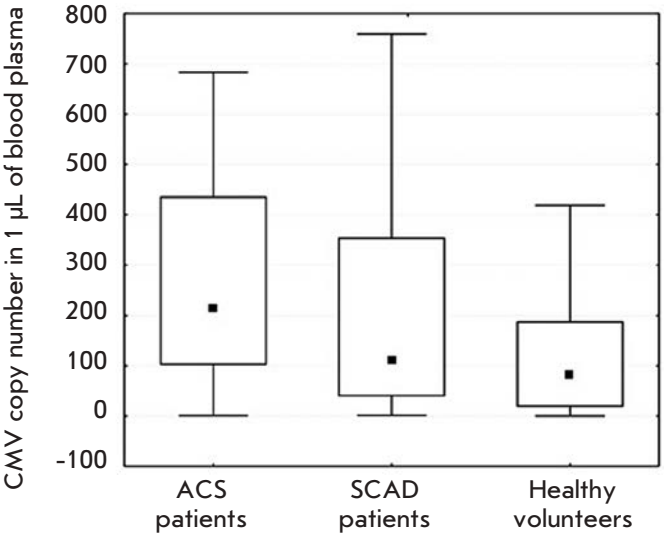


Fig. 1. Comparison of the CMV DNA copy number in the blood plasma of patients in the study groups. The median and 25th–75th percentiles of the CMV DNA copy number in the three groups are presented. Statistically significant differences were found between the ACS group and the healthy volunteer group ($p = 0.012$).

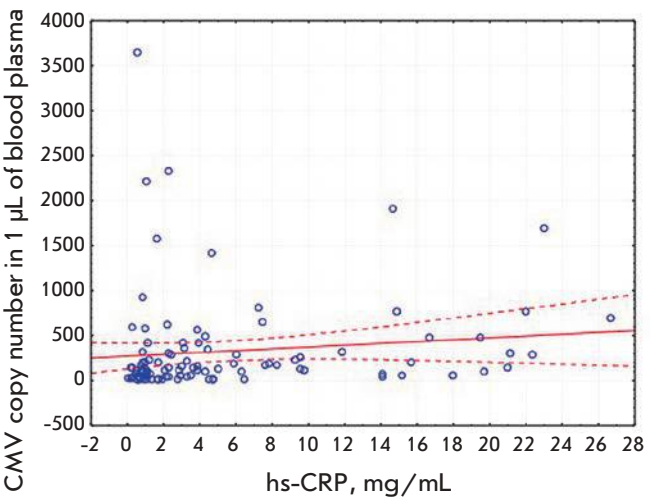


Fig. 2. A correlation between the CMV genome copy number and the hs-CRP level is shown. Results of an individual analysis of the CMV copy number and hs-CRP level are presented. A correlation between the indicators with 95% confidence intervals is demonstrated. Two samples exceeding the mean cohort values by almost 10 times were excluded from the analysis. The correlation coefficient R was 0.25 ($p = 0.011$) before excluding the samples and 0.30 ($p = 0.002$) after exclusion.

niques have demonstrated that the plaques contain activated lymphocytes and macrophages [11, 12, 39–42]. Previously, we used an original technique for isolation of cells from the plaque, preserving cell surface antigens, and their evaluation by flow cytometry [43]. This enabled us to quantitatively evaluate the number of activated lymphocytes ($CD8^+CD25^+$ and $CD8^+HLA\text{-}DR^+$) in the plaques, which happened to be significantly higher than that in the blood. In other studies, along with those by our group, a number of bacteria and viruses, including CMV, were found in blood vessels using RT-PCR [38]. This may be the cause of chronic activation of the immune system in vessels, stimulating the development of atherosclerosis [44]. The role of either oxidized lipoproteins or microorganisms in this activation remains unclear. It may not be excluded that detection of viruses in blood vessels is not related to atherosclerosis itself. They may be present in the vascular wall without playing any pathogenetic role in the development of this pathology. The data obtained in this study disprove this assumption: an elevated CMV DNA level in the plasma of ACS patients indicated enhanced virus replication upon atherosclerosis exacerbation. It is not clear whether the CMV activation plays the major role in the atherosclerosis progression, or other microorganisms may also be involved in this process. Also, the relationship between two factors, CMV reproduction and hyperlipidemia, has not been determined yet. A combination of both mechanisms is possible: CMV reproduction in the plaque may be accompanied by more active lipoprotein accumulation by macrophages. Lipoproteins subjected to oxidization, in turn, may enhance inflammatory reactions in the vascular wall. To answer these questions, further research is needed. The promising area seems to be further analysis of the CMV plasma level in patients with various forms of coronary atherosclerosis and comparison of the virus level with changes in the disease clinical picture.

## CONCLUSION

Thus, we have demonstrated the fact of CMV activation in ACS patients. The number of CMV DNA copies in the plasma is correlated with the level of hs-CRP, a systemic inflammation marker. CMV activation is probably one of the mechanisms triggering the inflammatory process in the atherosclerotic plaque, which leads to disruption of the plaque integrity and subsequent thrombus formation. Further investigation of the mechanisms of CMV effects on atherosclerosis progression may be helpful in developing new approaches to the treatment of CAD.

*This work was supported by a grant of the Ministry of Education and Science of the Russian Federation (o. 14.V25.31.0016).*

*Collaborative research by J.-C. Grivel and L.B. Margolis was supported by an internal program of the U.S. National Institutes of Health.*

REFERENCES

1. Hamm C.V., Murray C.J., Lopez A.D. // Lancet. 1997. V. 349. P. 1498–1504.
2. Hamm C.W., Bassand J.P., Agewall S., Bax J. Boersma E., Bueno H., Caso P., Dudek D., Gielen S., Huber K., et al. // Eur. Heart J. 2011. V. 32. P. 2999–3054.
3. Steg P.G., James S.K., Atar D., Badano L.P., Blömstrom-Lundqvist C., Borger M.A., Di Mario C., Dickstein K., Ducrocq G., Fernandez-Aviles F., et al. // Eur. Heart J. 2012. V. 33. P. 2569–2619.
4. Virchow R. // Cellular pathology. Translation from German. Mocow Medicine, 1859.
5. Galkina E., Ley K. // Annu. Rev. Immunol. 2009. V. 27. P. 165–197.
6. Harja E., Bu D.X., Hudson B.I., Chang J.S., Shen X., Hallam K., Kalea A.Z., Lu Y., Rosario R.H., Oruganti S., et al. // J. Clin. Invest. 2008. V. 118. № 1. P. 183–194.
7. Muller W.A. // Circ. Res. 2009. V. 105. № 3. P. 223–230.
8. Galkina E., Kadl A., Sanders J., Varughese D., Sarembock I.J., Ley K. // J. Exp. Med. 2006. V. 203. № 5. P. 1273–1282.
9. Ait-Oufella H., Taleb S., Mallat Z., Tedgui A. // Arterioscler. Thromb. Vasc. Biol. 2011. V. 31. № 5. P. 969–979.
10. van Berkel T.J., Out R., Hoekstra M., Kuiper J., Biessen E., van Eck M. // Curr. Opin. Lipidol. 2005. V. 16. № 5. P. 525–535.
11. Geng Y.J., Libby P. // Arterioscler. Thromb. Vasc. Biol. 2002. V. 22. № 9. P. 1370–1380.
12. Kruth H.S. // Curr. Opin. Lipidol. 2002. V. 13. № 5. P. 483–491.
13. Zhu J., Nieto F.J., Horne B.D., Anderson J.L., Muhlestein J.B., Epstein S.E. // Circulation. 2001. V. 103. № 1. P. 45–51.
14. Padilla C., Lobos O., Hubert E., Gonzalez C., Matus S., Pereira M., Pereira M., Hasbun S., Descouvieres C. // J. Periodontal Res. 2006. V. 41. № 4. P. 350–353.
15. Rafferty B., Dolgilevich S., Kalachikov S., Morozova I., Ju J., Whittier S., Nowygrod R., Kozarov E. // J. Atheroscler. Thromb. 2011. V. 18. № 1. P. 72–81.
16. Lo J., Abbara S., Shturman L., Soni A., Wei J., Rocha-Filho J.A., Nasir K., Grinspoon S.K. // AIDS. 2010. V. 24. № 2. P. 243–253.
17. Pesonen E., El-Segaier M., Persson K., Puolakkainen M., Sarna S., Ohlin H., Pussinen P.J. // Ther. Adv. Cardiovasc. Dis. 2009. V. 3. № 6. P. 447–454.
18. Roizman B., Pellet P.E. Fields' Virology 5th ed. N.Y.: Lippincott-Williams and Wilkins, 2007. P. 2479–2499.
19. Stowe R.P., Peek M.K., Cutchin M.P., Goodwin J.S. // J. Med. Virol. 2012. V. 84. № 11. P. 1797–1802.
20. Roberts E.T., Haan M.N., Dowd J.B., Aiello A.E. // Am. J. Epidemiol. 2010. V. 172. № 4. P. 363–371.
21. Simanek A.M., Dowd J.B., Pawelec G., Melzer D., Dutta A. // PLoS One. 2011. V. 6. № 2. e16103.

22. Gredmark S., Jonasson L., van Gosliga D., Ernerudh J., Söderberg-Nauclér C. // Scandinavian Cardiovasc. J. 2007. V. 41. P. 230–234.
23. Tomtishen III J.P. // Virology J. 2012. V. 9. P. 22.
24. Ross S.A., Novak Z., Pati S., Boppana S.B. // Infect. Disord. Drug Targets. 2011. V. 11. P. 466–474.
25. Gimeno C., Solano C., Latorre J.C., Hernández-Boluda J.C., Clari M., Remigia M.J., Furió S., Calabuig M., Tormo N., Navarro D. // J. Clin. Microbiol. 2008. V. 46. P. 3311–3318.
26. Thygesen K., Alpert J.S., Jaffe A.S., Simoons M.L., Chaitman B.R., White H.D., Lindahl B., Morrow D.A., Chaitman B.A., Clemmensen P.M., et al. // Eur. Heart J. 2012. V. 33. P. 2551–2567.
27. Montalescot G., Sechtem U., Achenbach S., Andreotti F., Arden C., Budaj A., Bugiardini R., Crea F., Cuisset T., Di Mario C., et al. / / Eur. Heart J. 2013. V. 34. № 38. P. 2949–3003.
28. Lagrand L.K., Visser C.A., Hermens W.T., Niessen H.W., Verheugt F.W., Wolbink G.J., Hack C.E. // Circulation. 1999. V. 100. № 1. P. 96–102.
29. Tanabe K., Tokumoto T., Ishikawa N., Koyama I., Takahashi K., Fuchinoue S. // Transplantation. 1997. V. 64. № 12. P. 1721–1726.
30. Staras S.A., Dollard S.C., Radford K.W., Flanders W.D., Pass R.F., Cannon M.J. // Clin. Infect. Dis. 2006. V. 43. № 9. P. 1143–1151.
31. Ji Y.N., An L., Zhan P., Chen X.H. // Mol. Biol. Rep. 2012. V. 39. № 6. P. 6537–6546.
32. Nieto F.J., Adam E., Sorlie P., Farzadegan H., Melnick J.L., Comstock G.W., Szklo M. // Circulation. 1996. V. 94. № 5. P. 922–927.
33. Ridker P.M., Hennekens C.H., Stampfer M.J., Wang F. // Circulation. 1998. V. 98. № 25. P. 2796–2799.
34. Smieja M., Chong S., Natarajan M., Petrich A., Rainen L., Mahony J.B. // J. Clin. Microbiol. 2001. V. 39. № 2. P. 596–600.
35. Melnick J.L., Petrie B.L., Dreesman G.R., Burek J., McCollum C.H., DeBakey M.E. // Lancet. 1983. V. 2. № 8351. P. 644–651.
36. Ridker P.M., Hennekens C.H., Buring J.E., Kundsin R., Shih J. // Ann. Intern. Med. 1999. V. 131. № 8. P. 573–577.
37. Izadi M., Fazel M., Saadat S.H., Nasseri M.H., Ghasemi M., Dabiri H., Aryan R.S., Esfahani A.A., Ahmadi A., Kazemi-Saleh D., et al. // Cardiovasc. J. 2012. V. 8. № 2. P. 42–46.
38. Nikitskaya E.A., Grivel J.-C., Ivanova O.I., Lebedeva A.M., Shpektor A.V., Margolis L.B., Vasilieva E.Yu. // Creative Cardiology. 2014. № 4. P. 50–62.
39. Ferrante G., Nakano M., Prati F., Niccoli G., Mallus M.T., Ramazzotti V., Montone R.A., Kolodgie F.D., Virmani R., Crea F. // Circulation. 2010. V. 122. № 24. P. 2505–2513.
40. Nakajima T., Goek O., Zhang X., Kopecky S.L., Frye R.L., Goronzy J.J., Weyand C.M. // Circ. Res. 2003. V. 93. № 2. P. 106–113.
41. Liuzzo G., Stephen L., Kopecky S.L., Robert L., Frye, W., O' Fallon M. // Circulation. 1999. V. 100. № 21. P. 2135–2139.
42. Weyand C.M., Goronzy J.J., Liuzzo G., Kopecky S.L., Holmes D.R., Frye R.L. // Mayo Clin. Proc. 2001. V. 76. № 10. P. 1011–1020.
43. Grivel J.-C., Ivanova O., Pinegina N., Blank P.S., Shpektor A., Margolis L.B., Vasilieva E. // Arterioscler. Thromb. Vasc. Biol. 2011. V. 31. № 12. P. 2929–2937.
44. Margolis L. // Am. J. Med. 2015. V. 128. № 6. P. 562–566.

# Inhibition of Poly(ADP-Ribose) Polymerase by Nucleic Acid Metabolite 7-Methylguanine

D. K. Nilov[1,2], V. I. Tararov[3], A. V. Kulikov[4], A. L. Zakharenko[5], I. V. Gushchina[2], S. N. Mikhailov[3], O. I. Lavrik[5], V. K. Švedas[1,2*]

[1]Lomonosov Moscow State University, Belozersky Institute of Physicochemical Biology, Leninskie Gory 1, bldg. 40, Moscow, 119991, Russia

[2]Lomonosov Moscow State University, Faculty of Bioengineering and Bioinformatics, Leninskie Gory 1, bldg. 73, Moscow, 119991, Russia

[3]Engelhardt Institute of Molecular Biology, Russian Academy of Sciences, Vavilov str. 32, Moscow, 119991, Russia

[4]Lomonosov Moscow State University, Faculty of Fundamental Medicine, Lomonosovsky avenue 31-5, Moscow, 119192, Russia

[5]Institute of Chemical Biology and Fundamental Medicine, Russian Academy of Sciences, Siberian Branch, Lavrentiev avenue 8, Novosibirsk, 630090, Russia

*E-mail: vytas@belozersky.msu.ru

Received: 01.12.2015



**ABSTRACT** **The ability of 7-methylguanine, a nucleic acid metabolite, to inhibit poly(ADP-ribose)polymerase-1 (PARP-1) and poly(ADP-ribose)polymerase-2 (PARP-2) has been identified *in silico* and studied experimentally. The amino group at position 2 and the methyl group at position 7 were shown to be important substituents for the efficient binding of purine derivatives to PARPs. The activity of both tested enzymes, PARP-1 and PARP-2, was suppressed by 7-methylguanine with $IC_{50}$ values of 150 and 50 μM, respectively. At the PARP inhibitory concentration, 7-methylguanine itself was not cytotoxic, but it was able to accelerate apoptotic death of BRCA1-deficient breast cancer cells induced by cisplatin and doxorubicin, the widely used DNA-damaging chemotherapeutic agents. 7-Methylguanine possesses attractive predictable pharmacokinetics and an adverse-effect profile and may be considered as a new additive to chemotherapeutic treatment.**

**KEYWORDS** **PARP inhibitors, molecular modeling, docking.**

**ABBREVIATIONS** **PARP – poly(ADP-ribose)polymerase, MD – molecular dynamics.**

## INTRODUCTION

Exposure of a human organism to different stress factors induces genotoxic DNA lesions that should be removed in order to ensure complete and accurate DNA replication and transcription, to avoid genomic instability, and to prevent, for example, cancer formation. Cellular repair pathways involve numerous proteins that recognize and clear DNA base modifications and DNA strand breaks [1]. Poly(ADP-ribose)polymerases (PARP; EC 2.4.2.30) are a group of eukaryotic proteins with diverse functions mainly related to DNA repair and cell death. The most studied PARP family members, PARP-1 and PARP-2, have DNA-damage-dependent enzymatic activity and catalyze the synthesis of poly(ADP-ribose) [2]. The donor of the ADP-ribose unit in the polymer synthesis is the $NAD^+$ molecule, and nicotinamide is released while a glycosidic bond between the units is formed. Binding of the PARP-1 and PARP-2 proteins to damaged DNA results in their poly(ADP-ribosyl)ation and that of the other proteins involved in DNA metabolism [3–6]. This kind of posttranslational modification leads to the activation and assembly of repair systems in the damaged locus of DNA: for example, automodified PARP-1 recruits the base excision repair protein XRCC1 associated with DNA polymerase $\beta$ and DNA ligase III [7–9]. The crucial role of PARP-1 and PARP-2 has been demonstrated by observations that both *parp-1*$^{-/-}$ and *parp-2*$^{-/-}$ mice are more sensitive to ionizing radiation, and *parp-1*$^{-/-}$*parp-2*$^{-/-}$ double mutants die early in development at the onset of gastrulation [10].

The DNA-binding domain (DBD) of PARP-1 is made of specialized zinc fingers, whereas the DBD structure of PARP-2 is unknown and has no sequence homology

with any identified DNA-binding motif. In contrast, the catalytic domains and the active sites of PARP-1 and PARP-2 in the apo form, as well as in a complex with inhibitors, have extensive structural similarity [11,12]. The $NAD^+$ substrate bound in the active site interacts with Gly863 and Tyr907 residues (the numeration is for PARP-1) similar to inhibitors that mimic nicotinamide moiety. The Gly863 backbone forms two hydrogen bonds with the amide group of nicotinamide, while the Tyr907 side chain stacks with the nicotinamide ring [13]. Several known classes of PARP inhibitors are composed of a carbamoyl group attached to an aromatic ring or a lactam group built in an aromatic ring system [14–19], which makes possible the formation of the abovementioned interactions with the Gly863 and Tyr907 residues. Besides compounds competing with $NAD^+$ for the active site, the minor groove binding ligands may also serve as inhibitors that target the DNA-dependent pathway of PARP-1 regulation [20].

The PARP's involvement in DNA repair systems makes this enzyme an attractive target for anticancer therapy. Inhibitors of PARP-1 and PARP-2 may potentiate the effects of various DNA-damaging anticancer drugs, such as cisplatin or doxorubicin. When DNA is moderately damaged, PARPs participate in DNA repair so that cancer cells can survive. The combination of a DNA-damaging agent and PARP-1 or PARP-2 inhibitors can help to overcome drug resistance and promote apoptotic cell death, representing a promising strategy for cancer treatment [15, 21–23]. In addition, the use of inhibitors can exploit DNA repair defects in certain cancer cells. For example, the deficiency in homologous recombination in BRCA1/2-deficient cells makes them acutely sensitive to PARP inhibition [24–26]. Several PARP inhibitors tested as anticancer agents have failed to progress through preclinical or clinical trials because of their toxicity and insufficient efficacy [27–29]. In particular, a well-known PARP-1 inhibitor, 3-aminobenzamide, has a limited cell uptake and affects other metabolic processes. A first-in-class PARP-1 inhibitor, olaparib, was approved by the FDA in December 2014 as treatment for patients with advanced ovarian cancer [30]. This compound is a phthalazine derivative with a lactam group which decreases the enzyme's activity at a nanomolar concentration. Nevertheless, developing effective and non-toxic compounds targeting PARPs and able to suppress the progression of various types of cancers is an important, yet challenging task.

One of the promising classes of PARP inhibitors comprises natural nucleobases and their derivatives which contain a lactam group [31, 32]. However, so far identified compounds (e.g., thymine, hypoxanthine) exert a relatively weak inhibitory effect. In this paper, we report on the results of a computer screening of nucleobase derivatives as PARP inhibitors and *in vitro* studies of the selected compounds.

## EXPERIMENTAL SECTION

### Protein model preparation

The initial model of PARP-1 was built on the basis of the 1efy crystallographic structure of the enzyme complex with inhibitor [33] using the AmberTools 1.2 program package (http://ambermd.org). Hydrogen atoms were added to the protein structure, and then it was solvated by a 12 Å-thick layer of TIP3P water. Chloride ions were added to neutralize the system. To perform the energy minimization of the obtained model, the protein molecule was described by the *ff99SB* force field [34] and the inhibitor molecule was described by *GAFF* parameters [35] calculated automatically. The energy minimization (2,500 steps of the steepest descent algorithm followed by 2,500 steps of the conjugate gradient algorithm) was performed using the Amber 10 package [36] in order to optimize the positions of hydrogen atoms. During the minimization, the heavy atoms of the protein and inhibitor were kept fixed by positional restraints $k(\Delta x)^2$, where the force constant $k$ was 2 kcal/(mol Å$^2$). The inhibitor, water molecules, and chloride ions were removed from the system after the energy minimization to obtain a model for molecular docking.

### Molecular docking

The computer library of natural nucleobase derivatives was prepared with the ACD/ChemSketch program [37]. Molecular docking was performed using the Lead Finder 1.1.14 program [38]. The energy grid map surrounding the active site of the PARP-1 model was calculated, and the library was screened using the genetic search algorithm. A series of 20 independent docking runs was performed for each compound, and the probability of a successful docking $P_{dock}$ was defined as the ratio of the number of successful runs meeting the specified structural criterion to the total number of runs; i.e., $P_{dock} = N_{succ}/20$. The structural criterion was the presence of two hydrogen bonds between the lactam group of a docked compound and the Gly863 residue. Compounds with $P_{dock} \leq 0.8$ were sorted out automatically by a Perl script.

### Molecular dynamics simulation

To include the selected potential inhibitor in the simulation, its parameters, except partial charges, were taken from the *ff99SB* force field. To derive partial charges, the molecular electrostatic potential of the inhibitor was calculated at the HF/6-31G* level of theory with the PC GAMESS/Firefly program [39]. The

fitting of partial atomic charges was done using the RESP method [40]. An equilibration and subsequent 10 ns molecular dynamics (MD) simulation of the PARP-1 in complex with the inhibitor were carried out using AmberTools 1.2 and Amber 10. A model of the complex obtained by molecular docking was solvated by a 12 Å-thick layer of TIP3P water and described by the *ff99SB* force field. The energy minimization using the steepest descent and conjugate gradient algorithms was performed to relax the solvated system. The minimized system was heated up from 0 to 300 K over 50 ps and then equilibrated over 500 ps at 300 K. Finally, a 10 ns trajectory of an equilibrium simulation at constant pressure was calculated. All simulations were performed using periodic boundaries and the Particle Mesh Ewald method to calculate long-range electrostatic interactions.

The VMD 1.8.6 software [41] was used for the visualization of the structures. Parallel computations of the MD trajectory were performed at the Supercomputer Center, Lomonosov Moscow State University [42].

### Synthesis of compounds

7-Methylguanine, 7-methylxanthine, 7-methylhypoxanthine, and 7-ethylguanine were prepared by alkylation of the corresponding nucleosides, followed by N-glycosidic bond cleavage according to the earlier described procedures [43,44].

7-*Methylguanine*. 400 MHz $^1$H NMR (DMSO-$d_6$): δ = 3.82 (s, 3H, Me), 6.03 (brs, 2H, $NH_2$), 7.81 (s, 1H, H-8), 10.66 (brs, 1H, NH).

7-*Methylxanthine*. 400 MHz $^1$H NMR (DMSO-$d_6$): δ = 3.81 (s, 3H, Me), 7.85 (s, 1H, H-8), 10.79 (brs, 1H, NH), 11.48 (brs, 1H, NH).

7-*Methylhypoxanthine*. 400 MHz $^1$H NMR ($CDCl_3$-$CD_3OD$): δ = 3.94 (s, 3H, Me), 7.80 (s, 1H, H-2), 7.84 (s, 1H, H-8).

7-*Ethylguanine*. 400 MHz $^1$H NMR (DMSO-$d_6$): δ = 1.36 (t, 3H, J = 7.2 Hz, $CH_3$), 4.19 (q, 2H, Me, J = 7.2 Hz, $CH_2$), 6.09 (brs, 2H, $NH_2$), 7.90 (s, 1H, H-8), 10.26 (brs, 1H, NH).

### Enzyme assay

Recombinant human PARP-1 and murine PARP-2 proteins were purified as described previously [45, 46]. Reaction of poly(ADP-ribosyl)ation catalyzed by PARP-1 and PARP-2 was performed at optimal conditions for each enzyme [47,48]. Briefly, for PARP-1: 50 mM Tris-HCl pH 8.0, 20 mM $MgCl_2$, 150 mM NaCl, 7 mM β-mercaptoethanol, activated DNA (2 $o.u._{280}$/ml, degree of activation 25%), 300 μM $NAD^+$ (0.18 μCi [$^3$H]$NAD^+$), 37°C. The reaction was started by adding PARP-1 up to a final concentration of 0.2 μM and was stopped after 1 min, placing the reaction mixture on paper filters (Whatman-1) soaked with a 5% solution of trichloroacetic acid. For PARP-2: 50 mM Tris-HCl pH 8.0, 40 mM NaCl, 0.1 mg/ml BSA, 8 mM $MgCl_2$, 1 mM DTT, activated DNA (2 $o.u._{280}$/ml, degree of activation 25%), 400 μM $NAD^+$ (0.4 μCi [$^3$H]$NAD^+$), 37°C. The reaction was started by adding PARP-2 up to a final concentration of 0.2 μM and was stopped after 5 min, placing the reaction mixture on the paper filters. The filters were washed four times by the 5% trichloroacetic acid, then by 90% ethanol (to remove acid), and air-dried. The quantity of radiolabel included into the acid insoluble product was registered on a scintillation counter Tri-Carb 2800 (Perkin Elmer) in a toluene scintillator. The quantity of the radiolabeled product was determined at the initial rate period.

The PARP-inhibiting activity of the synthesized compounds was evaluated in a reaction of auto-poly(ADP-ribosyl)ation at a $NAD^+$ concentration of 0.3 mM for PARP-1 and 0.4 mM for PARP-2. Different concentrations of the tested compounds were added to the reaction mixture before adding the enzyme. Reaction and detection of the products were performed as described above. To determine the $IC_{50}$ value (concentration of the compound required to reduce the enzyme activity by 50%), the effect of different concentrations of the inhibitor on the enzyme activity was examined. Measurements were done in at least two independent experiments. $IC_{50}$ values were calculated using the Origin Pro 8.0 software by nonlinear regression analysis.

### Cytotoxicity assay

The cytotoxic activity of 7-methylguanine, cisplatin, doxorubicin, and their combinations was evaluated by the analysis of cell cycle distribution and measurement of the Sub-G1 population by flow cytometry, as well as by measurement of caspase-3-like activity as a marker of the apoptotic pathway. A BRCA1-deficient human breast cancer line HCC1937 (ATCC CRL-2336) was cultured in DMEM supplemented with 10% heat-inactivated fetal bovine serum, penicillin/streptomycin (100 U/ml), and pyruvate (0,11 mg/ml) at 37°C in 20% $O_2$ humidified atmosphere. The cells were maintained in a logarithmic growth phase for all experiments. After 24 h of culturing, the cells were pretreated with 7-methylguanine (150 μM) for 3 h, followed by addition of either cisplatin (70 μM) or doxorubicin (1 μM).

To perform cell cycle analysis, the cells were then harvested after 72 hours, fixed with 70% EtOH (final concentration) for 60 min on ice, rinsed in PBS, and stained in a 500 μl solution containing 50 μg/ml propidium iodide and 25 μg/ml RNase A for 15 min. Data were acquired by a BD FACS CantoII flow cytometer (BD Biosciences) and analyzed using the FACSDiva software. The cleavage of the fluorogenic

peptide substrate Ac-DNLDAMC was measured using a fluorometric assay. Upon treatment with cytotoxic agents, the cells were incubated for 48 hours, then harvested and washed with PBS. After centrifugation, they were re-suspended in PBS at a concentration of $2 \times 10^6$ cells/100 μl. Then, 25 μl of the suspension was added to a 96-well plate and mixed with a DEVD peptide substrate dissolved in a standard reaction buffer (100 mM HEPES, 10% sucrose, 5 mM DTT, 0.001% NP-40, and 0.1% CHAPS, pH 7.2). Cleavage of the fluorogenic peptide substrate was monitored by AMC liberation in a VarioScan Flash multimode detector (Thermo Scientific) using 380 nm excitation and 460 nm emission wavelengths. Measurements were done in at least two independent experiments.

### Pharmacokinetics and adverse-effect modeling

Pharmacokinetics and adverse-effect profiling of 7-methylguanine was done with ACD/Percepta [49]. This software *in silico* predicts ADME properties (absorption, distribution, metabolism, excretion) and toxicity by QSAR models based on an analysis of similar compounds from the experimental data library. In case of 7-methylguanine, among library compounds were acyclovir, caffeine, theobromine, and theophylline.

## RESULTS AND DISCUSSION

### Virtual screening

A model of PARP-1, the most characterized member of the PARP family, was built on the basis of the crystallographic structure of the catalytic fragment in a complex with the inhibitor (PDB ID 1efy, 2.2 Å resolution). Hydrogen atoms were added taking into account ionization of amino acid side chains, and then their positions were optimized to achieve complementarity to the inhibitor scaffold. A computer library of natural nucleobase derivatives with a lactam structural fragment was prepared comprising nearly a hundred diverse purine and pyrimidine modifications which could be synthesized on a preparative scale. Virtual screening for derivatives able to bind in the active site of the PARP-1 was performed by molecular docking. In order to provide a better sampling of the conformational space, a series of 20 independent docking runs was performed for each compound in the library. Then, we applied the procedure of structural filtration, which allows one to sort out false-positive docking results [47]. As it has been noticed previously, the substrate and the known PARP inhibitors have a common structural feature – their amide (or lactam) group forms two hydrogen bonds with the Gly863 residue. This interaction is apparently crucial for an effective binding in the PARP active site and was used as a criterion for selection of potential inhibitors. Docking poses of compounds meeting the structural criterion were further analyzed for favorable hydrophobic contacts as well as electrostatic interactions in the PARP-1 active site, and the 7-methylguanine molecule ($P_{dock} = 0.95$, $\Delta G^{calc} = -6.8$ kcal/mol) was selected as the most promising PARP inhibitor.

MD simulations were further performed to evaluate the geometric characteristics of 7-methylguanine in the PARP-1 active site and examine the stability of the enzyme-inhibitor complex. The formation of two hydrogen bonds between the lactam group of 7-methylguanine and the Gly863 residue was observed along the MD trajectories as well as the pi stacking of purine rings with the side chain of Tyr907 and the hydrophobic interaction of the methyl group at position 7 with the Ala898 side chain (*Fig. 1*). We also revealed an electrostatic interaction between the amino group of 7-methylguanine at position 2 and the backbone oxygen of Gly263, which appeared to be a non-conventional hydrogen bond. The mean $NH_2$:H···Gly863:O distance was 2.42 Å, and the mean $NH_2$:N···$NH_2$:H···Gly863:O angle 137°, whereas the corresponding distance of a regular hydrogen bond is expected to be 1.8–2.1 Å and the angle not less than 150°. Distance and angle characteristics are presented in *Table 1*.

Interestingly, the structural analogue of 7-methylguanine, namely, 7-methylxanthine, was previously shown to be a moderate inhibitor of PARP-1 [32]. This compound differs from 7-methylguanine by an oxo substituent at position 2 (*Fig. 2*). However, 7-methylxanthine was sorted out by our procedure of structural filtration ($P_{dock} = 0.45$), indicating that its binding has to be less effective. We also docked 7-methylhypoxanthine, analogue with no substituent at position 2, and the predicted binding parameters ($P_{dock} = 0.85$, $\Delta G^{calc} = -6.4$ kcal/mol) were less encouraging, as well. Analysis of the modeled poses demonstrated that the amino group at position 2 can substantially increase the effectiveness of the inhibitor's binding in the PARP active site due to the favorable electrostatic interaction with Gly863. The methyl group at position 7 is another substituent responsible for the complementarity of the inhibitor to the PARP-1 active site, as the unmodified xanthine does not show inhibition [32]. However, the calculated parameters of 7-ethylguanine binding ($P_{dock} = 0.7$, $\Delta G^{calc} = -6.7$ kcal/mol) indicate that the inhibitory effect cannot be further increased with a growing alkyl chain at this position.

### Inhibitory properties of purine derivatives

We synthesized 7-methylguanine, 7-methylxanthine, 7-methylhypoxanthine, and 7-ethylguanine to test their ability to suppress PARP and assess the effect

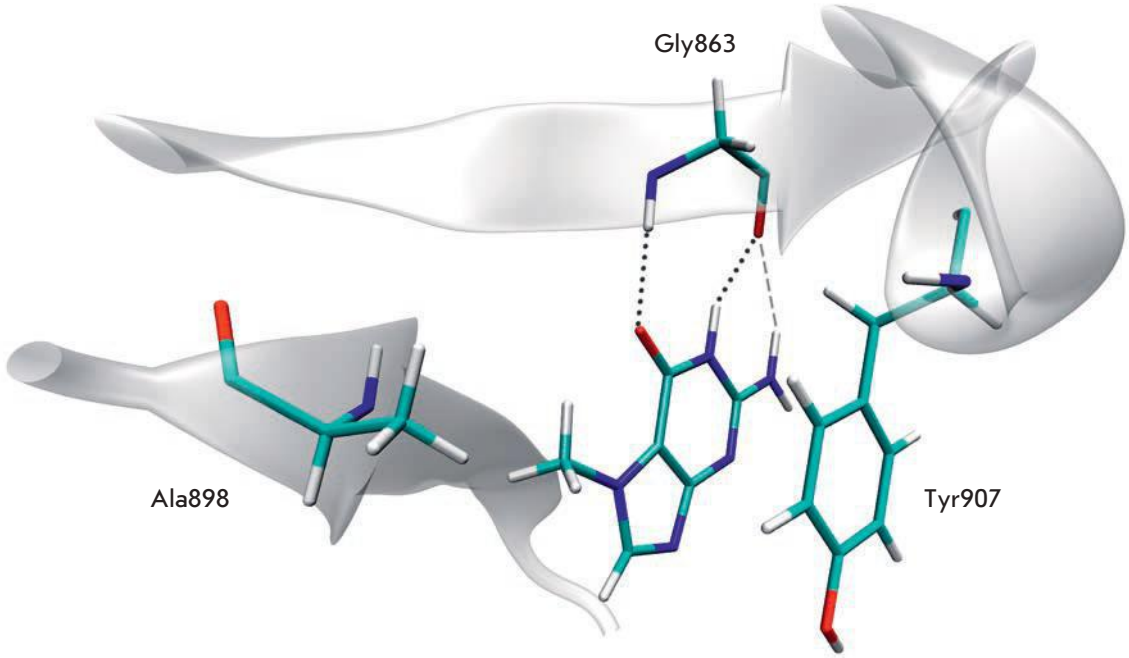


Fig. 1. The position and interactions of the 7-methylguanine molecule in the PARP-1 active site revealed by molecular modeling: two hydrogen bonds of the lactam group with Gly863 shown as dotted lines, an electrostatic interaction of the amino group as dashed line, pi stacking of purine rings with Tyr907, and hydrophobic interaction of the methyl group with Ala898.

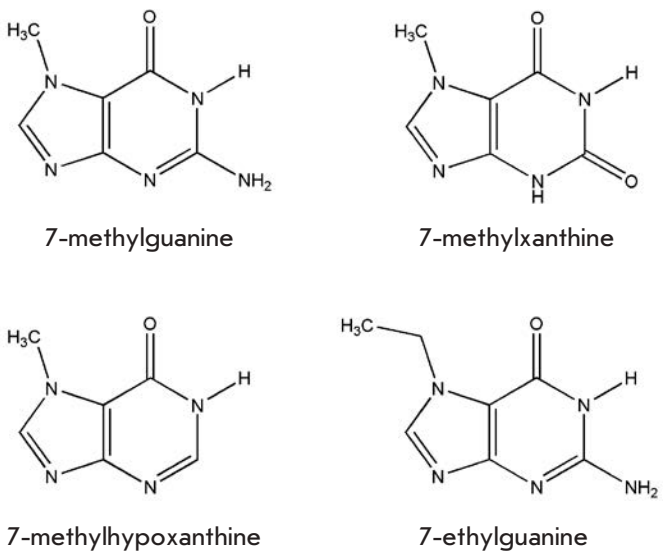


Fig. 2. Chemical structures of the synthesized and tested compounds.

Table 1. Distance and angle characteristics of the position of 7-methylguanine (7-MG) in the PARP-1 active site determined by MD simulations. Mean values are presented together with the standard deviations.

| Distance (Å) | |
|---|---|
| 7-MG:CO:O ··· Gly863:H | 2.0 ± 0.2 |
| 7-MG:NH:H ··· Gly863:O | 1.9 ± 0.1 |
| 7-MG:$NH_2$:H ··· Gly863:O | 2.4 ± 0.4 |
| 7-MG:$CH_3$:C ··· Ala898:CB | 4.0 ± 0.3 |
| *C*(7-MG fused rings) ··· *C*(Tyr907 benzene ring)* | 3.6 ± 0.2 |
| **Angle (deg)** | |
| 7-MG:CO:O ··· Gly863:H ··· Gly863:N | 160 ± 11 |
| 7-MG:NH:N ··· 7-MG:NH:H ··· Gly863:O | 159 ± 9 |
| 7-MG:$NH_2$:N ··· 7-MG:NH:H ··· Gly863:O | 137 ± 10 |

* Distance between the geometric center of 7-methylguanine fused rings and the center of the Tyr907 benzene ring.

of the substituent on the activity of the inhibitor. The inhibitory properties of 7-methylguanine and related compounds were studied using two purified proteins of the PARP family – human PARP-1 and murine PARP-2. Experimental data presented in *Table 2* demonstrate that 7-methylguanine, as predicted, is the most effective inhibitor, with $IC_{50}$ values of 150 and 50 μM for PARP-1 and PARP-2, respectively. Replacement of the 2-oxo group of 7-methylxanthine by the amino group led to a 5- and 3-fold increase in the ability to inhibit PARP-1 and PARP-2. 7-Methylguanine was a more effective inhibitor compared to 7-ethyl-

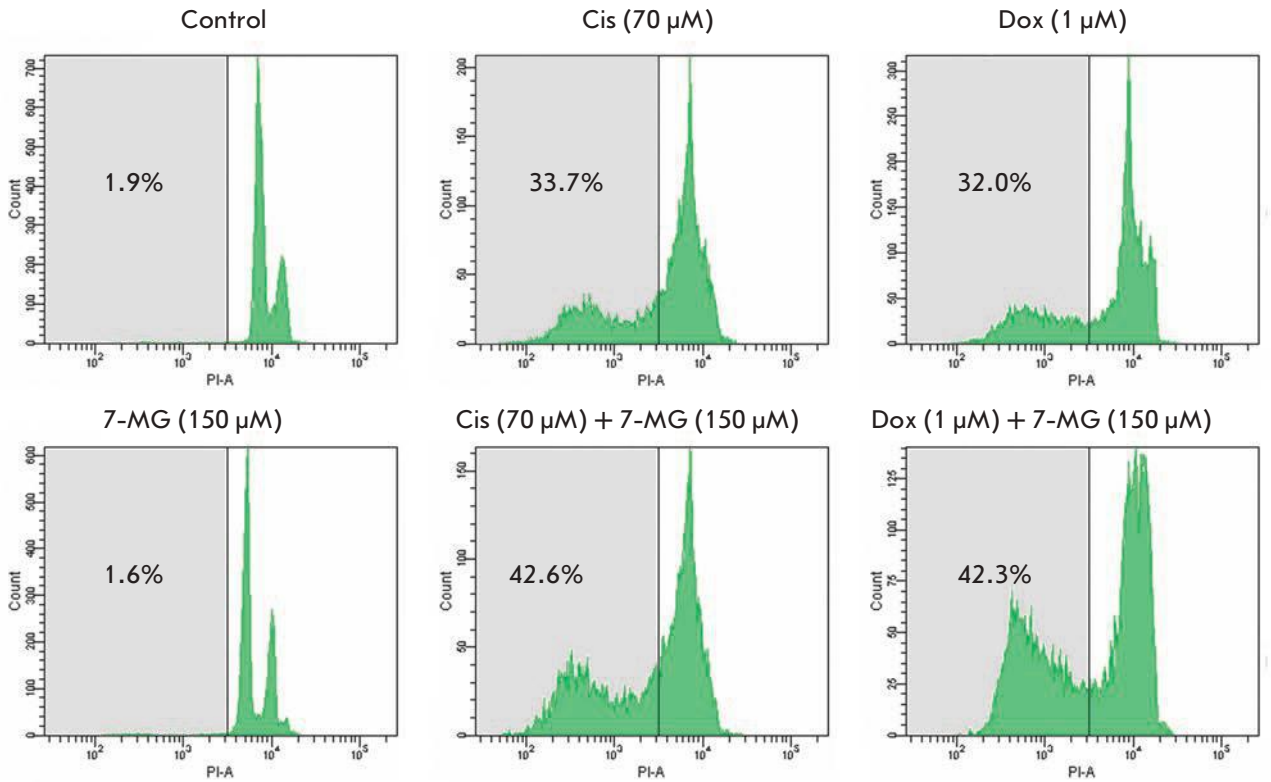


Fig. 3. Estimation of the Sub-G1 population of HCC1937 cells subjected to cisplatin (Cis), doxorubicin (Dox), and 7-methylguanine (7-MG) in single and combined treatment for 72 h. The area of the Sub-G1 population is shown in gray.

guanine, indicating that the methyl group is an optimal alkyl substituent at this position. It is worth mentioning that all tested purine derivatives were more effective inhibitors of PARP-2 despite the very similar organization of the binding sites of both enzymes. We can assume that the reason for this selectivity is the different inhibitor delivery trajectories to the active centers of the PARP proteins.

### Analysis of cytotoxicity

Analysis of cytotoxicity was performed on a human breast cancer line HCC1937, which is thought to be sensitive to the inhibition of PARP due to deficiency in the DNA repair gene BRCA1 [22, 50, 51]. Cell death induced by the conventional anticancer drugs cisplatin and doxorubicin and by 7-methylguanine was estimated by flow cytometry analysis of a Sub-G1 population, which corresponds to an apoptotic cell population with fragmented DNA (*Fig. 3*). Treatment of the cells with 7-methylguanine itself did not increase the cells' number in the Sub-G1 phase (it was around 2%), which was comparable to the control. Comparison of cell death level revealed that 7-methylguanine sensitizes HCC1937 to treatment with cisplatin and doxorubicin. With the exposure of cells to a combination of 7-methylguanine and 70 μM cisplatin, the population of cells in the Sub-G1 phase increased from 34% to 43% and addition of 7-methylguanine to 1 μM doxorubicin increased the Sub-G1 population from 32% to 42%. Thus, the level of cell death elevation at addition of 7-methylguanine was very similar in the cases of cisplatin and doxorubicin.

We also analyzed the activation of caspase-3 in HCC1937 cells, which is an important and obligatory event in the apoptotic cell death program. Active caspase-3 cleaves various cellular molecules, which re-

Table 2. Inhibitory effect of 7-methylguanine and related compounds on PARP-1 and PARP-2.

| | $IC_{50}$ (μM) | |
|---|---|---|
| | PARP-1 | PARP-2 |
| 7-methylguanine | 150 | 50 |
| 7-methylxanthine | 800 | 160 |
| 7-methylhypoxanthine | 780 | 620 |
| 7-ethylguanine | 230 | 90 |

sults in apoptotic morphology of cells. Thus, the degree of caspase-3 activation, measured by cleavage of the specific fluorogenic substrate, corresponds to the level of apoptotic cell death. *Figure 4* demonstrates that stimulation of caspase-3 activity was increased by the addition of 7-methylguanine to either cisplatin or doxorubicin by 27–39%, whereas 7-methylguanine alone demonstrated no caspase-3 activation. These data are in agreement with cell death induction observed by flow cytometry.

### Pharmacokinetics and adverse-effect profiling

Finally, we evaluated the pharmacokinetic properties and adverse-effect profile of 7-methylguanine using QSAR models based on literature data on its structural analogues (acyclovir, caffeine, theobromine, theophylline, etc.). In particular, human intestinal permeability was estimated to be very high, and the oral bioavailability was predicted to be optimal (83%). The calculated plasma protein bound fraction of 7-methylguanine was 17%, which should not considerably affect its efficiency. It is unlikely that 7-methylguanine binds to estrogen receptor alpha (no risk of reproductive toxicity), hERG potassium ion channel (no risk of cardiotoxicity), P-glycoprotein efflux transporter, and cytochrome P450 enzymes (CYP3A4, CYP2D6, CYP2C9, CYP2C19, CYP1A2). Thus, the predicted properties provide evidence of the safety and efficacy of 7-methylguanine for humans.

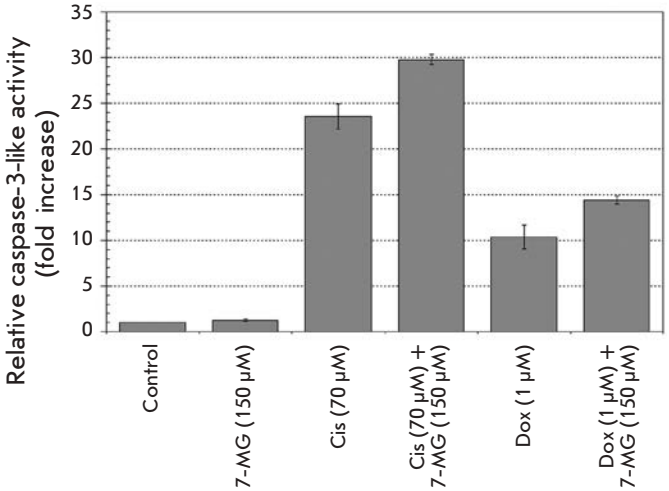


Fig. 4. Estimation of caspase-3-like activity in HCC1937 cells subjected to cisplatin (Cis), doxorubicin (Dox), and 7-methylguanine (7-MG) in single and combined treatment for 48 h.

## CONCLUSIONS

Despite the ability of DNA-damaging drugs to kill cancer cells, resistance to chemotherapy and drug toxicity remain serious problems. DNA repair systems involving PARP-1 and PARP-2 play an important role in the normal development of the organism, but in anticancer treatment with DNA-damaging agents these proteins may decrease the therapeutic effect. A nucleic acid metabolite 7-methylguanine was identified *in silico* as a novel inhibitor of PARP catalytic activity and studied experimentally. Two structural features of purine derivatives were shown to be important for efficient binding - the amino group at position 2 and the methyl group at position 7. At PARP inhibitory concentration, 7-methylguanine itself was not cytotoxic but able to sensitize BRCA1-deficient breast cancer cells to commonly used chemotherapeutic agents (cisplatin and doxorubicin). 7-Methylguanine is a nucleic acid metabolite observed in human serum and excreted in urine [52]. Despite the fact that 7-methylguanine is a weaker inhibitor than olaparib and some other PARP inhibitors, we believe that this natural compound possesses better pharmacokinetics and an adverse-effect profile compared to synthetic inhibitors and may be considered as a promising new constituent of anticancer therapy.

*This work was supported by the Russian Ministry of Education and Science (State agreement № 14.604.21.0018, ID RFMEFI60414X0018). The chemical synthesis of purines was supported by the Russian Foundation for Basic Research (grant 14-04-00835_a).*

REFERENCES

1. Cline S.D., Hanawalt P.C. // Nat. Rev. Mol. Cell Biol. 2003. V. 4. P. 361–373.
2. Drenichev M.S., Mikhailov S.N. // Nucleosides Nucleotides Nucleic Acids. 2015. V. 34. P. 258–276.
3. Lautier D., Lagueux J., Thibodeau J., Ménard L., Poirier G.G. // Mol. Cell. Biochem. 1993. V. 122. P. 171–193.
4. Schreiber V., Dantzer F., Ame J.-C., de Murcia G. // Nat. Rev. Mol. Cell Biol. 2006. V. 7. P. 517–528.
5. Hassa P.O., Haenni S.S., Elser M., Hottiger M.O. // Microbiol. Mol. Biol. Rev. 2006. V. 70. P. 789–829.
6. Hassler M., Ladurner A.G. // Curr. Opin. Struct. Biol. 2012. V. 22. P. 721–729.
7. Masson M., Niedergang C., Schreiber V., Muller S., Menissier-de Murcia J., de Murcia G. // Mol. Cell. Biol. 1998. V. 18. P. 3563–3571.
8. Ryu K.W., Kim D.-S., Kraus W.L. // Chem. Rev. 2015. V. 115. P. 2453–2481.

9. Cazzalini O., Donà F., Savio M., Tillhon M., Maccario C., Perucca P., Stivala L.A., Scovassi A.I., Prosperi. E. // DNA Repair (Amst.). 2010. V. 9. P. 627–635.
10. Ménissier de Murcia J., Ricoul M., Tartier L., Niedergang C., Huber A., Dantzer F., Schreiber V., Amé J.C., Dierich A., LeMeur M. et al. // EMBO J. 2003. V. 22. P. 2255–2263.
11. Ruf A., Mennissier de Murcia J., de Murcia G., Schulz G.E. // Proc. Natl. Acad. Sci. USA. 1996. V. 93. P. 7481–7485.
12. Karlberg T., Hammarström M., Schütz P., Svensson L., Schüler H. // Biochemistry. 2010. V. 49. P. 1056–1058.
13. Ruf A., de Murcia G., Schulz G.E. // Biochemistry. 1998. V. 37. P. 3893–3900.
14. Banasik M., Komura H., Shimoyama M., Ueda K. // J. Biol. Chem. 1992. V. 267. P. 1569–1575.
15. Jagtap P., Szabó C. // Nat. Rev. Drug Discov. 2005. V. 4. P. 421–440.
16. Ferraris D.V. // J. Med. Chem. 2010. V. 53. P. 4561–4584.
17. Ekblad T., Camaioni E., Schüler H., Macchiarulo A. // FEBS J. 2013. V. 280. P. 3563–3575.
18. Efremova A.S., Zakharenko A.L., Shram S.I., Kulikova I.V., Drenichev M.S., Sukhanova M.V., Khodyreva S.N., Myasoedov N.F., Lavrik O.I., Mikhailov S.N. // Nucleosides Nucleotides Nucleic Acids. 2013. V. 32. P. 510–528.
19. Ekblad T., Lindgren A.E.G., Andersson C.D., Caraballo R., Thorsell A.-G., Karlberg T., Spjut S., Linusson A., Schüler H., Elofsson M. // Eur. J. Med. Chem. 2015. V. 95. P. 546–551.
20. Kirsanov K.I., Kotova E., Makhov P., Golovine K., Lesovaya E.A., Kolenko V.M., Yakubovskaya M.G., Tulin A.V. // Oncotarget. 2014. V. 5. P. 428–437.
21. Cepeda V., Fuertes M.A., Castilla J., Alonso C., Quevedo C., Soto M., Pérez J.M. // Recent Pat. Anticancer Drug Discov. 2006. V. 1. P. 39–53.
22. Martin S.A., Lord C.J., Ashworth A. // Curr. Opin. Genet. Dev. 2008. V. 18. P. 80–86.
23. Brock W.A., Milas L., Bergh S., Lo R., Szabó C., Mason K.A. // Cancer Lett. 2004. V. 205. P. 155–160.
24. Curtin N.J., Szabo C. // Mol. Aspects Med. 2013. V. 34. P. 1217–1256.
25. Farmer H., McCabe N., Lord C.J., Tutt A.N.J., Johnson D.A., Richardson T.B., Santarosa M., Dillon K.J., Hickson I., Knights C., et al. // Nature. 2005. V. 434. P. 917–921.
26. Boerner J.L., Nechiporchik N., Mueller K.L., Polin L., Heilbrun L., Boerner S.A., Zoratti G.L., Stark, K., LoRusso, P.M., Burger, A. // PLoS One. 2015. V. 10. P. e0119614.
27. Milam K.M., Cleaver J.E. // Science. 1984. V. 223. P. 589–591.
28. Mateo J., Ong M., Tan D.S.P., Gonzalez M.A., de Bono J.S. // Nat. Rev. Clin. Oncol. 2013. V. 10. P. 688–696.
29. Madison D.L., Stauffer D., Lundblad J.R. // DNA Repair (Amst.). 2011. V. 10. P. 1003–1013.
30. Frampton J.E. // BioDrugs. 2015. V. 29. P. 143–150.
31. Virág L., Szabó C. // FASEB J. 2001. V. 15. P. 99–107.
32. Geraets L., Moonen H.J.J., Wouters E.F.M., Bast A., Hageman G.J. // Biochem. Pharmacol. 2006. V. 72. P. 902–910.
33. White A.W., Almassy R., Calvert A.H., Curtin N.J., Griffin R.J., Hostomsky Z., Maegley K., Newell D.R., Srinivasan S., Golding B.T. // J. Med. Chem. 2000. V. 43. P. 4084–4097.
34. Hornak V., Abel R., Okur A., Strockbine B., Roitberg A., Simmerling C. // Proteins. 2006. V. 65. P. 712–725.
35. Wang J., Wolf R.M., Caldwell J.W., Kollman P.A., Case D.A. // J. Comput. Chem. 2004. V. 25. P. 1157–1174.
36. Case D.A., Darden T.A., Cheatham T.E., III, Simmerling C.L., Wang J., Duke R.E., Luo R., Crowley M., Walker R.C., Zhang W., et al. // AMBER 10. University of California, San Francisco. 2008.
37. ACD/ChemSketch Freeware, version 8.17. Advanced Chemistry Development, Inc., http://www.acdlabs.com. 2005.
38. Stroganov O.V., Novikov F.N., Stroylov V.S., Kulkov V., Chilov G.G. // J. Chem. Inf. Model. 2008. V. 48. P. 2371–2385.
39. Granovsky A.A. Firefly, version 7.1.F, http://classic.chem.msu.su/gran/firefly/index.html. 2009.
40. Bayly C.I., Cieplak P., Cornell W.D., Kollman P.A. // J. Phys. Chem.; 1993. V. 97. P. 10269–10280.
41. Humphrey W., Dalke A., Schulten K. // J. Mol. Graph. 1996. V. 14. P. 33–38.
42. Voevodin Vl.V., Zhumatiy S.A., Sobolev S.I., Antonov A.S., Bryzgalov P.A., Nikitenko D.A., Stefanov K.S., Voevodin Vad.V. // Open Systems J. (Mosc.). 2012. V. 7. P. 36–39.
43. Jones J.W., Robins R.K. // J. Am. Chem. Soc. 1963. V. 85. P. 193–201.
44. Vidal A., Giraud I., Madelmont J.-C. // Synth. Commun. 2004. V. 34. P. 3359–3365.
45. Sukhanova M.V., Khodyreva S.N., Lavrik O.I. // Biochemistry (Mosc.). 2004. V. 69, P. 558-568.
46. Amé J.C., Rolli V., Schreiber V., Niedergang C., Apiou F., Decker P., Muller S., Höger T., Ménissier-de Murcia J., de Murcia G. // J. Biol. Chem. 1999. V. 274. P. 17860–17868.
47. Zakharenko A.L., Sukhanova M.V., Khodyreva S.N., Novikov F.N., Stroylov V.S., Nilov D.K., Chilov G.G., Švedas V.K., Lavrik O.I. // Mol. Biol. (Mosc.). 2011. V.45. P. 517-521.
48. Kutuzov M.M., Khodyreva S.N., Amé J.-C., Ilina E.S., Sukhanova M.V., Schreiber V., Lavrik O.I. // Biochimie. 2013. V. 95. P. 1208–1215.
49. ACD/Percepta. Advanced Chemistry Development, Inc., http://www.acdlabs.com. 2012.
50. Benafif S., Hall M. // Onco Targets Ther. 2015. V. 8. P. 519–528.
51. Helleday T. // Mol. Oncol. 2011. V. 5. P. 387–393.
52. Topp H., Sander G., Heller-Schöch G., Schöch G.. // Anal. Biochem. 1987. V. 161. P. 49–56.

# A Fusion Protein Based on the Second Subunit of Hemagglutinin of Influenza A/H2N2 Viruses Provides Cross Immunity

L. A. Stepanova*, M. V. Sergeeva, M. A. Shuklina, A. A. Shaldzhyan, M. V. Potapchuk, A. V. Korotkov, L. M. Tsybalova
Research Institute of Influenza, Prof. Popova Str. 15/17, 197376, St. Petersburg, Russia
*E-mail: stepanoval60@mail.ru
Received 21.09.2015


**ABSTRACT** **Conserved fragments of the second subunit of hemagglutinin (HA2) are of great interest for the design of vaccine constructs that can provide protective immunity against influenza A viruses of different subtypes. A recombinant fusion protein, FlgMH, was constructed on the basis of flagellin and a highly conserved HA2 fragment (35–107) of influenza viruses of the subtype A/H2N2, containing B cell, CD4+ T cell, and CD8+ T cell epitopes. The native conformation of the HA2 fragment was partially preserved upon its attachment to the C-terminus of flagellin within the recombinant fusion protein FlgMH. FlgMH was shown to stimulate a mixed Th1/Th2 response of cross-reactive antibodies, which bind to influenza viruses of the first phylogenetic group (H1, H2, H5), to the target sequence as well as the induction of specific cytotoxic T cells (CD3+CD8+IFNγ+). Immunization with the recombinant protein protected animals from a lethal influenza infection. The developed FlgMH protein is a promising agent that may be included in an influenza vaccine with a wide spectrum of action which will be able to stimulate the T and B cell immune responses.**
**KEYWORDS** **vaccine, influenza, HA2, recombinant protein, flagellin.**
**ABBREVIATIONS** **HA2 – second subunit of hemagglutinin; Flg – flagellin; FlgMH – fusion protein comprising flagellin and a conserved HA2 fragment of influenza viruses A/H2N2; BAL – bronchoalveolar lavage; ELISA – enzyme-linked immunosorbent assay; OD – optical density; GMT – geometric mean titer; TLR5 – Toll-like receptor 5; MHC – major histocompatibility complex.**

## INTRODUCTION

Virus-neutralizing antibodies prevent infection by blocking the attachment of the influenza virus to the cell surface. These antibodies are mainly targeted at immunodominant epitopes of the first highly variable subunit of hemagglutinin (HA1). The narrow specificity of neutralizing antibodies makes existing vaccines ineffective against circulating influenza virus variants and against emerging viruses with a pandemic potential. T cell immunity significantly contributes to viral clearance and facilitates a mild infection. Therefore, vaccines inducing not only humoral, but also T cell responses are desirable for a better control of an influenza infection. The development of vaccines based on conserved antigens that enhance both the humoral and cellular responses is a universal strategy to control epidemics or pandemics.

Influenza virus hemagglutinin is a polypeptide synthesized as a precursor (HA0) that is trimerized in the endoplasmic reticulum and transported via the Golgi apparatus to the cell surface. Hemagglutinin (HA0) is post-translationally cleaved by host proteases into two subunits, HA1 and HA2, that remain linked by one disulfide bridge [1]. Unlike HA1, the second subunit of hemagglutinin (HA2) has a relatively conserved sequence among viral strains and is responsible for the fusion of the viral and cell membranes in endosomes, thereby ensuring entry of the ribonucleic complex into the cytoplasm [2].

Immunization with traditional vaccines and natural influenza infection do not lead to the formation of a significant amount of anti-HA2 antibodies, which is associated with the low immunogenicity of the HA2 stalk region in the presence of immunodominant receptor-binding regions of HA1 [3]. However, a number of monoclonal antibodies (mouse, human) have been recently isolated that interact with epitopes localized in the HA stalk. These are cross-reactive antibodies that neutralize influenza virus subtypes within the phylogenetic group, thereby providing a wide range of protection [4–11].

Monoclonal antibodies specific to the 1–38 (CF2) and 125–175 (FE1) HA2 regions are capable of *in vitro* inhibiting the fusogenic activity of the influenza A virus.

Intravenous administration of CF2 and FE1 monoclonal antibodies 2 h before infection of Balb/c mice with homologous and heterologous influenza viruses A/H3N2 at the $1LD_{50}$ dose provided 100% survival of animals [6]. The monoclonal antibody CR6261 specific to the hydrophobic pocket of the HA2 stalk inhibited pH-induced conformational change in HA of the A/H1N1 and A/H5N1 influenza viruses and had a neutralizing activity [4, 5]. The monoclonal antibody CR6261 was shown to interact predominantly with the HA2 α-helix, as well as with the adjacent amino acid residues of HA1 and HA2. Most amino acids in the small α-helix of HA2, which interact with CR6261, are identical by more than 99% (differences in 1–5 amino acid residues) within influenza virus subtypes of the first phylogenetic group. The monoclonal antibody CR6261 prevented a transition of HA to the post-fusogenic conformation at low pHs; i.e., it neutralized the virus through stabilization of the pre-fusogenic state and prevention of the pH-dependent fusion of the viral and cell membranes. The anti-H3N2 monoclonal antibody 12D1that interacts with the large, highly conserved α-helix (residues 76–106) of HA2 has a neutralizing ability and bounds to the A/H3N2 influenza viruses that circulated from 1968 to 2003 [8].

In recent years, a number of potential vaccines on the basis of HA2 of influenza A viruses from the phylogenetic group II have been developed [12–14]. The immunogenicity and efficacy of the vaccines in protecting from infection with lethal doses of homologous and heterologous viruses of one phylogenetic group have been demonstrated. The design of the antigen inducing an immune response to HA2 conserved epitopes may provide the basis for a broad-spectrum vaccine possessing prophylactic and therapeutic efficacy.

The aim of this work was to model and generate a recombinant fusion protein comprising the promising T and B cell epitopes of HA2 of the influenza viruses A/H2N2 and to study the immunogenicity and protective action of the protein. Flagellin, a mucosal adjuvant that enhances the immune response to attached antigens, was chosen as the basis for the fusion protein.

## MATERIALS AND METHODS

### Selection of a conserved HA2 region of the influenza A/H2N2 viruses

The search for amino acid sequences for analysis was carried out in the GenBank database; alignments were performed using the Vector NTI v10.0 software (Invitrogen, USA). The search for possible T cell epitopes was conducted using the NetCTLpan 1.1 Server [15] and default search parameters. The search for experimental B and CD4+ T cell epitopes homologous to HA2 fragments was performed in the Immune Epitope Database [16]. The three-dimensional structure of proteins was visualized using a Chimera 1.5.3 program [17]. A Phyre2 open web resource was used for primary sequence homology simulation of the three-dimensional protein structure [18].

### Construction of expression vectors and generation of *Escherichia coli* host expression

The nucleotide sequence encoding the recombinant fusion protein FlgMH was optimized for expression in *E. coli*, synthesized, and inserted into the pQE30 vector at the BamHI and HindIII restriction sites. To generate Flg (flagellin) and MH (hemagglutinin fragment) proteins, the appropriate nucleotide sequences were amplified using primers carrying the terminal restriction sites BamHI and HindIII and then inserted into the multicloning site of the pQE30 vector. DLT1270 *E. coli* cells were transformed with the pQE30/FlgMH, pQE30/MH, and pQE30/Flg plasmids to generate strains producing recombinant proteins. The DLT1270 strain, a derivative of the DH10B strain [19], contained the *lacI* lactose operon repressor gene integrated into the chromosome.

### Isolation and purification of recombinant proteins

DLT1270 *E. coli* strains transformed with the pQE30/FlgMH, pQE30/Flg, and pQE30/MH vectors were cultured in LB medium supplemented with ampicillin. Expression was induced by adding 1 mM IPTG. Cells were treated with lysozyme, and recombinant proteins were purified from the cell lysate using metal affinity chromatography on a Ni-sorbent.

### Electrophoresis and immunoblotting

Polyacrylamide gel electrophoresis (PAGE) under denaturing conditions was carried out according to the Laemmli method [20]. Samples were mixed with a loading buffer containing β-mercaptoethanol, boiled for 7 min, and loaded into 8–16% gradient PAG. Electrophoresis was performed at 10–12 mA for 1.5 h. The gel was fixed in 10% acetic acid and then stained with Coomassie G-250 for 18 h.

Horizontal transfer of the proteins from polyacrylamide gel to a nitrocellulose membrane (BioRad, USA) was performed in TB-buffer (0.03 M glycine, 0.04 M Tris, 0.037% sodium dodecyl sulfate, 20% ethanol) using a Mini Trans-Blot cell system (BioRad, USA) in a chilled chamber at +4°C and a constant current of 200 mA for 1.5 h. The membrane was then blocked in a 3% bovine serum albumin (BSA) solution (Amresco, EU) in phosphate-buffered saline (PBS) at room temperature overnight. The membrane was incubated with primary antibodies diluted in PBS with 0.1% Tween

20 (PBST) and 3% BSA at room temperature for 1 h and then washed in PBST. Flagellin was stained with rabbit polyclonal antibodies (Abcam, UK) at a 1 : 16,000 dilution. A hemagglutinin fragment was stained with cross-specific serum, which was produced by triple sequential immunization of mice with sublethal doses of influenza A viruses of the phylogenetic group I (H2, H5, and H1pdm), at a 1 : 2,000 dilution. Proteins were detected by staining the membrane with secondary antibodies labeled with horseradish peroxidase (goat anti-rabbit IgG or goat anti-mouse IgG, Invitrogen, USA) at a 1 : 2,000 dilution at room temperature for 1 h and then incubated with a tetramethylbenzidine (TMB) immunoblot substrate solution (Invitrogen, USA) for 15 min.

### Immunization of mice

The FlgMH recombinant protein immunogenicity was studied in linear mice Balb/c and C57Bl/6 (females, age of 6–8 weeks, weight of 18–20 g) received from the Stolbovaya mouse farm of the State Scientific Center of Biomedical Technologies of the Russian Academy of Medical Sciences. The animals were kept at the vivarium of the Research Institute of Influenza in accordance with working regulations. Mice (16 animals) were intranasally immunized with the recombinant protein FlgMH (after inhalation anesthesia with 2–3% isoflurane, 30% $O_2$, 70% $N_2O$) at a dose of 10 μg/mouse in a volume of 50 μL three times with a two-week interval. Control mice (16 animals) were intranasally administered the recombinant protein Flg at a dose of 10 μg/mouse three times with a two-week interval.

### Collection of sera and BAL

Blood samples were obtained from five mice from the experimental and control groups 2 weeks after the last immunization, following euthanasia in a $CO_2$-chamber (Vet Tech Solutions, UK). To obtain serum, blood samples were incubated at 37 °C for 30 min. After blood clot formation, the samples were placed on ice and cooled for 1 h, followed by centrifugation at 400*g* for 15 min. Serum aliquots (30 μL) from five mice of each group were frozen at −20°C.

Bronchoalveolar lavages (BALs) were obtained from five mice of each group 2 weeks after the last immunization of the animals, following euthanasia in the $CO_2$-chamber. An animal's corpse was fixed on the operating table, with the belly up. A skin incision was made along the midline, starting from the mandible. A catheter was inserted into the lower portion of the trachea to a depth of 3–5 mm towards the lungs. The bronchi and lungs were washed twice with 1 mL of PBS. BAL was centrifuged at 400*g* for 15 min. The supernatant was aliquoted and frozen at −20°C.

### Collection of mouse splenocytes

Mouse splenocytes were prepared according to the BD Pharmingen™ protocol. Mice from the experimental and control groups (three mice from each group) were euthanized using the $CO_2$-chamber on the 14th day after the last immunization. Mouse spleens were removed aseptically, homogenized using a Medimachine (BD Biosciences, USA), and purified from cell debris by filtration through a syringe filter with a 70 μm pore size (Syringe Filcons, BD Biosciences, USA). Erythrocytes were lysed with ACK lysing buffer (0.15 M $NH_4Cl$, 1.0 M $KHCO_3$, 0.1 mM $Na_2EDTA$, pH 7.2–7.4); splenocytes were washed with a complete RPMI-1640 medium with 10% FBS, 2 mM *L*-glutamine, 100 U/mL penicillin, and 100 μg/mL streptomycin. Cell viability was assessed by staining with a 0.4% trypan blue solution. The cell concentration was adjusted to $2 \times 10^6$ cells/mL.

### Synthetic peptides

The immunogenicity of recombinant proteins was evaluated using the following synthetic peptides synthesized by Verta (Russia):

G-47 (24 amino acids): AADKESTQKAFDGITNKVNSVIEK, the small α-helix (35–58) of HA2; G-48 (15 amino acids): MNTQFEAVGKEFSNL, an unfolded "linker" segment (59–72) of HA2 in native hemagglutinin; G-49 (34 amino acids): ERRLENLNKKMEDGFLDVWTYNAELLVLMENERT, a fragment of the large α-helix (73–107) of HA2.

### Enzyme-linked immunosorbent assay

ELISA was performed according to a conventional method. 96-well plates with a high sorption capacity (Greiner, Germany) were coated with the recombinant protein FlgMH at a concentration of 5 μg/mL or purified viruses A/Singapore/1/57 (H2N2), A/PR/8/34 (H1N1), A/Aichi/1/68 (H3N2), A/Kurgan/05/2005/RG (H5N1) at a concentration of 2 μg/mL; sorption was performed in PBS, pH 7.2, at 4°C overnight. After virus sorption, parts of the plates were immersed in citrate buffer (pH 5.0) for 30 min and then washed once by PBS. Plates were treated with blocking buffer (0.01 M PBS with 5% FBS, pH 7.2) at room temperature for 1 h and washed 3 times with PBST. Plate wells were filled with 100 μL of two-fold dilutions of sera (starting with 1 : 400) in blocking buffer and incubated at room temperature for 1 h. Polyclonal HRPO-labelled goat anti-mouse IgG, IgG1, IgG2a, IgG2b, IgG3, and IgA antibodies (Abcam, UK) a 1 : 20,000 dilution were used. TMB (BD Bioscience, USA) was used as a substrate; the incubation time was 15 min. The optical density (OD) was measured using the i-Mark microplate reader (Bio-Rad) at a wavelength of 450 nm. The maximal se-

rum dilution that had an optical density at least 2 times higher than the double mean value of the blank was taken as the titer.

### Flow cytometry

Multiparameter flow cytometry was performed according to the BD Pharmingen™ protocol. The ability of the G-47, G-48, and G-49 synthetic peptides and the influenza virus A/Singapore/1/57 (H2N2) to activate the production of IFN-γ by specific CD8+ T cells in the spleen was determined. Splenocytes of Balb/c and C57Bl/6 mice were obtained on the 14th day after the last immunization; $2 \times 10^6$ of splenocytes from mice of the experimental and control groups were stimulated (at 37°C for 6 h) with 10 μg of the G-47, G-48, and G-49 peptides or 1 μg of the virus A/Singapore/1/57 (H2N2) in the presence of brefeldin A (1 μg/mL) (BD Bioscience, USA). Cells were washed, and Fc-receptors were blocked by CD16/CD32 antibodies (Mouse BD Fc Block, BD Pharmingen, USA) and stained with anti-CD3a-FITC and anti-CD8-PerCP (BD Pharmingen, USA), at 4°C for 30 min. Then, the cells were permeabilized in accordance with the Cytofix/Cytoperm Plus kit protocol (BD Bioscience, USA) and stained with anti-IFN-γ-PE antibodies (BD Pharmingen, USA). The fluorescence intensity was measured on a BD FACS Canto II flow cytometer (Becton Dickinson, USA). Results were analyzed using the BD FACSDiva v6.1.3 (BD Bioscience, USA) software.

### Viruses and infection of mice

We used strains received from the Collection of influenza and ARD viruses of the Laboratory of Evolutionary Variability of Influenza Viruses of the Research Institute of Influenza: A/Singapore/1/57 (H2N2), A/PR/8/34 (H1N1), A/Aichi/2/68 (H3N2), and A/Kurgan/05/2005/RG (H5N1). In experiments with lethal infection, we used a variant of the influenza A/Singapore/1/57 (H2N2) virus adapted to reproduce in the mouse lungs that was produced at the Laboratory of Influenza Vaccines of the Research Institute of Influenza. Viruses were accumulated in 10- to 12-day-old chicken embryos and purified by ultracentrifugation in a sucrose gradient.

Immunized mice (11 mice each from the experimental and control groups) were infected with the mouse-adapted influenza virus A/Singapore/1/57 (H2N2) at a $2LD_{50}$ dose. The virus was administered intranasally in a volume of 50 μL per mouse after inhalational anesthesia (2–3% isoflurane, 30% $O_2$, 70% $N_2O$). After infection, the animals were subjected to everyday monitoring. The protective effect of FlgMH was evaluated based on two parameters: dynamics of body weight loss and survival of mice after infection.

### Statistical processing

Statistical data processing was carried out using the GraphPad Prizm v5.1 program. The statistical significance of antibody titer differences was evaluated using the nonparametric Mann-Whitney test. Comparison of survival rates was performed using the Mantel-Cox test. The differences were considered significant at $p < 0.05$.

## RESULTS AND DISCUSSION

### Construction of the MH-fragment of the HA2 consensus sequence of the influenza virus A/H2N2

Two highly conserved fragments, (1–24) and (89–104), were found in the alignment of consensus sequences of HA2 (*Fig. 1A*). The identity of the first fragment was 78.3%, but the fragment contained a highly hydrophobic HA fusion peptide prone to aggregation. Although the second fragment was less conserved (62.5%), the majority of its amino acid substitutions were not associated with changes in the physicochemical properties of side chains, which gives hope for a small change in the ability to be presented in certain HLA alleles. Furthermore, the conserved sequence YNAELLVL, which is a part of this fragment, was found in most B and CD4+ T epitopes in HA2 (*Fig. 2A*). The H3 and H7 sequences (phylogenetic group II) were the most differentianted from the consensus sequence; their exclusion increased the fragment identity to 87.5%. A fragment of the HA2 consensus sequence of human influenza viruses A/H2N2 (phylogenetic group I) was chosen for construction of the target recombinant fusion protein.

The fusion protein included the conserved HA2 fragment (89–104), as well as the small α-helix (35–58) of HA2, which was exposed to the trimer surface and was potentially available for binding to antibodies (*Fig. 1B*). To preserve the tertiary structure, the fusion protein FlgMH included a continuous HA2 fragment (35–107).

The HA2 fragment (35–107) of human H2 influenza viruses has the highest amino acid composition homogeneity. The most variable amino acid (occurrence of 58.3%) was arginine (R) at position 75 (position 415 in the HA0 numbering), with lysine (K) occurring in this position in 41.7% of the cases. Both amino acids were positively charged, but the arginine side chain was larger; therefore, it is preferable to provoke a humoral immune response (*Fig. 1B*).

Furthermore, the HA2 sequence (35–107) contained fragments homologous to experimental B and CD4+ T cell epitopes present in the IEDB database (*Fig. 2A*). The theoretical search revealed the presence of multiple potential CD8+ T cell epitopes in the HA2 fragment (35–107) for a representative set of alleles (*Fig. 2B*).

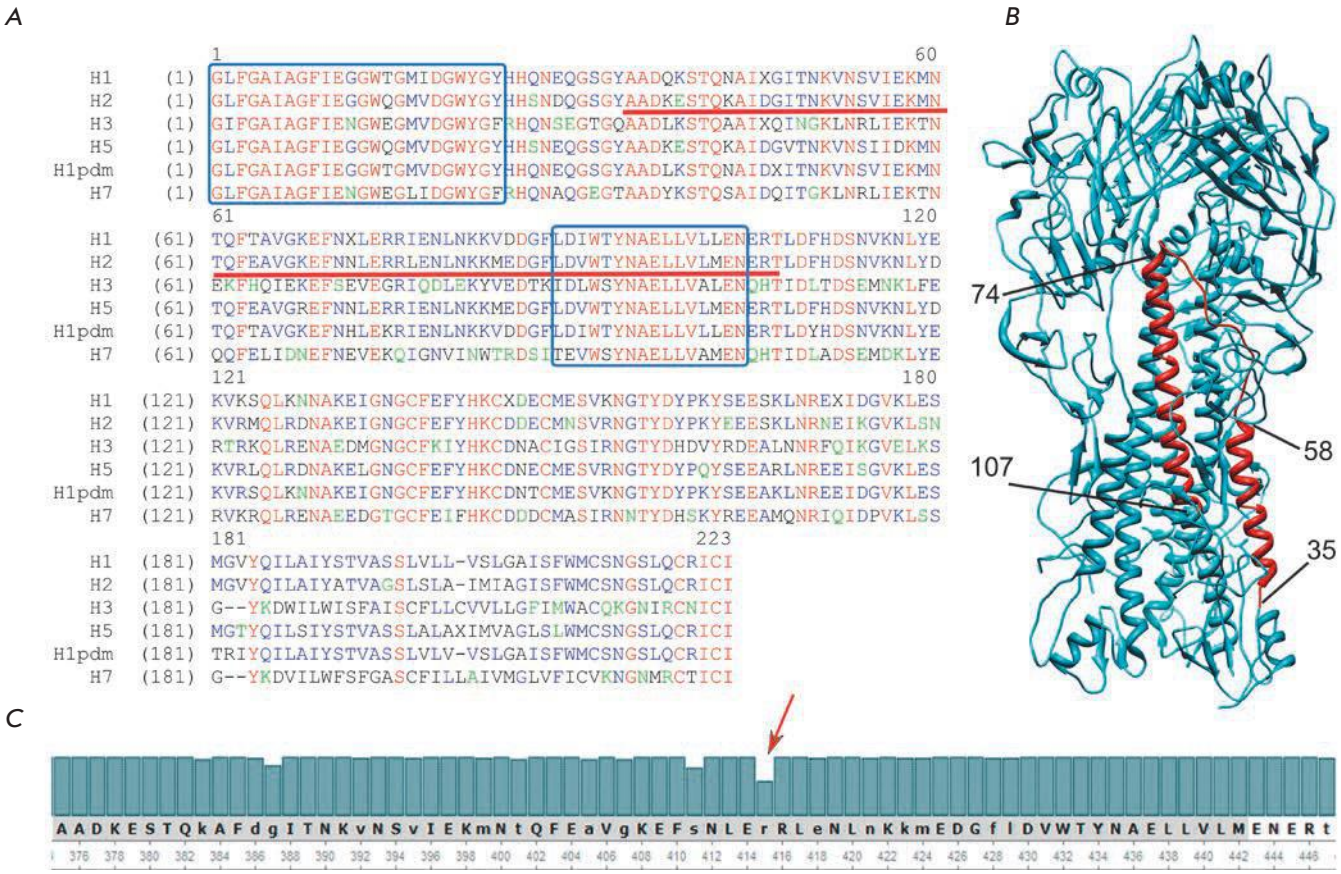


Fig. 1. *A* – alignment of HA2 consensus sequences of influenza A viruses of different subtypes. Two highly conserved fragments with sequence identities of 78.3 and 62.5%, respectively, are shown in blue boxes. A fragment selected for inclusion in the fusion protein is underlined. *B* – the three-dimensional structure of the hemagglutinin molecule (trimer, a model 3WR7 from the Protein Data Bank). The HA2 fragment (35–107) of one of the monomers is shown in red. Main fragments: the small α-helix (35–58); an unstructured region (59–73); a fragment of the large α-helix containing a highly conserved fragment (74–107). *C* – amino acid frequency plot of a HA2(35-107) fragment of human influenza A/H2N2 hemagglutinin (in HA0 numbering), the less conserved residue (Arg416 – 58.3%) is indicated by a red arrow.

### Design of the recombinant fusion protein FlgMH

The chimeric protein was constructed using the commercial plasmid pQE30 containing a start codon and a histidine tag before the cloning site. The fusion protein FlgMH included the full-length sequence of flagellin (FliC), lacking a start codon, and the target MH sequence that were encoded by a single reading frame with the histidine tag (*Fig. 3A*). Therefore, the recombinant protein FlgMH consisted of flagellin, with the histidine tag at the N-terminus and the HA2 consensus sequence (35–107) of human influenza A/H2N2 viruses at the C-terminus. Homologous modeling of the three-dimensional FlgMH structure demonstrated preservation of the α-helix structure in MH regions corresponding to HA2 fragments (38–56) and (75–107) (*Fig. 3B*), suggesting that most of the native structure was preserved, and the fusion protein would stimulate the formation of antibodies, in particular to structural epitopes typical of native HA.

### Production and purification of recombinant proteins

The nucleotide sequences encoding the fusion protein FlgMH, as well as its components Flg and MH, were cloned into the pQE30 vector and expressed in the DLT1270 *E. coli* strain (*Fig. 4A*). The theoretical molecular weights of the proteins were as follows: FlgMH (61.3 kDa), Flg (52.9 kDa), and MH (9.8 kDa), which coincided with their electrophoretic mobility in polyacrylamide gel (*Fig. 4B*). The Flg and FlgMH proteins were soluble in PBS, unlike the MH protein that accumulated in inclusion bodies and dissolved only in 2 M urea. In western blotting, the purified proteins FlgMH

*A*

```
                35   40        50        60        70        80        90        100
                     0    5    0    5    0    5    0    5    0    5    0    5    0    5
                AADKESTQKAFDGITNKVNSVIEKMNTQFEAVGKEFSNLERRLENLNKKMEDGFLDVWTYNAELLVLMENERT
Epitope
13172                                                                   ELLVLMENERTLDFHD
19567                                                              GFLDVWTYNAELLVLMENER
79805                              EKMNTQFTAVGKE
79809                                                                   ELLVLLENERTLD
80042                           SVIEKMNTQFTAV
95623                         NKVNSVIEKMNTQFTAVG
96007                                                                WTYNAELLVLLENERTLD
113324                                                             DGFLDIWTYNAELLV
122152                                                                NAELLVLMENERTLDFHDSN
125912                                                                ELLVLLENERTLDFHDS
125913                                                                ELLVLLENERTLDYHDS
127161                          SVIEKMNTQFTAVGKE
130108                        TNKVNSVIEKMNTQFTA
130227                         VIEKMNTQFTAVGKEFN
144630                                                                  ELLVLLENERTLDYHDSNVK
151060                          SVIEKMNTQFTAVGK
151075                                                                YNAELLVLLENERTL
167880        DKESTQKAFDGITNKVNSVI
167894                                                             EDGFLDVWTYNAELLVLMEN
167981                       NSVIEKMNTQFEAVGKEFSN
168022                                                                TYNAELLVLMENERTLDFHD
173555                                                                TYNAELLVLMENERTLDF
182401                        NKVNSVIEKMNTQFT
188765                      TNKVNSVIEKMNTQFTAVGK
195290                    FDGITNKVNSVIEKMNTQFE
225949                      EITNKVNSVIEKMNTQFTAV
```

*B*

```
                   35   40        50        60        70        80        90        100
                        0    5    0    5    0    5    0    5    0    5    0    5    0    5
MH fragment        AADKESTQKAFDGITNKVNSVIEKMNTQFEAVGKEFSNLERRLENLNKKMEDGFLDVWTYNAELLVLMENERT
Allele (supertype)
A1                                                                   MEDGFLDVWTY
A2                                                                       FLDVWTYNA
A2                                                                       FLDVWTYNAEL
A3                                KVNSVIEK                        RLENLNKK
A3                             KAFDGITNK      KMNTQFEAVGK
A3                                  ITNKVNSVIEK
A24                                                                          TYNAELLVL
A26                                    SVIEKMNTQF                            WTYNAELLVLM
B7
B8
B27                                                            RRLENLNK
B27                                                            RRLENLNKK
B27                                                            RRLENLNKKM
B39                                                                        YNAELLVL
B44                                                                  MEDGFLDV
B44                                          FEAVGKEF
B44                                               KEFSNLERRL
B44                                          FEAVGKEFSNL           MEDGFLDVWTY
B58                                                                 KMEDGFLDVW
B62                                    SVIEKMNTQF
```

Fig. 2. *A* – experimental B and CD4+ T cell epitopes homologous to the HA2 consensus sequence fragment (35–107) at least by 90%; based on the search in the IEDB database. *B* – potential CD8+ T cell epitopes included in the HA2 fragment (35–107) for a representative set of HLA alleles; the result of an analysis using the NetCTLpan1.1 Server [19].

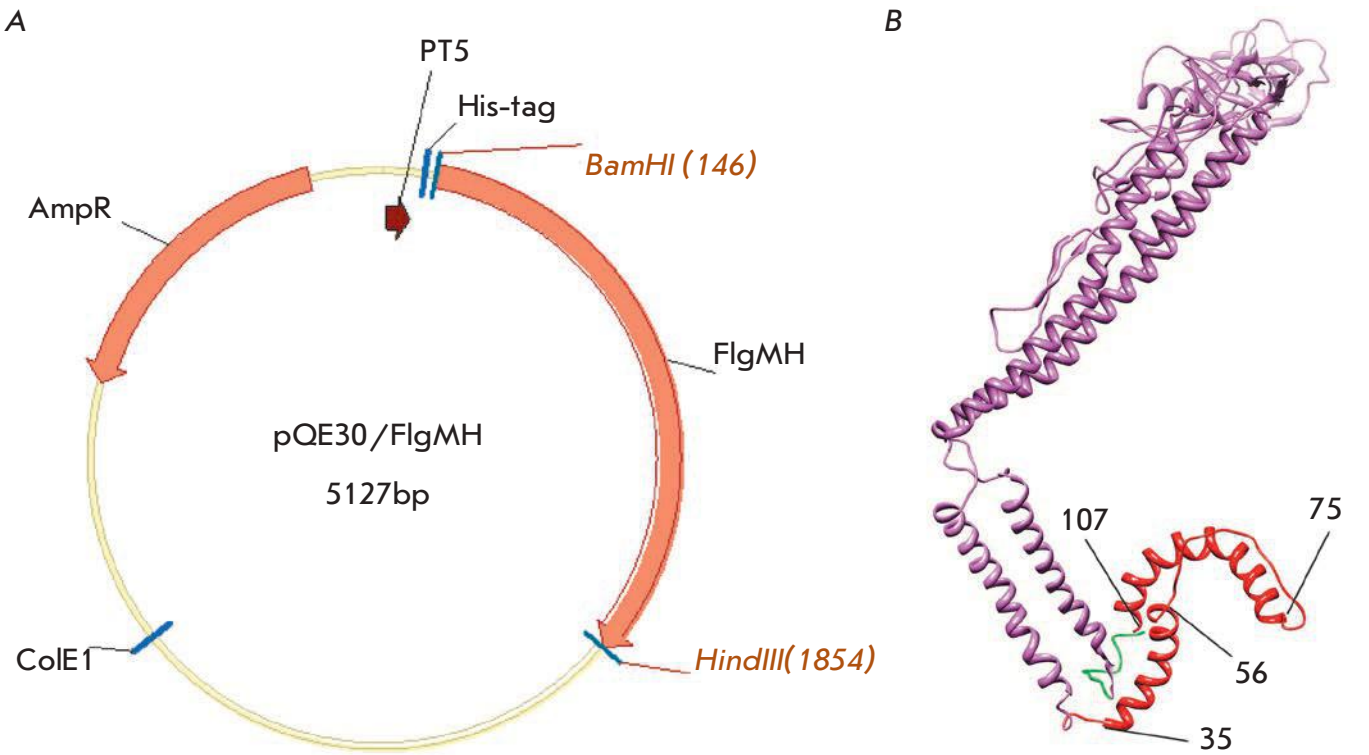


Fig. 3. *A* – map of a plasmid encoding the protein FlgMH. BamHI and HindIII are cloning sites of the gene encoding the fusion protein FlgMH into the vector pQE30. ColE1 – origin of replication; PT5 – the T5 promoter; AmpR – the β-lactamase gene, an ampicillin resistance marker; His-tag – a N-terminal histidine tag. *B* – a theoretical model of the three-dimensional structure of a monomer of the fusion protein FlgMH: the HA2 fragment (35–107) is shown in red; flagellin is shown in violet; the histidine tag is shown in green.

and Flg interacted with anti-flagellin rabbit polyclonal serum and the proteins FlgMH and MH interacted with mouse cross-specific serum against HA of influenza viruses of phylogenetic group I (*Fig. 4B*).

### Immunogenicity and protective ability of the recombinant protein FlgMH

The HA2 consensus sequence (35–107) included in the FlgMH protein contains B, CD4+, and CD8+ T cell epitopes. Thus, we assessed the ability of the recombinant protein FlgMH to stimulate both the B and T cell immune responses.

To investigate the ability of the recombinant protein FlgMH to induce the formation of HA2-specific antibodies, Balb/c mice were immunized intranasally three times with the FlgMH protein without the adjuvant; mice of the control group were administered the Flg protein. The intranasal route of antigen administration induces both systemic and local immune responses. Therefore, on day 14 after the last immunization, we determined the serum and BAL levels of IgA to the target antigen and the serum titers of IgG to influenza viruses of the first and second phylogenetic groups and evaluated the profile of IgG subclasses (IgG1, IgG2a, IgG2b, IgG3). The local response is associated with secretory sIgA, whose multimer form has effective antiviral activity, inhibiting viral replication [21, 22]. Intranasal immunization of mice with the recombinant protein FlgMH stimulated a high level of anti-HA2 IgA in the serum and BAL of the immunized animals (*Fig. 5A*).

The type of immune response by flagellin and flagellin-based recombinant proteins is known to be determined by the flagellin shape. Soluble flagellin (monomeric and polymeric) induces an immune response specific to flagellin and the co-administered target antigen, with a strong predominance of the Th2-type response [23–29]. At the same time, membrane-anchored flagellin induces primarily a Th1-type immune response [24, 28]. On the other hand, the type of an immune response to the target antigen was shown to be also dependent on the flagellin-fused antigen [23]. As shown in *Fig. 5B*, immunization with the soluble recombinant protein FlgMH led to induction of almost equal levels of HA2-specific antibodies IgG1 (type Th2 response) and IgG2a and IgG2b (type Th1 response):

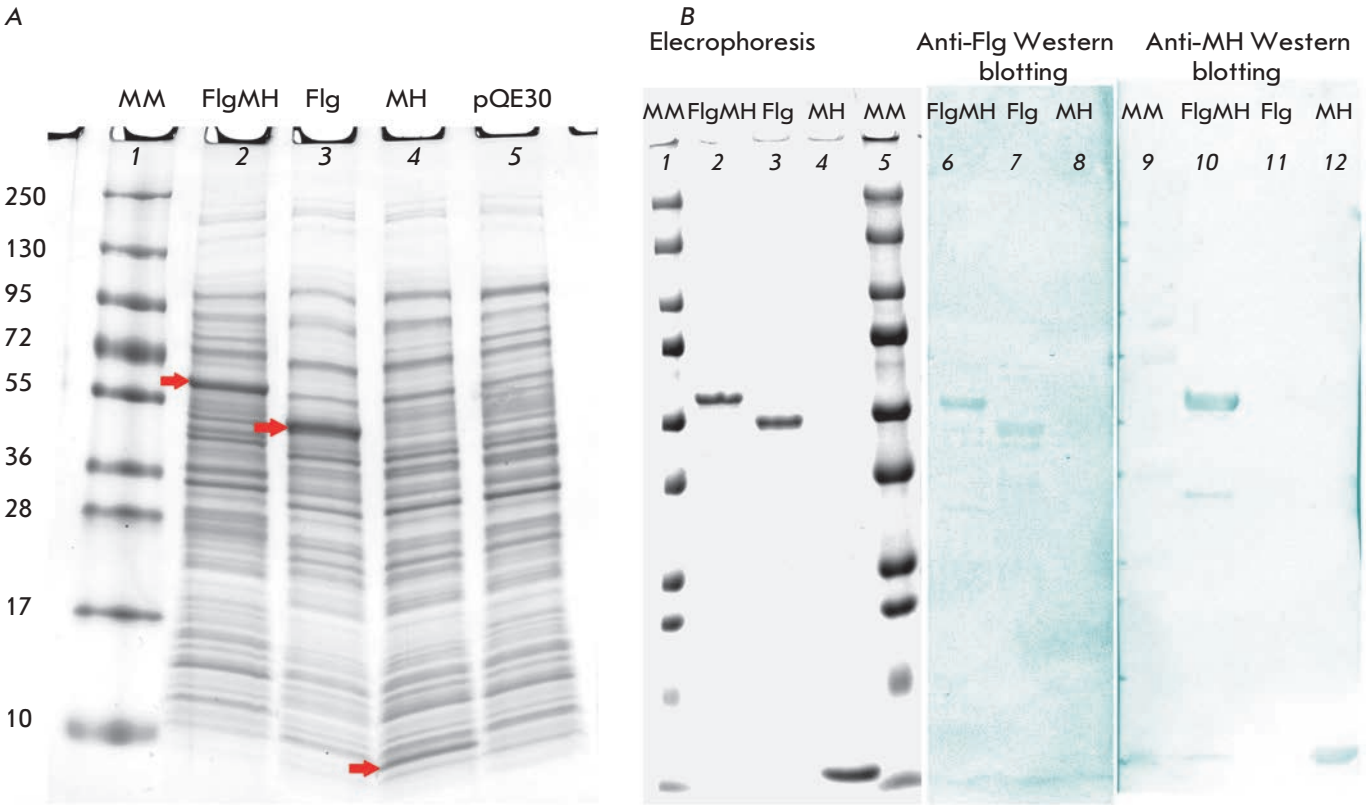


Fig. 4. *A* – expression of recombinant proteins in *E. coli* cells. 1 – molecular weight markers (Fermentas, EU) denoted in kDa; 2–4 – lysates of cells transformed with the plasmid pQE30 carrying an indicated insert; 5 – a lysate of cells transformed with the vector pQE30 without an insert. Bands of recombinant proteins are indicated by arrows. *B* – recombinant proteins FlgMH, Flg, and MH after chromatographic purification on a Ni-sorbent. Results of electrophoresis and Western blot using polyclonal antibodies to flagellin (6–8) and antiserum to a fragment MH (9–12) are presented.

IgG1 – 40.0%, IgG2a – 30.3%, IgG2b – 26.4%, and IgG3 – 3.3%. The absence of significant differences in IgG subclasses (IgG1, IgG2a, IgG2b) for the target antigen after immunization of mice with the recombinant protein FlgMH suggests a mixed Th1 and Th2 immune response.

The selected HA2 consensus sequence (35–107) is quite conserved in influenza viruses of the first phylogenetic group (87.5% homology); therefore, it was important to evaluate the formation of cross-reactive antibodies after immunization of mice with the FlgMH protein. According to the ELISA, FlgMH-induced HA2-specific IgGs bound not only to the influenza virus of the A/H2N2 subtype (geometric mean titer, GMT = 12,800), but also to other influenza A virus subtypes from the first phylogenetic groups: H1 (GMT = 4,160) and H5 (GMT = 2,880) (*Fig. 5B*). However, titers of antibodies to influenza viruses of the H5 and H1 subtypes were significantly lower than that to the H2 subtype ($p < 0.05$, Mann-Whitney test). In addition, induced antibodies bound to hemagglutinin in native conformation (pH 7.2) and to an acidic form of hemagglutinin (pH 5.0) with the same affinity (*Fig. 5B*), indicating the accessibility of the target HA2 sequence on the virion surface for antibodies.

The ability of the recombinant protein FlgMH to induce a cellular response was determined based on the production of IFN-γ by spleen CD3+CD8+ T cells after re-stimulation with synthetic peptides ($HA2_{35-58}$, $HA2_{59-72}$, $HA2_{73-107}$) corresponding to the target HA2 sequence or with a purified influenza virus A/H2N2. The number of activated IFN-γ secreting CD3+ CD8+ T cells both in Balb/c mice (haplotype H-2d) and in C57Bl/6 mice (haplotype H-2b) immunized with the recombinant protein FlgMH was shown to be significantly higher ($p < 0.05$, Mann-Whitney test) than that in mice immunized with the carrier protein flagellin (*Fig. 6A, B*).

Flagellin provides an antigen-specific CD4+ T cell response [30] through activation of TLR5 expressed on CD11c+ cells [31], which leads to a strong humoral response. However, the ability of flagellin to stimulate a specific CD8+ T cell response remains unclear. Several

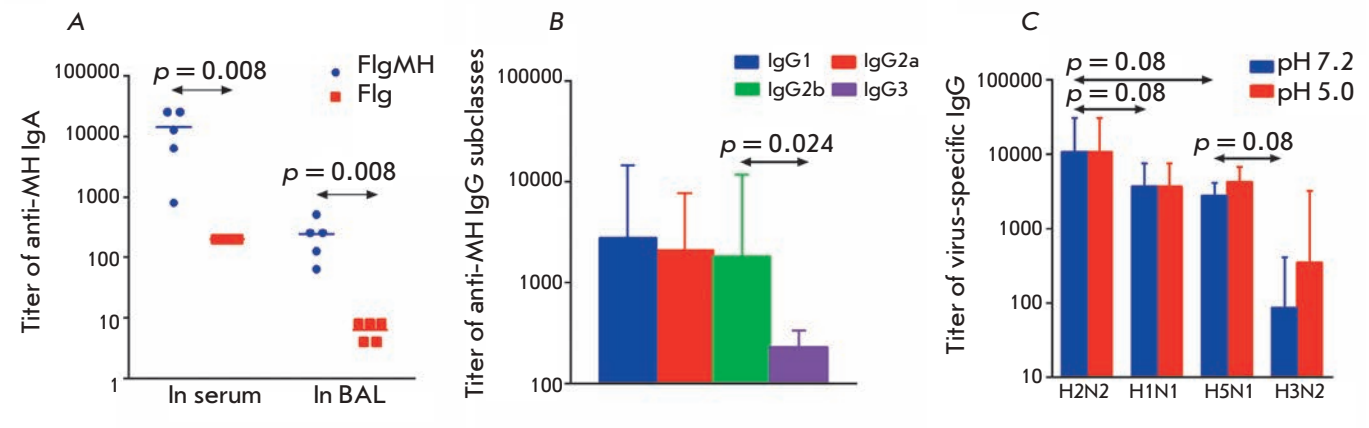


Fig. 5. Antibody titers in mice of the experimental and control groups 2 weeks after triple immunization. *A* – titers of IgA antibodies, in serum and BAL, to the target antigen MH. *B* – GMT of IgG subclasses to the target antigen MH in mice of the experimental group. *C* – GMT of serum IgG to influenza viruses A/PR/8/34 (H1N1), A/Singapore/1/57 (H2N2), A/Aichi/2/68 (H3N2), and A/Kurgan/05/2005 (H5N1). The Mann-Whitney test was used to calculate the *p* value.

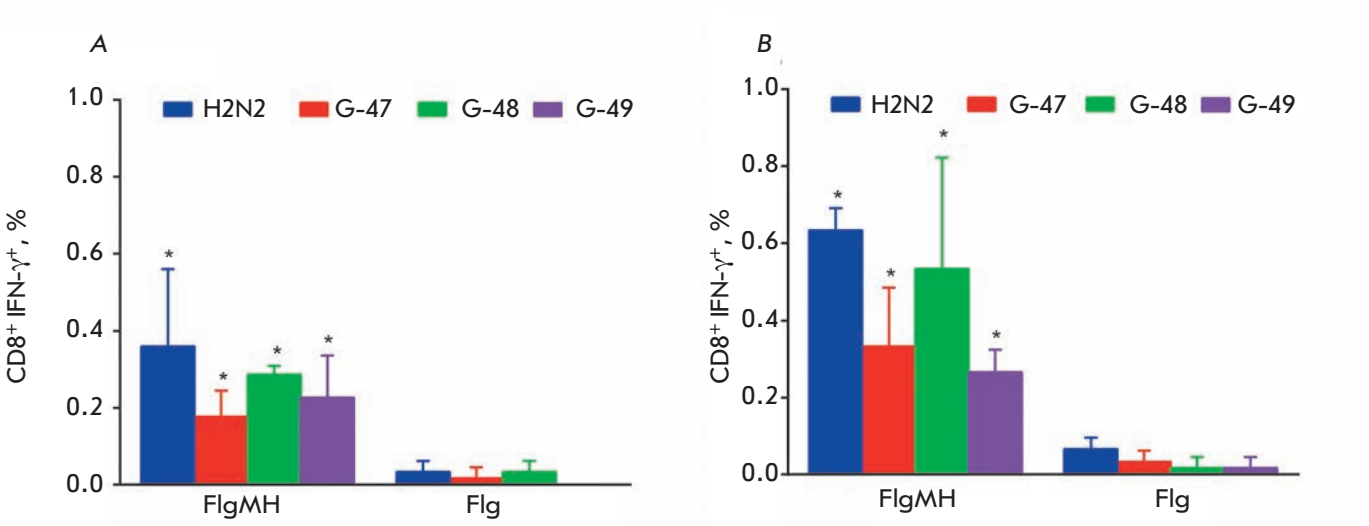


Fig. 6. IFNγ production by spleen CD8+ T-cells after re-stimulation with the G-47, G-48, and G-49 peptides and the influenza virus A/Singapore/1/57 (H2N2) in mice C57Bl/6 (*A*) and Balb/c (*B*). The spleens were taken from three mice each of the experimental and control groups 14 days after triple immunization. * – the difference from control $p < 0.05$ (Mann-Whitney test).

studies have shown that immunization of mice with a fusion protein (flagellin-GFP, flagellin-OVA) stimulates a CD8+ response to the antigen, contrary to immunization with the flagellin-free antigen, only [26, 32]. On the other hand, soluble flagellin fused with an antigen was found to induce predominantly the Th2 response and not to generate antigen-specific CD8+ cells [23–36]. To be presented in the MHC-complex, the antigen undergoes exogenous proteolytic degradation, before which it should be unfolded [33]. Reduction of disulfide bonds in a protein is a key element of the unfolding process [34], and cross-presentation of the antigen, which contains disulfide bridges, by dendritic cells depends on the IFN-γ-induced expression of thiol reductases [35]. Fusion of MHC I-restricted immunogenic epitopes to flagellin was shown [36] to be able to create a pseudo-adjuvant effect that functions via enhanced presentation of the antigen on the cell surface and not to be dependent on TLR5, MyD88, and conserved flagellin fragments. This is related to a more effective processing of the flagellin-fused antigen compared to processing of the antigen in its native state. This means that the antigen, not the TLR5 sig-

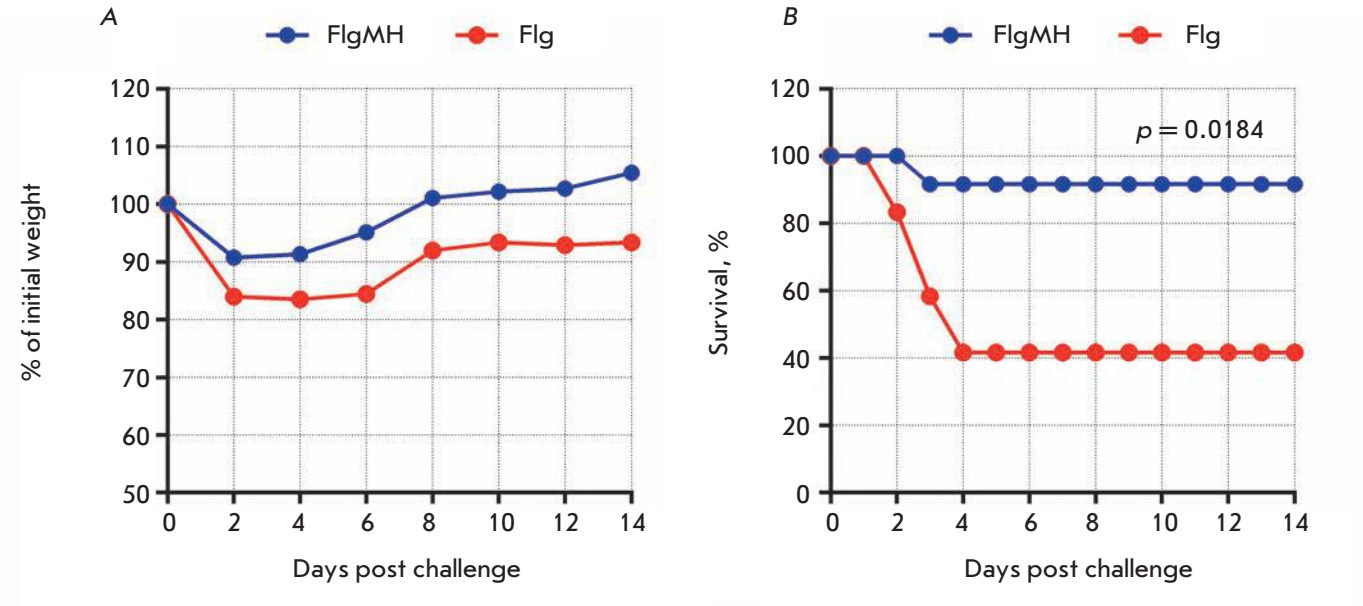


Fig. 7. Efficacy of FlgMH immunization. Two weeks post second boost mice were challenged with $2LD_{50}$ A/Singapore/1/57 (H2N2). Body weight (A) and survival rate (B) were monitored daily during 14 days. The *p* value was calculated using the Mantel-Cox test.

nal, is a limiting factor in the formation of the CD8+ T cell response. Thus, flagellin may serve as a platform for vaccines containing poorly processed antigens bearing CD8+ epitopes [36].

We found that a soluble form of flagellin fused with the sequence $HA2_{35-107}$ containing CD8+ epitopes stimulates the formation of HA2-specific CD8+ T cells.

The ability of the recombinant protein FlgMH to protect mice was demonstrated upon infection of immunized animals with a lethal dose ($2LD_{50}$) of the adapted influenza virus A/Singapore/1/57 (H2N2). Immunization led to differences in body weight dynamics in experimental and control mice: maximum body weight loss was 10% in immunized mice and 16.6% in control mice (*Fig. 7A*). Immunization with the recombinant protein FlgMH protected mice from infection (*Fig. 7B*). The survival rate was 91.0% in the experimental group in contrast to 41% in the control group. The observed differences were statistically significant ($p = 0.0184$, Mantel-Cox test).

## CONCLUSIONS

Conserved fragments of the second HA subunit are of particular interest for the design of vaccine constructs that can provide broad-spectrum immunity against influenza A viruses. The recombinant fusion protein FlgMH based on flagellin and the highly conserved hemagglutinin HA2 fragment (35–107) of influenza viruses of the A/H2N2 subtype includes potential B cell and CD4+ and CD8+ T cell epitopes. It combines the adjuvant activity of flagellin due to its specific binding to TLR5 and the conserved sequences of the hemagglutinin stalk region involved in conformational changes leading to the fusion of the bilayer lipid membranes of the virus and the host cell during a pH-induced fusion reaction. The target sequence including the small α-helix, a fragment of the larger α-helix, and a linker connecting the helices is part of the second hemagglutinin chain and is characterized by very high stability of the amino acid composition within the subtype.

The recombinant protein FlgMH stimulates a mixed Th1/Th2-response to the target sequence, formation of cross-reactive antibodies that bind to influenza viruses of the first phylogenetic group (H1, H2, H5), and induction of specific cytotoxic T cells (CD3+CD8+IFN-γ+). Immunization with the fusion protein protected immunized animals from a lethal influenza infection. The constructed recombinant fusion protein FlgMH is a promising basis for the development of an influenza vaccine with a wide spectrum of action and ability to stimulate the T and B cell immune responses. The cross-protective potential of HA2 fragments can be amplified through optimization of their delivery and increased immunogenicity using ligands of TLR-receptors for effective stimulation of innate immunity and subsequent amplification of the adaptive immune response.

*This work was supported by the Russian Science Foundation (Project No. 15-14-00043).*

REFERENCES

1. Skehel J.J., Wiley D.C. // Annu. Rev. Biochem. 2000. V. 69. P. 531–569.
2. Gerhard W., Mozdzanowska K., Zharikova D. // Emerg. Infect. Dis. 2006. V. 12. № 14. P. 569–574.
3. Kwong P.D., Wilson I.A. // Nat. Immunol. 2009. V. 10. № 6. P. 573–578.
4. Ekiert D.C., Friesen R.H., Bhabha G., Kwaks T., Jongeneelen M., Yu W., Ophorst C., Cox F., Korse H.J., Brandenburg B., et al. // Science. 2011. V. 333. № 6044. P. 843–850.
5. Trosby M., van den Brink E., Jongeneelen M., Poon L.L., Alard P., Cornelissen L., Bakker A., Cox F., van Deventer E., Guan Y., et al. // PLoS One. 2008. V. 3. № 12. P. e3942.
6. Gocnik M., Fislova T., Sladkova T., Mucha V., Kostolansky F., Vareckova E. // J. Gen. Virol. 2007. V. 88. № 3. P. 951–955.
7. Prabhu N., Prabakaran M., Ho H.T., Velumani S., Qiang J., Goutama M., Kwang J. // J. Virol. 2009. V. 83. № 6. P. 2553–2562.
8. Wang T.T., Tan G.S., Hai R., Pica N., Petersen E., Moran T.M., Palese P. // PloS Pathog. 2010. V. 6. № 2. P. e1000796.
9. Wei C.J., Boyington J.C., McTamney P.M., Kong W.P., Pearce M.B., Xu L., Andersen H., Rao S., Tumpey T.M., Yang Z.Y., et al. // Science. 2010. V. 329. № 5995. P. 1060–1064.
10. Corti D., Voss J., Gamblin S.J., Codoni G., Macagno A., Jarrossay D., Vachieri S.G., Pinna D., Minola A., Vanzetta F., et al. // Science. 2011. V. 333. № 6044. P. 850–856.
11. Wrammert J., Koutsonanos D., Li G.M., Edupuganti S., Sui J., Morrissey M., McCausland M., Skountzou I., Hornig M., Lipkin W.I., et al. // J. Exp. Med. 2011. V. 208. № 1. P. 181–193.
12. Wang T.T., Tan G.S., Hai R., Pica N., Ngai L., Ekiert D.C., Wilson I.A., Garcia-Sastre A., Moran T.M., Palese P. // Proc. Natl. Acad. Sci. USA. 2010. V. 107. № 44. P. 18979–18994.
13. Bommakanti G., Citron M.P., Hepler R.W., Callahan C., Heidecker G.J., Najar T.A., Lu X., Joyce J.G., Shiver J.W., Casimiro D.R., et al. // Proc. Natl. Acad. Sci. USA. 2010. V. 107. № 31. P. 13701–13706.
14. Stanekova Z., Adkins I., Kosova M., Janulíkova J., Sebo P., Vareckova E. // Antiviral Res. 2013. V. 97. № 1. P. 24–35.
15. Stranzl T., Larsen M.V., Lundegaard C., Nielsen M. // Immunogenetics. 2010. V. 62. № 6. P. 357–368.
16. Vita R., Zarebski L., Greenbaum J.A., Emami H., Hoof I., Salimi N., Damle R., Sette A., Peters B. // Nucl. Acids Res. 2010. V. 38. Database issue. P. D854–D862.
17. Pettersen E.F., Goddard T.D., Huang C.C., Couch G.S., Greenblatt D.M., Meng E.C., Ferrin T.E. // J. Comput. Chem. 2004. V. 25. № 13. P. 1605–1612.
18. Kelley L.A., Sternberg M.J. // Nat. Protoc. 2009. V. 4. № 3. P. 363–371.
19. Grant S., Jessee J., Bloom F., Hanahan D. // Proc. Natl. Acad. Sci. USA. 1990. V. 87. № 12. P. 4645–4649.
20. Laemmli U.K. // Nature. 1970. V. 227. № 5259. P. 680–685.
21. Arulanandam B.P., Raeder R.H., Nedrud J.G., Bucher D.G., Le J., Metzger D.W. // J. Immunol. 2001. V. 166. № 1. P. 226–231.
22. Bizanov G., Janakova L., Knapstad S.E., Karlstad T., Bakke H., Haugen I.L., Haugan A., Samdal H.H., Haneberg B. // Scand. J. Immunol. 2005. V. 61. № 6. P. 503–510.
23. Bobat S., Flores-Langarica A., Hitchcock J., Marshall J.L., Kingsley R.A., Goodall M., Gil-Cruz C., Serre K., Leyton D.L., Letran S.E. // Eur. J. Immunol. 2011. V. 41. № 6. P. 1606–1618.
24. Cunningham A.F., Khan M., Ball J., Toellner K.M., Serre K., Mohr E., MacLennan I.C. // Eur. J. Immunol. 2004. V. 34. № 11. P. 2986–2995.
25. Didierlaurent A., Ferrero I., Otten L.A., Dubois B., Reinhardt M., Carlsen H., Blomhoff R., Akira S., Kraehenbuhl J.P., Sirard J.C. // J. Immunol. 2004. V. 172. № 11. P. 6922–6930.
26. Huleatt J.W., Jacobs A.R., Tang J., Desai P., Kopp E.B., Huang Y., Song L., Nakaar V., Powell T.J. // Vaccine. 2007. V. 25. № 4. P. 763–775.
27. Sanders C.J., Franchi L., Yarovinsky F., Uematsu S., Akira S., Nunez G., Gewirtz A.T. // Eur. J. Immunol. 2009. V. 39. № 2. P. 359–371.
28. Gat O., Galen J.E., Tennant S., Simon R., Blackwelder W.C., Silverman D.J., Pasetti M.F., Levine M.M. // PLos One. 2011. V. 5. № 11. P. e1373.
29. Stepanova L.A., Kotlyarov R.Y., Kovaleva A.A., Potapchuk M.V., Korotkov A.V., Sergeeva M.V., Kasianenko M.A., Kuprianov V.V., Ravin N.V., Tsybalova L.M., et al. // PLoS One. 2015. V. 10. № 3. P. e0119520.
30. McSorley S.J., Ehst B.D., Yu Y., Gewirtz A.T. // J. Immunol. 2002. V. 169. № 7. P. 3914–3919.
31. Bates J.T., Uematsu S., Akira S., Mizel S.D. // J. Immunol. 2009. V. 182. № 12. P. 7539–7547.
32. Cuadros C., Lopez-Hernandez F.J., Dominguez A.L., McClelland M., Lustgarten J. // Infect. Immun. 2004. V. 72. № 5. P. 2810–2816.
33. Jensen P.E. // Semin. Immunol. 1995. V. 7. № 6. P. 347–353.
34. Collins D.S., Unanue E.R., Harding C.V. // J. Immunol. 1991. V. 147. № 12. P. 4054–4059.
35. Singh R., Cresswell P. // Science. 2010. V. 328. № 5984. P. 1394–1398.
36. Bates J.T., Graff A.H., Phipps J.P., Grayson J.M., Mizel S.B. // J. Immunol. 2011. V. 186. № 11. P. 6255–6262.

# Decrease in the Sensitivity of Myocardium to M3 Muscarinic Receptor Stimulation during Postnatal Ontogenisis

S.V. Tapilina[1,2], D.V. Abramochkin[1,2]*
[1]Department of human and animal physiology, Lomonosov Moscow State University, Leninskie Gory 1 bldg. 12,119234,Moscow, Russia
[2]Department of physiology, Pirogov Russian National Research Medical University, Ministry of Healthcare of the Russian Federation, Ostrovityanova str. 1, 117997, Moscow, Russia
*E-mail: abram340@mail.ru
Received 10.11.2015


**ABSTRACT** **Type 3 muscarinic receptors (M3 receptors) participate in the mediation of cholinergic effects in mammalian myocardium, along with M2 receptors. However, myocardium of adult mammals demonstrates only modest electrophysiological effects in response to selective stimulation of M3 receptors which are hardly comparable to the effects produced by M2 stimulation. In the present study, the effects of selective M3 stimulation induced by application of the muscarinic agonist pilocarpine (10 μM) in the presence of the selective M2 blocker methoctramine (100 nM) on the action potential (AP) waveform were investigated in isolated atrial and ventricular preparations from newborn and 3-week-old rats and compared to those in preparations from adult rats. In the atrial myocardium, stimulation of M3 receptors produced a comparable reduction of AP duration in newborn and adult rats, while in 3-week-old rats the effect was negligible. In ventricular myocardial preparations from newborn rats, the effect of M3 stimulation was more than 3 times stronger compared to that from adult rats, while preparations from 3-week old rats demonstrated no definite effect, similarly to atrial preparations. In all studied types of cardiac preparations, the effects of M3 stimulation were eliminated by the selective M3 antagonist 4-DAMP (10 nM). The results of RT-PCR show that the amount of product of the M3 receptor gene decreases with the maturation of animals both in atrial and ventricular myocardium. We concluded that the contribution of M3 receptors to the mediation of cardiac cholinergic responses decreases during postnatal ontogenesis. These age-related changes may be associated with downregulation of M3 receptor gene expression.**
**KEYWORDS** **acetylcholine, muscarinic receptors, heart, action potential, ontogenesis.**
**ABBREVIATIONS** **acetylcholine – ACh, type 2 muscarinic receptors – M2 receptors, type 3 muscarinic receptors – M3 receptors, newborn rats – NR, 3-week old rats – TWR, adult rats – AR, real-time PCR – RT-PCR, action potential – AP, AP duration at 50% repolarization level – APD50, AP duration at 90% repolarization level – APD90**

## INTRODUCTION

Parasympathetic regulation of the heart is extremely important for its proper functioning. The neurotransmitter acetylcholine (ACh) secreted by intramural postganglionic parasympathetic nerve endings is a major effector of the parasympathetic nervous system. ACh affects pacemaker and working cardiomyocytes through type 2 muscarinic receptors (M2 receptors), causing negative chronotropic and inotropic effects, respectively [1]. However, there is plenty of recent evidence of the existence of functionally active type 3 acetylcholine receptors (M3 receptors) in the mammalian myocardium [2–4].

While M2 receptors are coupled with $G_i$ proteins and the main effects of their stimulation are associated with a decrease in the intracellular levels of cAMP, M3 receptors are coupled with $G_q$ proteins, and, therefore, their stimulation results in the activation of the intracellular phosphoinositide signaling cascade [1, 2]. In this process, the α-subunit of the $G_q$ protein activates phospholipase C, which ultimately leads to an increased intracellular level of $Ca^{2+}$ and activation of protein kinase C capable of affecting the functioning of various ion channels by phosphorylation. On the other hand, the channels carrying the potassium current ($I_{KM3}$) are apparently activated by direct interaction with $G_q$ protein subunits [3, 5]. Stimulation of M3 receptors leads to a decrease in AP duration, which is mainly observed in atrial myocardium of adult rats [6], mice [4], and guinea pigs [7]. Furthermore, M3 receptors mediate a number of ACh effects

that are not related to electrical activity; in particular its antiapoptotic effect on cardiomyocytes [8, 9].

Most research dealing with myocardial M3 receptors are limited to the study of their functions in adult animals, despite the fact that at the early stages of postnatal ontogeny, the role of parasympathetic cardiac regulation is generally higher than in adults due to underdevelopment or lack of sympathetic innervation of myocardium [10]. The results of *in vivo* experiments on infant rats [11], as well as preliminary results obtained by our group [12] for myocardium of newborn rats, suggest a higher sensitivity of myocardium to M3 receptor stimulation at the early stages of ontogeny.

In this regard, the present work included a comparative study of the electrophysiological effects of selective stimulation of M3 receptors in the atrial and ventricular myocardium of newborn rats (NRs) on the first day of life, three-week-old rats (TWRs), and adult rats aged 4 months (ARs). Electrophysiological data were compared to the expression of the M2 and M3 receptor genes measured by real-time PCR (RT-PCR).

## EXPERIMENTAL

We used four-month-old male albino rats (n = 26) weighing 300–350 g, TWRs weighing 24–28 g (n = 24, five different litters), and NRs weighing 4.5–6 g (n = 25). The animals were decapitated, the thorax was quickly opened, and the heart was isolated and washed with Tyrode's solution (composition in mmol/l: NaCl 133.47; KCl 4.69; $NaH_2PO_4 \cdot 2H_2O$ 1.35; $NaHCO_3$ 16.31; $MgSO_4 \cdot 7H_2O$ 1.18; $CaCl_2 \cdot 2H_2O$ 2.5; glucose 7.77), saturated with carbogen (gas mixture of 95% $O_2$ and 5% $CO_2$). Then, a preparation of the right atrial appendage and a preparation of the right ventricular wall were isolated from each heart. Each preparation was mounted on a 3-ml experimental chamber (temperature 38°C, flow rate 10 ml/min) with its endocardial surface upward and stimulated using silver electrodes with a frequency of 6 Hz (ARs and TWRs) or 4 Hz (NRs).

AP was recorded using a standard method of intracellular recording of bioelectric activity with 25–50 MOhm glass microelectrodes connected to a Neuroprobe-1600 amplifier (AM-Systems, USA). The signal was digitized using a E14-140 analog-to-digital converter (L-Card, Russia) and recorded on a computer using the Powergraph 3.3 software (DiSoft, Russia). Data processing was carried out using the MiniAnalysis v. 3.0.1 software (Synaptosoft, USA). When analyzing the records, we determined AP duration at 50 and 90% repolarization (APD50 and DPD90, respectively), as well as the AP amplitude and resting potential value.

In electrophysiological experiments, four compounds were used: selective blockers of the M1, M2, and M3 receptors; pirenzepine, methoctramine, and 4-DAMP,

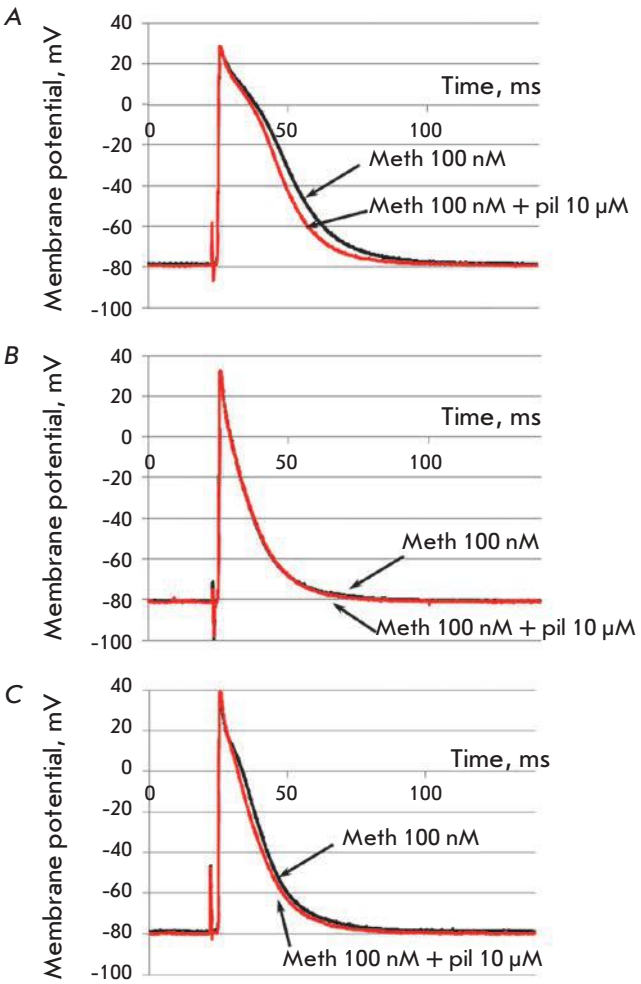


Fig. 1. Comparison of original AP traces recorded in isolated right ventricular wall preparations of NR (A), TWR (B), and AR (C) in the control or during the maximum effect of pilocarpine (10 μM) in the presence of the selective M2 blocker methoctramine (100 nM).

respectively; and the M receptor agonist pilocarpine, having low specificity to the M1 and M3 receptors as compared to the M2 and M4 receptors. All the substances were ordered from Sigma (USA). The concentrations of substances were selected based on data from previous studies [4, 7]. Each preparation was used no more than twice to record the pilocarpine effect under normal conditions and in the presence of a blocker.

Gene expression levels were compared by RT-PCR. Preparations of right atrial appendage and right ventricular walls from NRs, TWRs, and ARs obtained as described above were used for this purpose. The preparations were placed in a RNA stabilizing solution (IntactRNA, Evrogen, Russia) for 24 hours at 4C° and then stored at −20C° until RNA isolation. RNA was extracted

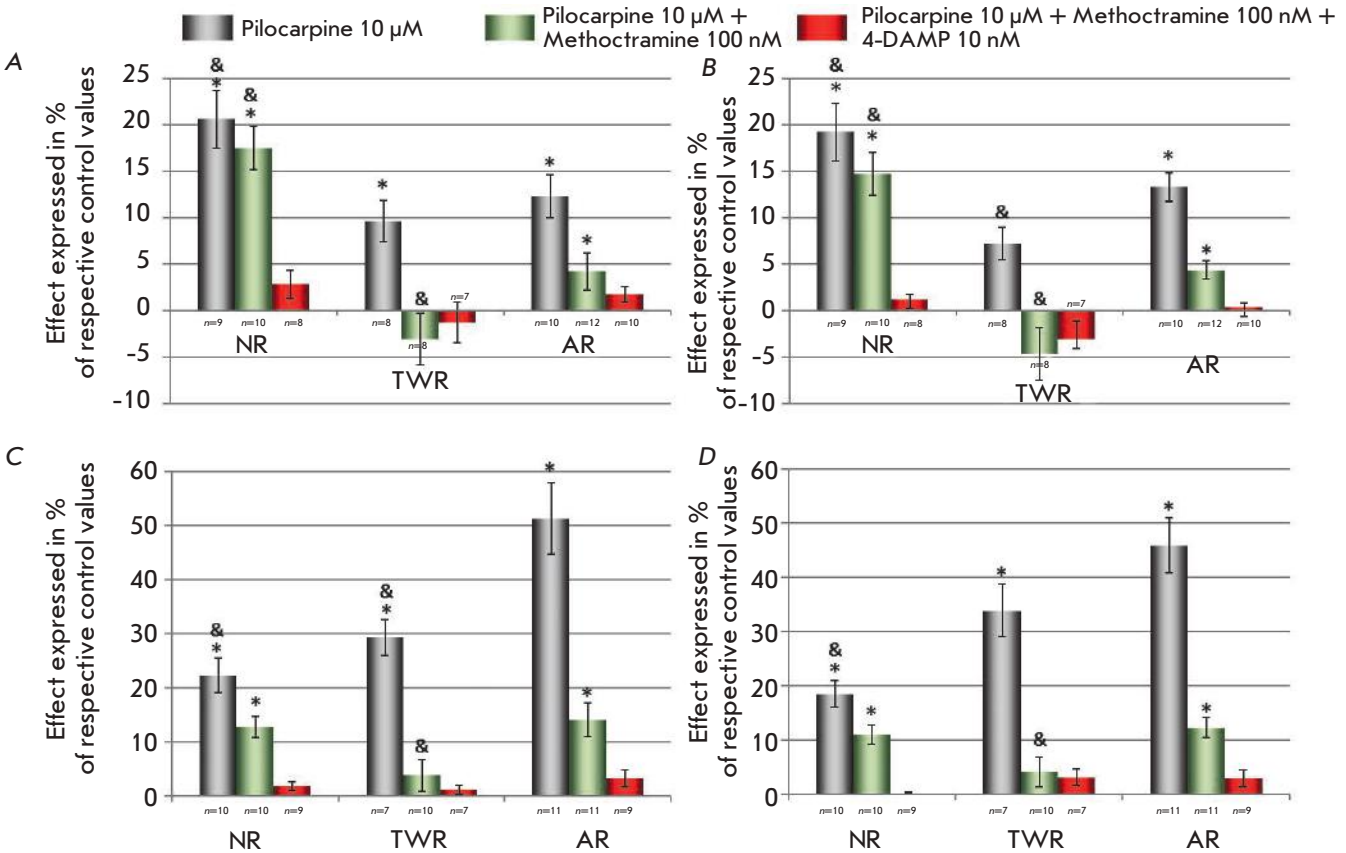


Fig. 2. Relative reduction in AP duration in ventricular (A, B) and atrial (C, D) myocardial preparations measured at a 50% (A, C) and 90% (B, D) repolarization level induced by 10 μM pilocarpine under normal conditions or in the presence of methoctramine (100 nM) and 4-DAMP (10 nM). Ordinates: maximal pilocarpine-induced decrease in APD50 or APD90 expressed in % of respective control values. *$p < 0.05$ vs. the respective control values, Wilcoxon test. &$p < 0.05$ vs. respective effects in AR, Mann-Whitney test.

using the guanidinium thiocyanate-phenol-chloroform method (ExtractRNA, Evrogen, Russia). RNA was purified from genomic DNA using DNase I (2000 act. units/ml, NEB, USA) for 60 min at 37C°. The RNA concentration was measured using a spectrophotometer (Nanodrop 2000, ThermoScientific, USA). For cDNA synthesis, the resulting RNA purified from genomic DNA was subjected to a reverse transcription reaction using a MMLVRTkit kit (Evrogen, Russia). All manipulations were carried out in accordance with the standard procedures using the protocols recommended by the manufacturer. cDNA was stored at −80C° until RT-PCR.

RT-PCR was performed on a BioRad instrument equipped with a CFX96 detection system using a Synthol reagent kit (Russia) and EvaGreen dye (BIOTIUM, USA). We used primers synthesized at Evrogen (5'−3'): M2 receptor − TCTACACTGTGATTGGTTACTGGC (forward), GCTTAACTGGGTAGGTCAGAGGT (reverse); M3-receptor − SAAGTGGTCTTCATTGCCTTCT (forward), GCCAGGCTTAAGAGGAAGTAGTT (reverse); GAPDH − CAGCGATGCTTTACTTTCTGAA (forward), GATGGCAACAATGTCCACTTT (reverse).

The amplification program consisted of initial denaturation at 95C°, 5min; followed by 50 cycles of PCR (1 min at 95C°, 30 sec at 60C°, and 30 sec at 72C°); and then the last step at 72C° for 10 min. Data were analyzed by the threshold method using the software supplied with the thermocycler. The results were normalized to the amount of RNA taken for the reverse transcription reaction.

The results were statistically processed using the Statistica 6.0 software. The Wilcoxon test was used to assess the statistical significance of the differences for paired samples; The Mann-Whitney test was used for unpaired samples. We used nonparametric tests due to the small sample sizes, which could not provide a normal distribution.

## RESULTS

Muscarinic receptor agonist pilocarpine (10 uM) was used for selective stimulation of M3 receptors in elec-

trophysiological experiments. It was applied to the experimental chamber in the presence of the highly selective M2 receptor blocker methoctramine (100 nM). Special preliminary experiments, where pilocarpine was applied in the presence of the selective antagonist pirenzepine (100 nM), were used to eliminate a possible effect of M1 receptor activation. Since there were no differences in the intensity of pilocarpine effects in the presence of methoctramine and in the presence of two blockers, which is consistent with previous data showing the absence of M1 receptors in cardiomyocytes, pilocarpine was further applied in the presence of methoctramine alone for selective stimulation of M3 receptors.

In addition to registration of the M3 receptor stimulation effects, we conducted control experiments where pilocarpine was applied in the absence of blocking agents to assess the total effect of M2 and M3 receptor activation in myocardial preparations.

It was found that in the absence of blockers, pilocarpine significantly reduces AP duration both at 50% and 90% repolarization levels in the ventricular *(Fig. 1, 2A, B)* and atrial *(Fig. 2C, D)* rat myocardium in all three age groups. The maximum effect of pilocarpine developed within 250–300 s after the beginning of the application of the substance. Hereinafter, we will discuss only the maximum values of pilocarpine effects.

The effect of selective stimulation of M3 receptors in all series of experiments was qualitatively similar to the effect of pilocarpine in the absence of blockers, but it was significantly less pronounced. However, in the ARs and NRs, APD50 and APD90 were significantly reduced both in the ventricular *(Fig. 1A, C, 2A, B)* and atrial myocardium *(Fig. 2C, D)*. On the contrary, there was no significant effect of selective stimulation of M3 receptors in the TWR group *(Fig. 1B, 2)*. Almost no effects of the selective stimulation of M3 acetylcholine receptors were observed in the presence of 4-DAMP (10 nM), selective M3 receptor blocker; i.e., these effects were actually mediated by the activation of M3 receptors *(Fig. 2)*.

It should be noted that the effect of M3 receptor stimulation in the ventricular myocardium of NRs was threefold stronger compared to that in ARs *(Fig. 2A, B)*, while no significant differences in the intensity of this effect were observed in the atrial myocardium. Thus, the most pronounced effect of M3 stimulation in the ventricular myocardium was observed for NRs, and the least pronounced effect was observed in TWRs. In the atrial myocardium, the main difference between the three age groups was observed in response to pilocarpine applied without blockers. The intensity of the effect increases with animal age, and it is more than twofold higher in ARs compared to NRs.

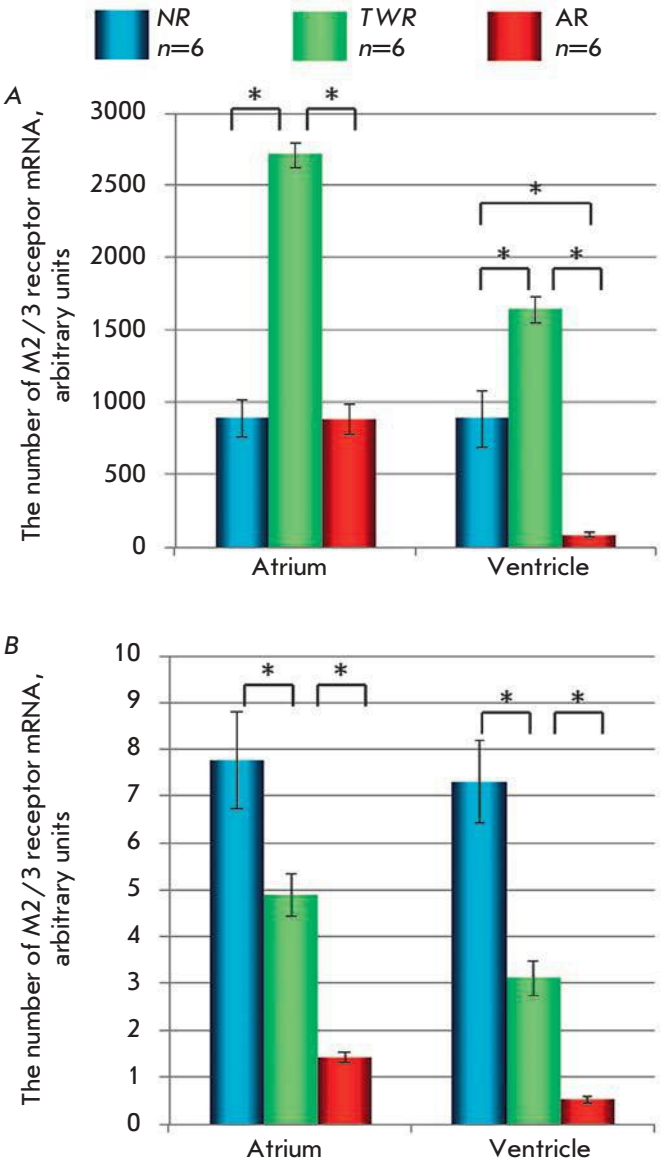


Fig. 3. Expression level of the M2 (A) and M3(B) receptor genes in the atrial and ventricular myocardium of NR, TWR, and AR. Ordinates: arbitrary units of mRNA quantity. * - $p < 0.05$ – difference between two groups, Mann-Whitney test.

According to the results of RT-PCR, mRNA of both the M2 and M3 receptors is synthesized in the myocardium of animals of all age groups. However, the expression of the M3 receptor gene is much weaker *(Fig .3)*. Furthermore, the expression level of the M3 receptor gene decreases both in the atrial and ventricular myocardium with maturation of the animal *(Fig. 3B)*. Thus, it is higher in the myocardium of TWRs compared to that in ARs. However, the expression level of the M2 receptor gene was highest in the TWR group. There-

fore, the ratio of M3 to M2 expression in the ventricular myocardium was higher in ARs compared to that in TWRs: 0.59 vs. 0.19%. In the atrial myocardium, the ratio was nearly the same: 0.16 and 0.18%, respectively.

## DISCUSSION

We were the first to obtain information on the change in the relative contribution of the M3 receptor to the regulation of the electrical activity of the ventricular and atrial myocardium during the postnatal ontogenesis of rats.

In electrophysiological experiments, selective stimulation of M3 receptors was achieved using a common method [4, 7]; more specifically, the application of 10 mM pilocarpine under conditions of total blockade of M2 receptors with 100 nM methoctramine. Please note that in our previous work, increase in the methoctramine concentration did not alter the pilocarpine effects, and, therefore, the effect observed in the presence of 100 nM of pilocarpine was unrelated to the activation of the residual M2 receptors. This fact is also confirmed by an almost complete elimination of the pilocarpine effect caused by both types of M receptor blockers: methoctramine and 4-DAMP.

Electrophysiological data suggest that the effect of M3 receptor stimulation on the electrical activity of the ventricular myocardium is maximal in NRs. In the atrial myocardium, sensitivity to pilocarpine in the absence of M receptor blockers increases with age, while sensitivity to pilocarpine under conditions of blockade of M2 receptors is identical in NRs and ARs. We can assume that the contribution of M2 receptors to electrical activity regulation increases with age both in atrial and ventricular myocardium, and in the ventricular myocardium of NRs M3 receptors play a key role.

The results of RT-PCR generally confirm these assumptions, since they show that expression of the M3 receptor gene decreases with age. It is still unclear why no effect of M3 receptor stimulation is observed in TWRs. On the one hand, this can be explained by the lowest ratio of M3 receptor mRNA to M2 receptor mRNA in this age group. On the other hand, the relative translational levels of M2 and M3 receptor proteins may differ from the expression levels of mRNA of the corresponding genes.

## CONCLUSION

In general, our results suggest an important functional role for the M3 receptor in the ventricles of newborn rats, which is leveled in ARs. Furthermore, M3 receptor functions are not limited to their action on the electrical activity investigated in our studies. For example, M3 receptors can participate in the realization of the cardioprotective effects of ACh [8, 9] under oxidative stress conditions experienced by a newborn's body. It is unlikely that change in the role of the M3 receptor is related to the beginning of sympathetic regulation of the myocardium, since there is no effect of M3 receptor stimulation as early as at the age of three weeks, before sympathetic regulation is switched on.

*This work was supported by the Russian Foundation for Basic Research (Grant No 14-04-01564).*

REFERENCES

1. Dhein S., van Koppen C.J., Brodde O. // Pharmacol. Res. 2001. V. 44. P. 161–182.
2. Wang H., Lu Y., Wang Z. // Auton. Autac.Pharmacol. 2007. V. 27. P. 1–11.
3. Shi H., Wang H., Yang B., Xu D., Wang Z. // J. Biol. Chem. 2004. V. 279. № 21. P. 21774–21778.
4. Abramochkin D.V., Tapilina S.V., Sukhova G.S., Nikolsky E.E., Nurullin L.F. // Pflug. Arch. 2012. V. 463. № 4. P. 523–529.
5. Shi H., Wang H., Lu Y., Yang B., Wang Z. // J. Membrane Biol. 1999. V. 169. P. 55–64.
6. Abramochkin D.V., Suris M.A., Borodinova A.A., Kuzmin V.S., Sukhova G.S. // Neurochem. J. 2008. V. 2. P. 90–94.
7. Wang H., Shi H., Lu Y., Yang B., Wang Z. // Br. J. Pharmacol. 1999. V. 126. P. 1725–1734.
8. Yang B., Lin H., Xu C., Liu Y., Wang H., Han H., Wang Z. // Cell. Physiol. Biochem. 2005. V. 16. № 4–6. P. 163–174.
9. Zhao J., Su Y., Zhang Y., Pan Z., Yang L., Chen X., Liu Y., Lu Y., Du Z., Yang B. // Br. J. Pharmacol. 2010. V. 159. № 6. P. 1217–1225.
10. Robinson R.B. // Cardiovasc. Res. 1996. V. 31. P. E68–E76.
11. Ziyatdinova N.I., Sergeeva A.M., Dement'eva R.E., Zefirov T.L. // Bull. Exp. Biol. Med. 2012. V. 154. No 7. P. 4–6.
12. Tapilina S.V., Abramochkin D.V. // Bull. Exp. Biol. Med. 2015. V. 159. № 1. P. 11–14.

## GENERAL RULES

*Acta Naturae* publishes experimental articles and reviews, as well as articles on topical issues, short reviews, and reports on the subjects of basic and applied life sciences and biotechnology.

The journal is published by the Park Media publishing house in both Russian and English.

The journal *Acta Naturae* is on the list of the leading periodicals of the Higher Attestation Commission of the Russian Ministry of Education and Science. The journal Acta Naturae is indexed in PubMed, Web of Science, Scopus and RCSI databases.

The editors of *Acta Naturae* ask of the authors that they follow certain guidelines listed below. Articles which fail to conform to these guidelines will be rejected without review. The editors will not consider articles whose results have already been published or are being considered by other publications.

The maximum length of a review, together with tables and references, cannot exceed 60,000 characters with spaces (approximately 30 pages, A4 format, 1.5 spacing, Times New Roman font, size 12) and cannot contain more than 16 figures.

Experimental articles should not exceed 30,000 symbols (approximately 15 pages in A4 format, including tables and references). They should contain no more than ten figures.

A short report must include the study's rationale, experimental material, and conclusions. A short report should not exceed 12,000 symbols (8 pages in A4 format including no more than 12 references). It should contain no more than four figures.

The manuscript and the accompanying documents should be sent to the Editorial Board in electronic form:
1) text in Word 2003 for Windows format;
2) the figures in TIFF format;
3) the text of the article and figures in one pdf file;
4) the article's title, the names and initials of the authors, the full name of the organizations, the abstract, keywords, abbreviations, figure captions, and Russian references should be translated to English;
5) the cover letter stating that the submitted manuscript has not been published elsewhere and is not under consideration for publication;
6) the license agreement (the agreement form can be downloaded from the website www.actanaturae.ru).

## MANUSCRIPT FORMATTING

The manuscript should be formatted in the following manner:

- Article title. Bold font. The title should not be too long or too short and must be informative. The title should not exceed 100 characters. It should reflect the major result, the essence, and uniqueness of the work, names and initials of the authors.
- The corresponding author, who will also be working with the proofs, should be marked with a footnote *.
- Full name of the scientific organization and its departmental affiliation. If there are two or more scientific organizations involved, they should be linked by digital superscripts with the authors' names. Abstract. The structure of the abstract should be very clear and must reflect the following: it should introduce the reader to the main issue and describe the experimental approach, the possibility of practical use, and the possibility of further research in the field. The average length of an abstract is 20 lines (1,500 characters).
- Keywords (3 – 6). These should include the field of research, methods, experimental subject, and the specifics of the work. List of abbreviations.
- INTRODUCTION
- EXPERIMENTAL PROCEDURES
- RESULTS AND DISCUSSION
- CONCLUSION

  The organizations that funded the work should be listed at the end of this section with grant numbers in parenthesis.
- REFERENCES

  The in-text references should be in brackets, such as [1].

## RECOMMENDATIONS ON THE TYPING AND FORMATTING OF THE TEXT

- We recommend the use of Microsoft Word 2003 for Windows text editing software.
- The Times New Roman font should be used. Standard font size is 12.
- The space between the lines is 1.5.
- Using more than one whole space between words is not recommended.
- We do not accept articles with automatic referencing; automatic word hyphenation; or automatic prohibition of hyphenation, listing, automatic indentation, etc.
- We recommend that tables be created using Word software options (Table → Insert Table) or MS Excel. Tables that were created manually (using lots of spaces without boxes) cannot be accepted.
- Initials and last names should always be separated by a whole space; for example, A. A. Ivanov.
- Throughout the text, all dates should appear in the "day.month.year" format, for example 02.05.1991, 26.12.1874, etc.
- There should be no periods after the title of the article, the authors' names, headings and subheadings, figure captions, units (s – second, g – gram, min – minute, h – hour, d – day, deg – degree).
- Periods should be used after footnotes (including those in tables), table comments, abstracts, and abbreviations (mon. – months, y. – years, m. temp. – melting temperature); however, they should not be used in subscripted indexes ($T_m$ – melting temperature; $T_{p.t}$ – temperature of phase transition). One exception is mln – million, which should be used without a period.
- Decimal numbers should always contain a period and not a comma (0.25 and not 0,25).
- The hyphen ("-") is surrounded by two whole spaces, while the "minus," "interval," or "chemical bond" symbols do not require a space.
- The only symbol used for multiplication is "×"; the "×" symbol can only be used if it has a number to its

right. The "·" symbol is used for denoting complex compounds in chemical formulas and also noncovalent complexes (such as DNA·RNA, etc.).
- Formulas must use the letter of the Latin and Greek alphabets.
- Latin genera and species' names should be in italics, while the taxa of higher orders should be in regular font.
- Gene names (except for yeast genes) should be italicized, while names of proteins should be in regular font.
- Names of nucleotides (A, T, G, C, U), amino acids (Arg, Ile, Val, etc.), and phosphonucleotides (ATP, AMP, etc.) should be written with Latin letters in regular font.
- Numeration of bases in nucleic acids and amino acid residues should not be hyphenated (T34, Ala89).
- When choosing units of measurement, SI units are to be used.
- Molecular mass should be in Daltons (Da, KDa, MDa).
- The number of nucleotide pairs should be abbreviated (bp, kbp).
- The number of amino acids should be abbreviated to aa.
- Biochemical terms, such as the names of enzymes, should conform to IUPAC standards.
- The number of term and name abbreviations in the text should be kept to a minimum.
- Repeating the same data in the text, tables, and graphs is not allowed.

## GUIDENESS FOR ILLUSTRATIONS

- Figures should be supplied in separate files. Only TIFF is accepted.
- Figures should have a resolution of no less than 300 dpi for color and half-tone images and no less than 500 dpi.
- Files should not have any additional layers.

## REVIEW AND PREPARATION OF THE MANUSCRIPT FOR PRINT AND PUBLICATION

Articles are published on a first-come, first-served basis. The members of the editorial board have the right to recommend the expedited publishing of articles which are deemed to be a priority and have received good reviews.

Articles which have been received by the editorial board are assessed by the board members and then sent for external review, if needed. The choice of reviewers is up to the editorial board. The manuscript is sent on to reviewers who are experts in this field of research, and the editorial board makes its decisions based on the reviews of these experts. The article may be accepted as is, sent back for improvements, or rejected.

The editorial board can decide to reject an article if it does not conform to the guidelines set above.

The return of an article to the authors for improvement does not mean that the article has been accepted for publication. After the revised text has been received, a decision is made by the editorial board. The author must return the improved text, together with the responses to all comments. The date of acceptance is the day on which the final version of the article was received by the publisher.

A revised manuscript must be sent back to the publisher a week after the authors have received the comments; if not, the article is considered a resubmission.

E-mail is used at all the stages of communication between the author, editors, publishers, and reviewers, so it is of vital importance that the authors monitor the address that they list in the article and inform the publisher of any changes in due time.

After the layout for the relevant issue of the journal is ready, the publisher sends out PDF files to the authors for a final review.

Changes other than simple corrections in the text, figures, or tables are not allowed at the final review stage. If this is necessary, the issue is resolved by the editorial board.

## FORMAT OF REFERENCES

The journal uses a numeric reference system, which means that references are denoted as numbers in the text (in brackets) which refer to the number in the reference list.

*For books:* the last name and initials of the author, full title of the book, location of publisher, publisher, year in which the work was published, and the volume or issue and the number of pages in the book.

*For periodicals:* the last name and initials of the author, title of the journal, year in which the work was published, volume, issue, first and last page of the article. Must specify the name of the first 10 authors. Ross M.T., Grafham D.V., Coffey A.J., Scherer S., McLay K., Muzny D., Platzer M., Howell G.R., Burrows C., Bird C.P., et al. // Nature. 2005. V. 434. № 7031. P. 325–337.

References to books which have Russian translations should be accompanied with references to the original material listing the required data.

References to doctoral thesis abstracts must include the last name and initials of the author, the title of the thesis, the location in which the work was performed, and the year of completion.

References to patents must include the last names and initials of the authors, the type of the patent document (the author's rights or patent), the patent number, the name of the country that issued the document, the international invention classification index, and the year of patent issue.

The list of references should be on a separate page. The tables should be on a separate page, and figure captions should also be on a separate page.

**The following e-mail addresses can be used to contact the editorial staff: vera.knorre@gmail.com, actanaturae@gmail.com, tel.: (495) 727-38-60, (495) 930-87-07**

# NANOTECHNOLOGIES *in Russia*

## Peer-review scientific journal

*Nanotechnologies in Russia (Rossiiskie Nanotekhnologii)* focuses on self-organizing structures and nanoassemblages, nanostructures including nanotubes, functional nanomaterials, structural nanomaterials, devices and facilities on the basis of nanomaterials and nanotechnologies, metrology, standardization, and testing in nanotechnologies, nanophotonics, nanobiology.

→ **Russian edition:** http://nanoru.ru

→ **English edition:** http://www.springer.com/materials/nanotechnology/journal/12201

Issued with support from:

The Ministry of Education and Science of the Russian Federation

МОСКВА

# F-2016

## XI ВСЕРОССИЙСКАЯ КОНФЕРЕНЦИЯ с международным участием «ХИМИЯ ФТОРА»

1906–1990

**посвящается 110-летию со дня рождения академика И. Л. Кнунянца**

***Уважаемые коллеги!***

***ОРГКОМИТЕТ ПРИГЛАШАЕТ ВАС ПРИНЯТЬ УЧАСТИЕ В РАБОТЕ КОНФЕРЕНЦИИ***

**Конференция состоится 26–30 июня 2016 г. в Москве в Институте элементоорганических соединений им. А.Н.Несмеянова Российской академии наук (Россия, Москва, ул. Вавилова, 28).**

**ЦЕЛЬ конференции – обсуждение достижений и актуальных проблем развития химии фторсодержащих соединений, выявление приоритетных направлений исследований, развитие научных и коммерческих контактов научно-исследовательских институтов и вузов с промышленными предприятиями**

**НАУЧНАЯ ПРОГРАММА конференции охватывает все важнейшие аспекты и общемировые тенденции развития химии и технологии соединений фтора: *синтез и реакционная способность органических и неорганических соединений фтора; биологически активные фторсодержащие вещества для медицины и сельского хозяйства; фторполимеры; проблемы технологии и перспективы использования фторсодержащих веществ и материалов.***

**Программа включает доклады ведущих ученых о последних достижениях в химии органических и неорганических соединений фтора, о результатах исследований, которые открывают путь к созданию новых технологий. Планируется проведение круглых столов с представителями промышленности и бизнес-сообщества.**

**Получить дополнительную информацию можно на сайте конференции http://fluorine.moscow/, и по телефону** +7(499)135-6994

**ОРГАНИЗАТОРЫ КОНФЕРЕНЦИИ: ИНЭОС РАН, ОТДЕЛЕНИЕ ХИМИИ И НАУК О МАТЕРИАЛАХ РАН, ФЕДЕРАЛЬНОЕ АГЕНТСТВО НАУЧНЫХ ОРГАНИЗАЦИЙ РФ, РФФИ, АНО НИЦ ИНЭОС, ЗАО НПО «ПИМ-ИНВЕСТ»**

# Научный журнал
# выходит 6 раз в год

Доступно для загрузки из App Store


# Теперь на iPad

Наше приложение доступно в «Киоске» AppleStore в разделе «Наука».